Western and Central Pacific Fisheries Commission

SCIENTIFIC COMMITTEE
TWENTY-FIRST REGULAR SESSION

Nuku'alofa, Tonga
13–21 August 2025

Stock assessment of skipjack tuna in the western and central Pacific Ocean: 2025

WCPFC-SC21-2025/SA-WP-02 (REV3)
05 August 2025

T. Teears[1], N. Davies[2], P. Hamer[1], A. Magnusson[1], T. Peatman[3], J. Scutt Phillips[1], G. Pilling[1], R. Scott[1] T. Vidal[1], J. Hampton[1]

[1]Oceanic Fisheries Programme of the Pacific Community
[2]Te Takina
[3]Shearwater Analytics Ltd.

1 Author contribution

Thomas Teears: lead analyst, prepared data inputs, performed the analysis, contributed to results interpretation, and primary author of the report. **Nick Davies:** provided technical support, guidance, and assistance with results interpretation. **Paul Hamer:** oversaw the assessment work and contributed to results interpretation. **Arni Magnusson:** performed external growth analysis. **Tom Peatman:** performed analyses on tagger effects, tag seeding, and re-weighting of length compositions. **Joe Scutt Phillips:** performed tag mixing analysis. **Graham Pilling:** performed projections and recalibration of iTRP. **Rob Scott:** performed projections and recalibration of iTRP **Tiffany Vidal** provided updated catch, effort, and length data provided by the member countries. **John Hampton:** contributed to data preparation, performed the analysis, contributed to results interpretation and the report production.

Revision 1: This revision involves various technical corrections in Section 6.1.2, Section 6.1.3, Section 11.3.3, Section 11.3.6, Section 6.1.4, Section 6.1.6, and Section 6.3.1.

Revision 2: This revision involves the status quo projections and the recalibration of the iTRP in Section 11.6. The table of references points is also updated with the ratio of $SB_{recent}/SB_{F=0}$ to the iTRP (Table 5).

Revision 3: This revision involves correcting the hyper link to the MSE shiny app in the the executive summary (Section 2) and in Section 11.6.

Contents

2 Executive Summary

This paper describes the 2025 stock assessment of skipjack tuna, *Katsuwonus pelamis*, in the western and central Pacific Ocean (WCPO). An additional three years of data were available since the previous assessment in 2022, and the model extends through to the end of 2024. The structure of the assessment was similar in most respects to recent WCPO skipjack assessments, including:

- The model was catch-conditioned, and used the same key data sources of catch, length-frequency, standardised catch-per-unit-effort (CPUE) and tagging data as used in previous WCPO skipjack assessments.
- The same 8–region model structure that was used in the 2019 and 2022 assessments.
- A quarterly time-step for the period from 1972 to 2024 for the computation of the population dynamics, with recruitment assumed to occur at the beginning of each year-quarter.
- A quarterly time-step for the specification of catch and size composition for the fisheries.
- A series of relative abundance indices based on CPUE for the Japanese pole-and-line fishery, the multi-flag free-school purse seine fishery and the Philippines small-scale purse seine fishery.
- Tag mixing assumptions for tag release groups were informed by IKAMOANA simulations (Scutt Phillips et al., 2022) to account for the fine-scale distribution of tag releases in relation to fishing effort and movement patterns estimated from the SEAPODYM model.

Key changes to the stock assessment since 2022 include:

- Natural mortality-at-age (M_{age}) was assumed to be inversely proportional to mean length-at-age (Lorenzen, 1996). The scaling of M was estimated internally.
- An orthogonal polynomial recruitment (OPR) system was used to parameterise recruitment, replacing the previously used recruitment deviations approach, in order to more efficiently parameterise recruitment variability.
- Effort creep was incorporated into the pole-and-line CPUE indices, utilising the results of Nishimoto et al. (2024).
- Not all growth parameters could be estimated internally; therefore, the von Bertalanffy growth coefficient k was fixed at 0.3 quarter^{-1} in the diagnostic case model and sampled from a uniform distribution (0.2–0.4 quarter^{-1}) in the model ensemble. All other growth parameters, including two offset parameters for age-classes 2 and 3, were estimated internally.
- The early Skipjack Survey and Assessment Programme (SSAP) tagging data was excluded from the assessment (as suggested by the 2025 PAW) in order to moderate a likely negative bias in early recruitment and resulting biomass.

- The structure of tag reporting rate groupings by fishery and tagging programme was substantially modified, in order to allow the model to estimate reporting rate parameters only where sufficient tagging data were available and to minimise the number of such estimates converging at the upper bound.

A number of smaller technical changes to the model were introduced, including:

- Longline length-frequency data were aggregated into an arbitrary time period (Q3 2000) in each region and their selectivity ungrouped to remove any potential for the data to impact trends (2025 PAW recommendation). Additionally, asymptotic constraints on selectivity with increasing size and age were removed to improve fits to these data.
- The estimated Dirichlet Multinomial parameters were estimated separately for four fishery groups (instead of the previous three) comprising pole-and-line, purse seine, miscellaneous region 5 and longline fisheries.
- Length-based selectivity was used for all fisheries.
- The selectivity and catchability parameters for all CPUE indices were ungrouped to allow improved fits to CPUE and length data.
- Time-varying CVs were used in fitting to the CPUE indices.
- The initial equilibrium population was specified in terms of an assumed small amount of fishing mortality that resulted in a stable level of spawning potential depletion over the first few years of the model period.
- Tag returns for the fisheries occurring in region 5 (Western Pacific East Asia region) were grouped for the purposes of the tag likelihood to mitigate the impacts of uncertainty in allocating many tag returns from this region to the correct fishery.
- Updates to tag seeding and tagger effects analyses were used in the treatment of tagging data and specification of reporting rate priors.
- The use of skipjack batch fecundity at size estimates (Ashida, 2020) to compute spawning potential.

A number of sensitivity analyses were used to investigate the impacts of various model settings and various sets of data, including reporting rate priors, the possibility of an increase in M-at-age for older age classes, the von Bertalanffy growth coefficient k, effort creep in pole-and-line indices, tag mixing scenarios, steepness in the stock-recruitment relationship and Indonesian catch uncertainty.

A multi-variate Monte Carlo sampling process was used to characterise uncertainty in key stock assessment metrics ($SB_{recent}/SB_{F=0}$, F_{recent}/F_{MSY} and SB_{recent}/SB_{MSY}). The factors included in the 300 model ensemble were steepness (Beta distribution with mode 0.85 and approximate limits of 0.6 and 0.99), pole-and-line index effort creep (Beta distribution of effort multipliers based

on the results of Nishimoto et al. (2024)), growth coefficient k (a uniform distribution 0.2–0.4) and tag mixing scenario (3 scenarios sampled with equal probability). Sampling was independent with respect to these factors and the ensemble was effectively weighted according to the shape of the individual distributions sampled. Of the 300 models run, 271 (90%) met the convergence criteria and were thus included in the final ensemble, from which the key stock assessment metrics were computed, including estimation error from the individual ensemble models.

We note that the main uncertainty factor affecting the stock status estimates was the tag mixing scenario used, with more optimistic metrics associated with stricter criteria for tags to be considered 'mixed'. We have provided results across all tag mixing scenarios in the main body of this report (which is our recommendation for producing management advice), and separately for individual scenarios in Section 20. Steepness was also an influential factor for the MSY-based reference points.

The general conclusions of this assessment are as follows:

- In contrast to previous assessments, recruitment is estimated to have been more variable and above average but declining slightly prior to 1990. Recruitment increased from 1990 to around 2005, after which there has been no particular trend. There is some evidence of high recruitment in recent years. The lack of a persistently increasing trend in recruitment that was estimated in previous assessments is due to the exclusion of the SSAP tagging data and the admission of effort creep in the pole-and-line CPUE indices.
- Spawning potential declined prior to about 1990 (largely in response to recruitment) but has remained relatively stable since. The ratio of fished to unfished spawning potential depletion declined gradually since the start of the model period to around 2010, after which it has been stable.
- Average fishing mortality rates for juvenile and adult age-classes increased to around 2010 and have been stable since.
- The key estimates (medians), and their 80% confidence intervals were:
  - $SB_{recent}/SB_{F=0}$ 0.51 (0.45–0.63)
  - F_{recent}/F_{MSY} 0.35 (0.24–0.45)
  - SB_{recent}/SB_{MSY} 3.90 (2.95–5.61)
- No models from the ensemble estimate the stock to be below the LRP of 20% $SB_{F=0}$.
- 2024 represents the first year of application of the skipjack interim management procedure (CMM 2022-01). The stock is on average at 98% of the recalibrated TRP (0.94 – 1.01). This is within the range expected through the MSE testing of the adopted interim skipjack MP (see MSE shiny; performance indicator: '$SB/SB_{F=0}$ relative to target').

The most notable feature of the assessment is the estimation that the stock has had fairly stable

spawning potential, spawning potential depletion and fishing mortality since around 2010. This is in contrast to the previous assessment finding that the stock is becoming increasingly depleted over time. This change appears to be driven by the removal of the long-term increasing trend in recruitment, and unfished spawning potential as a result, estimated in previous assessments. The current results are now more consistent with the recent catch history, whereby total catch increased linearly up to 2010, and has varied between 1.5 and 2 million tonnes since that time.

We believe that this assessment is a substantial improvement over the previous assessment. Model diagnostics are much improved – good convergence of 90% of models with positive definite Hessians, no parameters estimated at their bounds, no strong retrospective patterns, a very small number of high parameter correlations and improved fits to all data categories. However, there remains some level of data conflict, with the size data trying to push the population scale higher and the tagging and CPUE index data trying to constrain population scale.

Several of the key research needs identified in the 2022 assessment have been addressed, including effort creep effects on pole-and-line CPUE indices, rectifying the increasing trend in recruitment and improved model diagnostics around convergence. The remaining, and some new priorities include:

1. While not appearing to be overly sensitive to growth assumptions, the assessment could likely be improved through better information on growth and age structure. The epigenetic approach to age determination, should it be confirmed for skipjack, likely offers the best long-term solution for a better understanding of growth and age structure.

2. A better understanding of meta-population structure of skipjack, particularly focussed on improving understanding of the linkages between populations in the east Asian waters and those in the broader western and central Pacific, is still a priority area. With the 2024 record skipjack catch in both the eastern and western & central Pacific Ocean, understanding the east-west linkages across the Pacific more broadly will likely increase in importance.

3. The impact of assumed tag mixing period on the assessment is substantial. The use of finer-spatial-scale models would potentially allow less restrictive assumptions regarding tag mixing and should be a high priority for future research. As a first step, implementing an option in SEAPODYM to model tags in a release-conditioned mode (as opposed to the current recapture-conditioned approach) may provide more accurate information on skipjack abundance and fishing mortality as well as on movement. Such information could either be used directly for assessment purposes or provide the basis for informative priors in a MULTIFAN-CL model that would not then be required to model the tagging data directly. Furthermore, the external tagging analysis being explored as part of WCPFC project 123 may prove beneficial in this regard, and should continue to be supported through that project.

4. The impact of the tagging data on the assessment results is also impacted to an extent by tag reporting rate estimates and their prior distributions. It was noted that there is frequently a mismatch between the reporting rate priors and the model estimates – this is an area that

needs further investigation, e.g., in the way in which the tag seeding data are analysed.

5. Finally, further work in understanding the data conflict of the size data with CPUE and tag data is required. This should include testing of different filtering rules to enhance data quality and representativeness. Collaboration with the observer and port sampling programmes of CCMs providing these data will be essential in this work.

3 Introduction

This paper presents the 2025 stock assessment of skipjack tuna (*Katsuwonus pelamis*) in the western and central Pacific Ocean (WCPO; west of 150°W; Figure 1). Since 2000 (Bigelow et al., 2000), assessments for skipjack in the WCPO have been conducted regularly; the most recent assessments are documented in Hoyle et al. (2010); Rice et al. (2014); McKechnie et al. (2016); Vincent et al. (2019a); Castillo-Jordán et al. (2022). Consistent with previous assessments, the 2025 assessment is conducted using the MULTIFAN-CL (MFCL) stock assessment software (see MFCL for more information; Fournier et al. (1998); Hampton and Fournier (2001); Davies et al. (2025)) and continues the development of the WCPO skipjack stock assessment. Each new assessment can involve updates to fishery input data, implementation of new features in the MFCL software, and consideration of new information on biology, population structure and other important assumptions. These changes are part of ongoing efforts to improve the modelling procedures and reduce the uncertainty of estimates of stock status, fishing impacts, biological, and population processes. However, they can result in changes to the estimated historical population dynamics, status of the stock, and fishing impacts from previous assessments. Advice from the Scientific Committee (SC) on previous assessments, and the annual SPC (Pacific Community) run Pre-assessment Workshop (PAW; Hamer (2025)) guide this ongoing process. Notable new features of the 2025 assessment are summarised below and are described in the methods and supporting papers.

The objectives of this assessment are to estimate population parameters for skipjack in the WCPO, such as time series of recruitment, total biomass, spawning potential, spawning potential depletion and fishing mortality, that indicate the stock status and impacts of fishing. The outcomes of the stock assessment are used to provide a basis for management advice to the Western and Central Pacific Fisheries Commission (WCPFC). We summarize the stock status in terms of reference points adopted by the WCPFC. The methodology used for the assessment is based on the general approach of integrated modelling (Fournier and Archibald, 1982), and implements a size-based, age- and spatially-structured population model in MFCL. Model parameters are estimated by maximizing an objective function, consisting of both likelihood (data) and prior information components. The assessment uses an 'ensemble' of models as the basis for management advice. The ensemble is a suite of models that are selected to incorporate important axes of uncertainty that relate to plausible alternative biological assumptions, data inputs and/or data treatment. The variation in estimates of the key management quantities across the uncertainty grid represent the current appreciation of the uncertainty in stock status and should be considered carefully by managers.

This assessment report should be read in conjunction with several supporting papers, specifically the paper on data inputs and preparatory analyses (Teears et al., 2025; Nishimoto et al., 2025) and the papers on tag reporting rates and tagger effects estimations (Peatman et al., 2025; Peatman, 2025). Finally, the planning for this assessment was informed by the discussion at the 2025 PAW (Hamer, 2025). New features applied to this assessment, discussed in more detail in relevant sections of this paper,include:

- The application of the orthogonal polynomial recruitment parameterisation.
- The application of Lorenzen natural mortality parameterisation (Lorenzen, 1996).
- The removal of tagging data from the Skipjack Survey and Assessment Program (SSAP).
- The application of effort creep correction to the Japanese pole-and-line (JPPL) index fisheries.
- The application of length-based selectivity.
- The application of updated fecundity estimates.

4 Background

4.1 Stock structure

Skipjack tuna are widely distributed in tropical to sub-tropical waters in all the major oceans, with the populations in each ocean thought to comprise separate stocks (Wild and Hampton, 1994; Artetxe-Arrate et al., 2021).

In the Pacific Ocean, while skipjack tuna have a continuous east-west distribution (Figure 2), there is evidence from genetic and tagging studies for broad stock separation between the WCPO and the Eastern Pacific Ocean (EPO) (Grewe et al., 2019; Moore et al., 2020). In the western Pacific, warm, pole-ward-flowing currents near Japan and Australia seasonally extend the skipjack distribution to about 40°N and 40°S. These limits roughly correspond to the 20°C surface isotherm. In general, skipjack movement is highly variable and is thought to be influenced by large-scale oceanographic variability (Lehodey et al., 1997, 2008). The El Niño-Southern Oscillation (ENSO) cycle is influential on east-west distributional patterns in the equatorial region, where in La Niña phases pooling of warm waters towards the western Pacific tends to concentrate skipjack more towards the western Pacific. In the El Niño phase, skipjack are more distributed towards the central Pacific as the warm surface waters spread further to the central and eastern Pacific (Senina et al., 2016, 2025).

Finer scale population structure of skipjack in the WCPO is poorly understood, although 'meta-population' structure is thought to be present (Grewe et al., 2019; Moore et al., 2020). There is a need for further studies of meta-population structure, especially the relationships between skipjack in the east Asian waters and those in the equatorial western and central Pacific waters. Skipjack in the WCPO are considered a single but spatially partitioned stock for the purpose of this stock

assessment. Spatial structure of the assessment is based on the hypothesis and data that support sub-regional structure of population processes, the spatial structure inherent in the tagging and size composition data, and operational features of fishing fleets (Kiyofuji and Ochi, 2016).

4.2 Biology

Skipjack growth is rapid compared to yellowfin, albacore and bigeye tuna. Approximate age estimates from counting daily rings on otoliths suggest that growth may vary between areas of the Pacific. Analyses of tagging-recapture growth increments suggested that growth varies spatially in the eastern Pacific (Maunder, 2001) and the Atlantic (Gaertner et al., 2008). For the WCPO region, samples from the north Pacific region were estimated to reach approximately 40 cm fork length (FL) by 300 days age (Tanabe et al., 2003), whereas fish sampled closer to the equator, near Papua New Guinea, were estimated to reach 42 cm FL in around 150 days (Leroy, 2000). Despite these earlier studies, growth remains a significant biological uncertainty for skipjack (Ochi et al., 2016), largely because there is no method that can reliably estimate growth across their lifespan. There are no clear validated annual increment structures in skipjack otoliths and daily increments cannot be confidently interpreted beyond about 1 year of age. Ageing from spines is also not considered reliable and analysis of tag recapture growth increments is typical restricted to the portion of the growth curve that includes the sizes at which fish are large enough to be caught by hook and line, and the predominant sizes of recaptured fish by purse seine fishery (i.e., 35—60 cm FL). Tag-recapture growth analyses are also plagued by poor quality length measurement data. In this assessment we explore as a sensitivity an alternative growth model based on the analysis presented in the companion paper on skipjack growth by (Macdonald et al., 2022).

The maximum age of skipjack tuna is thought to be around 8–10 years, although most fish captured by the industrial purse seine and pole-and-line fisheries are thought to be less than 4 years old. They can reach sexual maturity by approximately 40–50 cm FL (i.e., within 6 months age) (Ashida et al., 2017; Ohashi et al., 2019) and may reach a maximum size of 90–100 cm.

Estimates of natural mortality rate (M) have previously been obtained using a size-structured tag attrition model (Hampton, 2000), which indicated that M was substantially larger for small skipjack (21–30 cm FL, M=0.8 mo^{-1}) compared to larger skipjack (51–70 cm FL, M=0.12–0.15 mo^{-1}). The longest period at liberty for a tag-recaptured skipjack to date is approximately 4.5 years.

4.3 Fisheries

Skipjack tuna comprise the largest component of the tuna fisheries throughout the WCPO and are caught using a wide variety of fishing gears. Fisheries can be broadly classified into the Japanese pole-and-line fleets (both distant-water (DW) and offshore (OS)); domestic pole-and-line fleets based in Pacific Island countries; artisanal fleets fishing a wide range of gears based in the Philippines (PH), Indonesia (ID), Vietnam (VN), and the Pacific Islands; and distant-water and Pacific Island

based industrial scale purse seine fleets that now account for most of the catch in the equatorial region of the WCPO.

The Japanese pole-and-line fleets have historically operated over a large area of the WCPO, although effort and the spatial extent of this fishery has declined substantially since the 1980's (Ducharme-Barth et al., 2022). A domestic pole-and-line fishery occurred in Papua New Guinea (PNG) from 1970 to 1985 and in Fiji since 1974, but this fishery is no longer operating. Pole and-line fishing in the Solomon Islands has occurred since 1971 but is now operating at a low level.

A variety of gear types (e.g., gillnet, hook and line, longline, purse seine, ring net, pole-and-line and unclassified gear types) capture a significant amount of skipjack in the waters around the PH, ID, and VN. Small, but locally important artisanal fisheries for skipjack and other tuna (mainly using traditional methods and trolling) also occur in many of the Pacific Islands.

The industrial purse seine fleets usually operate in equatorial waters from 10°N to 10°S; although a Japanese offshore purse seine fleet operates in the temperate North Pacific (model regions 1, 2, 3; Figure 1), and takes skipjack seasonally in smaller quantities. The distant-water fleets from Japan, Korea, Chinese Taipei, and the United States capture most of the skipjack in the WCPO, although catches by fleets flagged to or chartered by Pacific Island countries, have increased considerably in recent years. The purse seine fishery is usually classified by set type categories – sets on floating objects such as logs and fish aggregation devices (FADs), which are termed 'associated sets' and sets on free-swimming schools, termed 'unassociated sets'. These different set types can have different spatial distributions, catch per unit effort (CPUE), and size selectivity of skipjack and other tuna.

Skipjack tuna catches in the WCPO increased steadily after 1970, approximately doubling during the 1980s (Figure 3). Catches further increased during the 1980s due to growth in the international purse seine fleet, combined with increased catches by domestic fleets from ID, PH, and VN. The catch was then relatively stable during the early 1990s, approaching 1 million mt per annum. Catches increased again from the late 1990s as the purse seine fishery further developed and have varied between about 1.5 and 2 million mt since 2007, with a record catch estimated at just over 2 million mt taken in 2019.

Pole-and-line fleets, primarily Japanese, initially dominated the fishery, with their catches peaking at 380,000 mt in 1984, but the relative importance of this fishery has declined steadily over time. Historically, most of the catch has been taken from the equatorial Pacific (model regions 5, 6, 7,and 8; Figure 4, Figure 5). During the 1990s, combined annual catches from this region fluctuated around 500,000–800,000 mt before increasing sharply to approximately 1.2 million mt in 2007–2009 (Figure 4). Since the late 1990s, there has been a large increase in the purse seine fishery in the eastern equatorial region of the WCPO (Region 8, Figure 1), although catches from this region have been highly variable among years depending on the ENSO conditions (Figure 6). Catches in the central-eastern equatorial region tend to be higher in region 8 under the influence of strong El Niño conditions, which are thought to drive greater eastward displacement of skipjack (Lehodey

et al., 1997; Wang et al., 2014).

5 Data compilation

Data used in the stock assessment of skipjack tuna using MFCL consist of catch, effort and length frequencies for the fisheries defined in the analysis and tag-recapture data (Figure 2). Improvements in these data inputs are ongoing and more detailed summaries of the analyses and methods of producing the necessary input files are given by Teears et al. (2025). In general, data preparation methods for the 2025 assessment largely follow the previous assessments Vincent et al. (2019b); Teears et al. (2022).

The full details of these analyses are not repeated here, rather, a brief overview of the key features is provided and readers are directed to the relevant papers referenced throughout this section. A summary of the data available for the assessment is provided in Figure 7.

5.1 Spatial stratification

The geographical area considered in the assessment corresponds to the WCPO (from 50°N to 20°S between 120°E and 150°W) and oceanic waters adjacent to the east Asian coast (110°E between 20°N and 20°S). The eight model regions (Figure 1) were created as part of the 2019 assessment in an attempt to capture the seasonal movement dynamics and differences in size composition observed in the Japanese pole-an-line fishery in this region (Kiyofuji and Ochi, 2016; Kiyofuji et al., 2019a). Additional consideration of the region boundaries attempted to ensure there was sufficient tag releases within each region to estimate the biomass within the regions. The 8-region model was compared to the previous 5-region model structure in the 2019 assessment (Vincent et al., 2019a). SC15 preferred to use the 8-region model as the basis for management advice, although management quantities differed slightly between the two model structures. Noting it was endorsed as the preferred structure for management advice at SC15, it is maintained as the spatial structure for this assessment with one slight alteration where the lower boundary of region 5 was changed from 20°S to 10°S to ensure data from the Indian Ocean would not inadvertently be included in the assessment.

5.2 Temporal stratification

The time period covered by the assessment is 1972–2024. Within this period, data were compiled into quarters (1; Jan–Mar, 2; Apr–Jun, 3; Jul–Sep, 4; Oct–Dec). The assessment included data from the most recent full calendar year (2024), which are finalized late in the development of this assessment and may be subject to some change as they are refined. However, recent experience suggests these changes are likely to be relatively minor and not expected to be consequential for the assessment results and management advice. All data are available up until and including 2024 except for the Japanese pole-and-line CPUE that was updated through 2023.

5.3 Fisheries definitions

Extraction fisheries: MFCL requires the definition of 'fisheries' that consist of relatively homogeneous fishing units. Ideally, the defined fisheries will have selectivity and catchability characteristics that do not vary greatly over time and space, although some allowance can be made for time-series variation. For most pelagic fisheries assessments, fisheries are defined according to gear type, fishing method, region, and sometimes by vessel flag or fleet.

The extraction fishery definitions for the 2025 assessment are very similar to the 2019 and 2022 assessments, with one exception. In the previous two assessments, there were 31 fisheries defined to account for the harvest of skipjack. Specifically, in region 5 catch and length compositions from the purse seine and ring net gears from vessels flagged as PH or ID operating in their respective EEZs were combined into a common fishery. However, there were significant differences in length composition patterns between the PH and ID data, therefore, the Indonesia flagged data were separated into an additional fishery (see Table 1 for fishery descriptions).

Equatorial purse seine fishing activity was aggregated over all flags, but stratified by region and set type, in order to sufficiently capture the variability in fishing operations. Set types were grouped into 'associated' (which includes all of log, FAD, whale, dolphin, and unknown set types) and 'unassociated' (free-school) sets. A fishery for the Japanese purse seine fleet for all set types was assumed in regions 1–3. Purse seine catch in region 4 by all flags was insufficient (less than 1,000 metric tons) to warrant creating a fishery. Additional fisheries were defined for pole-and-line fisheries in each region and miscellaneous fisheries (gillnets, ringnets, handlines etc.) in the western equatorial area, mostly region 5. Catch data from the Japanese troll fishery in region 1 was combined with the pole-and-line fishery in this region. Miscellaneous gears from ID, PH, and VN were aggregated by flag, with the exception of the two fisheries created for the domestic ID and PH purse seine fleets (as described above). The catch time-series by gear and region that were input to the assessment are shown in Figure 8, Figure 9, and Figure 10.

A longline fishery was defined in each region to hold the long time series of skipjack length composition data from Japanese research longline cruises in the WCPO and more recently, observer-measured length composition samples. Longline length compositions were an important topic of discussion in the pre-assessment workshop (Hamer, 2025). Longline catches of skipjack are relatively low by comparison to other gears, and are primarily included in the assessment with logistic selectivity in order to allow other fisheries to have dome shaped selectivity. Therefore, it was recommended to aggregate these compositions into one time step to allow them to characterize selectivity while not influencing population scaling and dynamics. This suggestion was adopted and applied in the 2025 stock assessment by aggregating each longline fishery catches and length compositions to the 3^{rd} quarter of the year 2000.

CPUE indices: As was done in the previous assessment, the catch-conditioned approach (Davies et al., 2022) was applied in the 2025 stock assessment which, allows the specification of 'CPUE

indices' that are used to provide standardised indices of abundance. CPUE indices may be derived from the same fisheries as the extraction fisheries, but when used as a survey they do not take any catch. For this assessment, we have defined ten CPUE indices, six based on standardised Japanese pole-and-line CPUE (Nishimoto et al., 2025) in regions 1-4, 7 and 8, and four based on standardised purse seine CPUE in regions 5–8 (Teears et al., 2025; Nishimoto et al., 2025).

The purse seine CPUE index in region 5 is based on a generalised linear model (GLM) standardised CPUE of smaller PH based vessels that operate differently than the more industrial fleets operating in regions 6–8 for which a spatiotemporal CPUE model was developed (Table 1). These CPUE indices cover varying periods of time depending on the availability and coverage of data (Figure 7, Figure 11, and Figure 12) (Teears et al., 2025).

5.4 Catch data

Catch data were compiled by year and quarter according to the fisheries defined in Table 1. When using the catch-conditioned approach, effort data are not a necessary input and were not included in the MULTIFAN-CL input summary. See Appendix 2: *Catch and length frequency data summaries by fishery* in Teears et al. (2025) for detailed plots. The catches of all fisheries were expressed in weight of fish, with the exception of the longline fishery, the catches of which are very small and set at a nominal low level expressed in numbers of fish (i.e., 500).

Total annual catches by major gear categories for the WCPO are shown in Figure 3 and a regional breakdown is provided in Figure 4. The spatial distribution of catches over the past ten years is provided in Figure 5 and an annual spatial distribution for the past ten years for the equatorial regions in Figure 6. Discarded catches are estimated to be minor and were not included in the analysis. Quarterly catch histories provided to the model for the different fishery groupings are displayed in: pole-and-line fisheries (Figure 8), ID, PH, and VN domestic fisheries (Figure 9), and purse seine fisheries (Figure 10).

5.4.1 Purse seine

For the industrial purse seine extraction fisheries predominantly operating in regions 6, 7, and 8, catch by species within each set type (associated or unassociated) is determined by applying estimates of species composition from observer-collected samples to total catches estimated from raised logsheet data (Hampton and Williams, 2016; Peatman et al., 2023b). For the Japanese (JP) fleet for which there is greater confidence in species-based reporting, reported catch by species is used. Purse seine catch for PH and ID domestic purse seine fisheries, predominantly operating in region 5, was derived from raised port sampling data provided by these countries.

Effort data for purse seine fisheries are defined as number of sets (except for the PH and ID domestic purse seine fisheries where effort is vessel days), specified by set type (associated or unassociated). Effort is not used in the main assessment models used for management advice, it is only used

to estimate and effort-fishing mortality relationship to allow effort based projections. This step is performed on the fitted models with the other parameters fixed at there converged values. The main purse seine fisheries effort was defined as number of sets in the model and is consistent with procedures applied in management strategy evaluation and projections (SPC-OFP, 2013).

5.4.2 Longline

Longline fisheries take a negligible proportion of the total skipjack catch. These fisheries were included in the model solely to utilize the available size frequency data. Catches are set at low, arbitrary levels.

5.4.3 Pole-and-line

Pole-and-line catches are provided to SPC for the Japanese DW and OS fleets from logbook data since 1972 (Figure 8).

5.4.4 Other fisheries

Catch estimates for ID, PH, and VN fisheries are derived from various port sampling programmes dating back to before the start year of the stock assessment model (1972) for ID and the PH,and early 2000s for VN (SPC-OFP, 2024).

5.5 CPUE data

5.5.1 Purse seine

CPUE indices were created for purse seine fisheries in regions 5, 6, 7, and 8 using standardised CPUE indices developed using different approaches. In region 5 a standardised CPUE index was developed for the PH domestic purse seine fishery. In the 2022 stock assessment, the region 5 CPUE index was developed using data from the PH archipelagic waters and the high seas pocket 1 (HSP-1; Bigelow et al. (2019)). However, in the 2025 stock assessment, the fisheries data from the high seas pocket were considered to not be representative of the entirety of region 5 as the length composition patterns were progressively more variable over time. Therefore, the CPUE index in region 5 was developed using only data from the Philippines EEZ using a GLM following the methods of Bigelow et al. (2019), consistent with the 2019 and 2022 assessments. Briefly, standardised year-quarterly CPUE was estimated by removing effects due to vessel identification (fishing ground was considered but did not improve the model) and the results are shown in (Figure 12; Teears et al. (2025).

Additionally, in the previous assessment, the selectivity associated with the domestic purse seine CPUE index mirrored the selectivity with the corresponding extraction fishery. This index was developed using data from the PH EEZ and data from international waters in the high seas pocket that extends across the eastern most border where region 5 adjoins region 7. However, in the 2025 assessment, length data from the high seas pocket was evaluated and determined to be progressively

more variable over time and was not considered representative of the wider region 5. Thus, the length data corresponding to the domestic purse seine CPUE index in region 5 came exclusively from data from PH EEZ which, was considered to be more representative of region 5.

CPUE for the purse seine CPUE indices operating within regions 6, 7 and 8 were analysed based on observer data available from the Pacific Islands Regional Fisheries Observer Program since 2010. Observer data were chosen over the longer time series of logbook data due to it being considered more accurate and consistent in the approach used to estimate species composition of the purse seine catches (Hamer, 2022). As was done in the previous stock assessment, the index was developed based on unassociated sets only to remove the hyper-stability effects from FAD fishing and vessels that primarily fish on FADs during the non-closure period were removed to reduce bias from differing fishing practices. However, in the 2025 stock assessment, FAD specialists were identified over the whole time-series instead of annually (as done previously) based on recommendations from the 2025 PAW (Hamer, 2025). Therefore, the derived indices were essentially based on unassociated fishing without FAD specialists (Teears et al., 2025).

Consistent with the 2022 assessment, effort for the purse seine CPUE indices in region 6, 7, and 8 was defined as the cumulative daytime path length between unassociated sets derived using the Vessel Monitoring System (VMS). In the 2022 stock assessment, 'failed sets' (i.e., low catch of tuna, typically caused by equipment failure or entanglement) were defined as sets with ≤ 5 tonnes of total tuna, however; in the 2025 analysis, failed sets were defined as sets with ≤ 5 tonnes of skipjack. This had the effect of removing yellowfin dominated sets which are not indicative of skipjack. This change also has the effect of removing all zero catch skipjack sets.

A spatiotemporal delta generalised linear mixed model (GLMM) approach implemented in sdmTMB (Anderson et al., 2022) was used to develop the unassociated purse seine survey indices for regions 6, 7 and 8. Full details of the CPUE standardisation are in Teears et al. (2025). Briefly, an sdmTMB model with 242 spatial knots with uniform distribution was developed. Building on the previous research (Vidal et al., 2020; Teears et al., 2022), the model selection was performed using 5-fold cross validation for predictive performance which, identified six variables as influential on catch rates. Two of the variables were assumed to affect catchability but not density and these were vessel identification (as a random effect) and detection method (i.e, information from anchored FADs, bird radar, information from other vessels, marked with beacon, seen from helicopter, seen from vessel, sonar/depth sounder). The remaining three variables were assumed to affect density and were ENSO and the interaction between sea-surface temperature and chlorophyll (as spatially varying variables).

The purse seine CPUE indices in regions 6, 7, and 8 (Figure 12) are assumed to have the same catchability and are grouped to provide information on biomass scaling among those model regions. Time invariant penalty weights of 27, 15, and 23 (equivalent to coefficient of variation (CV)s of 0.27, 0.15, and 0.23, respectively) were applied to the purse seine CPUE indices in regions 6, 7, and 8, respectively. A time and space invariant penalty weight of 19 (CV of 0.19) was applied to the

region 5 pure seine index. These penalty weights/CV's were derived from the CPUE standardisation analyses. However, due to spatiotemporal heterogeneity in fishing effort, high uncertainty during instances of low sample size can go unaccounted for while modelling large areas jointly (e.g., regions 6–8 in WCPFC; see Teears et al. (2025) for further details). Therefore, for the purse seine in regions 6, 7, and 8, the time-varying and time-invariant penalty weights/CVs were derived from the region-specific models and the relative abundance estimates were derived from the global model (where regions 6, 7, and 8 were modelled jointly).

5.5.2 Pole-and-line

CPUE indices were created for the Japanese pole-and-line fisheries in regions 1, 2, 3, 4, 7, and 8. These indices were developed consistent with the spatiotemporal delta GLM approach used for the 2019 and 2022 assessments (Ducharme-Barth et al., 2019; Kinoshita et al., 2019; Teears et al., 2022), and further described in Nishimoto et al. (2025). Nominal fishing-vessel-day was used as the unit of effort for the pole-and-line CPUE indices. The spatiotemporal CPUE model was fit to the DW and OS (fishing closer to Japan) fleet data together and included spatial and environmental components.

The following information was included for the CPUE calculation: date, skipjack catches in weight, number of poles, gross registered tonnage (GRT), and vessel identity. The data were further categorized by vessel size with vessels between 20 and 199 GRT defined as OS and vessels $\geq$ 200 GRT defined as DW. The implementation of important technological innovations are available only in the DW fleet, and these are low temperature live bait tank, the first and second generations of bird radar, sonar, and onboard National Oceanic and Atmospheric Administration (NOAA) meteorological satellite image receiver.

In order to have more complete spatiotemporal coverage within the model time period and regions, the DW and OS trips were combined in the CPUE modelling following methods in Kinoshita et al. (2019) who showed that for nominal CPUE in spatiotemporal strata that were fished by both DW and OS vessels, the magnitude and trend of mean catch rates was similar. Given the joint modelling approach of the DW and OS trips, and the fact that device information were unavailable for OS vessels, device covariates were not included in the spatiotemporal model. The analysis used 260 spatial knots uniformly distributed across the spatial domain, as recommended by Ducharme-Barth et al. (2019) to improve estimation in the case of the contracting spatial coverage of the data over time. Final model configurations include number of knots, a uniform knot distribution, random effects (RE) for vessel identification, catchability covariates (number of poles, vessel class (OS, DW), vessel GRT), and density covariate sea-surface temperature (SST).

The Japanese pole-and-line CPUE indices in regions 1–4, 7, and 8 (with effort creep included; see Section 5.5.3 below) are displayed in Figure 11 and are assumed to have the same catchability and are grouped to provide information on biomass scaling among those model regions. A time invariant penalty weight of 27, 28, 18, 19, 22, and 24 (equivalent to CVs of 0.27, 0.28, 0.18, 0.19, 0.22, and

0.24, respectively) were applied to the Japanese pole-and-line CPUE indices in regions 1–4, 7, and 8, respectively. These penalty weights/CV's were derived from the CPUE standardisation analyses. Similar to the purse seine CPUE (see Purse seine), for the Japanese pole-and-line in regions 1–4, 7, and 8, the time-varying and time-invariant penalty weights/CVs were derived from the bi-regionally grouped models (i.e., region 1 with 2, 3 with 4, 7 with 8) while the relative abundance estimates were derived from the global model (i.e., all regions modelled jointly).

As was done in the 2022 stock assessment, the Japanese pole-and-line in region 8 was truncated to remove all estimates before 1975 and after 1997 due to inadequate spatiotemporal coverage (see Teears et al. (2022) for further details). Similarly, the Japanese pole-and-line in region 7 was truncated to not include estimates after 2009 since the purse seine CPUE index in region 7 begins in 2010.

5.5.3 Application of effort creep to survey indices

CPUE indices can be affected by gradual (Palomares and Pauly, 2019) and/or abrupt (Matsubara et al., 2022) increases in capture effectiveness per unit of effort (referred to hereafter as 'effort creep'; e.g., increased use and/or effectiveness of technology over time). This has potential to influence rates of harvest per unit of effort (i.e., catchability) and the purse seine fisheries in regions 6, 7, and 8, are likely subject to some level of effort creep. However, the rates and dynamics of such effectiveness changes over time are unclear. Developing purse seine indices based on unassociated fishing removes confounding factors for effort creep related to the use of technologies such as FADs with satellite/sonar buoys and their sophisticated associated software.

Purse seiners make a set only after a substantial school of tuna has been identified and so the bulk of the effort involved in catching free-swimming schools of skipjack by purse seiners is in the searching to find schools of skipjack to set on. As such, free-school indices using the cumulative daytime path length between sets as an effort metric would be less prone to hyper-stability than using set as the metric of effort. While technology can also influence searching efficiency, the inclusion of vessel identification and detection method help to standardise out differences in catchability adopted by individual vessels. Furthermore, the purse seine indices are only calculated from 2010, so any effectiveness changes are expected to be of minimal influence on the trend in the index as most modern searching technologies such as sonar, bird radars, etc... were implemented by the purse seine fishery prior to 2010.

Pole-and-line fisheries also exhibit effort creep as Matsubara et al. (2022) demonstrated using the Japanese pole-and-line data to show the temporal uptake of fishing technology (Figure 13). Furthermore, Nishimoto et al. (2024) quantified the change in catchability over time due to technological progress in the Japanese pole-and-line fishery. For this assessment, we applied an increase in effectiveness of the effort metric for the Japanese pole-and-line CPUE indices using the median estimated change in catchability over time (Figure 13) from the Gompertz parameterisation indicated in Nishimoto et al. (2024). The resulting normalised effort multiplier is shown in Figure 13.

5.6 Size data

5.6.1 Purse seine

Only length frequency data (fork length (FL) in 2 cm bins) are used in the skipjack assessment. Length frequency data available for the 2025 assessment are summarised in Teears et al. (2025). The purse seine length frequency data are derived from long-term port sampling of primarily US purse seiners in Pago Pago, and samples taken at sea by observers corrected for grab-sample bias (Lawson, 2011). Size data are available for both associated and unassociated set types (Figure 14), with sample numbers for most fisheries increasing from the early 2000s (Teears et al., 2025). Sample numbers increased greatly in region 5 from 2010 onwards due to increased sampling of the PH and ID purse seine fisheries under improved port sampling programmes.

In the previous assessment, length compositions from the domestic purse seine and ring net gears in region 5 from vessels flagged as PH or ID operating in their respective EEZs were combined into a common fishery. However, there were significant differences in length composition patterns between the PH and ID therefore, the ID flagged data was separated into an additional fishery (Table 1; Teears et al. (2025)).

5.6.2 Pole-and-line

Size composition data for pole-and-line fisheries primarily come from port samples or tagging cruises, with the exception of regions 1, 2, 3, 4, and 7 where length data are available from the Japanese offshore and distant-water fleets from the beginning of the model period until 2024 (Teears et al., 2025). These data are derived from port sampling and sampling onboard research and training vessels. The length frequency for the Japanese pole-and-line fishery in the database held by SPC were revised in 2019 based on the methods described in Kiyofuji et al. (2019b). Length data for the equatorial pole-and-line fisheries are available from both the Japanese distant-water fleet and domestic fleets.

The data from the pole-and-line fishery in region 8 are dominated by data for the Japanese fleets (1974–2004) with additional data from Fiji in the 1990s. Length data from the pole-and-line fishery in region 5 were filtered to only include data from ID because it constituted the majority of the catch. The data from the pole-and-line fishery in region 6 are a large dataset from multiple countries with the Solomon Island and PNG contributing the majority of the length composition samples. The pole-and-line fisheries in the northern regions generally catch smaller fish than the equatorial fisheries in regions 5–8, although over the model period, there is a slight increase in the length of fish sampled from the pole-and-line fisheries in the four northern regions, with a substantial change in region 3 during the early 2000s (Teears et al., 2025). The region 5 length compositions indicated smaller fish caught after 2010 compared to the data prior to 2000. No systematic trends in the length composition were evident in regions 6–8.

5.6.3 Longline

Longline fisheries typically do not target skipjack but do catch small numbers of larger skipjack within the 50–90 cm FL range as by-catch, that are usually discarded. Japanese research vessels have routinely collected measurements of the length of skipjack caught by longline since the start of the assessment time period. Japanese research data are only available sporadically in several regions and sample sizes have decreased or ceased to exist in areas where Japanese longline fishery effort has declined. From the 2019 stock assessment, data for other flags conducting longline fishing have been added to these fisheries, resulting in substantial increases in sample size and temporal coverage. Most of these samples were collected by observer programs (since the 2000s).

Longline catches are primarily included in the assessment with logistic selectivity in order to allow other fisheries to have dome shaped selectivity. This provides the assessment model important information regarding the presence of larger-sized skipjack that are not typically caught by the purse seine and pole-and-line surface fisheries. Without this information, the model would have difficulty estimating this "cryptic biomass" component of the population. Longline length compositions were an important point of discussion in the pre-assessment workshop (Hamer, 2025). It was recommended to aggregate these compositions into one time-step to allow them to characterize selectivity while not influencing population scaling and dynamics. This suggestion was adopted and applied in the 2025 stock assessment.

5.6.4 Other fisheries

Size composition data for the PH domestic fisheries were collected by a sampling program conducted in the PH in 1993–1995 and augmented with data from the 1980s. In addition, data collected during 1997–2006 under the National Stock Assessment Project (NSAP), and in more recent years under the various West Pacific East Asia (WPEA) projects, were included in the current assessment. The ID domestic fishery is given its own selectivity function as a result of the addition of data from the large number of measurements from recent sampling under the WPEA project. Similarly, length data for the VN domestic fishery has increased substantially in recent years and is given a separate selectivity in the model (Table 1).

5.7 Reweighting of the size composition data

Statistical correction of size composition data is required as length samples are often collected unevenly in space and time. The methods for reweighting of the size composition data are detailed in Teears et al. (2025). For the extraction fisheries, reweighting of composition data is required to ensure that sampling biases in space, time, and the fleets providing data, are minimised so that size composition data better reflect the composition of the overall removals. Strata-specific size data samples are therefore reweighted by catch for the extraction fisheries based on the approach used for the 2023 bigeye and yellowfin assessments for extraction fisheries (Peatman et al., 2023a). For the CPUE indices, reweighting of composition data is required to ensure that the size composition

of the CPUE indices reflect the size component of the population that is being sampled by the index fisheries through time. Strata specific samples are therefore reweighted by relative abundance using the standardised CPUE following the approach used for the 2022 skipjack assessment for CPUE indices (Teears et al., 2022). A summary of length sample coverage across time for the fishery/region groups is provided in Figure 14.

5.8 Tagging data

A large amount of tagging data is available for incorporation into the assessment. The treatment of the tagging data for this assessment followed the methods described in Vincent et al. (2019b) and is further summarised in Teears et al. (2025). The data were available from SPC's Skipjack Survey and Assessment Program (SSAP) carried out during 1977–1980, the Regional Tuna Tagging Project (RTTP) during 1989–1992 (including affiliated in-country projects in the Solomon Islands, Kiribati, Fiji and the Philippines), and the Pacific Tuna Tagging Program (PTTP) which has been ongoing since 2006 with the most recent tagging data included in the assessment from the Central Pacific 16 (CP16) tagging cruise in 2023 (Figure 2 and Figure 15). Data from the SSAP were used in previous assessments but, based on suggestions from the pre-assessment workshop (Hamer, 2025), this tagging data was not included in the 2025 stock assessment due to concerns with representativeness and appropriate mixing periods. Tags were released using standard tuna tagging equipment and techniques by trained scientists and technicians. Tags have been returned mostly from purse seine vessels via processing and unloading facilities throughout the Asia-Pacific region.

Tagging data from regular Japanese research tagging cruises were available for the period 1989–2024 (Figure 2 and Figure 15). Assessments prior to the 2019 assessment did not use Japanese programme tag releases prior to 1998 because the tag releases were not measured at the time of tagging. However, for the 2019 assessment these earlier data were included with release lengths estimated by sampling from the available measured release lengths from the Japanese tagging program (Vincent et al., 2019b). The same approach was used for the 2022 and 2025 stock assessments.

As in recent tropical tuna assessments, the numbers of tag releases were adjusted for a number of sources of tag data reduction such as unusable recaptures due to a lack of adequately resolved recapture data, estimates of tag loss (shedding and initial mortality) due to variable skill of taggers, and estimates of base levels of tag shedding/tag mortality, in combination referred to as 'tagger effects'. The procedures used in re-scaling the releases for tagger effects are described in detail in Peatman et al. (2025). Essentially, the re-scaling preserves the recovery rates of tags from the individual tag groups that would otherwise be biased low when an often significant proportion of recaptures cannot be assigned to a recapture category in the assessment.

There is a delay between tagged fish being caught, the tag being reported, and the data being entered into the tagging database. If this delay is significant then reported recapture rates for very recent release events will be biased low and will impact estimates of fishing mortality in the terminal

time periods of the assessment. For the Japanese tagging program, tags are generally returned more promptly; thus it was possible to include tag releases to the end of 2022 in the assessment. For the PTTP, efforts have been made to improve the timeliness of tag recaptures being reported to SPC and the validation of recaptures. This has meant that tag releases up to and including the 2022 CP16 tagging cruise can be used in this assessment, with recapture data included up to 2024 for the Japanese tagging programme and the PTTP.

For incorporation into the assessment, tag releases were stratified by release region, year/quarter of release, and length at release using the same size bins as the length-frequency data. Tag release events that had less than 30 tags released per event were removed from the analysis to reduce the computational load otherwise created by the many small release events, and allow for better model convergence.

Since the 2022 skipjack stock assessment, improvements have been made to the tagging database as well as increased filtering (as recommended at the 2025 pre-assessment workshop, Hamer (2025)) of tagging data to increase the quality of the resulting tagging data inputs and subsequent stock assessment results (see Teears et al. (2025) for more details). The final tagging input file has 14 fewer release groups than the 2022 assessment (largely due to removal of SSAP data) with a total of 289,627 effective releases classified into 314 tag release groups. The returns from each size-class of each tag release group (57,809 total usable tag returns; Table 2) were then classified by recapture fishery and time period (quarter). A summary of tags recaptured by release and recapture regions is presented in Figure 15. Tag return data were aggregated (for the purpose of the tagging data likelihood) across set types for the purse seine fisheries in each region because tag returns by purse seiners were often not accompanied by information concerning the set type. Likewise, the tag returns reported from the Indonesian and Philippines fisheries in region 5 were frequently difficult to allocate to the specific fisheries. Therefore, these returns were also aggregated internally in the model to a group consisting of these fisheries.

6 Model description

The model comprises of several components, (i) the dynamics of the fish population; (ii) the fishery dynamics; (iii) the observation models for the data; (iv) the parameter estimation procedure; (v) the uncertainty estimation procedure (both parameter and model uncertainty); and (vi) stock assessment interpretations. Detailed technical descriptions of components (i)–(iv) are given in Hampton and Fournier (2001) and Davies et al. (2025). In addition, we describe the procedures followed for estimating the parameters of the model, the uncertainty, and the way in which stock assessment conclusions are drawn using a series of reference points. In this section, model settings primarily refer to those used within the 'diagnostic case' model. Some of these settings are later varied in sensitivity analyses.

6.1 Population dynamics

The model partitions the population into eight spatial regions and 16 quarterly age-classes. The last age-class comprises a 'plus group' in which mortality and other vital rates are assumed to be constant. The population is 'monitored' in the model at quarterly time steps, extending through a time window of 1972–2024. The main population dynamics processes are as follows.

6.1.1 Recruitment

Recruitment is defined as the appearance of age-class 1 quarter fish (i.e., fish averaging ∼23cm given the current diagnostic model growth curve) in the population. Tropical tuna spawning does not generally follow a clear seasonal pattern but occurs sporadically when food supplies are plentiful (Itano, 2000). The assessment model assumed that recruitment occurs instantaneously at the beginning of each quarter. This is a discrete approximation to continuous recruitment, but provides sufficient flexibility to allow a range of variability to be incorporated into the estimates as appropriate.

In previous assessments, recruitment was estimated using recruitment deviates as year-quarter and region-specific deviates from the mean recruitment (referred to as 'Rec-Devs'). The 2022 skipjack assessment consisted of 1,809 parameters (of 2,010 in total) relating to recruitment – 1 for each year/season/region (some constrained by sum-to-zero conditions). There has been a long-standing concern that the Rec-Devs approach poses a risk of over-parameterisation, with resulting poor statistical performance, including difficulties with convergence. To address these concerns, MFCL has an orthogonal polynomial recruitment (OPR) feature in which:

- A linear hierarchical structure for year, region, season, and region-season interaction levels is implemented using a Gram-Schmidt orthogonalisation basis matrix;
- A user-specified number of degrees is estimated for each of the four levels to control the extent of time-series variation; and
- A common effect can be used for a specified number of terminal years of a specified level.

The system gives a large degree of user control over recruitment variability, ranging from the simplest (constant total recruitment by year equally allocated to seasons and regions – 1 parameter) to a 'fully saturated' system equivalent to the Rec-Devs approach (1600 parameters).

As reported to the 2025 PAW, we undertook an extensive comparison (using AIC) of many alternative OPR structures using the 2022 assessment data. The conclusions of that analysis were that:

- A close to fully saturated year effect (1 parameter per year) was optimal;
- A single average seasonal effect (i.e. the overall seasonal distribution of recruitment is constant over time) was optimal;

- A regional effect varying over time with a 10^{th} order polynomial (i.e. the way the overall annual regional distribution varies over time); and
- A close to fully saturated region-season interaction, allowing flexibility in the variation of the seasonal distribution by region and the regional distribution by season over year, was optimal.

Initial application of this approach to the 2025 assessment data estimated unrealistically high recruitments towards the end of the time series (this also occurred to an even greater extent with the Rec-Devs version). To control this, we set a common recruitment pattern for the terminal 3 years of the assessment. This resulted in 1,195 recruitment parameters being estimated. This is a considerable reduction from the 1,696 parameters that would be required to be estimated under the Rec-Devs approach. The recruitment pattern (Figure 16, Figure 17) and other stock-assessment related quantities estimated using the Rec-Devs and OPR approaches were very similar.

Spatially-aggregated recruitment was assumed to have a weak relationship (CV of log-recruitment deviates set to 0.707) with total spawning potential in the preceding quarter, according to a Beverton and Holt stock-recruitment relationship (SRR) with a fixed value of steepness (h). Steepness is defined as the ratio of the equilibrium recruitment produced by 20% of the equilibrium unexploited spawning potential to that produced by the equilibrium unexploited spawning potential (Francis, 1992; Harley, 2011). As has been the practice in other tuna stock assessments, (h) was fixed at 0.80 in the diagnostic model. The SRR was estimated over the period 1984–2020 to prevent the earlier recruitments, which appear to be part of a less productive recruitment regime, from influencing the relationship.

6.1.2 Initial population

The initial equilibrium population was assumed to be lightly exploited, arising from a small amount (2% of the natural mortality) of pre-existing fishing mortality. The value of 2% was determined by trial and error so as to result in a stable level of spawning potential depletion over the first few years of the model period.

6.1.3 Growth

The standard assumptions made concerning age and growth are (i) the lengths-at-age are normally distributed for each age-class; (ii) the mean lengths-at-age follow a von Bertalanffy growth curve; (iii) the standard deviations of length for each age-class are a log-linear function of the mean lengths-at-age; and (iv) the probability distributions of weights-at-age are a deterministic function of the lengths-at-age and a specified weight-length relationship. These processes are assumed to be regionally invariant.

During model development for this assessment, it became apparent that, unlike for the 2022 assessment, estimating growth internally in the assessment model was not feasible. We found that the von Bertalanffy growth coefficient k was being estimated at a high value, hitting successively higher

upper bounds settings. This was likely caused by an interaction of the growth and Lorenzen shape of the M-at-age. The higher estimates of k were improving primarily the tagging data likelihood, seemingly because the tagging data favour high tag attrition of the early age classes. This can be most easily facilitated in the model estimation though a rapidly declining M for the first few age classes, which in turn is facilitated by a rapidly increasing mean length for those initial age classes. The latter is provided for by having a high value of k. We felt that it was somewhat perverse for k to be impacted in this way, and therefore opted to constrain the growth curve by fixing k at a value of 0.3 q^{-1} for the diagnostic case model. A range of fixed k was explored in a sensitivity analysis (Section 11.5.3) and in the model ensemble (see Section 11.6). The remaining growth parameters, the mean lengths of the first and last age classes and the two parameters required to parameterise the variability in length-at-age, continued to be estimated. In the process of exploring growth options, it also became apparent that model behaviour, in particular obtaining good convergence properties, was enhanced by allowing deviations in mean length at age for age classes 2 and 3, so those 'offset' parameters were also estimated in all models.

We also investigated the possibility of applying an externally estimated growth curve for skipjack, as was done in the 2022 assessment. This approach used data from daily otolith ageing (Leroy, 2000; Aoki et al., 2024) and growth increment data from tag recaptures, in a joint likelihood estimation of the standard von Bertalanffy growth parameters using the Schnute (1981) parameterisation. Use of this growth curve in the assessment model however was problematic, as the relatively low estimate of mean length of the oldest age class did not enable acceptable fits to the longline size data. Therefore, we did not pursue use of an external growth curve in this assessment.

6.1.4 Movement

Movement was assumed to occur instantaneously at the beginning of each quarter. Parameters were estimated for regions that shared a common boundary, but fish can move between non-contiguous regions in a single time step due to the 'implicit transition' computational algorithm employed (see Hampton and Fournier (2001) and Davies et al. (2025) for details). Movement can also be re-cast as the proportion of fish in a given region that move to the adjacent region. Across each regional boundary in the model, movement is possible in both directions for the four quarters. As was done in 2019 and 2022 assessments, movement was assumed to be constant across ages for this assessment because the increased number of parameters does not yield sufficient improvement in model fit to the data to warrant their inclusion (Vincent et al., 2019a; Castillo-Jordán et al., 2022). The seasonal pattern of movement persists from year to year with no allowance for inter annual variation in movement. A prior mean of 0 was assumed for all movement coefficients, but the penalty was weak for deviations from the mean. Starting parameter estimates for the movement coefficients were specified based on the proportion of tags returned within each region and quarter relative to total tags returned for releases in the same region.

6.1.5 Natural mortality

The Center for the Advancement of Population Assessment Methodology (CAPAM) at the 2023 'Tuna Stock Assessment Good Practices Workshop' recommended applying an age-specific pattern in M by using the inverse mean length-at-age method developed by Lorenzen (1996). In MFCL, the asymptotic (lower) level of natural mortality for the Lorenzen function (at the oldest ages) can be estimated while holding the 'shape' parameter constant. Following the CAPAM Workshop advice, we allowed M-at-age to be inversely proportional to mean length-at-age following Lorenzen (1996) with the asymptotic scale of M estimated within the MFCL model and was assumed to be invariant over time and region.

6.1.6 Sexual maturity/fecundity

Age-specific sexual maturity was computed internally from a specified maturity-at-length ogive and the growth parameters. Recently, research was done by the Japan Fisheries Research and Education Agency (FRA) to estimate reproductive traits, including fecundity (Ohashi et al., 2019). Samples were analysed from temperate, subtropical and tropical areas. The majority of the skipjack population is believed to occur in the tropical region; therefore, the maturity-at-length ogive for skipjack sampled only from tropical waters was modelled as:

$$P_l = 1/(1 + exp(7.414 - 0.148FL)) \tag{1}$$

where the proportion mature (P) for each length bin (l; centered in each bin) was calculated based on fork length (FL) using Equation 1.

Unlike *Thunnus* species, the sex ratio for skipjack does not appear to vary with size and is believed to be 50:50 between sexes. Therefore no adjustment to the maturity ogive was necessary to reflect the proportion of females by length.

In previous skipjack assessments, it had been assumed that spawning potential of mature skipjack was proportional to their body weight. However, Ohashi et al. (2019) found that skipjack batch fecundity per unit of body weight increased with increasing size. Therefore, for this assessment we incorporated this body weight dependency into the maturity ogive, which shifts the maturity ogive to the right (Figure 32).

MFCL estimates the reproductive potential at age internally (using the model growth parameters) from the externally calculated reproductive potential ogive at length using a smooth-spline approximation (Davies et al., 2019). This allows for a more natural definition of reproductive potential as the product of three length-based processes: proportion females-at-length (sex-ratio; assumed to be 50:50), proportion of females mature-at-length (from Ohashi et al. (2019); Figure 32), and the fecundity-at-length (from Japan FRA estimates) of mature females.

6.2 Fishery dynamics

6.2.1 Selectivity

Selectivity is often modelled as a functional relationship with age to reduce the number of parameters estimated within the stock assessment model. Examples include a logistic curve to model monotonically increasing selectivity and various dome-shaped curves to model fisheries that select neither the youngest nor oldest fish. Modelling selectivity with separate age-specific coefficients (ranging from 0–1), constrained with smoothing penalties, allows more flexibility but has the disadvantage of requiring more parameters. Instead, we have used a method based on a cubic spline interpolation. This is a form of smoothing, but the number of parameters for each fishery is the number of spline 'nodes' that are deemed to be sufficient to characterize selectivity over the age range. The number of nodes varied by fishery and were selected because they provided an improvement in Akaike Information Criterion (AIC), increased model stability by reducing the number of parameters, or removed unreasonable patterns in the selectivity-at-age.

In the 2022 stock assessment, selectivity was modelled using an age-based functional form however, in the 2025 stock assessment, selectivity was modelled using the length-based form as recommended by Punt et al. (2023) to assume length-based selectivity unless it is known to be age-based (e.g., due to ontogenetic movement).

In MFCL, a single selectivity function could be 'shared' among a group of fisheries that have similar length compositions or were assumed to operate in a similar manner to reduce parameters or share information where data is lacking. In the 2022 stock assessment, some extraction fishery selectivities were grouped based on similarities (e.g., Japanese pole-and-line fisheries, equatorial purse seine fisheries). However, in the 2025 stock assessment, all extraction fishery selectivities were assumed to be time-invariant and fishery-specific to allow for differences in availability among fisheries due to spatial heterogeneity of the population. All selectivities were modelled with splines with the number of nodes and selectivity groupings indicated in Table 1. Japanese pole-and-line CPUE indices were assumed to share selectivity as was the equatorial purse seine CPUE indices in regions 6–8 until the latter phases of the estimation. Then, the groupings were removed to allow improved fit to the CPUE indices' length data and release the estimation of regional scaling that is primarily determined by CPUE indices while they are grouped.

6.3 Dynamics of tagged fish

Tagged fish are modelled as discrete cohorts based on the region, year, quarter, and length at release for the first 12 quarters after release. The tags released are assigned to a quarterly age bin according to the length at release and the estimated growth curve and its associated standard deviations. Subsequently, the tagged fish are pooled into a common release group in order to limit memory and computational requirements. Additionally, tag returns can also be grouped within MFCL to accommodate situations where recaptured tags lack adequate information to assign to

a specific fishery but can be assigned to one of several fisheries (e.g., purse seine associated or unassociated). The tag return groupings are shown in Table 1.

6.3.1 Tag reporting

In this assessment as in 2022, we continued to structure tag reporting rates by the three main tag-release programs included in the assessment – the RTTP, the PFRP and the JPTP – and by recapture fishery or fishery group (see Table 2 for grouping of reporting rates). In theory, tag-reporting rates can be estimated internally within the stock assessment model. In practice, experience has shown that independent information on tag-reporting rates for at least some fisheries tends to be required for reasonably precise estimates to be obtained. Also, some reasonable number of tag returns by a release program/fishery group is required to sustain a reporting rate estimate. We chose 5 tag returns as a cut-off and for any release program/fishery groups with fewer than 5 recaptures, we removed those recaptures from the tagging data and set the reporting rate to be zero. For release program/fishery groups for which reporting rates were being estimated, priors that reflect independent estimates based on tag seeding experiments (Peatman, 2025), or in some cases expert opinion, were specified. For the RTTP and PTTP purse seine fisheries in equatorial regions 6, 7 and 8, relatively informative priors were formulated given the larger extent of tag seeding information available. For the Japan tagging program (JPTP) moderately informative reporting rates for the Japanese pole-and-line and purse seine fisheries in the northern regions were provided by Japanese scientists familiar with tag recovery processes in Japan. For most other fisheries, uninformative priors were specified (see Section 18 for more details).

6.3.2 Tag mixing

The population dynamics of the fully recruited tagged and untagged populations are governed by the same model structures and parameters. Implicitly, we assume that the probability of recapturing a given tagged fish is the same as the probability of catching any given untagged fish in the same region and time period. For this assumption to be valid, either the distribution of fishing effort must be random with respect to tagged and untagged fish and/or the tagged fish must be randomly mixed with the untagged fish. The former condition is unlikely to be met because fishing effort is almost never randomly distributed in space. The second condition can only be met if sufficient time for mixing has transpired.

Depending on the distribution of fishing effort in relation to tag release sites, the probability of recapture of tagged fish soon after release may be different to that for the untagged fish. Thus, it is desirable to designate an appropriate number of time periods after release as 'pre-mixed' and compute fishing mortality for the tagged fish based on the actual recaptures, corrected for tag reporting and tagging effects, rather than use fishing mortalities based on the general population parameters. This, in effect, desensitizes the likelihood function to tag recaptures in the specified pre-mixed periods while correctly removing fish from the tagged population that is present after

the pre-mixed period.

For the 2022 assessment, variable mixing periods were implemented, for the first time, based on tag mixing simulations by Scutt Phillips et al. (2022). The approach simulated mixing periods specifically for each release group, taking into account the unique locational and temporal (environmental, fishing effort) contexts of each release event constituting the group that may result in different rates of mixing of released fish. It applies an individual based Lagrangian model (Ikamoana) (Scutt Phillips et al., 2018) to track movement of individual fish (particles) and quantify the fishing pressure that individuals experience across their dispersal trajectories. Ikamoana uses the forcings and parameters such as fishing mortality, growth, and natural mortality that have been estimated from real data by the Eulerian model SEAPODYM (Lehodey et al., 2008; Senina et al., 2020, 2025). The individual based modelling approach simulates post-tagging movement and probability of capture for all individual tagged fish in a release group while also simulating the broader untagged population as the simulated 'truth' with which to compare fishing pressure to the tagged groups. The key results from the individual simulations are trajectories of survival and capture probabilities that can be compared between tagged and untagged populations. By comparing distributions of capture probabilities for the tagged and untagged fish it is possible to use criteria to estimate at what period after release, fish from particular tagging events are experiencing sufficiently similar fishing mortality as the untagged fish for particular model regions to be considered to be well mixed.

The simulation studies provided summary distributions of recapture probability after increasing time-at-liberty from an assumed mixing period for both the tagged fish and the untagged population. By comparing the distributions of final recapture probability for individual release events assuming different mixing periods, i.e., 0, 1, 2, and 3 quarters after release, it is possible to make a judgement on whether the tagged fish are likely to be mixed (i.e., have sufficiently similar probability of recapture as the untagged population). For determining what constitutes sufficiently mixed we calculated the dissimilarity statistic (based on Kolmogorov dissimilarity K metric, referred in the 2022 assessment as the D statistic, but herein now referred to as K) to indicate the degree of similarity between the distributions of recapture probability for the tagged and the untagged (reference) population.

Median values of K were used to determine the earliest possible mixing period to be assigned to each release group in MFCL, using cut-off values of $K = 0.1$, 0.2, and 0.3 as alternatives for the uncertainty characterisation. The K of 0.1 results in generally requiring a longer mixing period than 0.2, which assumes a longer mixing period than 0.3. Hence the lower the K, the more conservative the mixing period assumption. A more conservative K statistic of 0.1 also results in only 8.3% of the total recaptures to be considered mixed and subsequently, included in the MFCL likelihood function (Figure 20; see Teears et al. (2025) for further details). Whereas a much less conservative K statistic of 0.3 results in 53.2% of the total recaptures to be considered mixed. An intermediate K statistic of 0.2 would result in 31.0% of the total recaptures to be considered mixed and thus, permitted to inform the MFCL model parameters.

The tagging data are very influential on parameter estimation and removing tagging data from the model can have notable impacts on estimation. Because there is some subjectivity in deciding the K value to apply, we included the mixing periods for the three K values as an axis in the uncertainty characterisation for this assessment, and for the diagnostic model apply the K value of 0.2.

The simulations were computationally demanding and, as such, not all release groups could be simulated from the tagging program data sets. Thus, various release groups from the PTTP and the JPTP were selected to be simulated to maximize the spatial coverage and the number of releases simulated. RTTP release groups (n=29) were not simulated and were assigned the region specific median estimates from the PTTP. There were 9 (of 49) PTTP release groups that were not simulated and were assigned the PTTP region-specific median estimates and there were 130 (of 236) JPTP release groups that were not simulated and were assigned the JPTP region-specific median mixing period calculated from simulated release groups. Resulting mixing periods of 0 quarters were not considered plausible and assigned a mixing period of 1 quarter. Similarly, resulting mixing periods of more than 4 quarters were assigned a mixing period of 4 quarters.

6.4 Likelihood components

There are three data components that contribute to the log-likelihood function for the skipjack stock assessment – the CPUE data, the length-frequency data, and the tagging data.

6.4.1 CPUE likelihood

In catch-conditioned models, CPUE indices differ from the regular extraction fisheries in that no catch is extracted and CPUE is modelled directly as a log-normal likelihood contribution. The contribution of each observation to the log likelihood is made up of time-varying CVs and a generic component, or scaled CV. The time-varying CVs are input from the standardisation models (Teears et al., 2025; Nishimoto et al., 2025) where each region was modelled separately (or small groups of regions – for Japanese pole-and-line regions 1 with 2, 3 with 4, and 7 with 8) with year-specific relative abundance input from the global models (where regions were modelled jointly). The generic CVs were derived from overall standard error from each region-specific standardisation model.

CPUE indices may be grouped if it is felt that the CPUE reflects differences in average abundance among regions. For this assessment, the pole-and-line CPUE indices were grouped, as are the purse seine CPUE indices in regions 6–8. This grouping allows the CPUE to inform regional as well as temporal abundance changes. However, this grouping was only applied in earlier phases of the MFCL estimation, CPUE likelihoods (and selectivity) were grouped to provide regional scaling information via the regional difference in scale from the resulting standardised relative abundance estimates. Then in the last estimation phase, the CPUE indices were ungrouped to improve the fits to the CPUE indices while also allowing regional scaling to be informed from other data sources.

6.4.2 Length frequency: Dirichlet-multinomial likelihood

In the 2025 stock assessment, we have implemented a Dirichlet multinomial (DM) likelihood for the length frequency data. Our implementation is similar to the DM implementation in Stock Synthesis (Thorson et al., 2017), which has been shown to be capable of estimating effective sample size (ESS) for compositional data and performs similarly to iterative re-weighting methods. In the MFCL implementation, two categories of parameter are estimated – an exponent for an ESS multiplier and an exponent for a sample size covariate. The ESS multiplier parameter estimates the relationship between the observed sample size (OSS) and ESS. With thousands of length-frequency samples in the model, it is obviously not feasible to estimate this parameter independently for each sample. Therefore, we estimate a sample size covariate parameter, which defines how ESS varies with OSS within a fishery, or group of fisheries. This keeps the parameter estimation tractable, with just two parameters estimated for each fishery, or group of fisheries.

In the 2022 stock assessment, three fishery groups were defined for the estimation of DM parameters according to gear type – large purse seine and pole-and-line, longline, and the small-fish miscellaneous gear fisheries in Indonesia, Philippines and Vietnam. The estimated relationships between OSS and ESS for these three fishery groups are shown in Figure 21. In early explorations of the 2025 stock assessment model, we explored the use of 4 DM groups where the large purse seine fisheries were separated from the pole-and-line fisheries (Figure 21) and another parameterisation where all the fisheries (a total of 41 fisheries at the time of exploration) were separated into their own DM groups.

The results indicated, as expected, that likelihood components were improved by the increase in the number of DM parameters (Table 3). There were slight differences in management quantities of interest between groups of 3 and 4 (Figure 22) however, estimating individual DM parameters for each fishery showed no differences in model outputs. Therefore, expanding out to 4 gear-specific DM groups was judged to be sufficient without the unnecessarily large increase in number of parameters required to provide each fishery with separate DM parameters. The relationships between OSS and ESS for the four-group model are also shown in Figure 21.

6.4.3 Tagging data

A log-likelihood component for the tag data was computed using a negative binomial distribution. The negative binomial is preferred over the more commonly used Poisson distribution because tagging data often exhibit more variability than can be attributed by the Poisson. We have employed a parameterisation of the overdispersion parameter (τ) such that as it approaches 1, the negative binomial approaches the Poisson. Therefore, if the tag return data show high variability (for example, due to non-independence of tags), then the negative binomial is able to provide an improved fit to data with higher variability than a Poisson distribution. Examples of this effect are shown in Figure 23. This should then provide a more realistic weighting of the tag return data in the overall log-likelihood and allow the variability in tag returns to impact the confidence intervals of

estimated parameters. Therefore, we allowed the overdispersion parameter (τ) to be estimated by the assessment model. A complete derivation and description of the negative binomial likelihood function for tagging data is provided in Davies et al. (2025).

6.4.4 Parameter and uncertainty estimation

The parameters of the model were estimated by maximizing the log-likelihood of all data components plus the log of the probability density functions of the penalties specified in the model. The maximisation to a point of model convergence was performed by an efficient optimisation using exact derivatives with respect to the model parameters (auto-differentiation, Fournier et al. (2012)). Estimation was conducted in a series of phases, the first of which used relatively arbitrary starting values for most parameters. A bash shell script, 'doitall' file (see Appendix 1: Doitall file for diagnostic case model doitall file), implements the phased procedure for fitting the model. After obtaining a converged model, the Hessian matrix was computed and its positive definite status verified by the absence of negative eigenvalues. Then, the estimation errors for the important stock assessment related dependent variables (including time series of recruitment, spawning potential (SB), dynamic depletion, and MSY-based reference points) were computed using the Delta method.

7 Diagnostics methods

As has been suggested in Carvalho et al. (2017) and Carvalho et al. (2021), diagnostic tools are vital for evaluating the quality of integrated stock assessment models for informing management advice and there is no single diagnostic tool that is capable of comprehensive evaluation for all models. As such, a suite of tools from the 'diagnostic toolbox' was applied to the current model assessment.

7.1 Convergence diagnostics

All models in this assessment were considered to be converged if 1) a maximum parameter gradient of 1e-03 was achieved; 2) the Hessian matrix was positive definite; 3) the model fit could not be significantly improved by jittering the estimated parameters (Carvalho et al., 2021); (4) estimated parameters should not be on their bounds; or (5) be highly correlated with each other ($-0.9 > r > 0.9$)

7.2 Model fit

Plots of observed and predicted index, LF and tagging data were examined, including residuals plots.

7.3 Age-structured production model (ASPM)

ASPM diagnostics (Carvalho et al., 2017, 2021; Maunder and Piner, 2015; Minte-Vera et al., 2017) for the diagnostic case model were estimated by 1) fixing growth and selectivity parameters at their estimated values; 2) removing the LF data from the model, leaving only the CPUE indices and tagging data as data to be fitted; 3) setting the orthogonal polynomial recruitment parameters such that there is no variability over time in year, season, region or season-region interaction effects; and 4) re-fitting the model estimating only the population scaling parameters. A comparison of biomass and depletion scaling and trends estimated by the ASPM and the full model gives an indication of the extent to which these estimates are informed by the CPUE indices and tagging data only. A second version of the ASPM, in which recruitment variability was estimated as for the diagnostic case, was also run.

7.4 Catch curve analysis (CCA)

A CCA is essentially the reverse of the ASPM, whereby the CPUE index data are removed from the model and all parameter estimation retained. The CCA indicates the information on population trends and scaling provided by the LF and tagging data.

7.5 Likelihood profile

A likelihood profile over a metric related to population scale is frequently used to evaluate conflict among data types. In this assessment, we profiled on the estimated population biomass averaged over the full model period (1972-2024) and examined the response of the likelihood of each data type (and their components). Ideally, we would like to see the negative log likelihood of each data component used in the model reaching a minimum at similar levels of average biomass.

7.6 Retrospective analysis

Retrospective analyses were undertaken as a general test of the stability of the model. A robust model, when rerun with data for the terminal year/s sequentially excluded (Cadigan and Farrell, 2005), should produce outputs that are variable across runs, and without a systematic pattern in either the scaling or time-series trends. The Mohn's rho statistic, a measure of the average relative bias of retrospective estimates, was computed for recruitment, SB and spawning potential depletion ($SB_t/SB_{F=0(t)}$) to indicate whether significant retrospective bias was present in the model. When calculating Mohn's ρ for recruitment, the antepenultimate year (2022) was used for comparison since the terminal and penultimate years' recruitment values were set to the arithmetic mean of the recruitment time-series, thereby having the effect of reducing any potential retrospective pattern.

8 Sensitivity analysis methods

Sensitivity analyses were undertaken to determine the sensitivity of important stock assessment results (recruitment, SB, $SB_{recent}/SB_{F=0}$, F_{recent}/F_{MSY}, and SB_{recent}/SB_{MSY}; see Table 4 for reference point definitions) to various structural assumptions, parameter settings, and decisions made during model development. For the purpose of these comparisons, we used the diagnostic case model as the reference model. The results of these tests informed decisions regarding the composition of the multi-model ensemble used to characterise uncertainty in the assessment results.

The range of sensitivity tests was developed by the assessment team over the course of model development, taking account of suggestions by the 2025 SPC Pre-Assessment Workshop (Hamer, 2025) as well as discussions with external scientists. The tests, hopefully, capture the main sources of potential uncertainty in the key model results given the time available.

The sensitivity tests conducted were (1) setting all tag reporting rate priors to be uninformative to see the impact of prior settings; (2) an alternative M-at-age shape that incorporated senescent mortality for older age classes; (3) alternative growth curves with k fixed at various values as 0.2, 0.3, 0.4, and 0.5; (4) alternative effort creep scenarios for Japanese pole-and-line CPUE indices using 20% and 90% percentiles of the effort creep posterior trajectories from Nishimoto et al. (2024); (5) alternative K statistics as the metric for release group mixing period assignments of K=0.1 and 0.3; (6) alternative steepness values of 0.65 and 0.95; and (7) setting the catch of Indonesian domestic fisheries to +/- 20% of the reported values.

It should be noted that the fixed k sensitivity was performed due to difficulties with estimates of k in preliminary model runs for the ensemble. Specifically, there was the propensity for the majority of the ensemble models to estimate values of k above 0.5 and, in some models, higher than 0.6. Although, growth parameters for skipjack are uncertain, this was considered to be problematic since these estimates were much higher than previous assessments.

9 Monte–Carlo model ensemble uncertainty estimation methods

Typically, three types of uncertainty could be incorporated into the estimates of stock status used for management advice. One involves the statistical uncertainty of the estimates produced by individual models, often referred to as 'estimation' uncertainty (described above). The second involves 'model' uncertainty, which is the uncertainty in the structural and fixed-parameter assumptions underpinning individual models, (e.g., fixed growth coefficient k, h, mixing periods, etc...). The third involves data inputs, such as alternative abundance indices (e.g., effort creep applied to CPUE indices) or other data inputs. Stock assessments of tuna for the WCPFC have often included an approach to assess the model uncertainty in the assessment model by running a factorial 'grid' of models to explore the interactions among selected 'axes of uncertainty'. The grid contains all combinations of two or more parameter settings or assumptions for each uncertainty axis and this

was commonly referred to as the 'structural uncertainty grid'.

In the 2025 assessment, the characterization of uncertainty in management reference points and quantities of interest was accomplished by applying a Monte Carlo model ensemble approach following the methods introduced by Ducharme-Barth and Vincent (2021), implemented in the 2021 stock assessment of south-west Pacific swordfish (Ducharme-Barth et al., 2021) and recommended as good practice by Neubauer et al. (2023). Building off the familiar model uncertainty grid, the model ensemble approach continues to consider the effects of model uncertainty while extending it to also account for the statistical estimation uncertainty from each model in the ensemble. This allows for a more holistic and transparent description of the uncertainty in estimates of stock status. Another key difference between the model ensemble and the model uncertainty grid is the relaxation of the full factorial design. Instead of choosing set levels for certain fixed parameters (e.g., $h \in 0.65$, 0.8, 0.95), a random set of the fixed parameters is drawn from an assumed prior distribution for each model in the ensemble. This approach has the advantage of implicitly weighting the ensemble to the most likely parameter combinations given the shape of the prior.

For aspects of model uncertainty that cannot be parametrized using assumed continuous prior distributions (e.g., in this assessment, the specification of the discrete K statistic limits for tag release group mixing period assignments), these scenarios can be selected randomly with specified probability using random numbers. This was the approach followed here for tag-mixing scenarios (see below).

The estimation uncertainty for each model in the ensemble was determined as described in Parameter and uncertainty estimation. However, for the ensemble models, we computed the estimation uncertainty (i.e., standard deviations of the estimates) for only the key reference point variables ($SB_{recent}/SB_{F=0(t)}$, F_{recent}/F_{MSY}, SB_{recent}/SB_{MSY}) and not the full set of time-series estimates as an efficiency measure. This was done for all models in the model ensemble and the estimation uncertainty was combined across models in a parametric bootstrap similar to the approach used in stock assessments conducted by the International Pacific Halibut Commission (Stewart and Martell, 2014) and applied in the 2023 yellowfin and bigeye assessments (Day et al., 2023; Magnusson et al., 2023).

Steepness, mixing periods, growth coefficient, and extent of effort creep emerged from the sensitivity analyses as the key sources of model uncertainty impacting stock assessment related estimates (see Sensitivity analysis methods). Therefore, prior distributions for these parameters were constructed as described below.

Diagnostics applied to the model ensemble were not as extensive as those applied to the diagnostic case model as described in Diagnostics methods due to the high number of models in the ensemble. Therefore, ensemble models were considered converged if 1) a maximum parameter gradient of 1e-3 was achieved; and 2) the Hessian matrix was positive definite.

9.1 Steepness (h) prior distribution

In the 2024 South Pacific albacore stock assessment (Teears et al., 2024), a prior for h was developed following the approach of Brodziak et al. (2011) which, uses various life history parameters. The prior was modified (to increase the percentage of converged models in the ensemble) with values at the extremes ($<$0.5 and $\geq$0.99) at low probabilities. Similarly, in the 2021 swordfish stock assessment (Ducharme-Barth et al., 2021), due to limited existing information, a prior for h was developed using a beta distribution with a median at 0.88. Following these approaches, in the 2025 skipjack stock assessment, a prior for h was developed with a mean of 0.84 and mode of 0.85 (Figure 24).

9.2 Effort creep prior distribution

In order to include uncertainty in effort creep, varying effort multiplier trajectories were included (i.e., a unique trajectory for each model in the ensemble; n=300) in the model ensemble by sampling from the estimated change in catchability from the Gompertz parameterisation from Nishimoto et al. (2024). Each effort multiplier trajectory was developed by randomly sampling from a beta distribution that matched the shape of the catchability estimates in 1972. For the remaining years in the time-series, values were sampled from year-specific distributions based on the percentile of the 1972 sampled value. The resulting catchability trajectories and effort multipliers are shown in Figure 25.

9.3 Growth coefficient (k) prior distribution

As described in Sensitivity analysis methods, estimates of k were frequently above 0.5 in preliminary model runs of the ensemble thus, it was necessary to fix k at various potential values more consistent with previous estimates of k. The inclusion of alternative k in the model ensemble was accomplished by sampling from a uniform distribution defined by U(0.2, 0.4) for each of the models in the ensemble (n= 300).

9.4 Mixing period scenarios

Various mixing period assumptions were defined by the K statistic of 0.1, 0.2, and 0.3 (as described in Tag mixing). In order to include these three categorical scenarios in the model ensemble, a uniform distribution from U(0,1) was randomly sampled and values $< 1/3$ were assigned the K=0.1 scenario, values $\geq 1/3$ and $< 2/3$ were assigned the K=0.2 scenario, and values ge 2/3 were assigned the K=0.3 scenario, effectively giving each scenario equal weighting within the ensemble.

10 Stock assessment interpretation methods

10.1 Reference points

The unfished spawning potential ($SB_{F=0}$) in each time period was calculated given the estimated recruitments and the Beverton-Holt SRR (see Section 6.1.1). This offers a basis for comparing the exploited population relative to the population subject to natural mortality only. The WCPFC adopted 20% $SB_{F=0}$ as a limit reference point (LRP) for the skipjack stock where $SB_{F=0}$ for this assessment is calculated as the average over the period 2014–2023. The iTRP has also been recalibrated according to the definition in CMM 2022-01 (Section 11.6.1). This requires stock projection and we hope to have the recalibrated value available by the SC21 in a rev1 of this paper. Stock status was referenced against these points by calculating the reference points; $SB_{recent}/SB_{F=0}$ and $SB_{latest}/SB_{F=0}$ where $SB_{F=0}$ is calculated over 2014–2023 and SB_{recent} and SB_{latest} are the mean of the estimated spawning potential over 2021–2024, and 2024 respectively (Table 4).

The other key reference point, F_{recent}/F_{MSY} , is the estimated average fishing mortality at the full assessment area scale over a recent period of time (F_{recent}; 2020–2023 for this stock assessment) divided by the fishing mortality producing MSY which is a product of the yield analysis and is detailed in Section 10.2.

For this assessment we also add a reference point for the ratio of the values of recent spawning depletion $SB_{recent}/SB_{F=0}$ to that for year 2012 $SB_{2012}/SB_{F=0}$. This is added in response to a request from SC17. Several ancillary analyses using the converged models were conducted in order to interpret the results for stock assessment purposes. The methods involved are summarized below and the details can be found in Davies et al. (2025).

10.2 Yield analysis

The yield analysis consists of computing equilibrium catch (or yield) and spawning potential, conditional on a specified basal level of age-specific fishing mortality (F_a) for the entire model domain, a series of fishing mortality multipliers ($fmult$), the M-at-age (M_a), the mean weight-at-age (W_a) and the SRR parameters. All of these parameters, apart from $fmult$, which is arbitrarily specified over a range of 0–50 (in increments of 0.1), are available from the parameter estimates of the model. The maximum yield with respect to $fmult$ can be determined using the formula given in Davies et al. (2025), and is equivalent to the MSY. Similarly, the spawning potential at MSY (SB_{MSY}) can be determined from this analysis. The ratios of the current (or recent average) levels of fishing mortality and spawning potential to their respective levels at MSY are determined for all models of interest. This analysis was conducted for all models in the structural uncertainty grid and thus includes alternative values of steepness assumed for the SRR.

Fishing mortality-at-age (F_a) for the yield analysis was determined as the mean over a recent period of time (2020–2023). We do not include 2024 in the average as fishing mortality tends to have high uncertainty for the terminal data year of the analysis and the catch data for this terminal year are

potentially incomplete. Additionally, recruitments for the last three years of the model are estimated by a common set of OPR parameters, producing identical estimates of recruitment by year, season and region for the 2022–2024. Earlier model runs in which this constraint was not imposed estimated unrealistically high recruitments in the last and/or second last year of the model. This constraint was therefore imposed to stabilise the terminal recruitments to more realistic levels.

MSY was also computed using the average annual F_a from each year included in the model (1972–2023). This enabled temporal trends in MSY to be assessed and a consideration of the differences in MSY levels under historical patterns of age-specific exploitation.

10.3 Depletion and fishery impact

Fishery depletion was calculated by computing the unexploited spawning potential time series (at the region level) using the estimated model parameters, but assuming that fishing mortality was zero. Both the estimated spawning potential SB_t (with fishing) and the unexploited spawning potential $SB_{F=0[t]}$ incorporate recruitment variability. Therefore, the ratio of these two quantities at each quarterly time step (t) of the analysis $SB_t/SB_{F=0[t]}$ can be interpreted as an index of fishery depletion. The computation of unexploited spawning potential includes an adjustment in recruitment to acknowledge the possibility of reduction of recruitment in exploited populations through stock-recruitment effects. To achieve this, the estimated recruitment deviations are multiplied by a scalar based on the difference in the equilibrium recruitment between the fished and unfished spawning potential estimates.

A similar approach was used to estimate depletion associated with specific fisheries or groups of fisheries. Here, fishery groups of interest (purse seine unassociated sets, pure seine associated sets, purse seine unidentified, pole-and-line, longline, and miscellaneous fisheries), are removed in-turn in separate simulations. The changes in depletion observed in these runs are then indicative of the depletion (fishing impact) caused by each of the removed fisheries.

10.4 Majuro and Kobe plots

For the standard yield analysis (Section 10.2), the fishing mortality-at-age, F_a, is determined as the average over some recent period of time (2020–2023). In addition to this approach, the MSY-based reference points (F_t/F_{MSY}), and SB_t/SB_{MSY}) and the depletion-based reference point ($SB_t/SB_{F=0[t]}$) were also computed by repeating the yield analysis for each year in turn. This enabled temporal trends in the reference points to be estimated and a consideration of the differences in MSY levels under historical patterns of age-specific exploitation. This analysis is presented in the form of dynamic Kobe plots and 'Majuro plots', which have been presented for all stock assessments in recent years.

10.5 Stock projections from the model ensemble

Projections of stock assessment models can be conducted within MFCL to ensure consistency between the fitted model and the simulated future dynamics, and the framework for performing this exercise is detailed in Pilling et al. (2016). Stochastic 30 year projections of recent catch and effort (2024) were conducted from each assessment model within the model ensemble. For each model, 30 stochastic projections, which incorporate future recruitments randomly sampled from historical deviates within the period used to estimate the SRR, are performed (see also Section 11.6.1).

Projections using specified effort levels require estimates of catchability to apply in the projection catch equations. In the current catch-conditioned model, effort data are not used and so catchability is not estimated as part of the assessment. A special catchability estimation was conducted as follows: (1) effort data from 2010 onwards were incorporated into the assessment data file for all fisheries requiring catchability estimates; (2) the converged assessment model was then run to estimate catchability by a students-t regression method, regressing the fishing mortality implied by each effort observation on the fishing mortality estimated for that fishery in the converged catch conditioned model; (3) catchability was constrained by a four-node spline over the period 2010-2024 to allow for temporal changes in catchability over this period; and (4) this estimation was carried out while preserving the parameterisation of the converged assessment model, i.e., only the parameters relating to the regression analysis were estimated in this phase.

11 Results

11.1 CPUE trends

The Japanese pole-and-line CPUE indices indicated relatively stable trends (Figure 11) however, with the application of effort creep, each index shows a slight decline in relative abundance over time. Similarly, the purse seine CPUE indices (Figure 12) indicated an overall decline in relative abundance. The region 8 purse seine CPUE index indicated high uncertainty in some time-steps due to very low sample sizes.

11.2 Consequences of key model developments

Aspects of the progression of model development (also referred to as 'stepwise') from the 2023 reference case (Castillo Jordan et al., 2023) to the model used as the diagnostic case in 2025 are described below with brief notes on the implication of the developments for SB and $SB_t/SB_{F=0}$, which are also displayed in Figure 26. A summary of the consequences of this progression through the model focusing on the key management quantities of recruitment, SB, and $SB_t/SB_{F=0}$ is as follows:

1. **Started with the 2023 reference case model** (Castillo Jordan et al., 2023).
2. **Application of Lorenzen natural mortality** (Lorenzen, 1996) **as recommended at the**

CAPAM 2023 'Tuna Stock Assessment Good Practices Workshop': resulted in a large increase in recruitment scale and a decrease in scale of both $SB_t/SB_{F=0}$ and SB.

3. **Ungrouping of extraction fisheries selectivities and relaxation of longline asymptotic selectivity at older ages:** resulted in virtually no differences with the exception of a moderate increase in $SB_t/SB_{F=0}$ and SB in the last two years.

4. **Increase in Dirichlet groupings from 3 (purse seine and pole-and-line, longline, and ID and PH fisheries) to 4 groups (separation of purse seine and pole-and-line)**: resulted in very little difference in recruitment and $SB_t/SB_{F=0}$ trends with the exception of a decrease in $SB_t/SB_{F=0}$ in the last two years. Further, there was an overall moderate decrease in scale in SB.

5. **Truncation of region 7 Japanese pole-and-line CPUE to include 1972–2009:** resulted in an overall slight decrease in the scale of recruitment and an overall increase in the scale of SB until 2009 and higher SB after 2009.

6. **Removal of Skipjack Survey and Assessment Program tagging data:** resulted in effectively no differences in management quantities.

7. **Application of effort creep to the Japanese pole-and-line CPUE indices:** resulted in large increases in recruitment, $SB_t/SB_{F=0}$, and SB until the mid 1990s after which the recruitment levels were similar to the previous step.

8. **Conversion from age-based selectivity to length-based selectivity:** resulted in decreased scale in recruitment with a more pronounced decrease in the 1970s and 1980s. The estimates of $SB_t/SB_{F=0}$ and SB were lower in the 1970s and 1980s and higher thereafter.

9. **Modified fecundity:** resulted in higher recruitment, $SB_t/SB_{F=0}$, and SB until approximately 1990 and relatively similar results thereafter. The modification in fecundity resulted in a slower maturity schedule as shown in Figure 27.

10. **Additional 3 years of data through 2024:** resulted in overall lower scale of recruitment throughout the time-series with estimates in $SB_t/SB_{F=0}$ and SB that differ slightly and inconsistently throughout the time-series.

11. **Application of orthogonal polynomial recruitment:** resulted in almost no difference throughout the time-series with the exception of the last two years which, is expected as recruitment is constrained to the geometric mean causing $SB_t/SB_{F=0}$ and SB to be subsequently lower in the terminal year.

12. **Ungrouping of the CPUE indices:** resulted in slightly higher recruitment and slightly lower $SB_t/SB_{F=0}$ and SB, mostly in the latter half of the time-series.

13. **Flexible growth curve in the first 3 quarterly ages (via VB-offsets):** resulted in an increase in overall scale in recruitment, $SB_t/SB_{F=0}$, and SB throughout the time-series.

14. **Relaxation of longline asymptotic selectivity:** resulted in a slight increase in scale of recruitment, $SB_t/SB_{F=0}$, and SB throughout the time-series.

11.3 Model parameter estimation

Estimates from the diagnostic case model are discussed in this section to explore model behaviour and parameter estimates and a table of parameter configurations is shown in Table 6 in Section 18.

11.3.1 Selectivity

A range of selectivity patterns are shown by the different fisheries in the model and can be largely classified by gear type. The length-specific selectivity coefficients are displayed in Figure 28. The pole-and-line fisheries (including the CPUE indices) select mostly younger fish that are three to seven quarters old and 30-60 cm FL, whereas the longline fisheries catch the largest and oldest fish, with their selectivity increasing rapidly at 60 cm FL, with very low selectivity below 60 cm. The purse seine associated and unassociated fisheries (and the related unassociated index fishery) have slightly different selectivities, with the associated fishery mostly selecting smaller fish in the length range 30–60 cm, compared to the unassociated fishery that selects fish in the length range 50–65 cm. The purse seine fisheries in regions 1, 2, and 3 select fish in the length range from 30–65 cm. Fisheries in Region 5, mostly select smaller fish around 30–50 cm.

11.3.2 Movement

Observed patterns of recapture rate among regions are compared to the estimated movement coefficients from the diagnostic case model among regions for each season in Figure 29. The tag return data show generally higher movement to adjacent regions with low movement between the northern regions 1–4 and the equatorial regions 5–8, but some movement of tagged fish is observed from regions 1, 3, and 4 to regions 5 and 7, particularly in quarters two and three. Model estimated movement coefficients predict low levels of movement to region 7 from multiple regions during various quarters, and high levels of movement to region 8 from multiple regions during various quarters, especially in quarter four when movement from regions 1–4 to region 8 was highest.

11.3.3 Growth

Growth estimates from the diagnostic case model indicated a slightly higher length-at-age for ages 2 and 3 quarters than the traditional VB curve as estimated by the VB offsets parametrization (Figure 30). The growth parameters estimated with fixed k=0.3 q^{-1} were $L1 = 21.87$ cm, $L16 = 80.08$ cm, with 4.08 cm and 5.06 cm estimated offsets for ages 2 and 3 quarters, respectively. The added flexibility from estimating offsets in early stage growth provided some deviation from the traditional shape of the VB growth curve specified by MFCL.

11.3.4 Natural mortality-at-age

The M-at-age curve with assumed Lorenzen shape and estimated scaling is shown in Figure 31.

11.3.5 Maturity-at-age

Maturity-at-age estimated by the 2025 diagnostic model ('13-LL-relax-asymptote' in Figure 32) differs from the 2023 model with a steeper initial incline resulting in higher maturity at earlier ages.

11.3.6 Tag reporting rates

Tag reporting rates were estimated for 22 fishery/tag release program groups (6 for the RTTP, 5 for the PTTP and 11 for the JPTP). The prior distributions, the model estimates of reporting rate and the upper limit imposed for each group are shown in Figure 33. In all cases where informative priors are provided, the model estimate is considerably higher than the prior mode, and is often far into the upper tail of the prior distribution. Where priors are more diffuse, several groups for the JPTP have estimates at the low end of the range. It seems that there is, more often than not, a mismatch between the priors based on tag seeding experiments or expert opinion, and what the model 'thinks' the reporting rates should be based on the large numbers of tag returns received from some reporting rate groups and other data in the model impacting fishing mortality and population size. This is an area where further research is required.

11.3.7 Recruitment

The estimated recruitment aggregated across all regions (Figure 34) shows high inter-annual variation, however, the trend in recruitment is stationary over the time-series. Large variability is indicated throughout the 1970s and 1980s and less variable, thereafter. From the early 1970s, the trend in recruitment shows a very gradual decrease until around 1990, after which there is a slight increase until approximately 2005 where the trend is very stable, onwards. As described in Section 6.1.1, the aggregated recruitment estimates in the last 3 years are derived from a common set of parameters – for year, season, region and region-season interaction.

The regional recruitments (Figure 35) indicated similar trends with high variability in recruitment at the beginning of the time-series. Regions 1–4 typically demonstrated decreased recruitment over time. Region 5 indicated very high recruitments in the 1970s and region 6 indicated high recruitments in the 1980s and early 1990s. Region 7 showed stable recruitment events until after 2000 when average recruitment began steadily increasing until the terminal year. High recruitment events typically occurred in the beginning and end of the time-series in region 8 with lower recruitment estimates from the 1980s through the early 2000s.

The estimated stock recruitment relationship for the diagnostic model is presented in Figure 36, which shows more variability in scale in the early years and lower scaled recruitments in more recent

years.

11.3.8 Biomass and spawning potential depletion

The 2025 diagnostic model predicted that spawning potential (Figure 37) declined steadily with strong seasonality throughout the time-series for regions 1–4 with regions 3 and 4 showing a slow increase in the last five years. However, regions 5–8 indicated less monotonic trends. Region 5 indicated the highest overall biomass with an initial decline until the 1980s, a stable trend until the early 2000s when biomass rose sharply, followed by a steady decline until the early 2020s. Region 6 indicated an overall slight declining trend with periodically sharp increases through the early 2000s and then less variability thereafter. Regions 7 and 8 demonstrated similar patterns with seasonality and a slow decline until approximately 1990 when spawning potential dropped sharply, recovered slightly in the mid 1990s, and then slowly increasing with variability until the terminal year. The aggregated spawning potential (over all regions) indicated an initial increase in the early 1970s and a steady decline until the early 1990s when spawning potential stabilised until the terminal year.

To interpret the trends in depletion, the individual trends in spawning potential, SB, should also be compared with the estimated spawning biomass in the absence of fishing (unfished; $SB_{F=0}$; Figure 38). $SB_{F=0}$ followed similar trends as spawning potential in regions 1–4 however, in regions 5–8, the $SB_{F=0}$ indicated a more pronounced increase from the 1990s onward.

The 2025 diagnostic model predicted that spawning depletion ($SB_{recent}/SB_{F=0}$; Figure 39) had a similar pattern as the spawning potential with overall declines in regions 1–4 and high seasonality however, there were stronger increases in spawning depletion (i.e., less depleted status) in the last 5-10 years of the model. Region 5 indicated less seasonality with high uncertainty in 1980s and an overall decline with periods of stability from 1990 through 2010 and an increase in the early 2020s. Region 6 showed an overall decline but with high variability. Region 7 indicated strong declines until around 2000, followed by a relatively stable period until around 2010, and then an increasing trend until the end of the model period. Region 8 indicated a similar trend with region 6 with overall declining spawning depletion with periods of temporary recovery. The aggregated spawning depletion (over all regions) estimates suggested a steady decline until approximately the early 2020s when spawning depletion increased until the terminal year when it decreases slightly.

11.3.9 Fishing mortality and age-specific exploitation

Estimates of F/F_{MSY} indicate a steady increase over time with a sharp decline in the early 2020s followed by a similar increase in the terminal year (Figure 40). All estimates (and confidence interval) were below 0.4 over the time-series.

Average fishing mortality rates for juvenile and adult age-classes (Figure 41) indicated variability in trends spatially as well as temporally. Overall, juveniles and adults showed similar trends with the exception of region 7 and all regions combined where juveniles indicated less severe increases in

fishing mortality. Regions 1–4 demonstrated relatively stable trends over time in fishing mortality but with periods of high variability and regions 3 and 4 indicated fishing mortality to be much lower in scale compared to other regions. Juveniles in region 1 experienced higher fishing mortality than adults. Regions 5–8 and the combined regions indicated overall increasing trends in fishing mortality with regions 6 and 7 being much higher in scale than region 8 and all regions combined (with the exception of juveniles in region 7) with differing periods of high variability. Regions 5, 6, and 7 had the highest fishing mortality and region 4 had the lowest. Region 5 shows a very strong increase in fishing mortality from around 2000.

Changes in fishing mortality-at-age and the population age structure are shown for decadal time intervals in Figure 42. Since the 1980s, the increase of fishing mortality to the current levels is due to the increases in catches of both juvenile and adult fish by the equatorial purse seine fisheries and the mixed gear fisheries of ID, PH, and VN in Region 5. Fishing mortality on ages 2–6 quarters also increased through time consistent with the increased fishing mortality from the purse seine fishery.

11.3.10 Fishing impact

Based on the diagnostic model, fishery impact was estimated with respect to depletion levels specific to fishery components (i.e., grouped by gear-type), in order to estimate which types of fishing activity have the most impact on the spawning potential (Figure 43). The early impacts on the population were primarily driven by pole-and-line fishing, which is still a dominant source of fishing impacts in regions 1–3 and 5, and less so in region 4. In regions 6–8, and the stock as a whole, pole-and-line impacts have slowly declined as purse seine associated and unassociated have had the most impact since the 1980s. Domestic fisheries have progressively more impacts on the population in region 5 with unidentified purse seine having increased impacts after 1980. Unidentified purse seine also has a substantial impact in regions 1–3 after 1980.

11.3.11 Yield Analysis

The yield analyses conducted in this assessment incorporates the spawner recruitment relationship (Figure 36) into the equilibrium biomass and yield computations. Importantly,in the diagnostic model, the steepness of the SRR was fixed at 0.8 so only the scaling parameter was estimated. Other models in the one-off sensitivity analyses and model ensemble assumed steepness values ranging between 0.62 and 0.96.

The yield distributions under different values of fishing effort relative to the current effort are shown in Figure 44 for several alternate values of steepness (i.e., the minimum, median, and maximum steepness values used in the model ensemble). For the median steepness model, it is estimated that MSY would be achieved at approximately 4 times the current fishing mortality and the resulting increase in yield would be approximately 1.7 times the current yield. The right-hand arm of the yield curve displays a decline in yield with increasing fishing mortality. The model at the minimum steepness indicates similar gains in yield with increases in fishing mortality but with a much steeper

decline after reaching maximum yield. The model at the maximum steepness shows a slower decline but a lower maximum yield (approximately 200,000 mt per year < the median model estimate).

11.4 Diagnostics results

In the following section, we present diagnostics for the diagnostic case model.

11.4.1 Convergence diagnostics

The following indicators of model convergence were recorded:

- The maximum parameter gradient for the diagnostic case model was 5.929e-05.
- The Hessian was positive definite.
- A jitter analysis was not able to improve on this solution, with all 35 jitters having total negative log likelihoods $\geq$ the diagnostic case model (Figure 45).
- The model consisted of 1,498 estimated parameters – 1,195 relating to recruitment, 96 to movement, 169 to selectivity, 8 to the Dirichlet Multinomial likelihood for length frequency data, 21 to tag reporting rates, 1 to overdispersion of the negative binomial likelihood for tagging data, 6 to growth, 1 to natural mortality and 1 to scaling of equilibrium recruitment in the stock-recruitment relationship. No parameters were estimated at their specified bound. However, 38 movement parameters were estimated to be very close to their lower bound of zero. While this could be a legitimate estimate of movement (e.g., zero observations of tag movements), and did not preclude good convergence properties, it might be preferable to adjust the parameterisation to fix those parameters at zero and not estimate them. This would require some substantial code development and is something to consider in any future new-generation integrated stock assessment software development.
- We examined the correlation matrix for the estimated parameters and found that 99.88% of all 1,121,253 correlations were between -0.9 and +0.9. There were only 9 correlations that were either >0.9 (3 correlations) or <-0.9 (4 correlations). The high positive correlations are both for the 1st and 2^{nd} parameters of selectivity spline quadruplets. Three of the high negative correlations were also for members of individual selectivity splines, two for the 1st and 4th parameter and, one for the 2^{nd} and 3^{rd} parameters. These correlations likely indicate some minor over-parameterisation of selectivity for some fisheries and is an area that could be investigated further. The last high negative correlation (of -0.971) was between the $L1$ and $L16$ growth parameters, which is not unexpected particularly when k is fixed.

11.4.2 Model fit

Pole-and-line CPUE regions 1–4, 7 and 8: There was substantial seasonal variability in the CPUE indices for the pole-and-line CPUE indices (Figure 46), but a slightly declining trend over

time. Overall the model-estimated CPUE predicted the seasonal variation in the CPUE indices relatively well and also the long-term trends. While the model-estimated CPUE largely captured the seasonal variability observed, for the temperate and equatorial pole-and-line fisheries (i.e., 35.PL.INDEX.ALL.3, 36.PL.INDEX.ALL.4, 38.PL.INDEX.ALL.7, and 39.PL.INDEX.ALL.8) the fit to the variability in the CPUE during the 1990s was relatively poor for the highest observations but better for the lower observations.

Purse seine CPUE Region 5: The model-estimated CPUE (Figure 47) showed a worse fit to the higher variability in the PH purse seine CPUE in the early part of the time series from 2005–2012, but after 2012 the model predicted the CPUE well, including the observed decreasing trend in CPUE.

Unassociated purse seine CPUE regions 6, 7, and 8: For the unassociated purse seine CPUE (Figure 47), the model underestimated the CPUE in region 6 from 2012-2014 and tended to overestimate from 2014–2019. For region 7, the model underestimated from 2010–2012 and overestimated after 2022. Otherwise, with the exception of region 6, the model had a reasonable fit to the purse seine CPUE indices.

ID, VN, PH fisheries' length compositions: The model fit to the composite length compositions of the domestic (DOM) fisheries in ID, VN, and PH was generally good. There was slight over estimation of smaller sizes and under estimation of larger sizes for 11.Z.ID.5 (Figure 48). Also, there was slight overestimation of larger sizes for 10.Z.PH.5. Across the model time series the model estimates of median lengths were very consistent with the temporal variation in the observed data (Figure 49).

Pole-and-line fisheries length compositions: The model fits to the aggregated length compositions for the pole-and-line fisheries were generally good, with some slight misfit to smaller sizes for some fisheries (Figure 50). Across the time series, the model estimates of median lengths were generally consistent with observations and predicted the temporal variation in the observed data. However, regions 7 and 8 showed worse fits, possibly due to low sample sizes and/or temporal patchiness in data coverage and therefore low weight in the model fitting process (Teears et al. (2025); Figure 14, Figure 51).

Pure seine fisheries' length compositions: The model estimation of the length composition for the purse seine fisheries for regions 1–3 indicated poor quality fits with over estimation of smaller and larger fish in comparison to the good fits from the purse seine associated and unassociated extraction and CPUE indices in regions 6–8 (Figure 52). Region 5 also indicated lower quality fit to the data though not as severely as regions 1–3. Across the time series the model estimates of median lengths were similar to and consistent with the temporal variation in the observed data, noting the low coverage for some of the observed data across the time period (Teears et al. (2025); Figure 14, Figure 53).

Longline fisheries length compositions: The model estimations of the length compositions for

the longline fisheries, noting the relatively low sample sizes (Figure 14), were reasonable for all regions, but with poorer fits in regions 1–4 (Figure 54).

Tagging data: The aggregated tag attrition estimates fit the observed tagging data closely (Figure 55). Some misfit was noted for the JPTP tagging data that indicated JPTP tagging data indicated over estimation of recaptures in region 5 from tags released in region 5, recaptures in region 8 from tags released in regions 1–4, 7 and 8, and recaptures in region 6 from tags released in region 7 (Figure 56). Recaptures in region 4 were also under estimated from tags released in regions 4 and 7 and recaptures in region 5 were underestimated from releases in regions 3, 4, 7 and 8.

The diagnostic model indicated high quality fits to the PTTP and RTTP tagging data as shown in Figure 57 with the exception of the underestimation of RTTP recaptures in region 8 from releases in region 8 with time-at-liberty above 3 quarters.

The predicted tag returns over time showed relatively good agreement with observed data (Figure 58, Table 2) although, some of the years with high recaptures are underestimated by the model such as tag groups 1, 2, 5, 14, 16, 18 and 19. Similarly, the model over estimated the high number of recaptures in tag group 21.

11.4.3 Age-structured production model (ASPM)

Two versions of the ASPM were run for the diagnostic case model, one that included and one that excluded estimated recruitment variability. The scaling and time series trends of recruitment, SB and spawning depletion ($SB/SB_{F=0}$) were very consistent between the diagnostic case and the ASPM with estimated recruitment variability (Figure 59). For the ASPM without estimated recruitment variability, the scaling of the three variables is consistent with the other two models. Also, the long-term decline in the SB and $SB/SB_{F=0}$ variables is replicated, but with less inter-annual variability. This indicates that much of the information on scaling and trends in the model is coming from the CPUE indices and tagging data.

11.4.4 Catch-curve analysis

The catch-curve analysis (CCA) omits the CPUE index data from the model leaving only the size data and tagging data. While the scale of recruitment, SB and $SB/SB_{F=0}$ is similar to that of the diagnostic case model, the time-series trends are quite different (Figure 60). This indicates that the CPUE indices inform trends while the size data informs shorter term variability, such as the very high recruitment estimates towards the end of the model period. It is likely that population scaling is informed by the tagging data, which remain in the CCA model.

11.4.5 Tag-free model

To examine the impact of the tagging data on the model, we re-fitted the diagnostic case model with the tagging data removed. Movement parameters estimated in the diagnostic case model were held

fixed in this model. The removal of tagging data results in a substantial increase in the population scaling, to the extent that recruitment, SB and $SB/SB_{F=0}$ are all substantially higher than in the diagnostic case (Figure 61). This suggests that the tagging data play a key role in moderation of population scaling and as a result, fishery impacts such as $SB/SB_{F=0}$.

11.4.6 Likelihood profile

Likelihood profiles by data component and by fishery for the CPUE indices and LF data are shown in Figure 62, Figure 63, and Figure 64, respectively. The aggregate profiles by data component indicate some consistency in scaling information from the CPUE and tagging data, whereas the LF data appear to be more consistent with higher scaling. Also of significance is the impact of the penalties resulting from priors for the tag reporting rates. On this evidence, it is likely that the reporting rate priors are constraining the population scaling to lower levels. Priors impacting key assessment results in this way is not desirable. We provide further information on reporting rate priors in a sensitivity analysis in a later section. JPPL CPUE indices have large changes in likelihood especially region 1 and 8 suggesting a lower scale than the region 4 index. The region 5 domestic fishery length data has the largest change in likelihood indicating a higher scale which, is consistent with most of the fisheries with high changes in likelihood with the exception of the unassociated purse seine in region 7 and the associated purse seine in region 6.

11.4.7 Retrospectives

The retrospective analysis indicated that the diagnostic model showed no significant retrospective patterns (Figure 65) with Mohn's ρ for recruitment, SB and $SB/SB_{F=0}$ being 0.2, -0.19, and -0.05, respectively.

11.5 Sensitivity analyses

One-off sensitivities from the diagnostic case model are used to inform choices regarding the construction of the multi-model ensemble.

11.5.1 Reporting rate priors

We noted earlier that the priors on tag reporting rates (informed by tag seeding experiments and expert opinion) appeared to have some impact on the population scaling as evidenced by the likelihood profiles. To provide additional insight into the impact of reporting rate prior specifications, we conducted a sensitivity in which all reporting rate priors were made to be uninformative. The reporting rate estimates for the diagnostic case model are all < 0.99, which was set as the upper bound (Figure 66). When the reporting rate priors are made to be uninformative, all estimated reporting rates (bar one) increase to some extent, and 12 converge to the upper bound.

As would be expected, there is some impact on the stock assessment quantities of interest when making the reporting rate estimates uninformative (Figure 67). Moderate increases in the scaling of

recruitment, SB and $SB/SB_{F=0}$ occur in the modified model. In the case of $SB/SB_{F=0}$, the ratio is raised by 5-10 percentage points in the recent years. While this adds some degree of uncertainty to the assessment, we opted to not incorporate this into the ensemble framework because of the undesirability of models having reporting rates at the upper bound, the likelihood of such models having convergence problems and the low plausibility of such models generally.

11.5.2 Natural mortality senescence

All models in this assessment including the diagnostic case have adopted a Lorenzen M-at-age function whereby the M-at-age is inversely proportional to the mean length-at-age (Lorenzen, 1996). This shape constraint means that M-at-age declines for successive age classes in the same manner that mean length increases. While this has now been adopted as the norm for many tuna assessments, it ignores the biological reality that natural mortality in the oldest age classes must ultimately increase due to physiological ageing as the fish approach their natural age expectancy. To test the impact of possible mis-specification of M-at-age, we constructed an alternative M-at-age shape for which M increases for the older age classes (Figure 68). The modified model actually provided an enhanced likelihood (by around 35 points overall) and in particular for the tagging data component. However, very little effect was seen on the key model outputs (Figure 69). For this reason, we deemed it not necessary to include M shape uncertainty in the model ensemble.

11.5.3 Growth

In this sensitivity we investigated the impact on the assessment of different k specifications, ranging from 0.2 q^{-1} to 0.5 q^{-1} (Figure 70).

Somewhat surprisingly, estimates of recruitment, SB and $SB/SB_{F=0}$ did not show strong sensitivity to the value of fixed k (Figure 71). Some scaling differences for recruitment and SB were noted, but $SB/SB_{F=0}$ in particular was found to be quite robust to the different k settings. Nevertheless, we opted to include a fixed k dimension in the uncertainty framework to allow for the possibility of interactions of k with the other uncertainty dimensions that were incorporated.

11.5.4 Effort creep in pole-and-line indices

Japanese pole-and-line CPUE provides a series of key region-based indices of relative abundance to the model. The CPUE standardisation procedure (Nishimoto et al., 2025) is likely able to capture to some extent catchability changes that occur through the covariates and categorical variables included in the standardisation model. However, it may be that this does not provide a complete picture of catchability trends due to technological innovation leading to better fishing performance. An analysis by Nishimoto et al. (2024) estimated the possible magnitude of so-called 'effort creep', which is summarised in Figure 13.

For the diagnostic case model, we used the median of the MCMC runs from Nishimoto et al. (2024), which results in an approximate 4-fold increase in effective effort from the first (1972) to the last

year (2023) of the abundance indices. For a sensitivity analysis we used effort multipliers close to the extremes of the MCMC runs, approximately 2- and 5-fold increases over time.

The estimates of recruitment, SB and $SB/SB_{F=0}$ are only moderately affected across this range of effort creep scenarios (Figure 72). The estimates of recruitment are mainly affected through the moderation of some of the early spikes in recruitment. In the low effort creep scenario the recruitment spikes are moderated due to the reduced declining trend in CPUE, compared to the high effort creep scenarios with a stronger decline in CPUE. A similar effect is seen in the SB estimates, with the low effort creep scenario resulting in a flatter time series. Likewise for the $SB/SB_{F=0}$ estimates, most of the divergence in estimates occurs in the first half of the time series. However, notably, the different scenarios appear to have only modest impact on the more recent results.

While the stock status indicators appear to be quite robust to effort creep, due to previous expressions of interest from SC and PAW scientists that effort creep should be included in the uncertainty framework, we opted to include sampling from the MCMC runs from the analysis of Nishimoto et al. (2024) in the model ensemble described in the next section.

11.5.5 Tag mixing

Tagging data are a key element of the skipjack assessment as they inform not only fish movement but also natural and fishing mortality rates and population scale. However, a key assumption that has to be made for tagging data is the length of time it takes for tagged fish to become adequately mixed with the untagged population, thereby experiencing similar capture probability. There is no perfect way of determining this time period as mixing is affected by both the movement of fish and the spatial/temporal disposition of the tag releases in relation to the untagged population and fishing effort in a region. As for the 2025 skipjack assessment, the method of Scutt Phillips et al. (2022) and described in Teears et al. (2025) was again used to define tag mixing scenarios. We used three values of K (the Kolmogorov-statistic; an index of similarity) – 0.1 (denoted Mix-$K1$), 0.2 (Mix-$K2$) and 0.3 (Mix-$K3$) to define acceptable levels of similarity of tagged and untagged capture probabilities.

The tag mixing scenarios have an important impact of the stock assessment results (Figure 73). In general, more tagging data admitted into the model (through shorter mixing periods) puts downward pressure on scaling of recruitment, SB and $SB/SB_{F=0}$. The Mix-$K2$ and Mix-$K3$ scenarios are reasonably similar, but the Mix-$K1$ (the longest mixing periods) scenario has substantially higher scaling of all variables. These differences are important and warranted the inclusion of tag mixing scenario in the ensemble model uncertainty analysis described in the next section.

11.5.6 Steepness

The steepness parameter (h) of the Beverton and Hold stock-recruitment relationship is almost always uncertain and cannot be estimated internally in the assessment. Here we have used three settings for h, 0.65, 0.8 and 0.95, to compare the key stock assessment results. This is the range of steepness values that have been typically used in WCPFC tuna assessments. The different steepness settings have virtually no effect on the estimates of recruitment and SB and have a slight effect on $SB/SB_{F=0}$ at lower levels of SB (Figure 74). However, in most assessments, there is a strong effect of steepness on the MSY-related reference point variables, F/F_{MSY} and SB/SB_{MSY}, with lower (higher) steepness producing more pessimistic (optimistic) outcomes. We have therefore included steepness in the multi-model ensemble to capture these effects.

11.5.7 Indonesian catch uncertainty

Catches in the domestic fisheries of Philippines, Vietnam and Indonesia are an important component of WCPFC tropical tuna stock assessments. In the past, there have been concerns regarding the accuracy of some of the catch estimates, which led to the development of the West Pacific East Asia (WPEA) project. The WPEA project has resulted in improvements in data quality, but uncertainties remain, particularly for the Indonesian fisheries, which are the largest and most complex fisheries in the WPEA region. For this reason, we conducted a sensitivity for different catch scenarios for the three Indonesian fisheries (11, 13 and 14) in the model. The scenarios used were simple modifications of the entire time series of reported catches by +/- 20%.

The modification of the catches had very little impact on the key model results (Figure 75). This provides some assurance that the assessment is robust to catch uncertainty of this magnitude. Of course, this result does not lessen the need to have accurate catch estimates from these fisheries, as catch and associated data are used in many different aspects of fisheries management apart from stock assessment.

11.6 Monte-Carlo model ensemble uncertainty estimation

Diagnostics for the 300 models in the ensemble indicated that 271 models converged based on the selected criteria and were, therefore, included in the final results. A table of diagnostics and likelihoods are available in Section 19.

The results of the ensemble uncertainty analysis are summarised in several forms: 1) histograms of model uncertainty estimated from Monte-Carlo draws from the model ensemble of $SB_{recent}/SB_{F=0}$, SB_{recent}/SB_{MSY}, and F_{recent}/F_{MSY} coloured by values of h, effort multiplier, and growth coefficient k in Figure 76, Figure 77, and Figure 78 (additional mixing period specific histograms are also provided in Section 20) combined with 2) estimates of $SB_{recent}/SB_{F=0}$, SB_{recent}/SB_{MSY}, and F_{recent}/F_{MSY} plotted by values of h, effort multiplier, and growth coefficient k for each model in the ensemble; 3) percentile trajectories (90% and 75%) are provided for $SB_{recent}/SB_{F=0}$, SB,

and fishing mortality in Figure 79, Figure 80, and Figure 81; 4) a table of summary statistics of reference points for the model ensemble is included in Table 5; and 5) Majuro and Kobe plots are shown for estimates from the model ensemble and the dynamic MSY analysis (Figure 82).

The models from the ensemble indicated the probability that $SB_{recent}/SB_{F=0}$ <0.2 was 0, the probability that F_{recent}/F_{MSY} >1 was 0, and the probability of $F_{recent}/F_{MSY} < 1$ was 0.

Mixing period assumptions had a high influence on $SB_{recent}/SB_{F=0}$, SB_{recent}/SB_{MSY}, and F_{recent}/F_{MSY} as evidenced by the differing distributions in Figure 76, Figure 77, and Figure 78. The relationships between h, effort multiplier, and k with $SB_{recent}/SB_{F=0}$ were less evident however, F_{recent}/F_{MSY} indicated a negative relationship with h and a positive relationship with k. Conversely, SB_{recent}/SB_{MSY} indicated a positive relationship with h and a negative relationship with k.

The time-series of percentiles indicated 90% of ensemble had terminal $SB_{recent}/SB_{F=0} \geq 0.426$ for the combined regions (Figure 79) and region 5 and 6 indicated 10^{th} percentiles as low as 0.302 and 0.335, respectively. The time-series of quantiles indicated 90% of ensemble models had terminal $SB \geq 27.5$ (100,000s of tons) for the combined regions (Figure 80) and regions 5–7 indicated more fluctuations over time but with more consistent estimates among models. The time-series of percentiles indicated 90% of ensemble models had terminal fishing mortalities ≤ 0.0349 for the combined regions and regions 2 and 5 indicated values as high as 0.140 and 0.123, respectively (Figure 81).

The dynamic MSY analysis indicated that for all time periods, the $SB_{recent}/SB_{F=0}$ was > 0.2, SB_{recent}/SB_{MSY} was > 1 and the F_{recent}/F_{MSY} was < 1 (Figure 82). Similarly, all models in the ensemble for the recent period (2021–2024) indicated the $SB_{recent}/SB_{F=0}$ was > 0.2, SB_{recent}/SB_{MSY} was > 1 and the F_{recent}/F_{MSY} was < 1.

11.6.1 'Status quo' stochastic projections

Two sets of projections were performed using the grid of skipjack models developed for SC21 consideration. Ultimately, results were developed from 270 models of that grid – projections from model 'Sim-71' were unsuccessful for technical reasons. The common settings for the two sets of projections were:

- Future fishing conditions were relative to those in 2024.
- Purse seine and pole and line fisheries were projected based upon effort, requiring catchabilities to be estimated from the 2025 catch-conditioned skipjack assessment. That fishery catchability was assumed then constant into the future. 'Other fisheries' in region 5 were projected on catch.
- Future recruitment was sampled from the period 1984-2020, consistent with the period over which the SRR was estimated within the assessment.

– Projections were run for 30 years and hence ended in 2054. This period was considered sufficient for the stock to have settled into equilibrium with the conditions being set for the future.

– Given the scale of the uncertainty grid and the computing capacity available, 30 projections were performed from each of the 271 models for the two future scenarios. Ultimately 16,200 projections were performed across those two scenarios.

The two sets of projections were:

'Recent conditions'

To evaluate the potential implications of recent fishing conditions, levels of fishing (effort/catch) in 2024 were projected into the future for 30 years. It should be noted that while 2024 was a record catch year, key components of the fishery (e.g., purse seine) were projected on effort and hence resulting catch would depend on underlying stock status.

'TRP recalibration'

To recalibrate the value of the agreed skipjack TRP based upon the 2025 assessment, projections were performed to support the calculation of the second component of the skipjack TRP. From CMM 2022-01 (para 2; italicised text below), the TRP is calculated based on two spawning potential depletion values:

- *The first value represents the estimated average depletion of the skipjack tuna stock over the period 2018-2021 ($SB_{2018-2021}/SB_{F-0}$).* For this element, the $SB_t/SB_{F=0,t-1\ to\ t-10}$ calculated within the assessment was identified for the years 2018, 2019, 2020 and 2021 (t) within each model. The mean of those values was taken within each model, and then the median across those models calculated.

- *The second value represents the long-term median equilibrium stock depletion that would be reached under the agreed baseline fishing conditions for skipjack tuna (purse seine effort at 2012 levels, pole and line effort at average 2001-04 levels, and the domestic fisheries in assessment region 5 at average 2016-18 levels).* Future fishing levels from each fishery were scaled up or down relative to those in 2024 to achieve the CMM 2022-01 specified baselines. Those conditions were projected forward 30 years, with 30 simulations across each of the assessment models, and the median of the resulting 8,100 depletion levels in 2054 calculated.

Both values are expressed as a percentage of the estimated average spawning potential in the absence of fishing ($SB_{F=0}$), calculated as described in paragraph 3 of CMM 2022-01. Values are calculated as medians based upon the grid of assessment models as agreed by the WCPFC Scientific Committee. The target reference point is the average of these two values (weighting of 50/50). As noted in the footnote, spawning potential depletion refers to the estimated spawning potential as a percentage of the estimated spawning potential in the absence of fishing (i.e., the unfished spawning potential). The metric is dynamic and is estimated for each model time step.

The projected stock depletion levels under recent conditions are presented in Figure 83. The year 2024 represents the first year of application of the skipjack interim management procedure (CMM 2022-01). The stock is on average at 98% of the recalibrated TRP (0.94 – 1.01). This is within the range expected through the MSE testing of the adopted interim skipjack MP (see MSE shiny; performance indicator: '$SB/SB_{F=0}$ relative to target').

12 Discussion

We believe that this assessment is a substantial improvement over the previous assessment. Model diagnostics are much improved – good convergence of 90% of models with positive definite Hessians, no parameters estimated at their bounds, no strong retrospective patterns, a very small number of high parameter correlations and improved fits to all data categories. However, there remains some level of data conflict, with the size data trying to push the population scale higher and the tagging and CPUE index data trying to constrain population scale.

The most notable feature of the assessment is the estimation that the stock has had fairly stable spawning potential, spawning potential depletion and fishing mortality since around 2010. This is in contrast to the previous assessment finding that the stock is becoming increasingly depleted over time. This change appears to be driven by the removal of the long-term increasing trend in recruitment, and unfished spawning potential as a result, estimated in previous assessments. The current results are now more consistent with the recent catch history, whereby total catch increased linearly up to 2010, and has varied between 1.5 and 2 million tonnes since that time.

A number of sensitivity analyses were used to investigate the impacts of various model settings and various sets of data, including reporting rate priors, the possibility of an increase in M-at-age for older age classes, the von Bertalanffy growth coefficient k, effort creep in pole-and-line indices, tag mixing scenarios, steepness in the stock-recruitment relationship and Indonesian catch uncertainty.

A multi-variate Monte Carlo sampling process was used to characterise uncertainty in key stock assessment metrics ($SB_{recent}/SB_{F=0}$, F_{recent}/F_{MSY} and SB_{recent}/SB_{MSY}). The factors included in the 300 model ensemble were steepness (Beta distribution with mode 0.85 and approximate limits of 0.6 and 0.99), pole-and-line index effort creep (Beta distribution of effort multipliers based on the results of Nishimoto et al. (2024)), growth coefficient k (a uniform distribution 0.2-0.4) and tag mixing scenario (3 scenarios sampled with equal probability). Sampling was independent with respect to these factors and the ensemble was effectively weighted according to the shape of the individual distributions sampled. Of the 300 models run, 271 (90%) met the convergence criteria and were thus included in the final ensemble, from which the key stock assessment metrics were computed, including estimation error from the individual ensemble models.

The main uncertainty factor affecting the stock status estimates was the tag mixing scenario used, with more optimistic metrics associated with stricter criteria for tags to be considered 'mixed'. Furthermore, steepness was also an influential factor for the MSY-based reference points.

12.1 Main assessment conclusions

The general conclusions of this assessment are as follows:

- In contrast to previous assessments, recruitment is estimated to have been more variable and above average but declining slightly prior to 1990. Recruitment increased from 1990 to around 2005, after which there has been no particular trend. There is some evidence of high recruitment in recent years. The lack of a persistently increasing trend in recruitment that was estimated in previous assessments is due to the exclusion of the SSAP tagging data and the admission of effort creep in the pole-and-line CPUE indices.
- Spawning potential declined prior to about 1990 (largely in response to recruitment) but has remained relatively stable since. The ratio of fished to unfished spawning potential depletion declined gradually since the start of the model period to around 2010, after which it has been stable.
- Average fishing mortality rates for juvenile and adult age-classes increased to around 2010 and have been stable since.
- The estimates of key management quantities (medians), and their 80% confidence intervals were:
  - $SB_{recent}/SB_{F=0}$ 0.51 (0.45–0.63)
  - F_{recent}/F_{MSY} 0.35 (0.24–0.45)
  - SB_{recent}/SB_{MSY} 3.90 (2.95–5.61)
- No models from the ensemble estimate the stock to be below the LRP of 20% $SB_{F=0}$.
- Overall, the outcomes of this assessment suggest that the skipjack stock in the WCPO is not overfished nor undergoing overfishing

12.2 Recommendations for further research and development

Several of the key research needs identified in the 2022 assessment have been addressed, including effort creep effects on pole-and-line CPUE indices, rectifying the increasing trend in recruitment and improved model diagnostics around convergence. However, there still remains several areas to focus research on for future assessments.

Although the assessment was not overly sensitive to growth assumptions, it could likely be improved through better information on growth and age structure. The epigenetic approach to age determination, should it be confirmed for skipjack, likely offers the best long-term solution for a better understanding of growth and age structure.

A better understanding of meta-population structure of skipjack, particularly focussed on improving understanding of the linkages between populations in the east Asian waters and those in the broader

western and central Pacific, is still a priority area. With the 2024 record skipjack catch in both the eastern and western & central Pacific Ocean, understanding the east-west linkages across the Pacific more broadly will likely increase in importance.

The impact of assumed tag mixing period on the assessment is substantial. The use of finer-spatial-scale models would potentially allow less restrictive assumptions regarding tag mixing and should be a high priority for future research. As a first step, implementing an option in SEAPODYM to model tags in a release-conditioned mode (as opposed to the current recapture-conditioned approach) may provide more accurate information on skipjack abundance and fishing mortality as well as on movement. Such information could either be used directly for assessment purposes or provide the basis for informative priors in a MULTIFAN-CL model that would not then be required to model the tagging data directly. Furthermore, the external tagging analysis being explored as part of WCPFC project 123 may prove beneficial in this regard, and should continue to be supported through that project.

The impact of the tagging data on the assessment results is also impacted to an extent by tag reporting rate estimates and their prior distributions. It was noted that there is frequently a mismatch between the reporting rate priors and the model estimates – this is an area that needs further investigation, e.g., in the way in which the tag seeding data are analysed.

Finally, further work in understanding the data conflict of the size data with CPUE and tag data is required. This should include testing of different filtering rules to enhance data quality and representativeness. Collaboration with the observer and port sampling programmes of CCMs providing these data will be essential in this work.

13 Acknowledgments

We are grateful to the member countries for committing to sharing their operational-level catch and effort data, which are invaluable for these analyses. We thank the European Union's "Pacific-European Union Marine Partnership Programme" for their vital support. We thank the various fisheries agencies and regional fisheries observers for their support with data collection, provision and preparatory analysis. We thank Sam McKechnie and Nan Yao for advice, comments, and edits. We thank the OFP-FEMA team for their ongoing work in the provision of tag-recapture data for the skipjack assessment. We especially thank Yoshi Aoki, Naoto Matsubara, Makoto Nishimoto, and Hidetada Kiyofuji for their support on developing the pole-and-line CPUE indices and the provision and analysis of the JPTP tagging and length composition data used in this analysis. We also thank Keith Bigelow who again provided standardized CPUE indices for the Philippines purse seine fishery, and Inna Senina for providing the movement coefficients, relative abundance estimates, and recruitment distribution estimates for the SEAPODYM sensitivity. We thank participants at the preparatory stock assessment workshop for their contributions to the assessment. We especially thank the SPC data management team and tagging data team for their hard work and support

to provide the data fuel for the assessment, and make special mention of the support from Benoit Pohl and Marc Ghergariu. Finally, we thank Fabrice Bouye for ensuring smooth operation of the computing resources required to do the assessment.

14 References

Anderson, S. C., Ward, E. J., English, P. A., and Barnett, L. A. (2022). sdmtmb: an R package for fast, flexible, and user-friendly generalized linear mixed effects models with spatial and spatiotemporal random fields. *BioRxiv*, pages 2022–03.

Aoki, Y., Tanaka, F., Aoki, A., Ohashi, S., and Kiyofuji, H. (2024). Re-evaluating age estimation using daily increments on otoliths of the skipjack tuna *Katsuwonus pelamis*. *Fisheries Research*, 269:106855.

Artetxe-Arrate, I., Fraile, I., Marsac, F., Farley, J. H., Rodriguez-Ezpeleta, N., Davies, C. R., Clear, N. P., Grewe, P., and Murua, H. (2021). A review of the fisheries, life history and stock structure of tropical tuna (skipjack (*Katsuwonus pelamis*), yellowfin (*Thunnus albacares*) and bigeye (*Thunnus obesus*)) in the Indian Ocean. *Advances in Marine Biology*, 88:39–89.

Ashida, H. (2020). Spatial and temporal differences in the reproductive traits of skipjack tuna *Katsuwonus pelamis* between the subtropical and temperate western Pacific Ocean. *Fisheries Research*, 221:105352.

Ashida, H., Tanabe, T., and Suzuki, N. (2017). Difference on reproductive trait of skipjack tuna (*Katsuonus pelamis*) female between schools (free vs fad school) in the tropical western and central Pacific Ocean. *Environmental Biology of Fishes*, 100:935–945.

Bigelow, K., Garvilles, E., Bayate, D. E., and Cecilio, A. (2019). Relative abundance of skipjack tuna for the purse seine fishery operating in the Philippines Moro Gulf (Region 12) and High Seas Pocket# 1. Technical Report WCPFC-SC15-2019/SA-IP-08.

Bigelow, K., Hampton, J., and Fournier, D. (2000). Preliminary application of the MULTIFAN-CL model to skipjack tuna in the tropical WCPO. Technical Report SCTB13 Working Paper SKJ-2.

Brodziak, J., Lee, H.-H., and Mangel, M. (2011). Probable values of stock-recruitment steepness for north pacific albacore tuna. Technical Report ISC/11/BILLWG-2/11.

Cadigan, N. G. and Farrell, P. J. (2005). Local influence diagnostics for the retrospective problem in sequential population analysis. *ICES Journal of Marine Science: Journal du Conseil*, 62(2):256–265.

Carvalho, F., Punt, A. E., Chang, Y.-J., Maunder, M. N., and Piner, K. R. (2017). Can diagnostic tests help identify model misspecification in integrated stock assessments? *Fisheries Research*, 192:28–40.

Carvalho, F., Winker, H., Courtney, D., Kapur, M., Kell, L., Cardinale, M., Schirripa, M., Kitakado, T., Yemane, D., Piner, K. R., et al. (2021). A cookbook for using model diagnostics in integrated stock assessments. *Fisheries Research*, 240:105959.

Castillo Jordan, C., Hampton, J., Teears, T., and Hamer, P. (2023). Follow up work on 2022 skipjack assessment recommendations. Technical Report WCPFC/SC19-SA-WP-07, Koror, Palau, 16–24 August 2023.

Castillo-Jordán, C., Teears, T., Hampton, J., Davies, N., Scutt Phillips, J., McKechnie, S., Peatman, T., MacDonald, J., Day, J., Magnusson, A., Scott, R., Scott, F., Pilling, G., and Hamer, P. (2022). Stock assessment of skipjack tuna in the western and central Pacific Ocean: 2022. Technical Report WCPFC-SC18-2022/SA-WP-01 (Rev5).

Davies, N., Bouye, F., and Hampton, J. (2025). Developments in the MULTIFAN-CL software 2024-25. Technical Report WCPFC-SC21-2025/SA-IP-02, Nuku'alofa, Tonga, 13-21 August 2025.

Davies, N., Fournier, D., Bouye, F., and Hampton, J. (2022). Developments in the MULTIFAN-CL software 2021-2022. Technical Report WCPFC-SC18-2022/SA-IP-03.

Davies, N., Fournier, D., and Hampton, J. (2019). Developments in the MULTIFAN-CL software 2018-2019. Technical Report WCPFC-SC15-2019/SA-IP-02, Pohnpei, Federated States of Micronesia.

Day, J., Magnusson, A., Teears, T., Hampton, J., Davies, N., Castillo Jordan, C., Peatman, T., Scott, R., Scutt Phillips, J., McKechnie, S., Scott, F., Yao, N., Pilling, G., Williams, P., and Hamer, P. (2023). Stock assessment of bigeye tuna in the western and central pacific ocean: 2023. Technical Report WCPFC-SC19-2023/SA-WP-05.

Ducharme-Barth, N., Castillo-Jordan, C., Hampton, J., Williams, P., Pilling, G., and Hamer, P. (2021). Stock assessment of swordfish in the southwest Pacific Ocean. Technical Report WCPFC-SC17-2021/SA-WP-04.

Ducharme-Barth, N. and Vincent, M. (2021). Focusing on the front end: A framework for incorporating in uncertainty in biological parameters in model ensembles of integrated stock assessments. Technical Report WCPFC-SC17-2021-SA-WP-05.

Ducharme-Barth, N., Vincent, M., Pilling, G., and Hampton, J. (2019). Simulation analysis of pole and line CPUE standardization approaches for skipjack tuna in the WCPO. Technical Report WCPFC-SC15-2019/SA-WP-04, Pohnpei, Federated States of Micronesia 12-20 August 2019.

Ducharme-Barth, N. D., Grüss, A., Vincent, M. T., Kiyofuji, H., Aoki, Y., Pilling, G., Hampton, J., and Thorson, J. T. (2022). Impacts of fisheries-dependent spatial sampling patterns on catch-per-unit-effort standardization: A simulation study and fishery application. *Fisheries Research*, 246:106169.

Fournier, D. and Archibald, C. P. (1982). A general-theory for analyzing catch at age data. *Canadian Journal of Fisheries and Aquatic Sciences*, 39(8):1195–1207.

Fournier, D., Hampton, J., and Sibert, J. (1998). MULTIFAN-CL: a length-based, age-structured model for fisheries stock assessment, with application to South Pacific albacore, *Thunnus alalunga*. *Canadian Journal of Fisheries and Aquatic Sciences*, 55:2105–2116.

Fournier, D. A., Skaug, H. J., Ancheta, J., Ianelli, J., Magnusson, A., Maunder, M. N., Nielson, A., and Sibert, J. (2012). AD Model Builder: using automatic differentiation for statistical inference of highly parameterized complex nonlinear models. *Optimization Methods and Software*, 27(2):233–249.

Francis, R. I. C. C. (1992). Use of risk analysis to assess fishery management strategies: A case study using orange roughy (ıt Hoplostethus atlanticus) on the Chatham Rise, New Zealand. *Canadian Journal of Fisheries and Aquatic Science*, 49:922–930.

Gaertner, D., gado de Molina, A., Ariz, J., Pianet, R., and Hallier, J. P. (2008). Variability of the growth parameters of the skipjack tuna (*Katsuwonus pelamis*) among areas in the eastern Atlantic: analysis from tagging data within a meta-analysis approach. *Aquatic Living Resources*, 21:349–356.

Grewe, P., Proctor, C., Adam, M., Jauhary, A., Schafer, K., Itano, D., Evans, K., Killian, A., Foster, S., Gosselin, T., et al. (2019). Population structure and connectivity of tropical tuna species across the Indo-Pacific Ocean region.

Hamer, P. (2022). Report from the SPC Pre-assessment Workshop – March 2022. Technical Report WCPFC-SC18-2022/SA-IP-02, Pacific Community.

Hamer, P. (2025). Summary report from the SPC Pre-assessment Workshop – April 2025. Technical Report WCPFC-SC21-2025/SA-IP-01, Pacific Community.

Hampton, J. (2000). Natural mortality rates in tropical tunas: size really does matter. *Canadian Journal of Fisheries and Aquatic Science*, 57:1002–1010.

Hampton, J. and Fournier, D. (2001). A spatially-disaggregated, length-based, age-structured population model of yellowfin tuna (*Thunnus albacares*) in the western and central Pacific Ocean. *Marine and Freshwater Research*, 52:937–963.

Hampton, J. and Williams, P. (2016). Annual estimates of purse seine catches by species based on alternative data sources. Technical Report WCPFC-SC12-2016/ST-IP-03, Bali, Indonesia, 3–11 August 2016.

Harley, S. J. (2011). A preliminary investigation of steepness in tunas based on stock assessment results. Technical Report WCPFC-SC7-2011/SA-IP-08, Pohnpei, Federated States of Micronesia, 9–17 August 2011.

Hoyle, S., Kleiber, P., Davies, N., Harley, S., and Hampton, J. (2010). Stock assessment of skipjack tuna in the western and central Pacific Ocean. Technical Report WCPFC-SC6-2010/ST-IP-02, Nuku'alofa, Tonga, 10–19 August 2010.

Itano, D. (2000). The reproductive biology of yellowfin tuna (*Thunnus albacares*) in Hawaiian waters and the western tropical Pacific Ocean: Project summary. JIMAR Contribution 00-328 SOEST 00-01.

Kinoshita, J., Aoki, Y., Ducharme-Barth, N., and Kiyofuji, H. (2019). Standardized catch per unit effort (CPUE) of skipjack tuna of the Japanese pole-and-line fisheries in the WCPO from 1972 to 2018. Technical Report WCPFC-SC15-2019/SA-WP-14, Pohnpei, Federated States of Micronesia.

Kiyofuji, H., Aoki, Y., Kinoshita, J., Okamoto, S., Masujima, M., Matsumoto, T., Fujioka, K., Ogata, R., Nakao, T., Sugimoto, N., and Kitagawa, T. (2019a). Northward migration dynamics of skipjack tuna (*Katsuwonus pelamis*) associated with the lower thermal limit in the western Pacific Ocean. *Progress in Oceanography*, 175:55–67.

Kiyofuji, H. and Ochi, D. (2016). Proposal of alternative spatial structure for skipjack stock assessment in the WCPO. Technical Report WCPFC-SC12-2016/SA-IP-09, Bali, Indonesia, 3–11 August 2016.

Kiyofuji, H., Ohashi, S., Kinoshita, J., and Aoki, Y. (2019b). Overview of historical skipjack length and weight data collected by the Japanese pole-and-line fisheries and Research vessel (R/V) from 1953 to 2017. Technical report, WCPFC-SC15-2019/SA-IP-12.

Lawson, T. (2011). Purse-seine length frequencies corrected for selectivity bias in grab samples collected by observers. Technical Report WCPFC-SC7-2011/ST-IP-02, Pohnpei, Federated States of Micronesia, 9–17 August 2011.

Lehodey, P., Bertignac, M., Hampton, J., Lewis, A., and Picaut, J. (1997). El Niño Southern Oscillation and tuna in the western Pacific. *Nature*, 389:715–718.

Lehodey, P., Senina, I., and Murtugudde, R. (2008). A spatial ecosystem and populations dynamics model (SEAPODYM) – Modeling of tuna and tuna-like populations. *Progress in Oceanography*, 78(4):304–318.

Leroy, B. (2000). Preliminary results on skipjack (*Katsuwonus pelamis*) growth. Technical Report SKJ-1, 13th Meeting of the Standing Committee on Tuna and Billfish. Noumea, New Caledonia.

Lorenzen, K. (1996). The relationship between body weight and natural mortality in juvenile and adult fish: a comparison of natural ecosystems and aquaculture. *Journal of Fish Biology*, 49(4):627–642.

Macdonald, J., Day, J., Magnusson, A., Maunder, M., Aoki, Y., Matsubara, N., Tsuda, Y., McKechnie, S., Teears, T., Leroy, B., et al. (2022). Review and new analyses of skipjack growth in the western and central Pacific Ocean. Technical report, WCPFC-SC18-2022/SA-IP-06.

Magnusson, A., Day, J., Teears, T., Hampton, J., Davies, N., Castillo Jordan, C., Peatman, T., Scott, R., Scutt Phillips, J., McKechnie, S., Scott, F., Yao, N., Pilling, G., Williams, P., and Hamer, P. (2023). Stock assessment of yellowfin tuna in the western and central pacific ocean: 2023. Technical Report WCPFC-SC19-2023/SA-WP-04.

Matsubara, N., Aoki, Y., and Tsuda, Y. (2022). Historical developments of fishing devices in japanese pole-and-line fishery. Technical Report WCPFC-SC18-2022/SA-IP-16.

Maunder (2001). Growth of skipjack tuna (*Katsuwonus pelamis*) in the easter Pacific Ocean, as estimate from tagging data. Technical Report Bulletin of the Inter-American Tropical Tuna Commision, vol. 22.

Maunder, M. N. and Piner, K. R. (2015). Contemporary fisheries stock assessment: many issues still remain. *ICES Journal of Marine Science*, 72(1):7–18.

McKechnie, S., Hampton, J., Pilling, G. M., and Davies, N. (2016). Stock assessment of skipjack tuna in the western and central Pacific Ocean. Technical Report WCPFC-SC12-2016/SA-WP-04, Bali, Indonesia, 3–11 August 2016.

Minte-Vera, C. V., Maunder, M. N., Aires-da Silva, A. M., Satoh, K., and Uosaki, K. (2017). Get the biology right, or use size-composition data at your own risk. *Fisheries research*, 192:114–125.

Moore, B. R., Bell, J. D., Evans, K., Farley, J., Grewe, P. M., Hampton, J., Marie, A. D., Minte-Vera, C., Nicol, S., Pilling, G. M., Scutt Phillips, J., Tremblay-Boyer, L., Williams, A. J., and Smith, N. (2020). Defining the stock structures of key commercial tunas in the Pacific Ocean I: Current knowledge and main uncertainties. *Fisheries Research*, 230:105525.

Neubauer, P., Kim, K., A'mar, T., and Large, K. (2023). Addressing uncertainty in wcpfc stock assessments: Review and recommendations from WCPFC project 113. Technical Report WCPFC/SC19-SA-WP-10, Koror, Palau, 16–24 August 2023.

Nishimoto, M., Aoki, Y., Matsubara, N., Hamer, P., and Tsuda, Y. (2024). Estimating fish stock biomass using a bayesian state-space model: accounting for catchability change due to technological progress. *Frontiers in Marine Science*, 11:1458257.

Nishimoto, M., Yoshinori, A., Matsubara, N., Tsuda, Y., Kiyofuji, H., Teears, T., Yao, N., and Hamer, P. (2025). Cpue standardization using sdmTMB for skipjack tuna stock assessment. Technical report, WCPFC-SC21-SA-IP-05.

Ochi, D., Ijima, H., and Kiyofuji, H. (2016). A re-consideration of growth pattern of skipjack on the western central Pacific. Technical Report WCPFC-SC12-2016/SA-IP-08, Bali, Indonesia, 3–11 August 2016.

Ohashi, S., Aoki, Y., Tanaka, F., Fujioka, K., Aoki, A., and Kiyofuji, H. (2019). Reproductive traits of female skipjack tuna (*Katsuwonus pelamis*) in the western central pacific ocean (wcpo). Technical Report WCPFC-SC15-2019/SA-WP-10, Pohnpei, Federated States of Micronesia.

Palomares, M. L. and Pauly, D. (2019). On the creeping increase of vessels' fishing power. *Ecology and Society*, 24(3).

Peatman, T. (2025). Analysis of tag seeding data for the 2025 skipjack assessment: reporting rates for purse seine fleets. Technical report, WCPFC-SC21-SA-IP-07.

Peatman, T., Day, J., Magnusson, A., Teears, T., Williams, P., Hampton, J., and Hamer, P. (2023a). Analysis of purse-seine and longline size frequency data for the 2023 bigeye and yellowfin tuna assessments. *19th Regular Session of the WCPFC Scientific Committee*, WCPFC-SC19-2023/SA-IP-03.

Peatman, T., Scutt Phillips, J., and Nicol, S. (2025). Analysis of tagging data for the 2025 skipjack assessment: corrections to tagrelease for tagging conditions. Technical report, WCPFC-SC21-SA-IP-06.

Peatman, T., Williams, P., and Nicol, S. (2023b). Project 60: Progress towards achieving SC18 recommendations.

Pilling, G., Scott, R., Davies, N., and Hampton, J. (2016). Approaches used to undertake management projections of WCPO tuna stocks based upon MULTIFAN-CL stock assessments. Technical Report WCPFC-SC12-2016/MI-IP-04, Bali, Indonesia, 3–11 August 2016.

Punt, A., Maunder, M., and Ianelli, J. (2023). Independent review of recent WCPO yellowfin tuna assessment. Working Paper WCPFC-SC19-2023/SA-WP-01. Nineteenth Regular Session of the ....

Rice, J., Harley, S., Davies, N., and Hampton, J. (2014). Stock assessment of skipjack tuna in the western and central Pacific Ocean. Technical Report WCPFC-SC10-2014/SA-WP-05, Majuro, Republic of the Marshall Islands, 6–14 August 2014.

Schnute, J. (1981). A versatile growth model with statistically stable parameters. *Canadian Journal of Fisheries and Aquatic Sciences*, 38(9):1128–1140.

Scutt Phillips, J., Lehodey, J., Hampton, J., Hamer, P., Senina, I., and Nicol, S. (2022). Quantifying rates of mixing in tagged, WCPO skipjack tuna. Technical Report WCPFC-SC18-2022/SA-WP-04.

Scutt Phillips, J., Sen Gupta, A., Senina, I., Sebille, E., Lange, M., Lehodey, P., J, H., and Nichol, S. (2018). An individual-based model of skipjack tuna (*Katsuwonus pelamis*) movement in the tropical Pacific Ocean. *Progress in Oceanography*, 164:63–74.

Senina, I., Bonnin, L., Lengaigne, M., Kiyofuji, H., Beunafe, K., Fuller, D., and Nicol, S. (2025). Reference model of skipjack tuna using SEAPODYM with catch, length, conventional tagging and early-life history stages data. Technical report, WCPFC-SC21-SA-IP-20.

Senina, I., Lehodey, P., Calmettes, B., Nichol, S. J., Caillot, S., J, H., and P, W. (2016). Predicting skipjack tuna dynamics and effects of climate change using SEAPODYM with fishing and tagging data. Technical Report WCPFC-SC12-2016/EB WP01.

Senina, I., Lehodey, P., Sibert, J., and Hampton, J. (2020). Integrating tagging and fisheries data into a spatial population dynamics model to improve its predictive skills. *Canadian Journal of Fisheries and Aquatic Sciences*, 77(3):576–593.

SPC-OFP (2013). Purse seine effort: a recent issue in logbook reporting. Technical Report WCPFC-TCC9-2013-18, Pohnpei, Federated States of Micronesia.

SPC-OFP (2024). Western and Central Pacific Fisheries Commission, Tuna Fishery Yearbook, 2024. Technical report, Oceanic Fisheries programme, Secretariat of the Pacific Community, Noumea, New Caledonia.

Stewart, I. J. and Martell, S. J. (2014). A historical review of selectivity approaches and retrospective patterns in the Pacific halibut stock assessment. *Fisheries Research*, 158:40–49.

Tanabe, T., Kayama, S., and Ogura, M. (2003). Precise age determination of young to adult skipjack tuna (ıt Katsuwonus pelamis) with validation of otolith daily increment. Technical Report SCTB16/SKJ-08, 16th Meeting of the Standing Committee on Tuna and Billfish, Mooloolaba, Queensland, Australia, 9–16 August.

Teears, T., Castillo-Jordan, C., Davies, N., Day, J., Hampton, J., Magnusson, A., Peatman, T., Pilling, G., Xu, H., Vidal, T., Williams, P., and Hamer, P. (2024). Stock assessment of South Pacific albacore: 2024. Technical Report WCPFC-SC20-2024/SA-WP-01, Manilla, Phillippines, 14–21 August 2024.

Teears, T., Ghergariu, M., Hampton, J., Peatman, T., Scutt Phillips, J., and Hamer, P. (2025). Background analyses and data inputs for the 2025 skipjack tuna stock assessment in the western and central Pacific Ocean. Technical Report WCPFC-SC21-2025/SA-IP-17.

Teears, T., Yoshinori, A., Matsubura, N., Tsuda, Y., Castillo-Jordan, C., Hampton, J., Scheitner, E., Scutt Phillips, J., Peatman, T., Bigelow, K., and Hamer, P. (2022). Background analyses and data inputs for the 2022 skipjack tuna stock assessment in the western and central Pacific Ocean. Technical Report SC18-SA-IP-05.

Thorson, J. T., Johnson, K. F., Methot, R. D., and Taylor, I. G. (2017). Model-based estimates of effective sample size in stock assessment models using the Dirichlet-multinomial distribution. *Fisheries Research*, 192:84–93.

Vidal, T., Hamer, P., Escalle, L., and Pilling, G. (2020). Assessing trends in skipjack tuna abundance from purse seine catch and effort data in the WCPO. Technical Report WCPFC-SC16-SA-IP-09 Rev 1.

Vincent, M., Pilling, G., and Hampton, J. (2019a). Stock assessment of skipjack tuna in the WCPO. Technical Report WCPFC-SC15-2019/SA-WP-05, Pohnpei, Federated States of Micronesia.

Vincent, M. T., Aoki, Y., Kiyofuji, H., Hampton, J., and Pilling, G. M. (2019b). Background analyses for the 2019 stock assessment of skipjack tuna. Technical Report WCPFC-SC15-2019/SA-IP-04, Pohnpei, Federated States of Micronesia.

Wang, X., Chen, Y., Truesdell, S., Xu, L., Cao, J., and Guan, W. (2014). The large-scale deployment of fish aggregation devices alters environmentally-based migratory behavior of skipjack tuna in the western Pacific Ocean. *PLoS One*, 9(5):e98226.

Wild, A. and Hampton, J. (1994). A review of the biology and fisheries for skipjack tuna, *Katsuwonus pelamis*, in the Pacific Ocean. FAO Fisheries Technical Paper (FAO) 336(2):1–51.

15 Tables

Table 1: Definition of fisheries by gear, model region (Region), flags, selectivity groupings (Sel Group), number of selectivity nodes (Sel Nodes), tag return groupings (Recap Group), and Dirichlet multinomial groupings (DM Group) for the 2025 MFCL skipjack tuna stock assessment (refer to Figure 1). Note: selectivity groupings for CPUE indices were removed in latter phases of estimation (see Section 6.2.1 for further information).

Fishery	Gear	Model Code-Fleets	Flags	Region	Sel Group	Sel Nodes	Recap Group	DM Group
1	PL	1.PL.ALL.1	ALL	1	1	4	1	1
2	PS	2.PS.ALL.1	ALL	1	2	4	2	1
3	LL	3.LL.ALL.1	ALL	1	3	3	3	2
4	PL	4.PL.ALL.2	ALL	2	4	4	4	1
5	PS	5.PS.ALL.2	ALL	2	5	4	5	1
6	LL	6.LL.ALL.2	ALL	2	6	3	6	2
7	PL	7.PL.ALL.3	ALL	3	7	4	7	1
8	PS	8.PS.ALL.3	ALL	3	8	4	8	1
9	LL	9.LL.ALL.3	ALL	3	9	3	9	2
10	Dom	10.Z.PH.5	PH	5	10	6	10	3
11	Dom	11.Z.ID.5	ID	5	11	5	10	3
12	PS	12.S.PH.5	PH	5	12	5	10	3
13	PS	13.S.ID.5	ID	5	13	5	10	3
14	PL	14.PL.ALL.5	ALL	5	14	6	10	1
15	PS.ASSOC	15.SA.DW.5	DW	5	15	4	10	4
16	PS.UNASSOC	16.SU.DW.5	DW	5	16	4	10	4
17	Dom	17.Z.VN.5	VN	5	17	5	11	3
18	LL	18.LL.ALL.5	ALL	5	18	3	12	2
19	PL	19.PL.ALL.6	ALL	6	19	4	13	1
20	PS.ASSOC	20.SA.ALL.6	ALL	6	20	4	14	4
21	PS.UNASSOC	21.SU.ALL.6	ALL	6	21	4	14	4
22	LL	22.LL.ALL.6	ALL	6	22	3	15	2
23	PL	23.PL.ALL.4	ALL	4	23	4	16	1
24	LL	24.LL.ALL.4	ALL	4	24	3	17	2
25	PL	25.PL.ALL.7	ALL	7	25	4	18	1
26	PS.ASSOC	26.SA.ALL.7	ALL	7	26	4	19	4
27	PS.UNASSOC	27.SU.ALL.7	ALL	7	27	4	19	4
28	LL	28.LL.ALL.7	ALL	7	28	3	20	2
29	PL	29.PL.ALL.8	ALL	8	29	4	21	1
30	PS.ASSOC	30.SA.ALL.8	ALL	8	30	4	22	4
31	PS.UNASSOC	31.SU.ALL.8	ALL	8	31	4	22	4
32	LL	32.LL.ALL.8	ALL	8	32	3	23	2
33	PL	33.PL.INDEX.JP.1	JP	1	33	4	24	1
34	PL	34.PL.INDEX.JP.2	JP	2	33	4	25	1
35	PL	35.PL.INDEX.JP.3	JP	3	33	4	26	1
36	PL	36.PL.INDEX.JP.4	JP	4	33	4	27	1
37	PS	37.PS.INDEX.PH.PH.5	PH	5	34	5	28	3
38	PL	38.PL.INDEX.JP.7	JP	7	33	4	29	1
39	PL	39.PL.INDEX.JP.8	JP	8	33	4	30	1
40	PS.UNASSOC	40.PS.UNASSOC.INDEX.ALL.6	ALL	6	35	4	31	4
41	PS.UNASSOC	41.PS.UNASSOC.INDEX.ALL.7	ALL	7	35	4	32	4
42	PS.UNASSOC	42.PS.UNASSOC.INDEX.ALL.8	ALL	8	35	4	33	4

Table 2: Reporting rate groupings (Group) and number of recaptures (Recaps) by fishery and program for the Pacific Tuna Tagging Program (PTTP), the Regional Tuna Tagging Program (RTTP), and the Japanese Tagging Program (JPTP) in the 2025 MFCL skipjack tuna stock assessment.

Fishery	Model Code-Fleets	Region	PTTP Recaps	RTTP Recaps	JPTP Recaps	PTTP Group	RTTP Group	JPTP Group
1	1.PL.ALL.1	1	0	0	752	1	1	12
2	2.PS.ALL.1	1	0	0	221	1	1	13
3	3.LL.ALL.1	1	0	0	0	1	1	1
4	4.PL.ALL.2	2	0	0	1278	1	1	14
5	5.PS.ALL.2	2	0	0	1051	1	1	15
6	6.LL.ALL.2	2	0	0	0	1	1	1
7	7.PL.ALL.3	3	0	0	1249	1	1	16
8	8.PS.ALL.3	3	0	0	50	1	1	17
9	9.LL.ALL.3	3	0	0	0	1	1	1
10	10.Z.PH.5	5	0	424	4	2	7	18
11	11.Z.ID.5	5	0	1	0	2	7	18
12	12.S.PH.5	5	235	1646	4	2	7	18
13	13.S.ID.5	5	4176	31	0	2	7	18
14	14.PL.ALL.5	5	0	826	5	2	7	18
15	15.SA.DW.5	5	410	169	54	2	7	18
16	16.SU.DW.5	5	1	7	0	2	7	18
17	17.Z.VN.5	5	0	0	0	1	1	1
18	18.LL.ALL.5	5	0	0	0	1	1	1
19	19.PL.ALL.6	6	0	0	0	1	1	1
20	20.SA.ALL.6	6	23168	2774	10	3	8	19
21	21.SU.ALL.6	6	4931	21	0	3	8	19
22	22.LL.ALL.6	6	0	0	0	1	1	1
23	23.PL.ALL.4	4	0	0	224	1	1	20
24	24.LL.ALL.4	4	0	0	0	1	1	1
25	25.PL.ALL.7	7	5	67	176	4	9	20
26	26.SA.ALL.7	7	6919	2263	738	5	10	21
27	27.SU.ALL.7	7	918	314	0	5	10	21
28	28.LL.ALL.7	7	0	0	0	1	1	1
29	29.PL.ALL.8	8	2	31	39	4	9	20
30	30.SA.ALL.8	8	1571	521	80	6	11	22
31	31.SU.ALL.8	8	121	322	0	6	11	22
32	32.LL.ALL.8	8	0	0	0	1	1	1

Table 3: Likelihoods by MFCL model component for Dirichlet groupings of 3, 4, and 41 fisheries groups.

Likelihood Component	DM-3 (3 groups)	DM-4 (4 groups)	DM-41 (41 groups)
LF	401,062.70	399,599.20	398,117.10
CPUE	1,211.80	1,286.30	1,190.10
Tags	31,134.50	31,395.30	31,435.80
Penalties	423.6	407.2	415.7
Total	433,851.30	432,706.50	431,175.50
No. of parameters	2010	2012	2086

Table 4: Description of symbols used in the yield and stock status analyses. For the purpose of this assessment, 'recent' for F is the average over the period 2020–2023 and for spawning potential is the average over the period 2021–2024 and 'latest' is 2024.

Symbol	Description
F_{MSY}	Fishing mortality-at-age producing the maximum sustainable yield (MSY)
f_{mult}	Fishing mortality multiplier at maximum sustainable yield (MSY)
$F_{\text{recent}}/F_{\text{MSY}}$	Average fishing mortality-at-age for a recent period (2020–2023) relative to F_{MSY}
MSY	Equilibrium yield at F_{MSY}
SB_{latest}	spawning potential in the latest time period (2024)
SB_{recent}	spawning potential for a recent period (2021–2024)
$SB_{F=0}$	Average spawning potential predicted in the absence of fishing for the period 2014–2023
$SB_{\text{latest}}/SB_{F=0}$	spawning potential in the latest time period (2024) relative to the average SB predicted to occur in the absence of fishing for the period 2014–2023
$SB_{\text{latest}}/SB_{\text{MSY}}$	spawning potential in the latest time period (2024) relative to that which will produce the maximum sustainable yield (MSY)
SB_{MSY}	spawning potential that will produce the maximum sustainable yield (MSY)
$SB_{\text{MSY}}/SB_{F=0}$	spawning potential that produces maximum sustainable yield (MSY) relative to the average spawning potential predicted to occur in the absence of fishing for the period 2014–2023
$SB_{\text{recent}}/SB_{F=0}$	spawning potential for a recent period (2021–2024) relative to the average spawning potential predicted to occur in the absence of fishing for the period 2014–2023
$SB_{\text{recent}}/SB_{\text{MSY}}$	spawning potential for a recent period (2021–2024) relative to the SB that produces maximum sustainable yield (MSY)
$Y_{F_{\text{recent}}}$	Equilibrium yield at average fishing mortality for a recent period (2020–2023)
$20\%SB_{F=0}$	WCPFC adopted limit reference point – 20% of spawning potential in the absence of fishing average over years $t-10$ to $t-1$ (2014–2023)
iTRP	WCPFC adopted interim target reference point (iTRP) – defined in CMM2022-01 skipjack managemen

Table 5: Summary of reference points over the model ensemble, along with results incorporating estimation uncertainty. Note that these values do not include estimation uncertainty, unless otherwise indicated.

	Mean	Median	Min	10%	90%	Max
F_{MSY}	0.28	0.28	0.22	0.25	0.32	0.37
f_{mult}	3.01	2.85	1.88	2.25	4.12	5.42
$F_{\text{recent}}/F_{\text{MSY}}$	0.35	0.35	0.18	0.24	0.44	0.53
MSY	2,506,046	2,374,800	1,819,600	2,090,400	3,200,800	4,204,000
SB_{latest}	3,715,913	3,365,822	2,320,595	2,747,472	5,231,863	5,801,571
SB_{recent}	3,681,316	3,248,438	2,337,134	2,641,802	5,337,579	6,023,691
$SB_{F=0}$	6,844,279	6,466,725	5,102,043	5,753,337	8,444,739	9,440,668
$SB_{\text{latest}}/SB_{F=0}$	0.54	0.53	0.42	0.46	0.62	0.82
$SB_{\text{latest}}/SB_{\text{MSY}}$	4.17	3.91	2.24	3.07	5.62	8.92
SB_{MSY}	924,241	893,900	399,400	624,900	1,232,000	1,908,000
$SB_{\text{MSY}}/SB_{F=0}$	0.13	0.14	0.07	0.10	0.16	0.20
$SB_{\text{recent}}/SB_{F=0}$	0.53	0.51	0.40	0.45	0.63	0.68
$SB_{\text{recent}}/SB_{\text{MSY}}$	4.11	3.91	2.14	2.98	5.60	8.92
$Y_{F_{\text{recent}}}$	440,394	438,000	362,400	398,500	486,800	562,600
$20\%SB_{F=0}$	1,368,856	1,293,345	1,020,409	1,150,667	1,688,948	1,888,134
$SB_{\text{recent}}/SB_{F=0}$:iTRP	0.98	0.98	0.83	0.94	1.01	1.05
Including estimation uncertainty						
$F_{\text{recent}}/F_{\text{MSY}}$	0.35	0.35	0.16	0.24	0.45	0.59
$SB_{\text{recent}}/SB_{F=0}$	0.53	0.51	0.37	0.45	0.63	0.74
$SB_{\text{recent}}/SB_{\text{MSY}}$	4.11	3.90	1.92	2.95	5.61	10.73

16 Figures

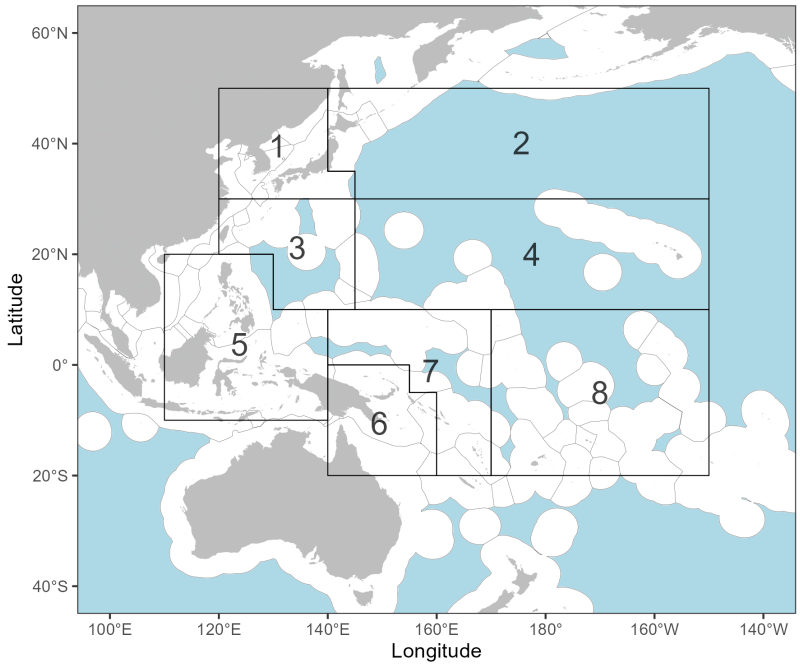

Figure 1: The geographical area covered by the stock assessment and the boundaries of the eight model regions used for the 2025 skipjack assessment.

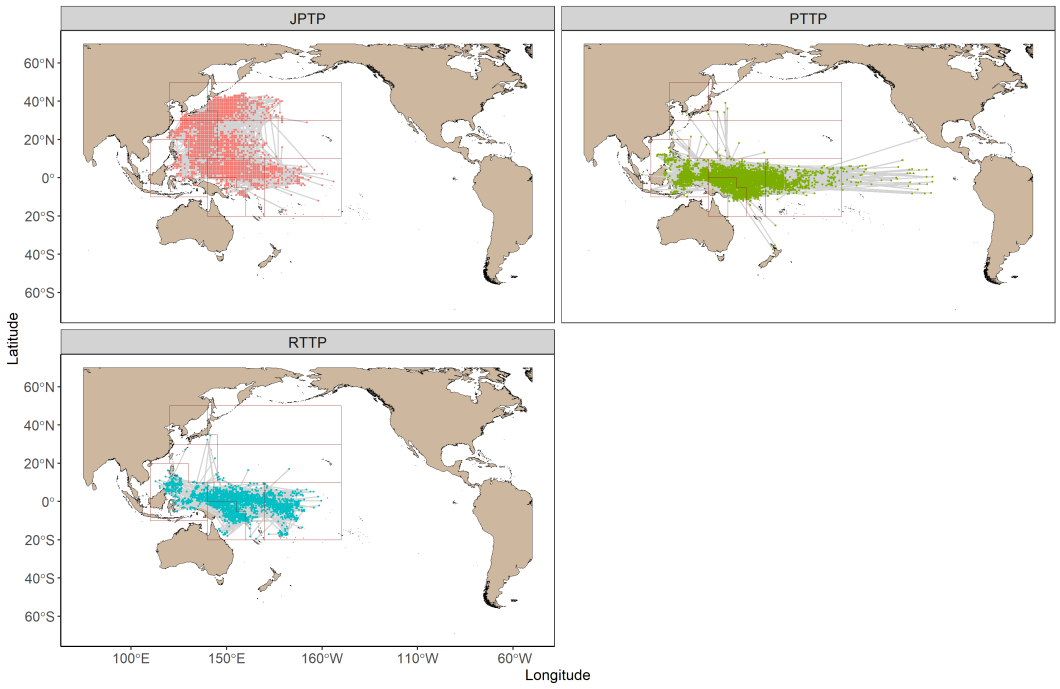

Figure 2: Mark-recapture tagging displacements for the Pacific Tuna Tagging Program (PTTP), the Regional Tuna Tagging Program (RTTP), and Japanese Tagging Program(JPTP).

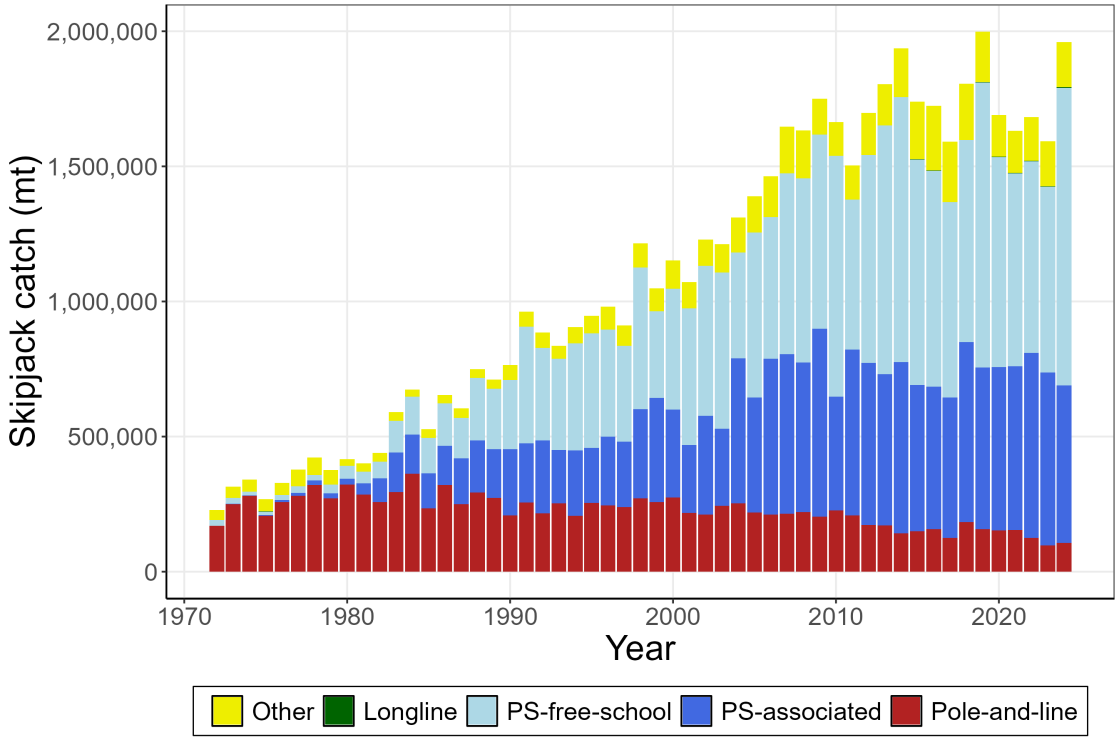

Figure 3: Annual catches of skipjack by gear type in the WCPO area covered by the assessment.

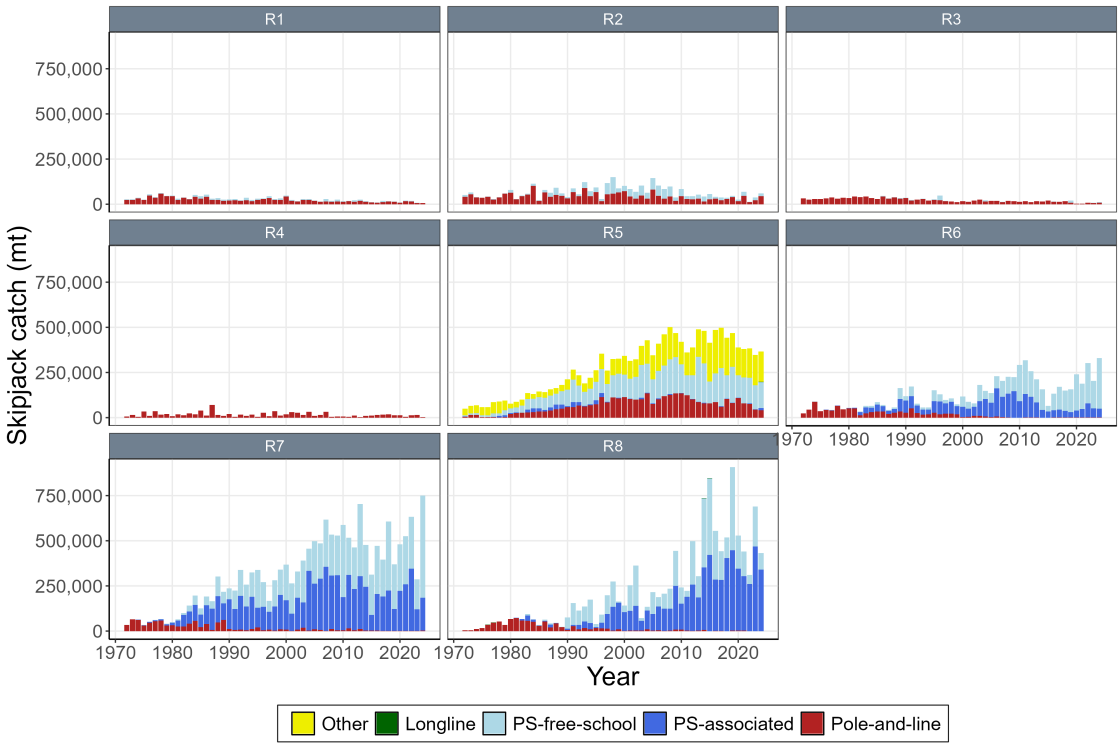

Figure 4: Annual catches of skipjack by gear type for each of the eight model regions.

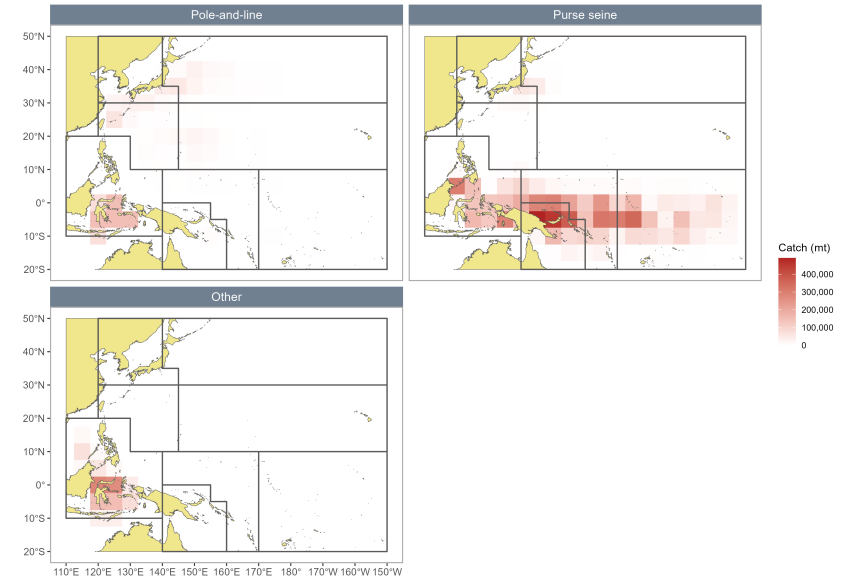

Figure 5: Distribution and magnitude of skipjack catches (mt) by gear type summed over the last 10 years (2015-2024) for 5°x5° cells.

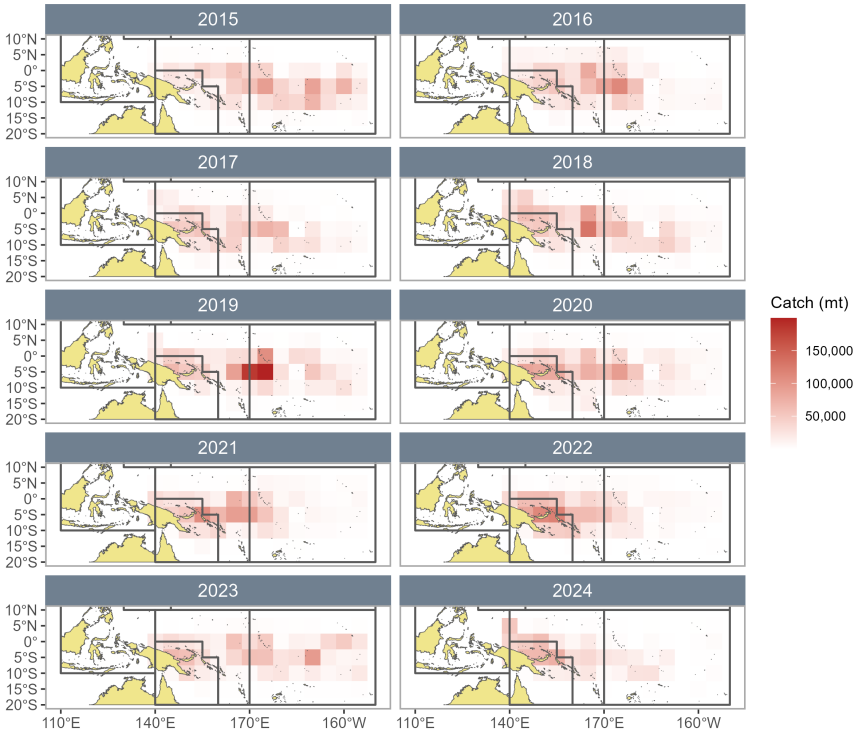

Figure 6: Annual distribution and magnitude of skipjack catches (mt) by gear type summed over the last 10 years (2015-2024) for 5°x5° cells in the equatorial regions.

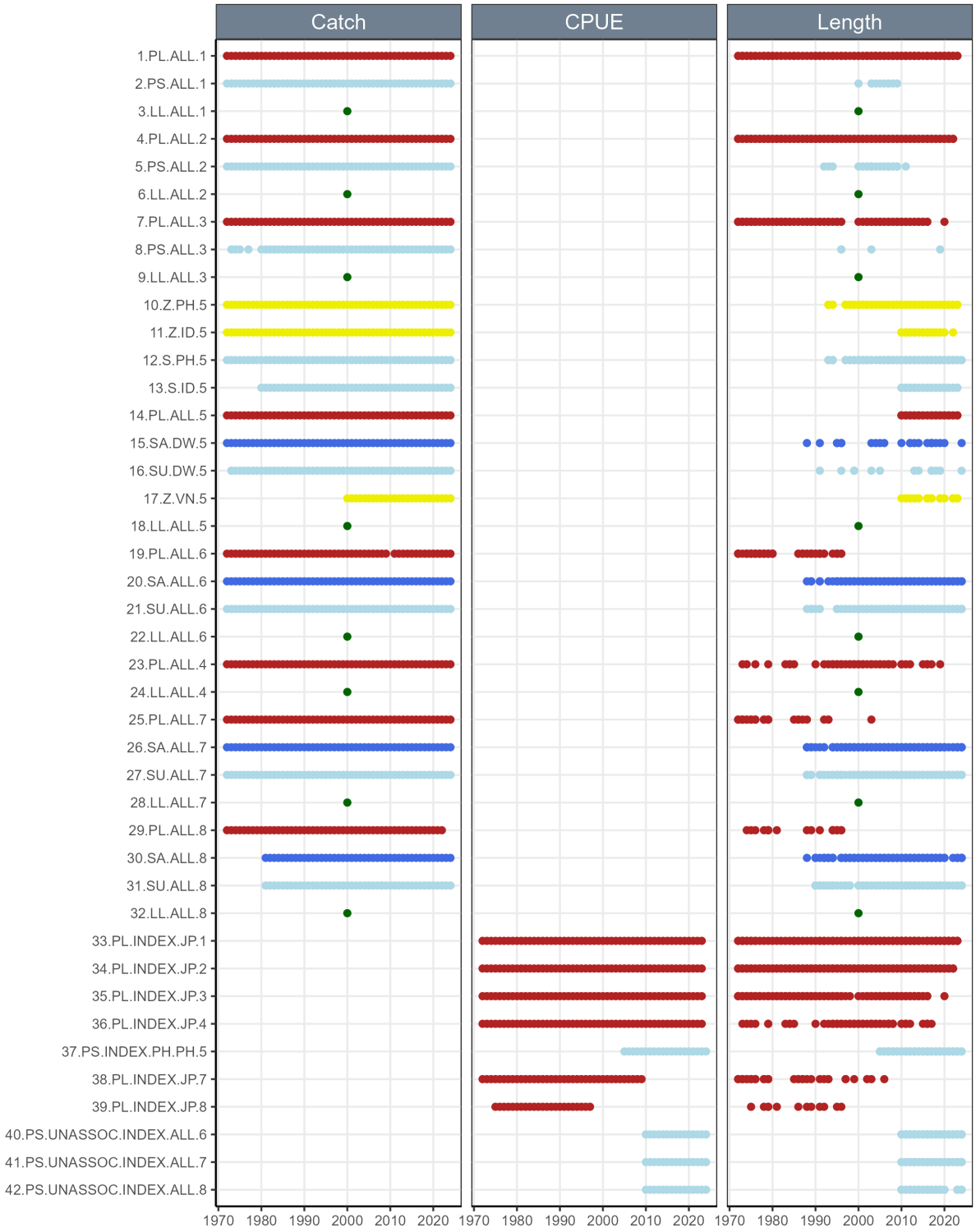

Figure 7: Summary of data coverage by fishery for the WCPO 2025 skipjack assessment.

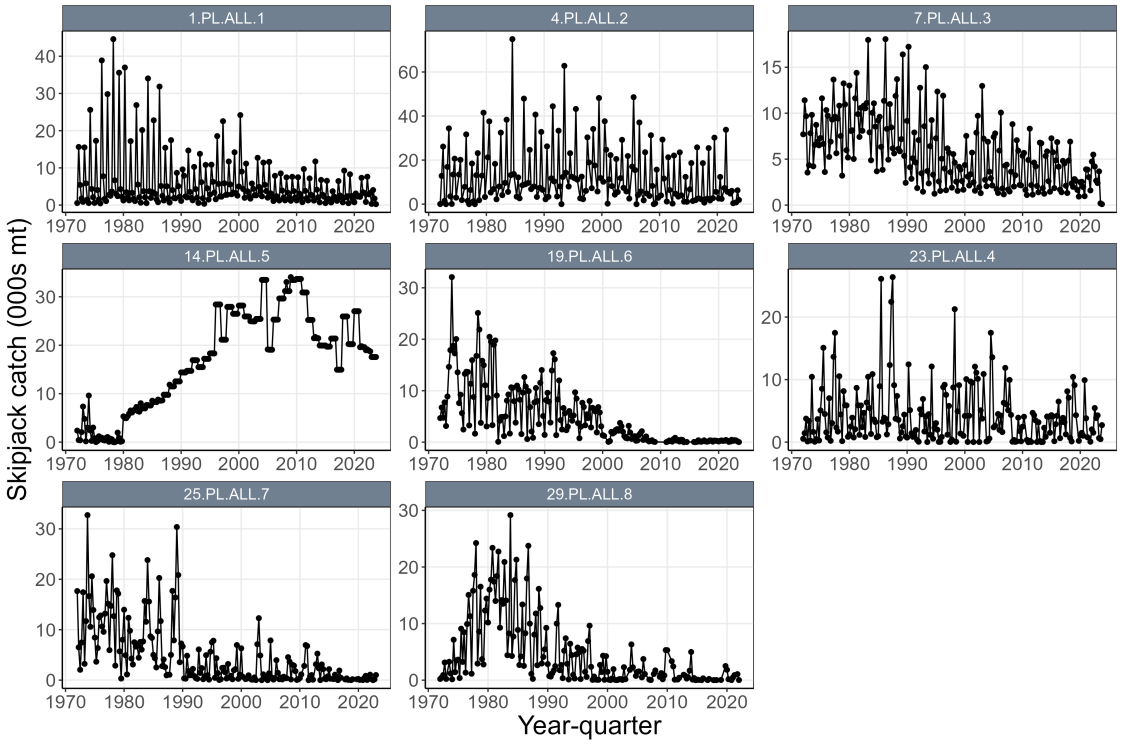

Figure 8: Time series of year-quarterly catches (mt) by fishery for the pole-and-line fisheries. Fishery labels indicate fishery number, gear type, flags, and region, respectively.

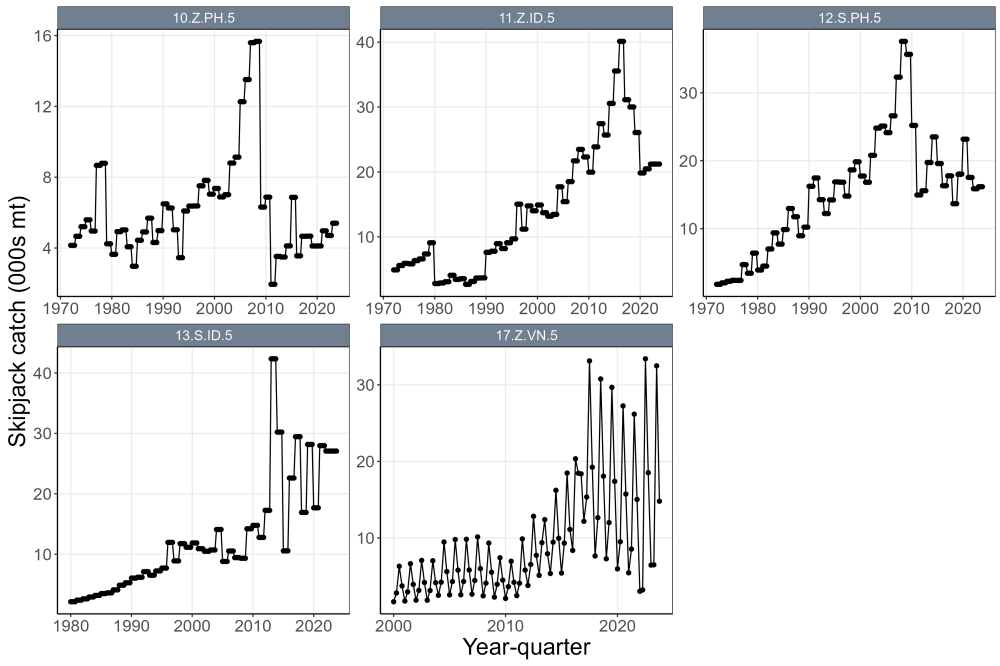

Figure 9: Time series of year-quarterly catches (mt) by fishery for the domestic fisheries in region 5 including ID, VN and PH for purse seine ('S') and assorted smaller gears ('Z'). Fishery labels indicate fishery number, gear type, flags, and region, respectively.

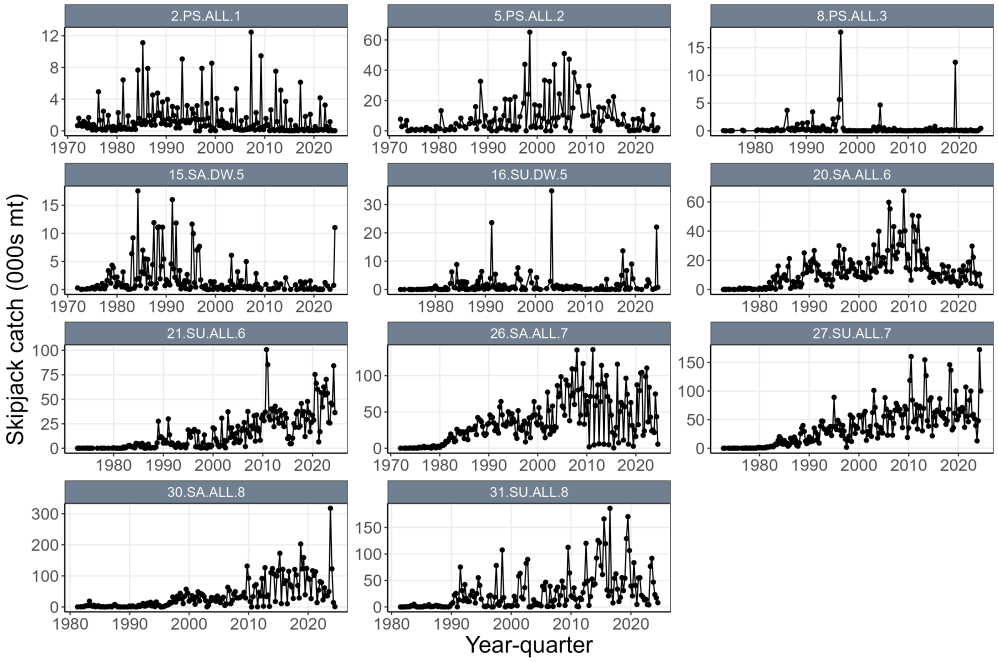

Figure 10: Time series of year-quarterly catches (mt) by fishery for the purse seine fisheries. Fishery labels indicate fishery number, gear type, flags, and region, respectively.

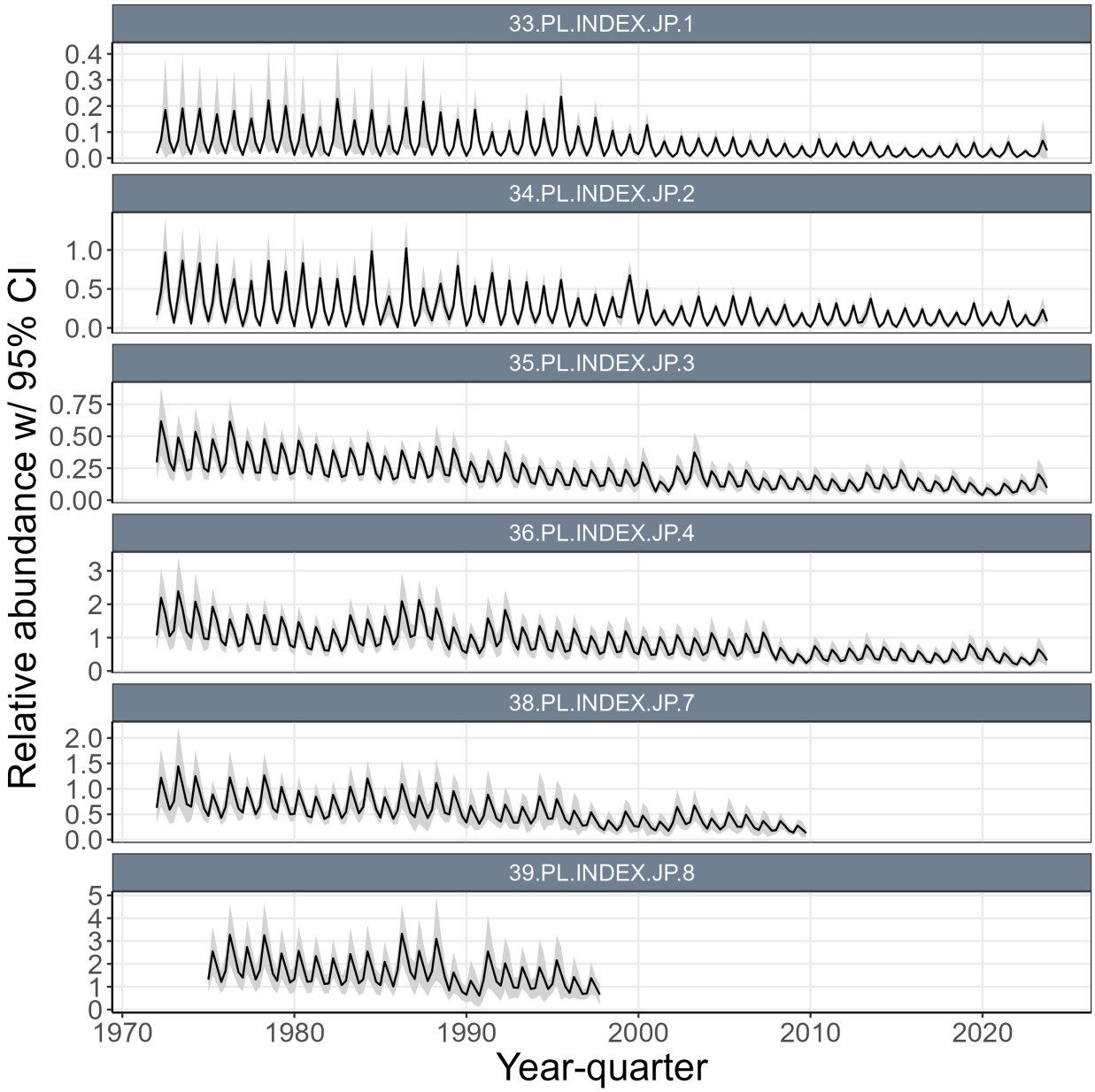

Figure 11: Standardised CPUE with 95% confidence interval (CI) for the Japanese pole-and-line fisheries in regions 1, 2, 3, 4, 7, and 8. Estimates include the application of effort creep adjustment and confidence intervals derived from bi-regionally grouped models (i.e., region 1 with 2, 3 with 4, and 7 with 8). Fishery labels indicate fishery number, gear type, flags, and region, respectively.

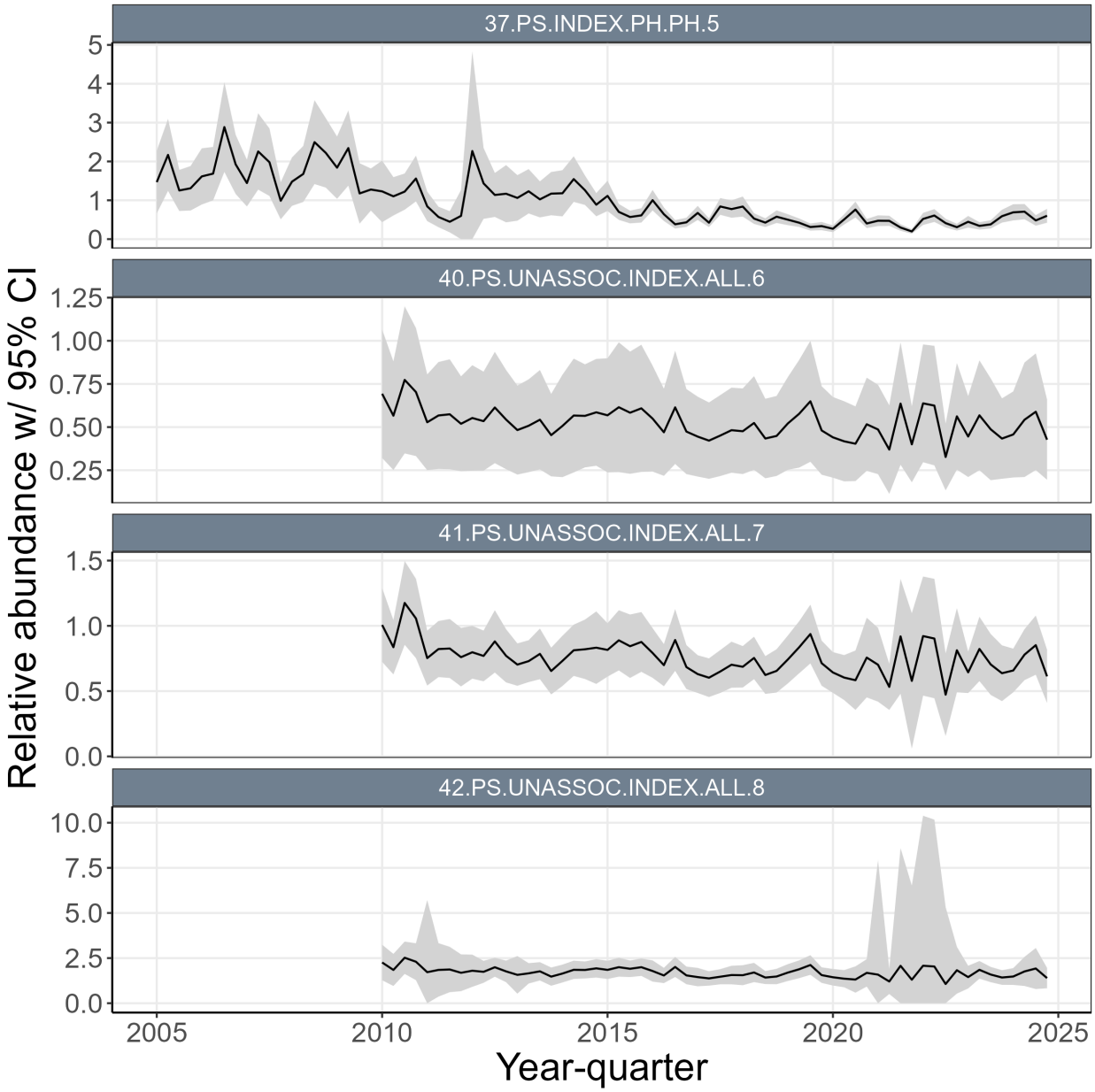

Figure 12: Standardised CPUE with 95% confidence interval (CI) for the 'unassociated' purse seine CPUE indices in regions 6, 7 and 8, and the Philippines purse seine index in region 5. Fishery labels indicate fishery number, gear type, flags, and region, respectively.

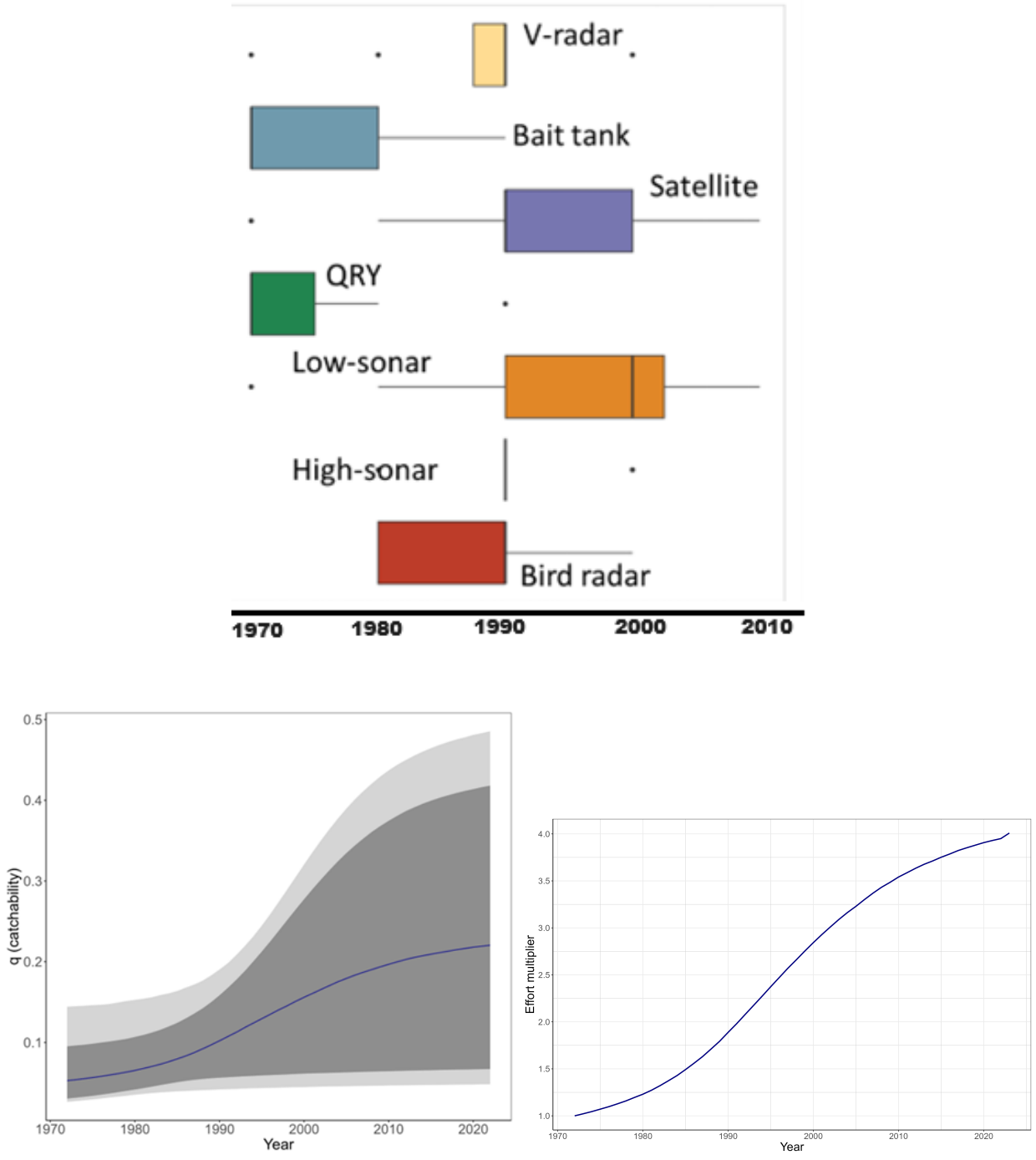

Figure 13: Boxplots of vessel adoption of various technologies for Japanese pole-and-line fishing (top), estimated catchability (q) parameter following a Gompertz parameterisation (bottom-left; blue line at median), and resulting effort multiplier derived by normalising the median q trajectory estimate (bottom-right). In the catchability plot (bottom-left), the dark grey shading indicates the 80% confidence interval (CI), and light grey shading indicates the 95% CI (plot adapted from Nishimoto et al. (2024)).

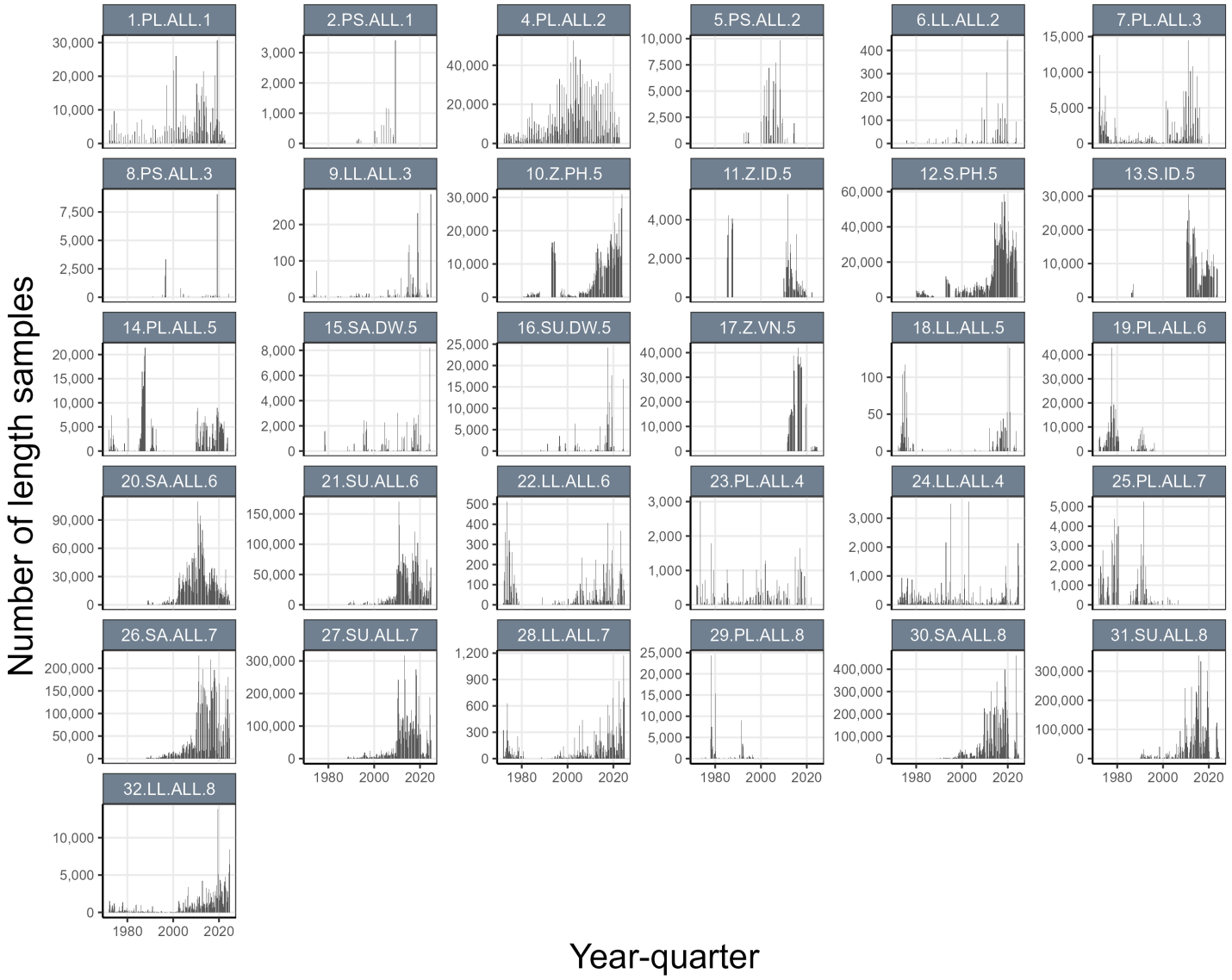

Figure 14: Plots of observed samples sizes for length composition for each fishery in the model across the model period. Note the difference in scale among fisheries.

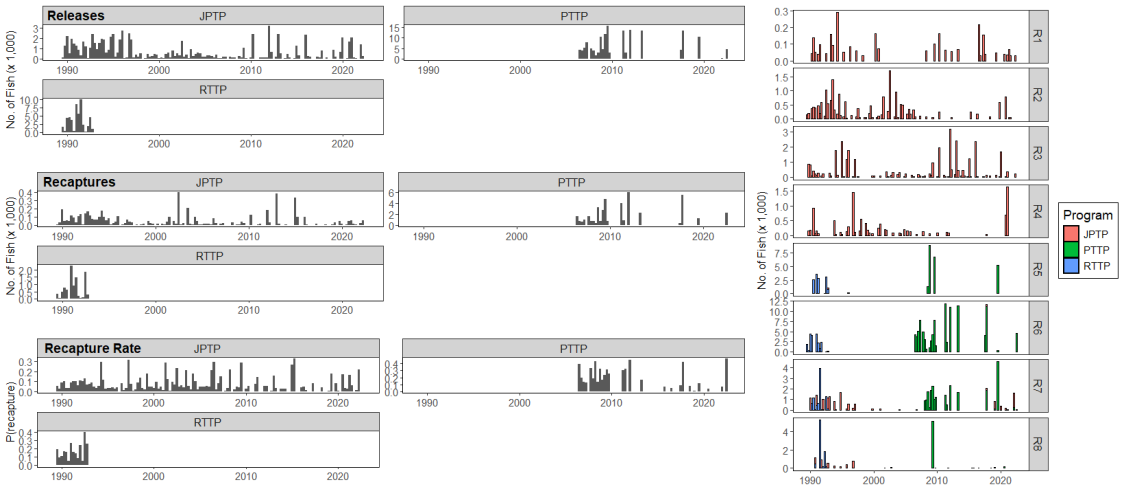

Figure 15: Summary plots of the number of releases, recaptures, and recapture rate of tags, by tagging program and region.

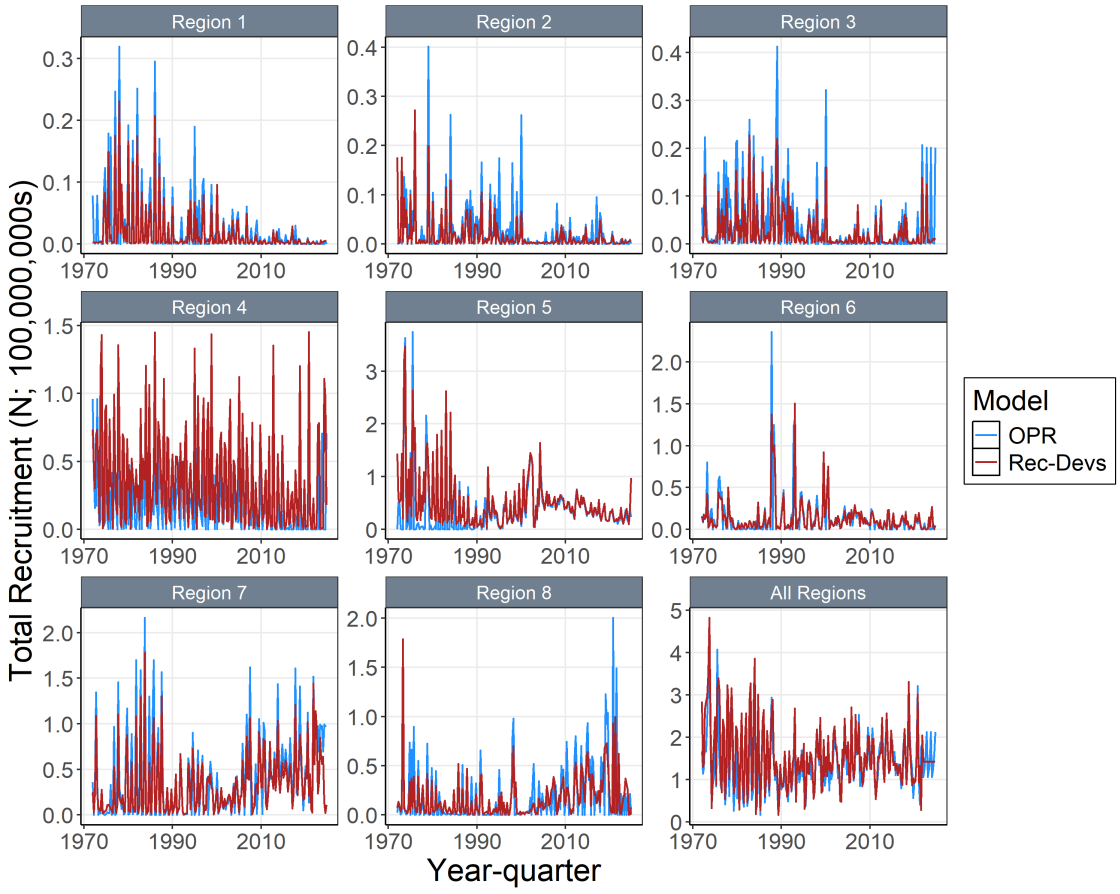

Figure 16: Annual time series of estimated quarterly recruitment summed across regions for the diagnostic model with orthogonal polynomial recruitment (OPR) in comparison to the equivalent 'Rec-Devs' version.

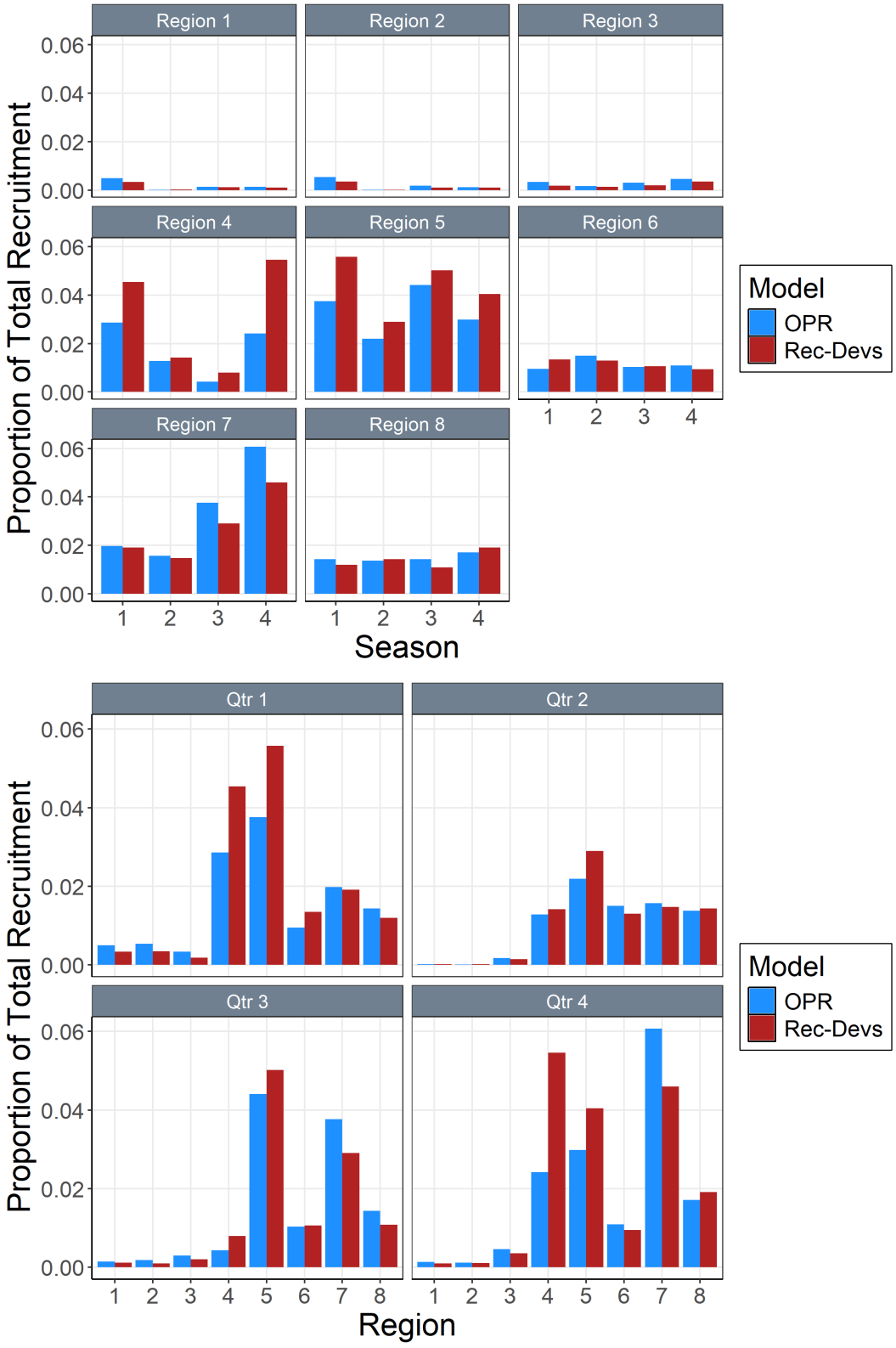

Figure 17: Estimated overall recruitment seasonal distribution among regions (top) and regional distribution among seasons (bottom) for the diagnostic model with orthogonal polynomial recruitment (OPR) in comparison to the equivalent 'Rec-Devs' version.

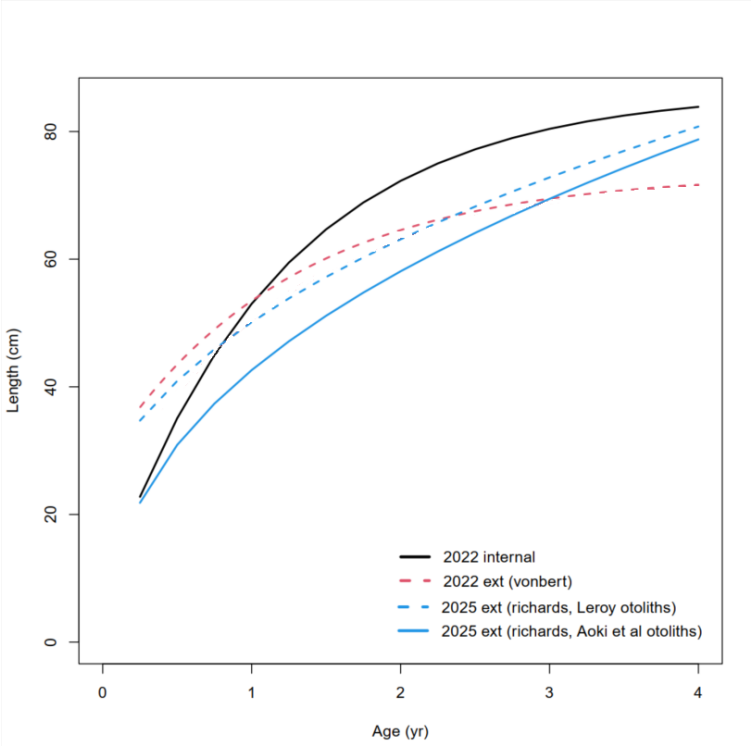

Figure 18: Growth curves estimated for skipjack including the 2022 MFCL estimated (2022 internal) , the 2022 externally estimated von Bertalanffy (2022 ext vonbert), the 2025 externally estimated Richards curve using the otolith data from Leroy (2000), and the 2025 externally estimated Richards curve using the otolith data from Aoki et al. (2024).

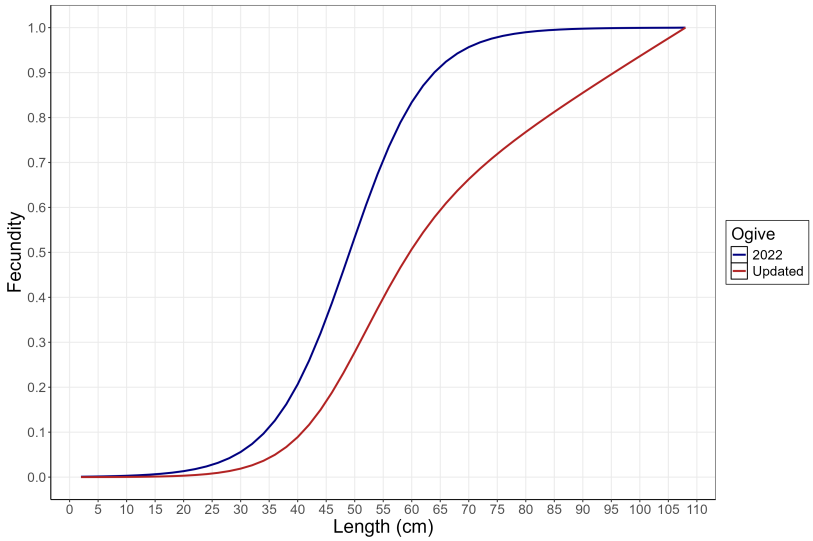

Figure 19: Maturity-at-length from the 2022 stock assessment (blue) and the Japan FRA updated (red) used in the 2025 stock assessment.

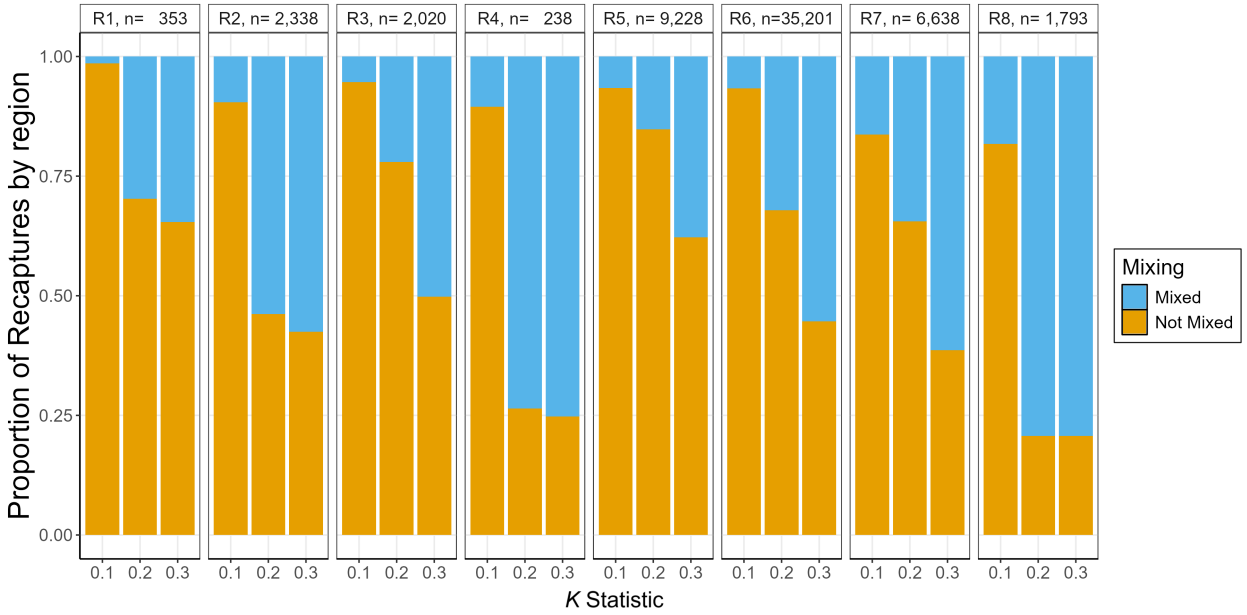

Figure 20: Proportion of recaptures by region and mixing assignment for dissimilarity statistic (K) at 0.1, 0.2, and 0.3 for skipjack tagging data in regions 1–8 from the Pacific Tuna Tagging Program (PTTP), Regional Tuna Tagging Program (RTTP), and the Japanese Tagging Program (JPTP). Total recaptures by region and program are indicated on each plot.

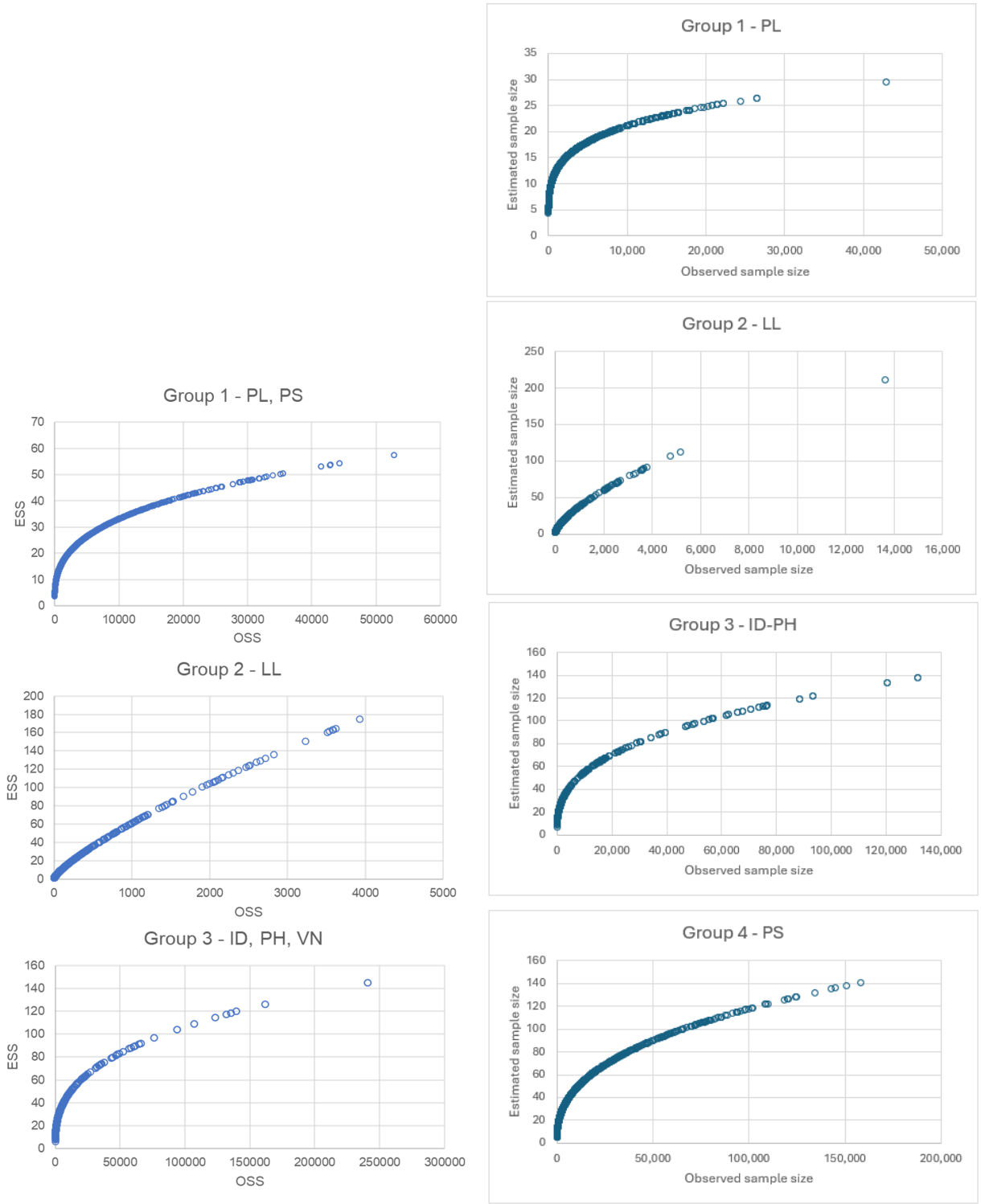

Figure 21: Plots of estimated effective sample (ESS) sizes versus observed sample sizes (OSS) from the MFCL implementation of Dirichlet-multinomial likelihood for the diagnostic 2022 (left) and 2025 (right) stock assessment models.

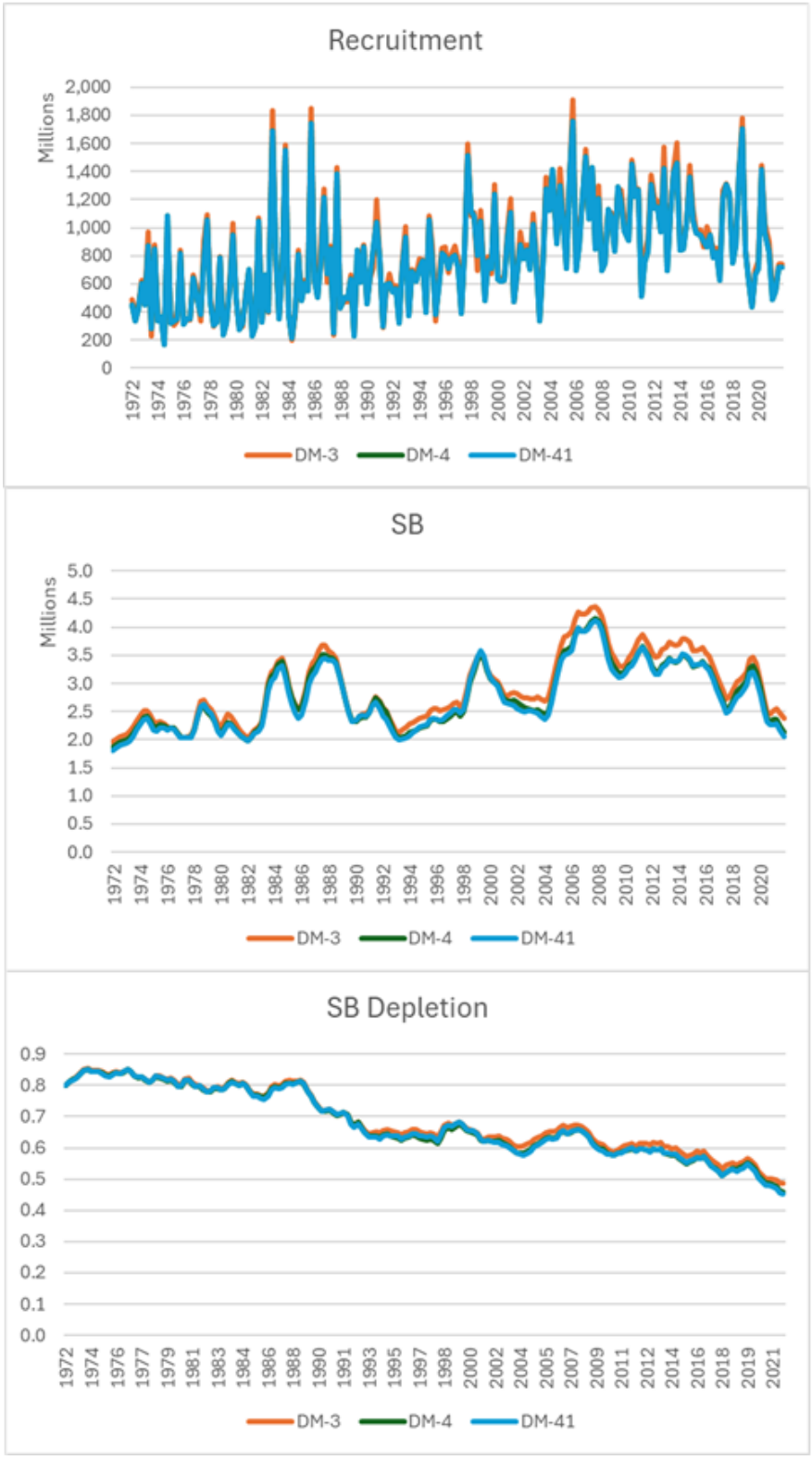

Figure 22: Estimates of recruitment, spawning potential (SB), and spawning potential depletion $SB/SB_{F=0}$ from models with 3 (DM-3), 4 (DM-4), and 41 (DM-41) Dirichlet multinomial groups.

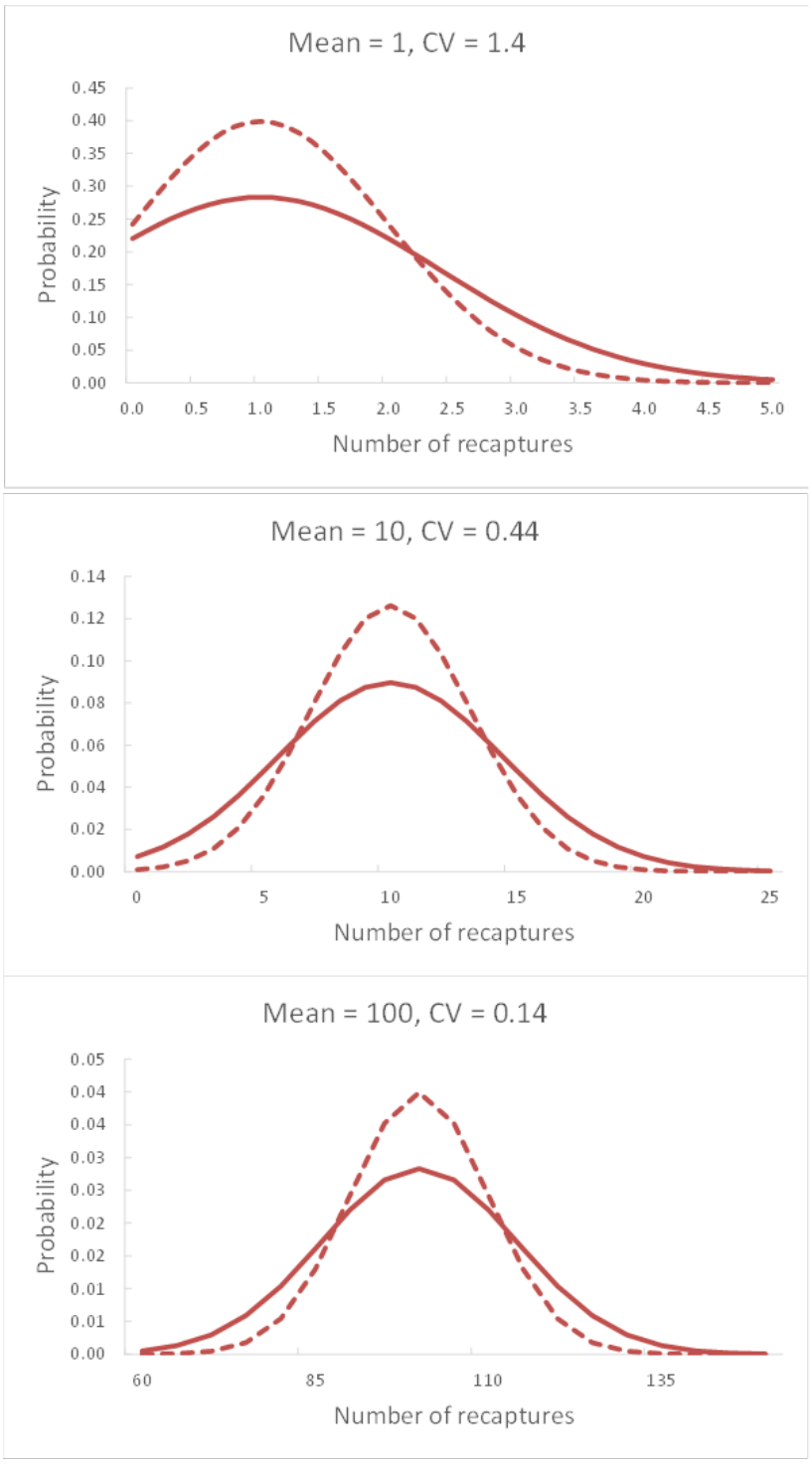

Figure 23: Example probability distributions for three example expected values of tag recoveries – 1 recapture, 10 recaptures and 100 recaptures. The solid lines show the negative binomial probability distributions with the estimated level of overdispersion ($\tau = 1.982$). The CV for each distribution is indicated in the title of each chart. For reference, a Poisson distribution (mean = variance) has $\tau = 1$, and those distributions are shown for comparison in the dashed lines.

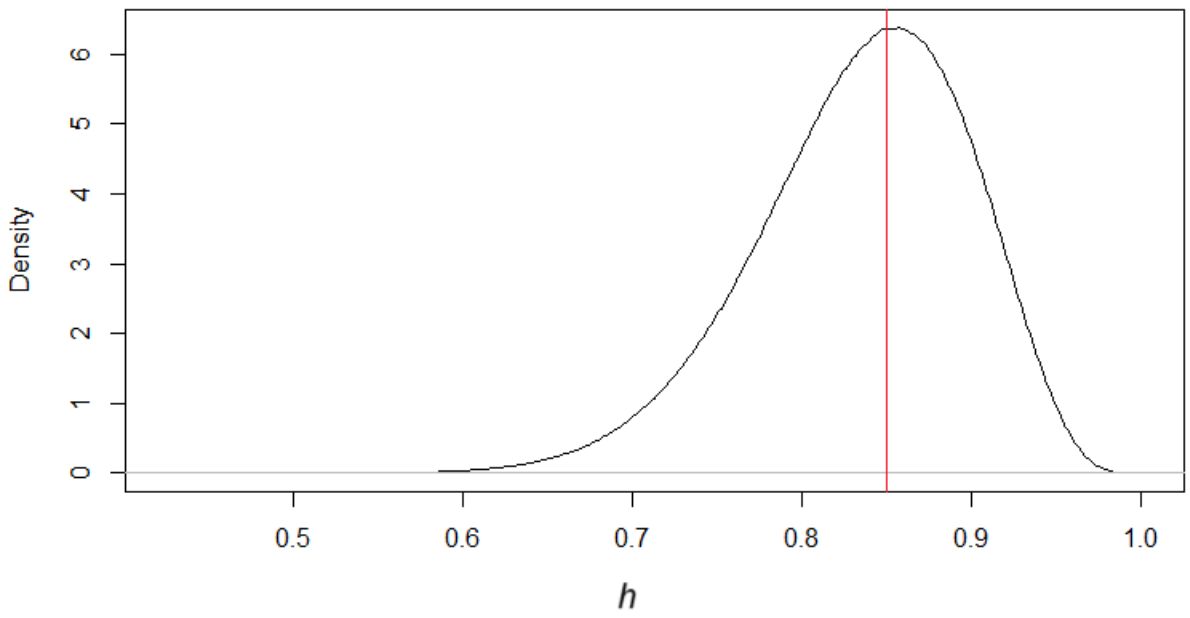

Figure 24: Assumed prior distribution of steepness (mode=0.85, red line) considered in the model ensemble uncertainty characterization.

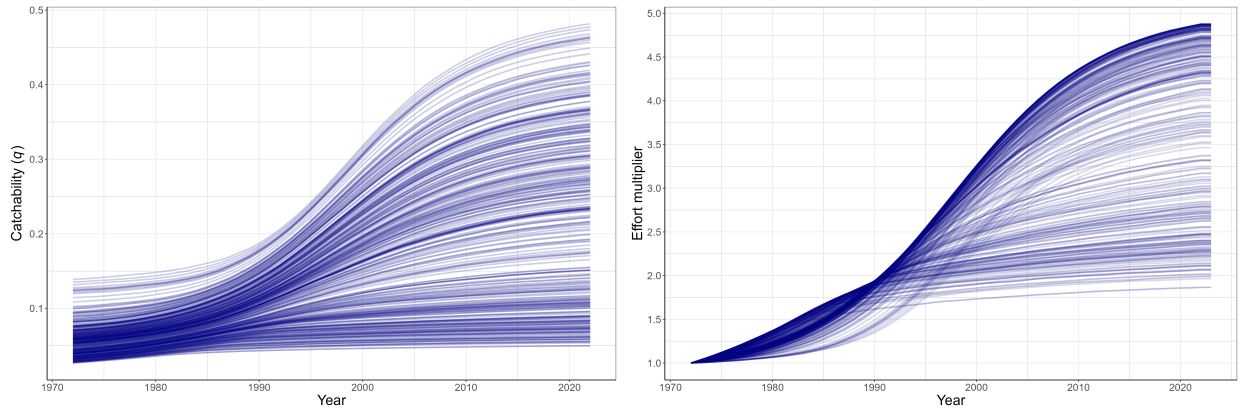

Figure 25: Catchability (left) and effort multiplier (right) trajectories applied to Japanese pole-and-line CPUE indices for inclusion of effort creep in the model ensemble for uncertainty characterisation.

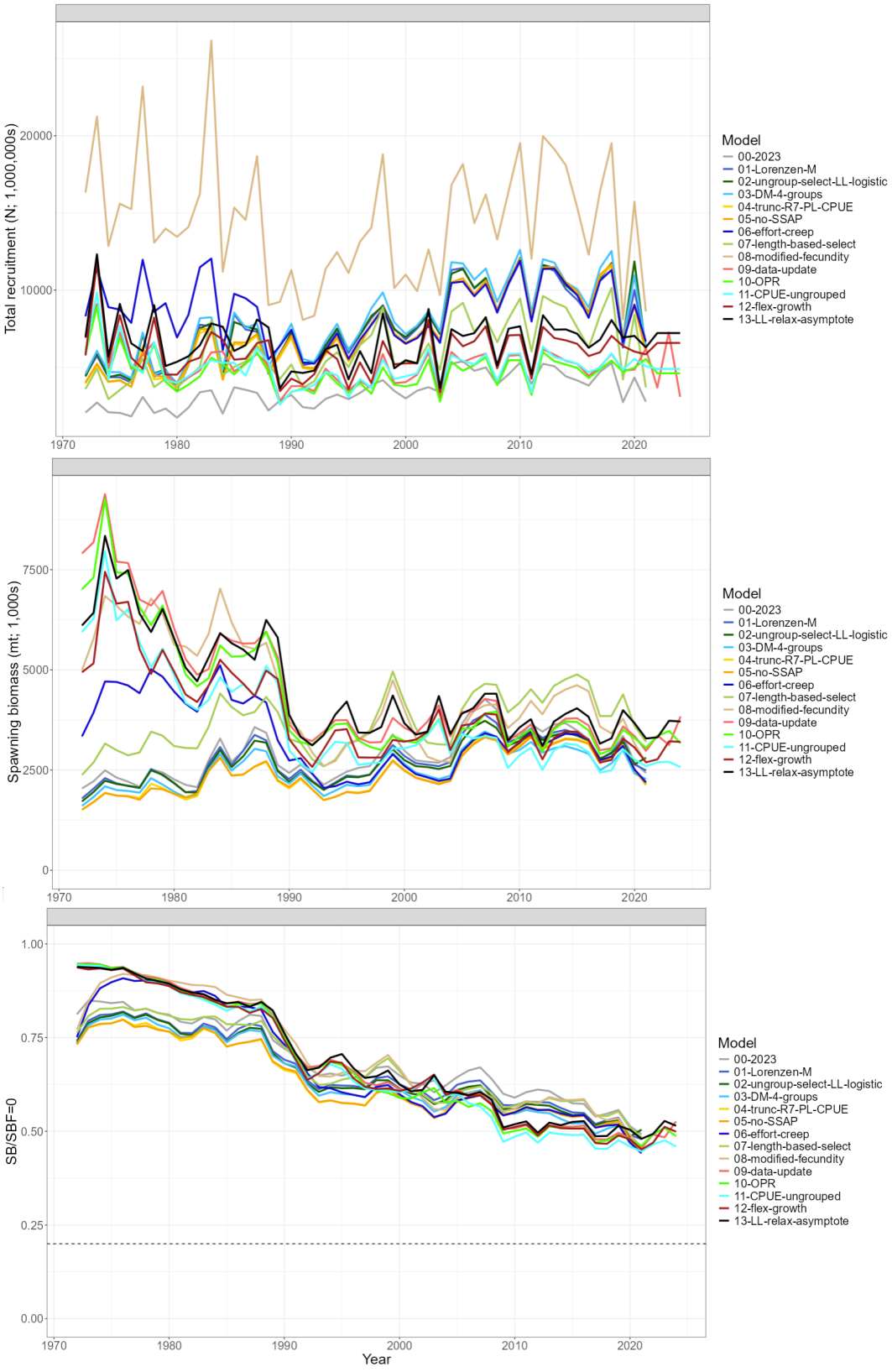

Figure 26: Model development change in recruitment (top), SB (middle), and $SB/SB_{F=0}$ (bottom) from the 2023 reference case model to the 2025 diagnostic case model (i.e., model 13 – black line).

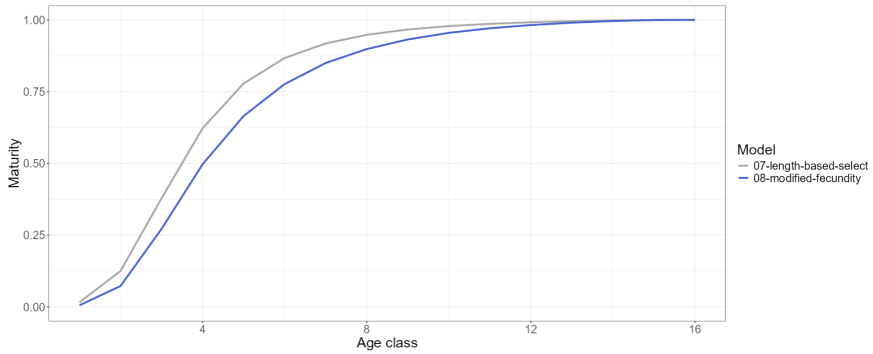

Figure 27: Estimated maturity-at-age for step 7 ('07-length-based-select') and step 8 ('08-modified-fecundity') in the stepwise model development.

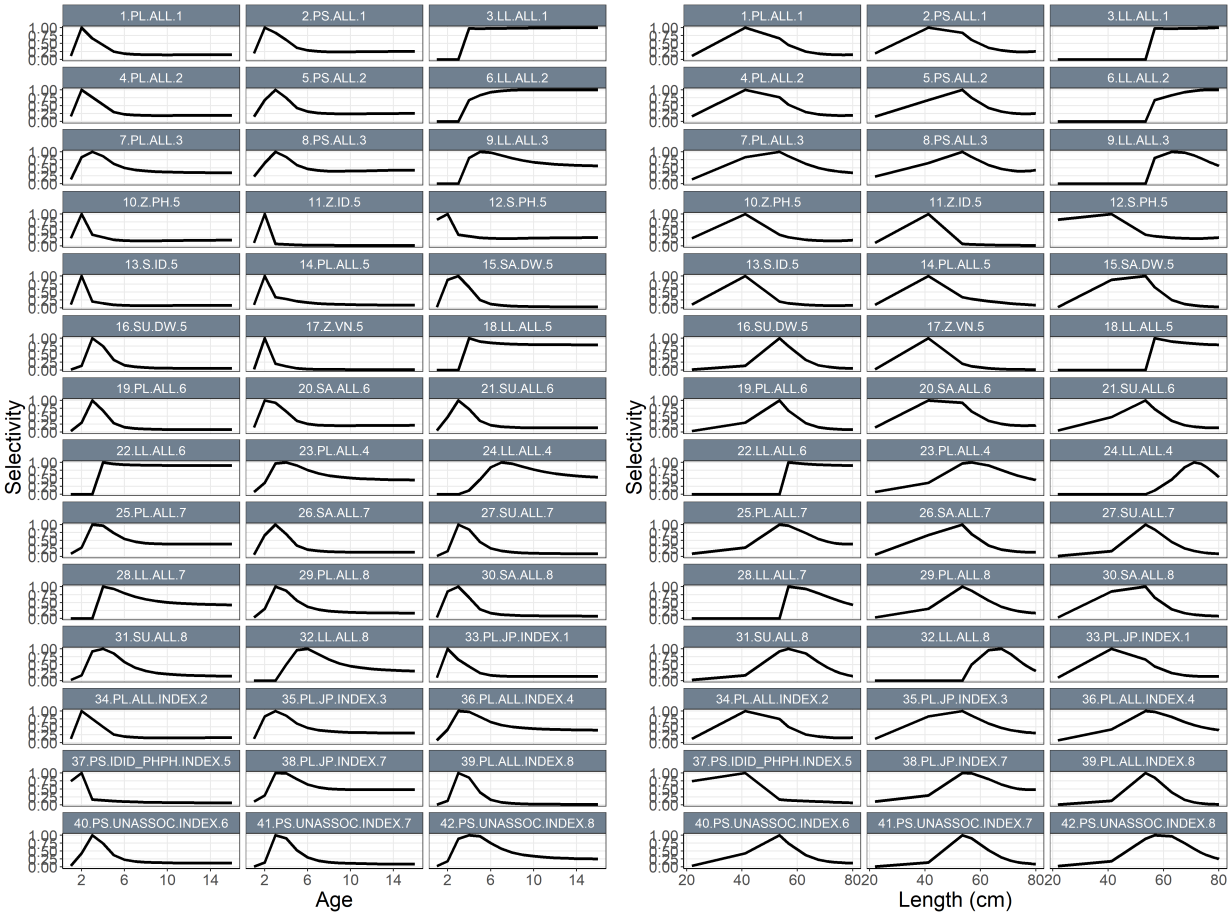

Figure 28: Estimated age-specific (left) and length-specific (right) selectivity coefficients by fishery for the diagnostic case model.

Q1	From 1	From 2	From 3	From 4	From 5	From 6	From 7	From 8
To 1	0.028		0.017	0.007			0.001	
To 2	0.028		0.010	0.011			0.001	
To 3			0.040	0.006			0.002	
To 4			0.003	0.030			0.004	
To 5			0.002		0.200	0.002	0.003	
To 6			0.000		0.001	0.222	0.043	
To 7			0.003	0.003	0.008	0.059	0.088	0.041
To 8			0.000	0.006	0.001	0.009	0.014	0.138

Q3	From 1	From 2	From 3	From 4	From 5	From 6	From 7	From 8
To 1	0.088	0.008		0.003				
To 2		0.107		0.001				
To 3	0.029	0.004	0.002	0.001				
To 4		0.003	0.002	0.003				
To 5	0.010	0.001	0.005	0.003	0.201	0.001	0.003	0.000
To 6					0.023	0.281	0.020	0.002
To 7		0.002	0.021	0.022	0.035	0.035	0.094	0.022
To 8		0.002		0.001	0.002	0.004	0.018	0.078

Q2	From 1	From 2	From 3	From 4	From 5	From 6	From 7	From 8
To 1	0.111	0.012	0.025	0.006				
To 2	0.059	0.149	0.002	0.015				
To 3	0.017	0.009	0.039					
To 4		0.003	0.004					
To 5					0.088	0.004	0.001	0.001
To 6					0.016	0.177	0.058	0.003
To 7	0.018	0.005	0.018		0.037	0.036	0.156	0.030
To 8					0.002	0.004	0.020	0.117

Q4	From 1	From 2	From 3	From 4	From 5	From 6	From 7	From 8
To 1	0.065	0.025	0.010	0.004			0.001	
To 2	0.056	0.040	0.004	0.002			0.001	
To 3	0.020	0.006	0.019	0.003	0.007		0.004	
To 4	0.014	0.003	0.004	0.007			0.003	0.002
To 5		0.002	0.002		0.292	0.001	0.004	0.004
To 6					0.008	0.289	0.062	0.004
To 7		0.003	0.004	0.007	0.017	0.042	0.095	0.012
To 8				0.001	0.001	0.005	0.010	0.023

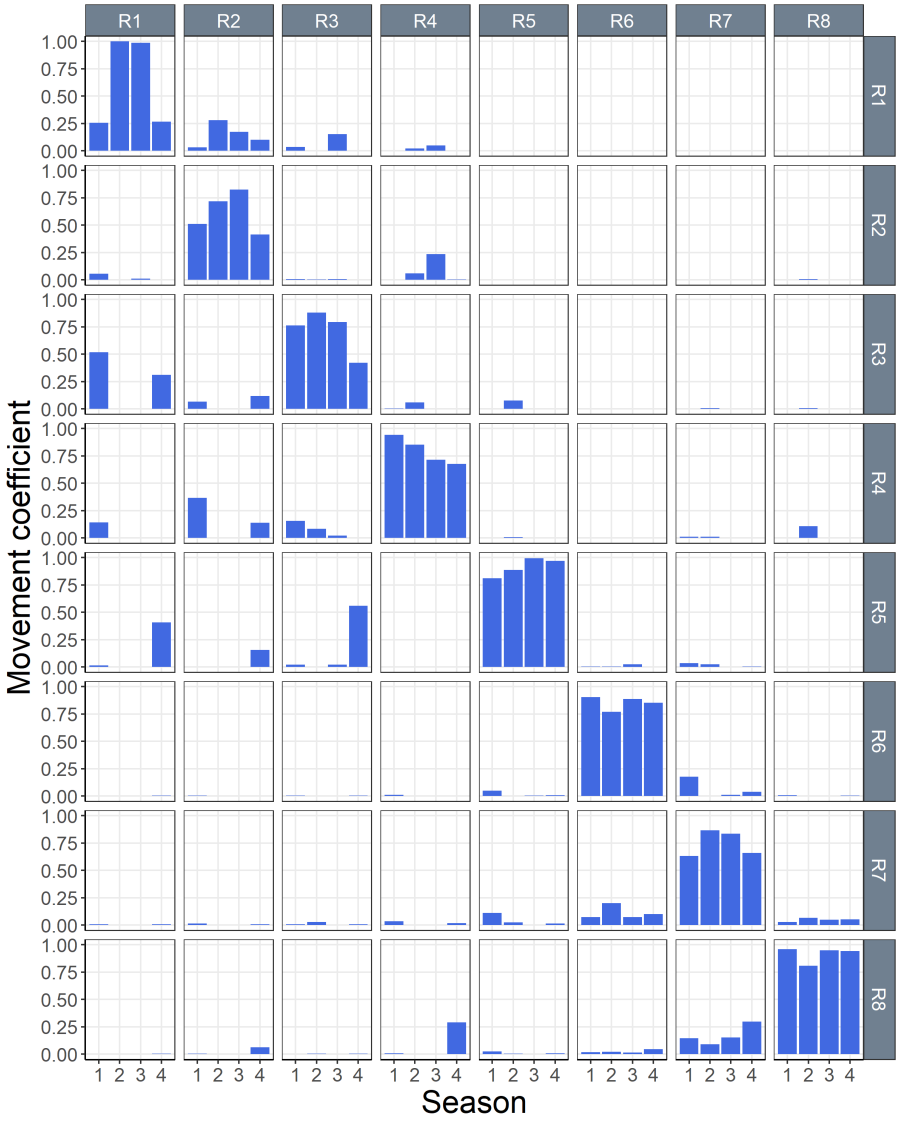

Figure 29: Observed recapture rate (top; intensity of color corresponds to proportion of recapture rate) by region released ('From') and region recaptured ('To') by season (Q1-Q4). Estimated movement coefficients (bottom) by season for the diagnostic case model.

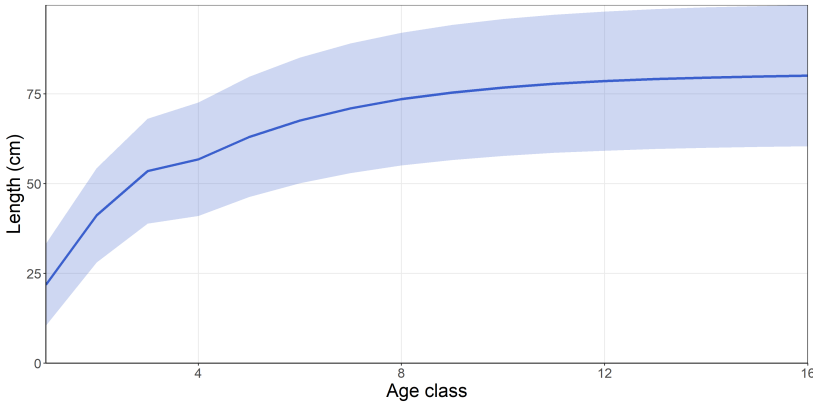

Figure 30: Estimated growth curve with 95% confidence interval for the diagnostic case model (quarterly age).

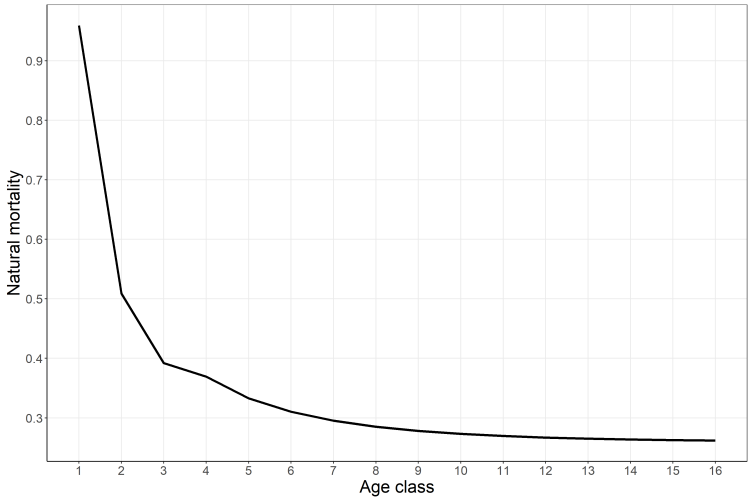

Figure 31: Estimated M-at-age from the von Bertalanffy (VB) growth parameters from the diagnostic case model.

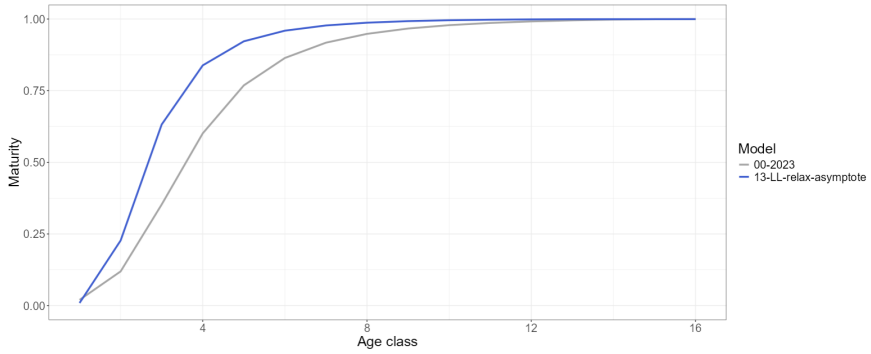

Figure 32: Maturity-at-age as estimated in step 0 ('00-2023') and the diagnostic case model ('13-LL-relax-asymptote') in the stepwise development for comparison.

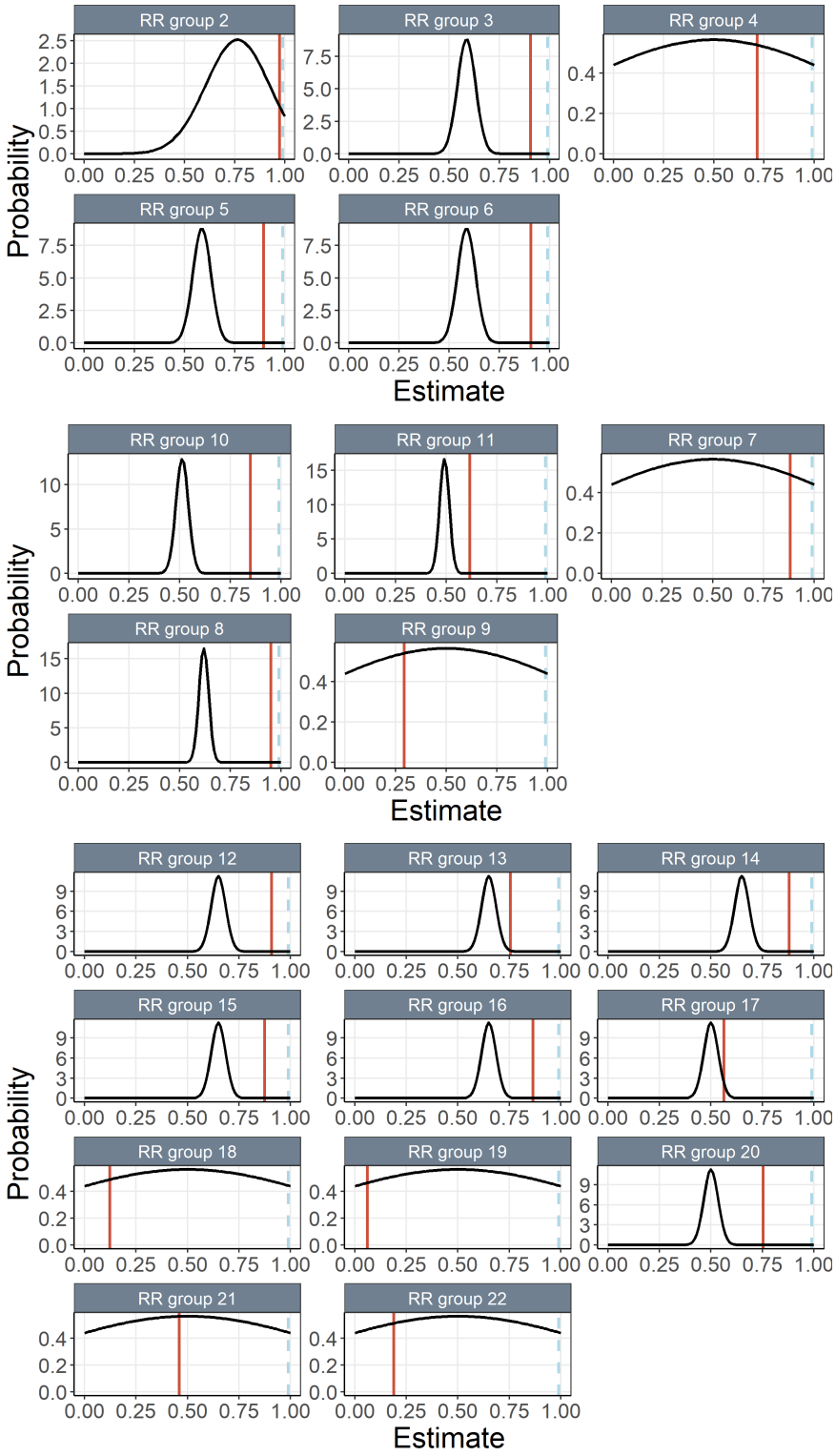

Figure 33: Estimated reporting rates for the diagnostic model (red lines) and the prior distribution for each reporting rate group (black lines) for RTTP (top), PTTP (middle), and JPTP (bottom). The imposed upper bound (0.99) on the reporting rate parameters is shown as a light blue dashed line. Reporting rates can be estimated separately for each release program and recapture fishery group but in practice are aggregated over some reporting rate groups (RR groups; see Table 2).

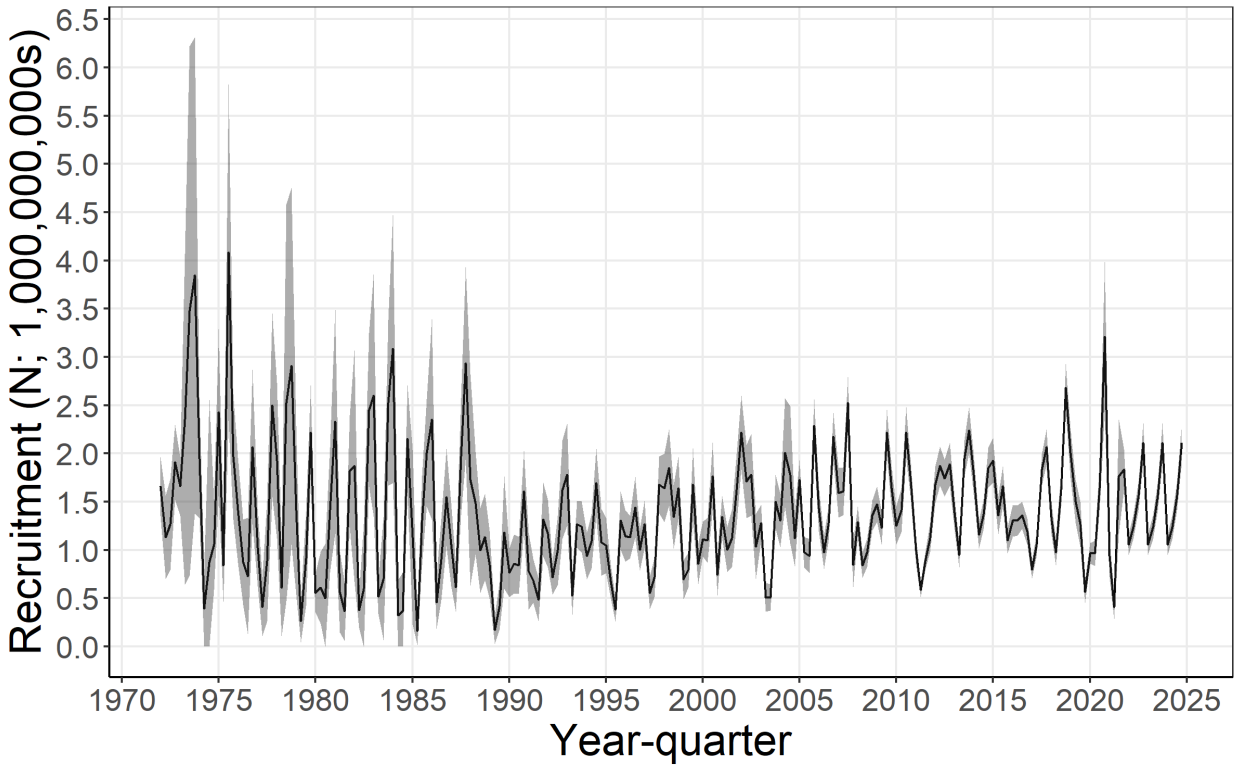

Figure 34: Annual time series of estimated quarterly recruitment summed across regions with 95% confidence interval for the diagnostic model.

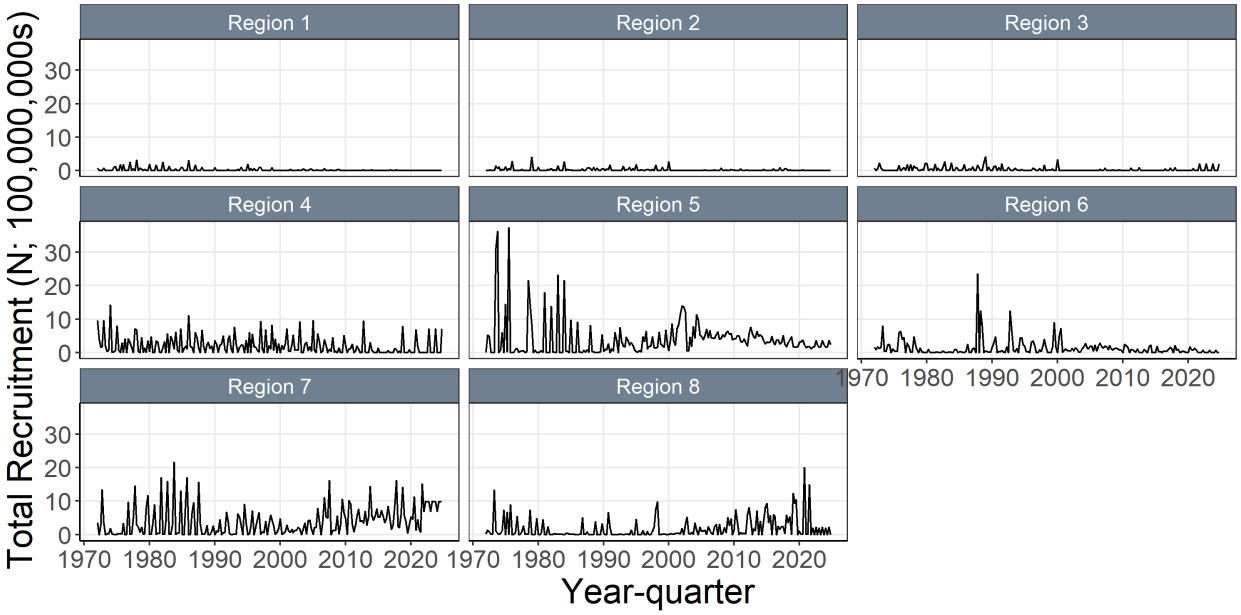

Figure 35: Annual time series of estimated quarterly recruitment among regions for the diagnostic model.

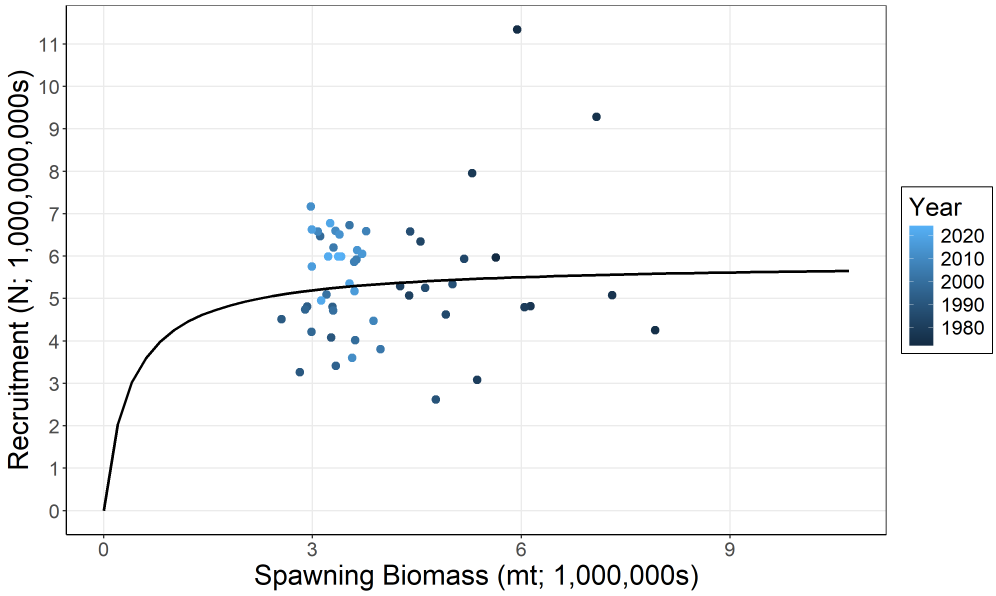

Figure 36: Estimated relationship between recruitment and spawning potential based on annual values for the diagnostic model. The darkness of the blue circles changes from light (more recent) to dark (earlier) through time.

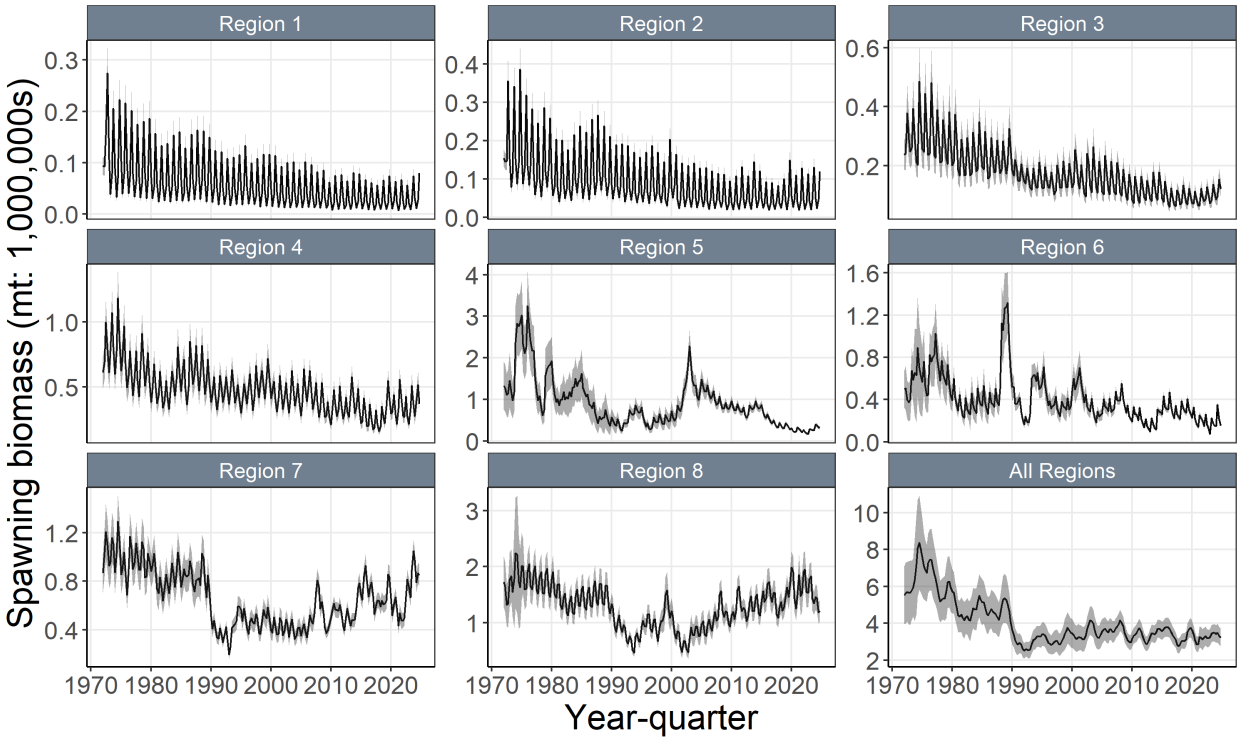

Figure 37: Time series of estimated quarterly spawning potential (spawning biomass) by region with 95% confidence interval for the diagnostic model.

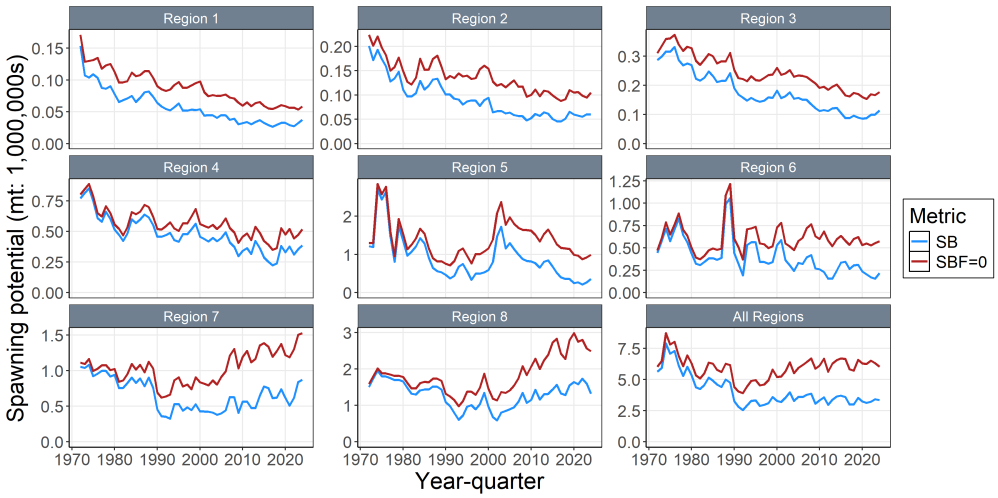

Figure 38: Comparison of the estimated average annual spawning potential (blue lines) with the estimated average spawning potential in the absence of fishing (red lines) for each region, for the diagnostic model.

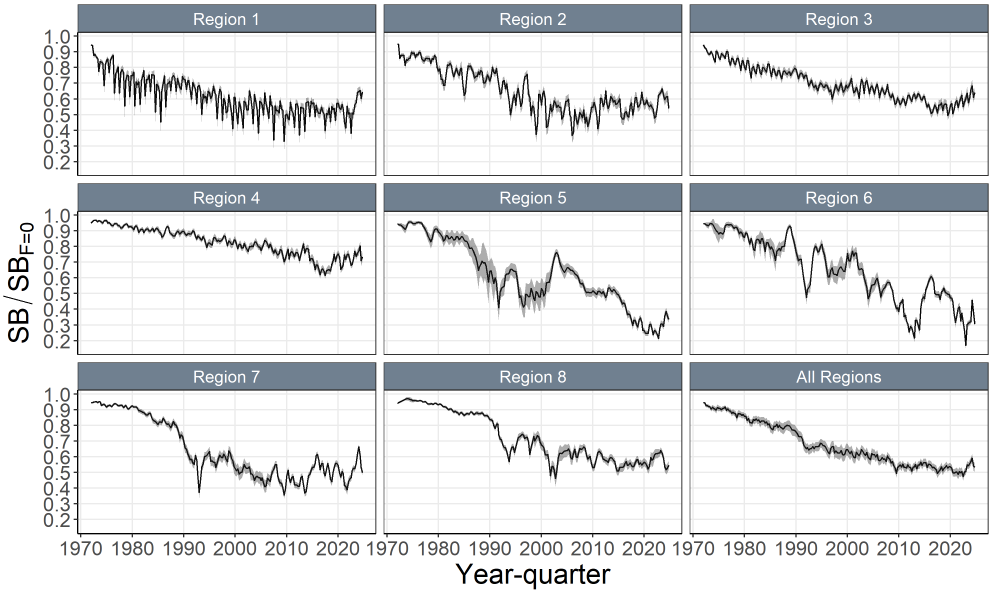

Figure 39: Time series of estimated quarterly spawning depletion ($SB_{recent}/SB_{F=0}$) by region with 95% confidence interval for the diagnostic model.

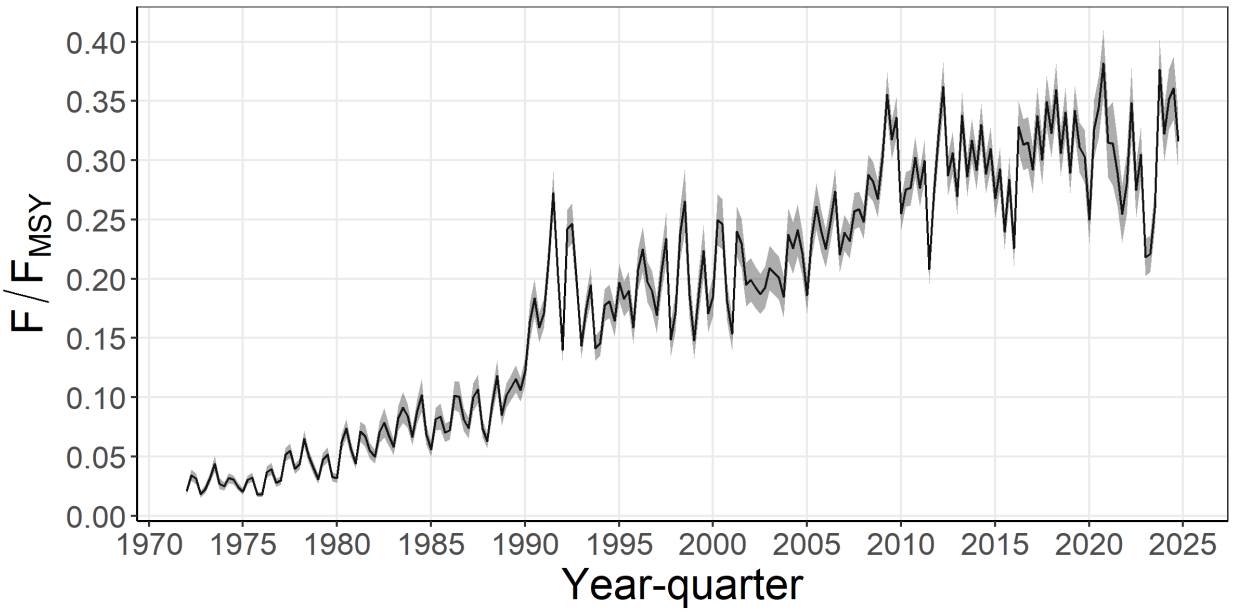

Figure 40: Time series of estimated F/F_{MSY} with 95% confidence intervals for the diagnostic model.

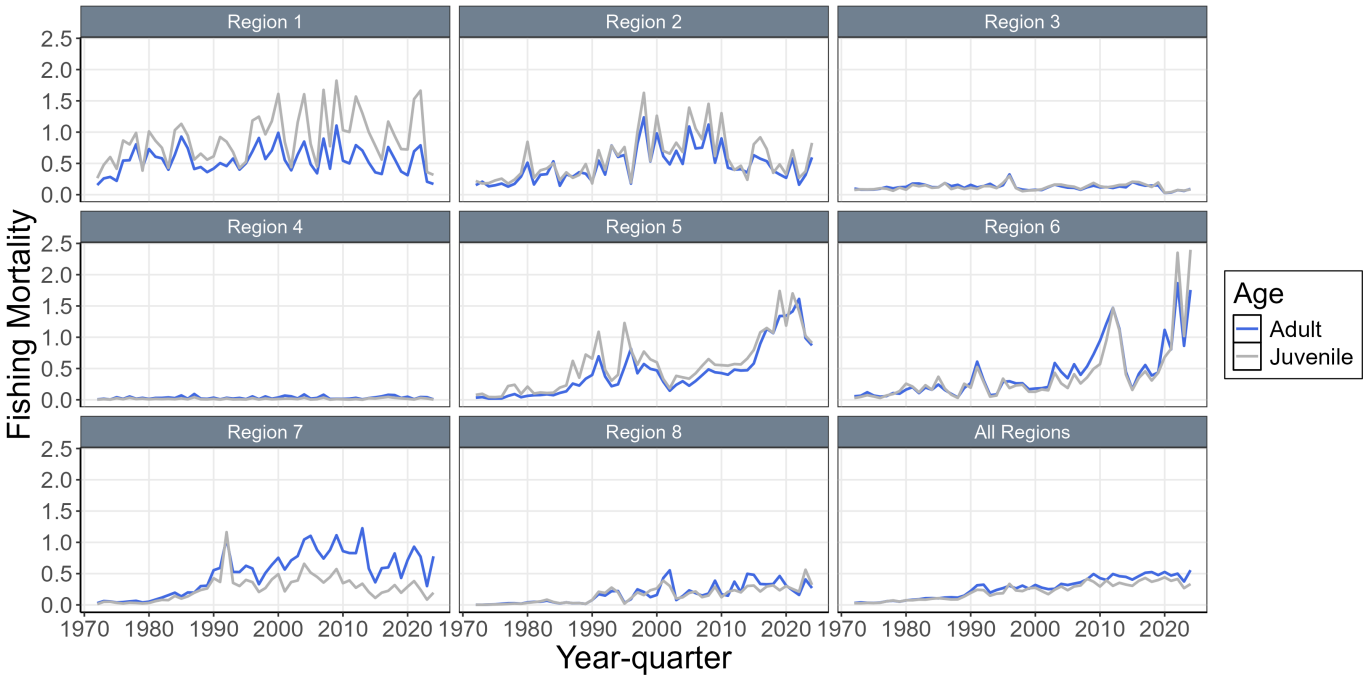

Figure 41: Time series of annual estimated fishing mortality for adults and juveniles by region for the diagnostic model.

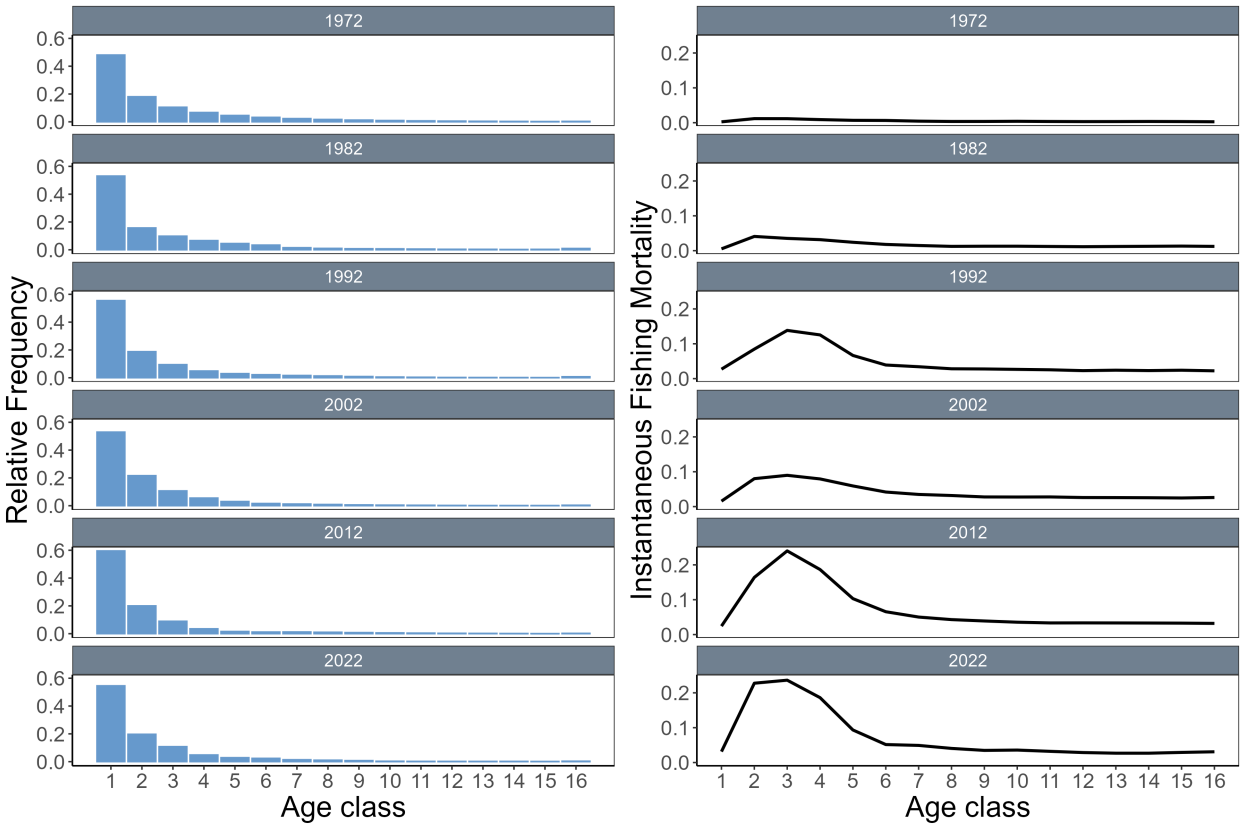

Figure 42: Estimated proportion-at-age (left) and fishing mortality-at-age (right), by quarter, at decadal intervals, for the diagnostic model.

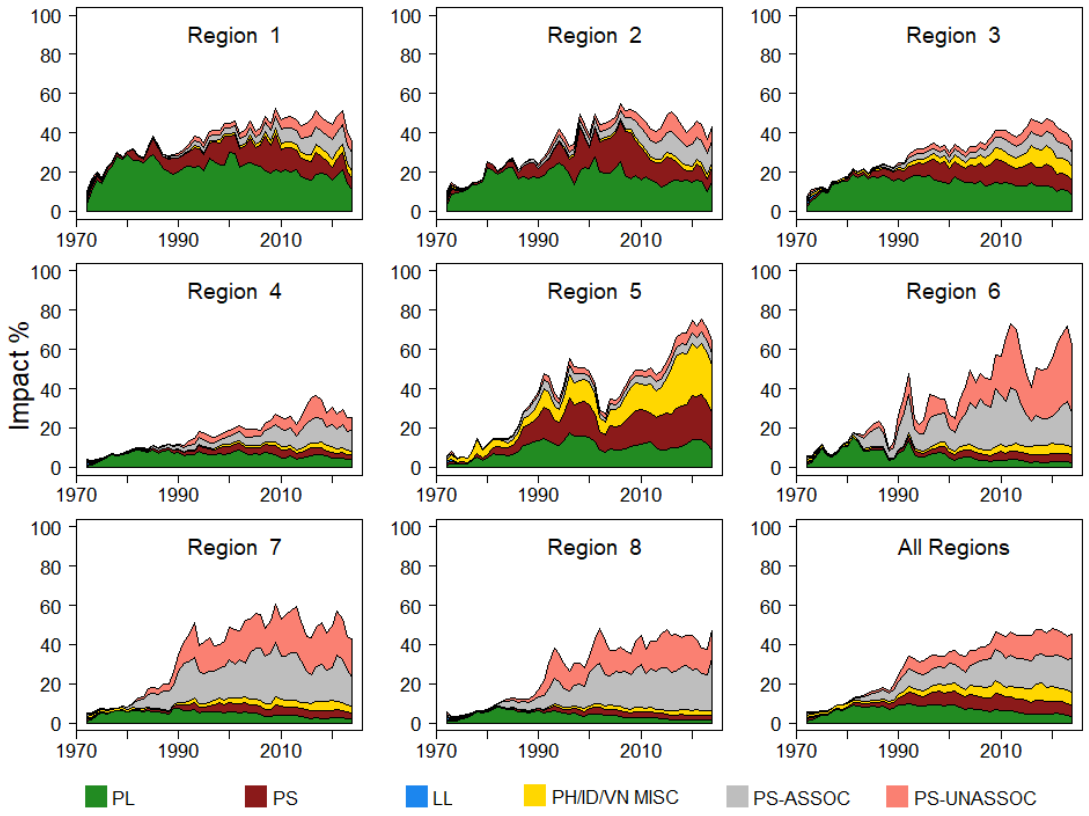

Figure 43: Estimates of reduction in spawning potential due to fishing (Fishery Impact = $1–SB_{latest}/SB_{F=0}$) by region, and over all regions (lower right panel), attributed to various fishery groups for the diagnostic model.

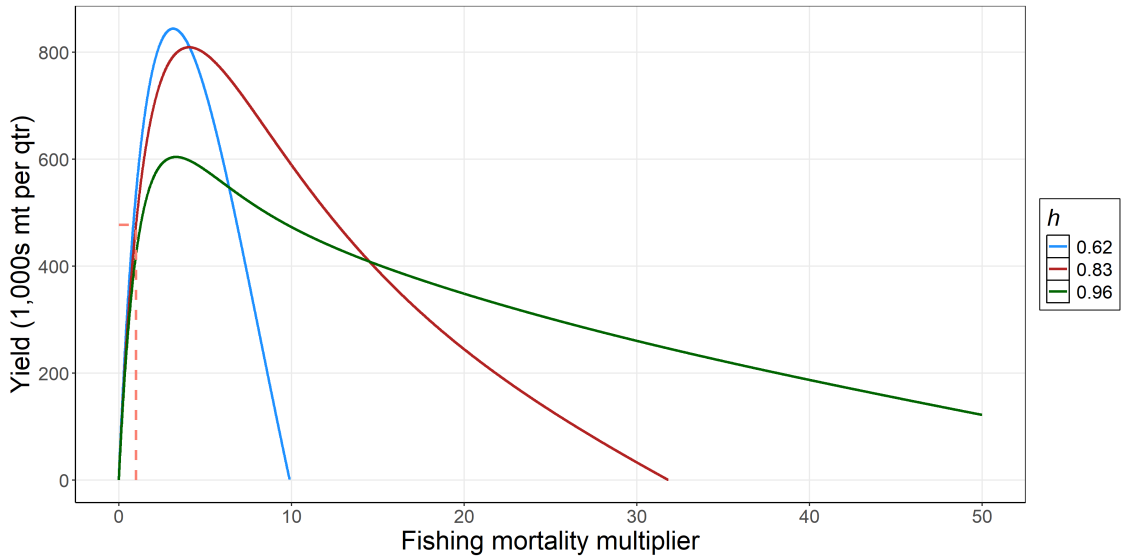

Figure 44: Estimated yield as a function of fishing mortality multiplier for the ensemble models at the minimum, median, and maximum steepness values. The salmon colored dashed line indicates the equilibrium yield at current fishing mortality for the model at median steepness.

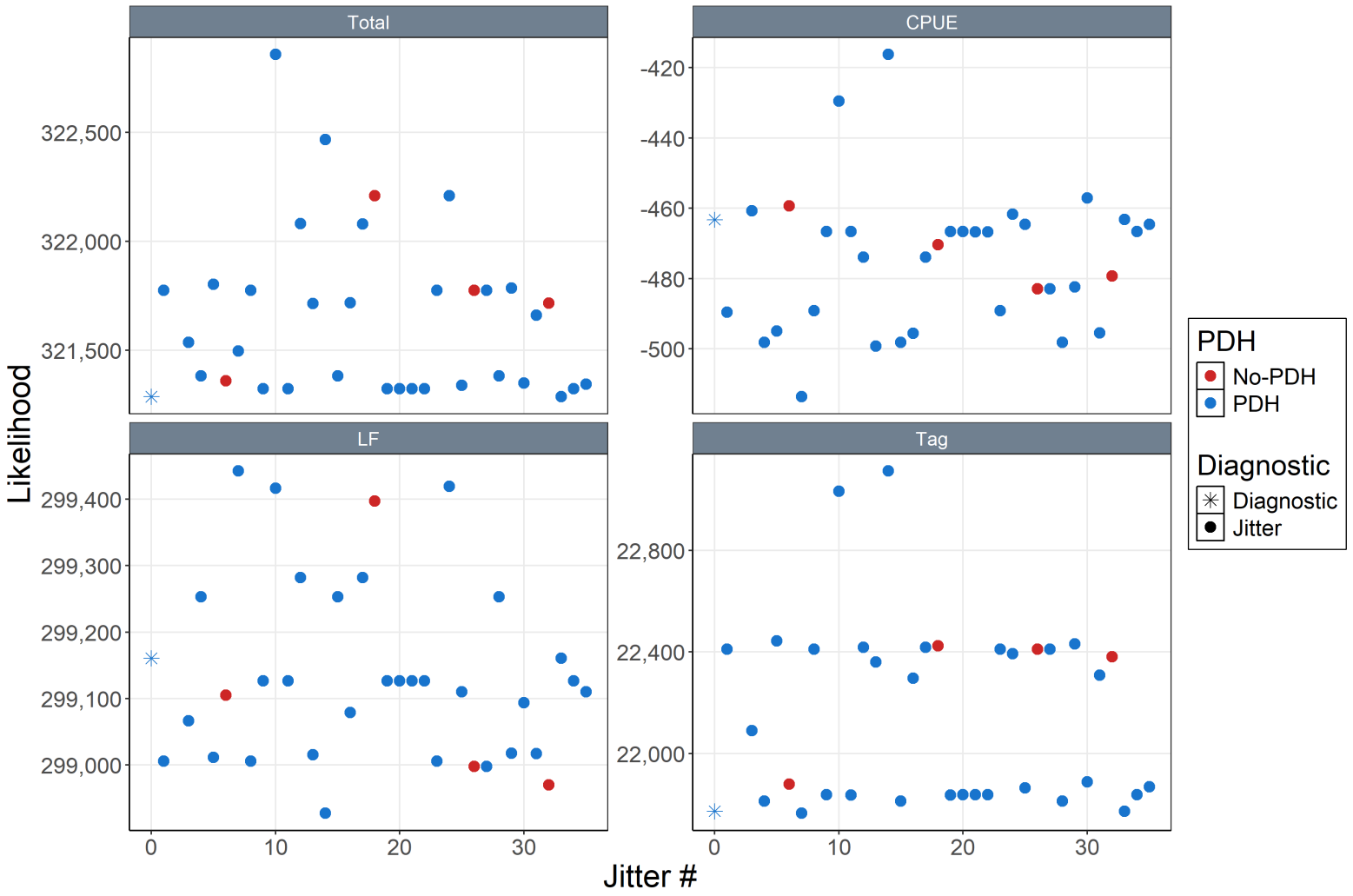

Figure 45: Negative log likelihood for total (top-left), CPUE (top-right), length-frequency data (LF; bottom-left), and tagging data (Tag; bottom-right) for 35 jittered models (coloured points; colours represent whether a PDH was achieved) and diagnostic case model (represented by an asterisk). Lower values (more negative) of negative log likelihood indicate an improvement in fit.

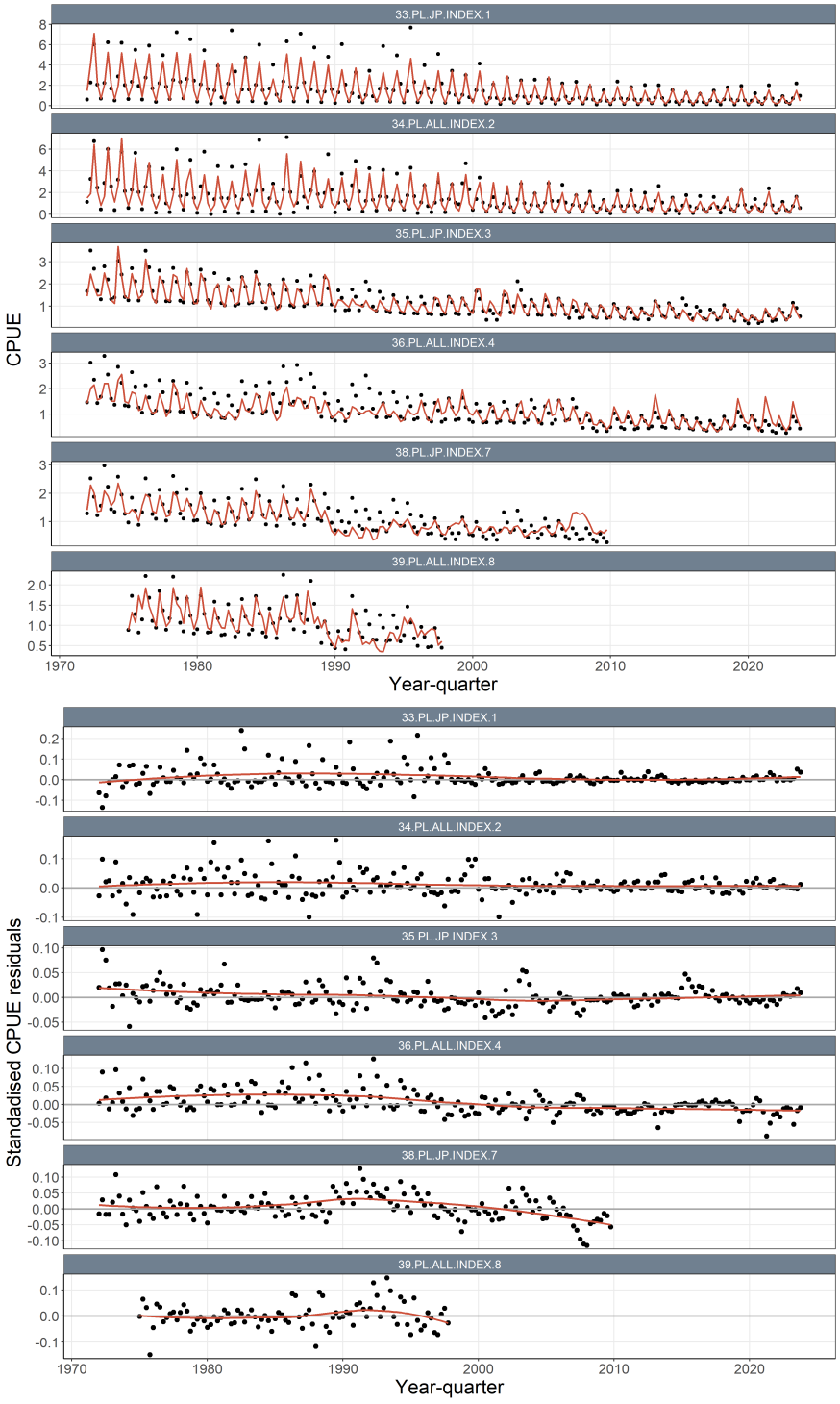

Figure 46: Comparison of quarterly model estimated (red line) and observed standardised CPUE (black dots) for the pole-and-line CPUE indices (top) for the 2025 diagnostic model. Plots of standardised residuals between estimated and observed with loess smoother (red line) standardised CPUE for the pole-and-line CPUE indices (bottom).

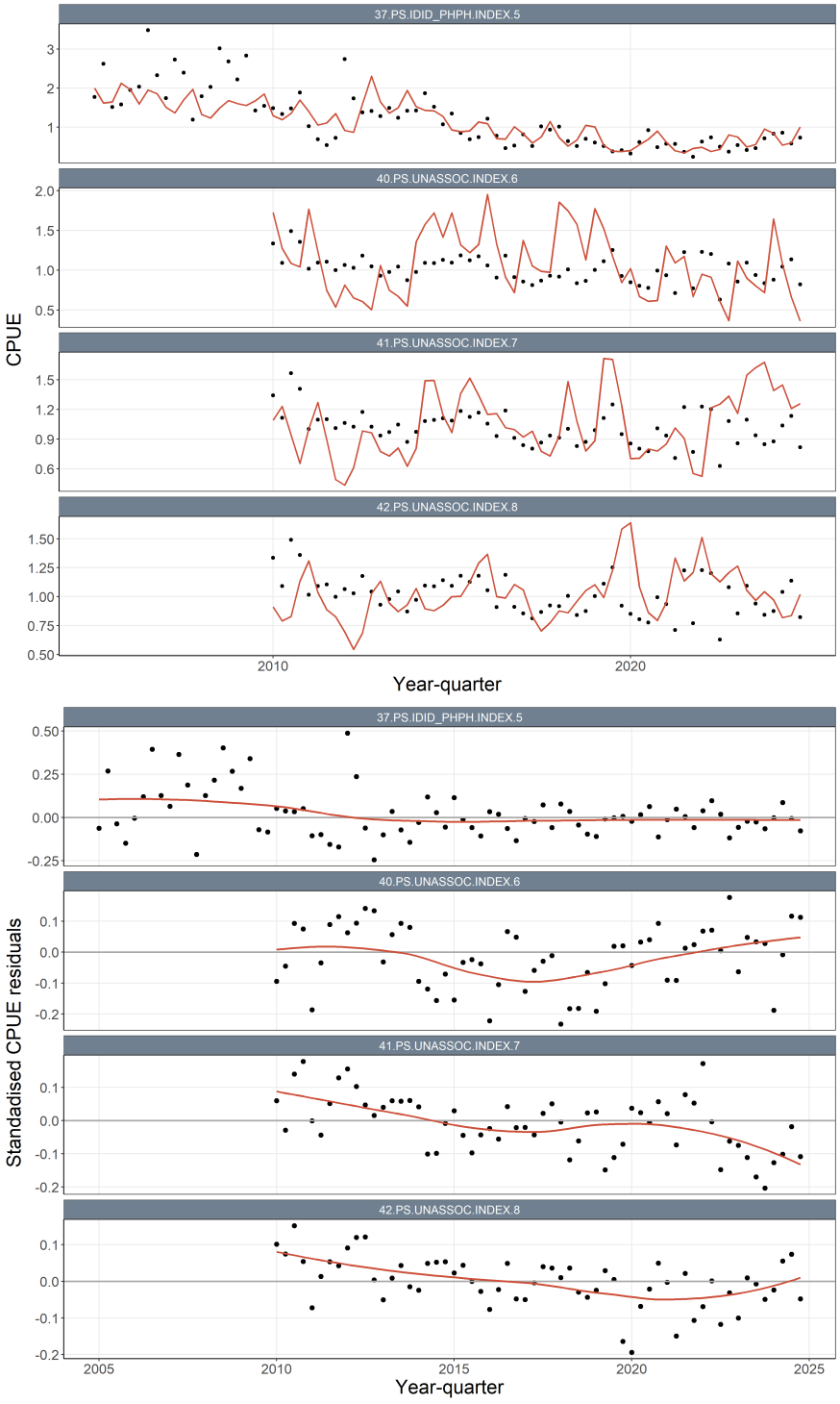

Figure 47: Comparison of quarterly model estimated (red line) and observed standardised CPUE (black dots) for the purse seine CPUE indices (top) for the 2025 diagnostic model. Plots of standardised residuals between estimated and observed with loess smoother (red line) standardised CPUE for the purse seine CPUE indices (bottom).

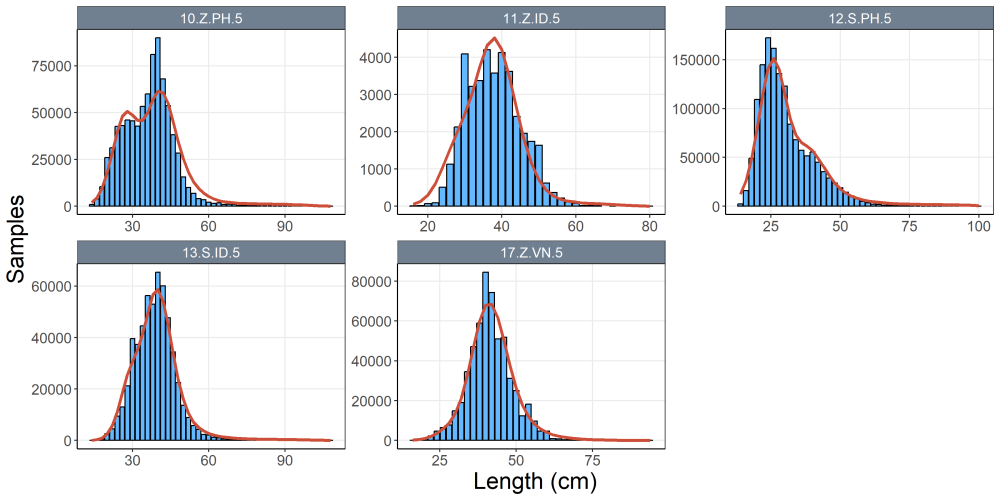

Figure 48: Composite (all time periods combined) observed (blue histograms) and predicted (red line) catch-at-length for ID, VN, and PH domestic fisheries in region 5 for the diagnostic model.

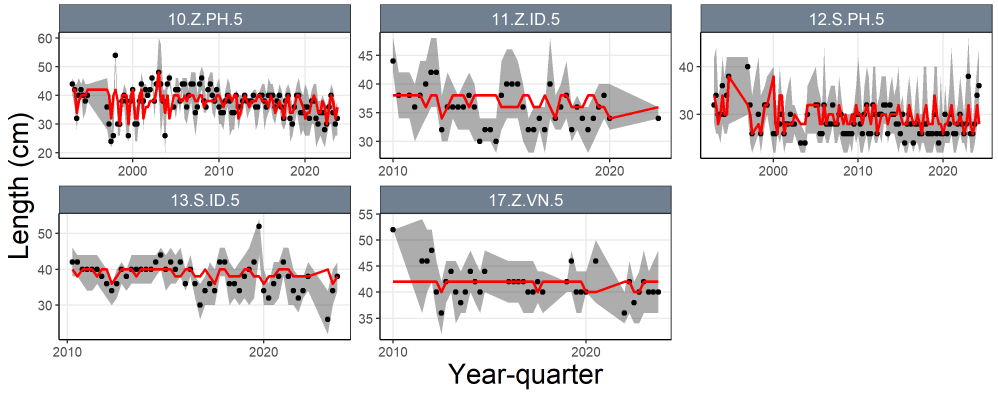

Figure 49: A comparison of the observed (black points) and predicted (red line) median fish length (FL, cm) for the ID, VN, and PH fisheries for the diagnostic model. The uncertainty intervals (gray shading) represent the values encompassed by the 25% and 75% quantiles.

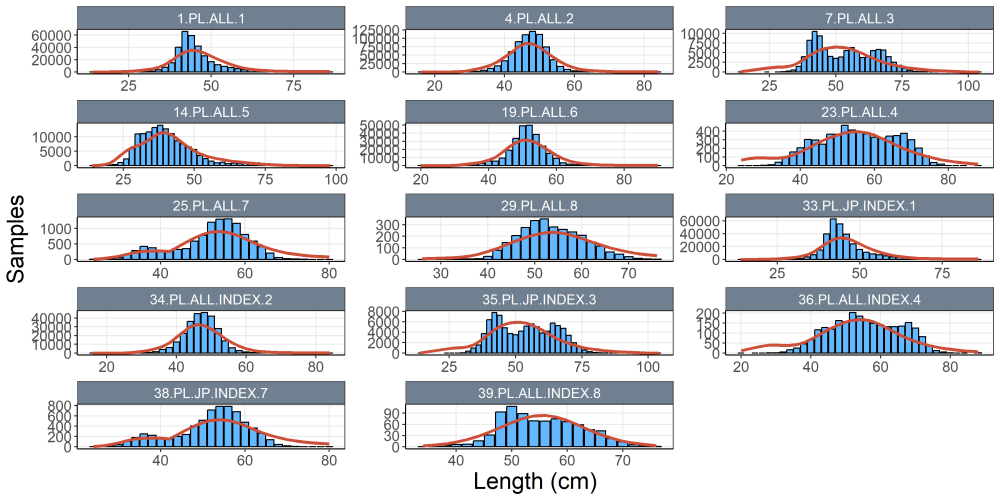

Figure 50: Composite (all time periods combined) observed (blue histograms) and predicted (red line) catch-at-length for the pole-and-line extraction and CPUE indices in regions 1–8 for the diagnostic model.

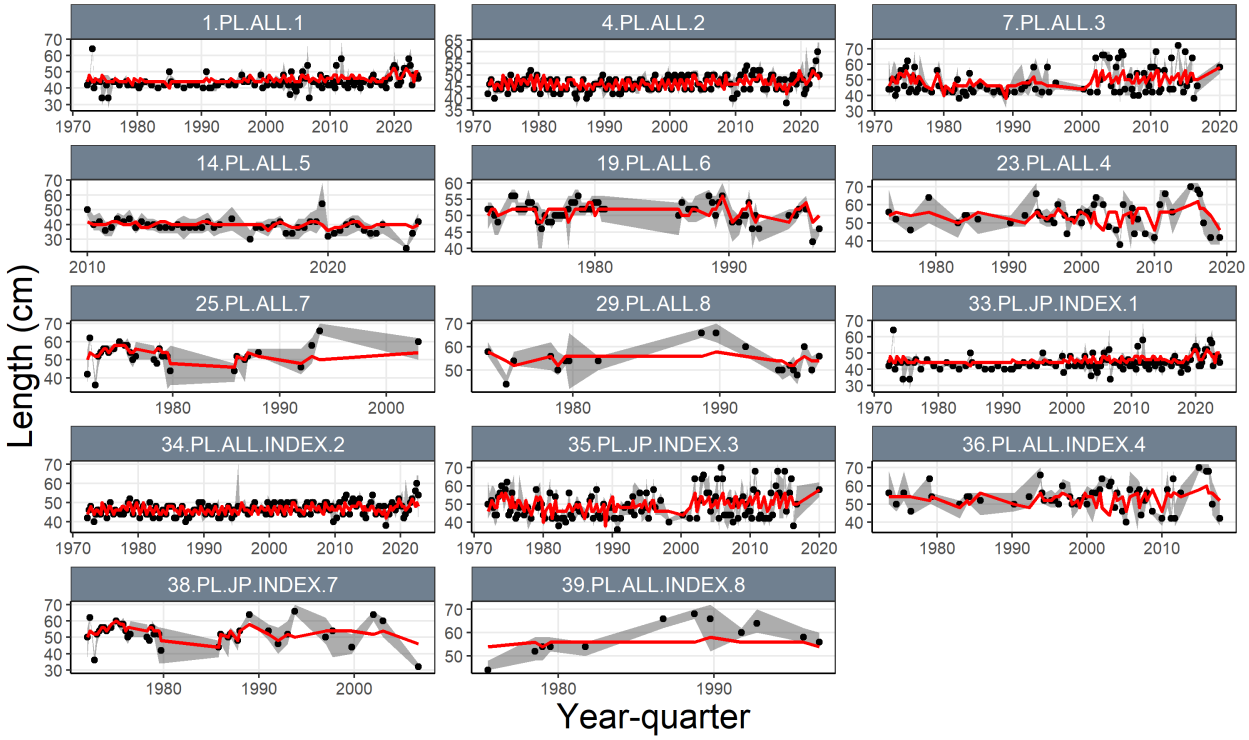

Figure 51: A comparison of the observed (black points) and predicted (red line) median fish length (FL, cm) for the pole-and-line extraction and CPUE indices for the diagnostic model. The uncertainty intervals (gray shading) represent the values encompassed by the 25% and 75% quantiles.

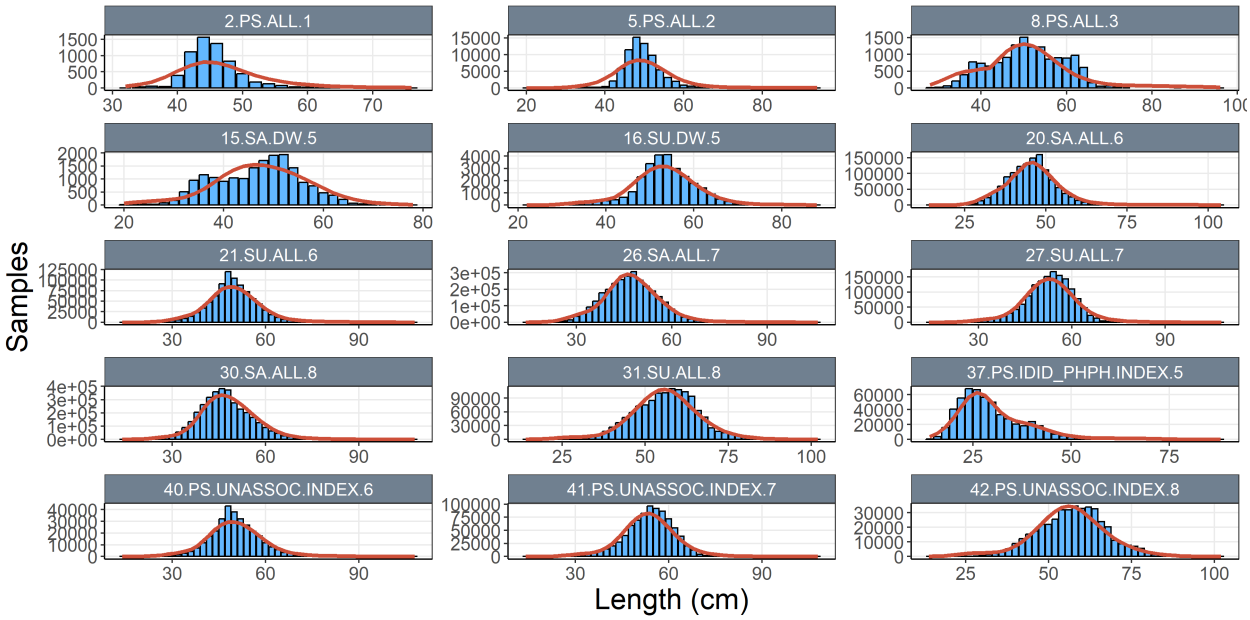

Figure 52: Composite (all time periods combined) observed (blue histograms) and predicted (red line) catch-at-length for the purse seine extraction and CPUE indices for the diagnostic model.

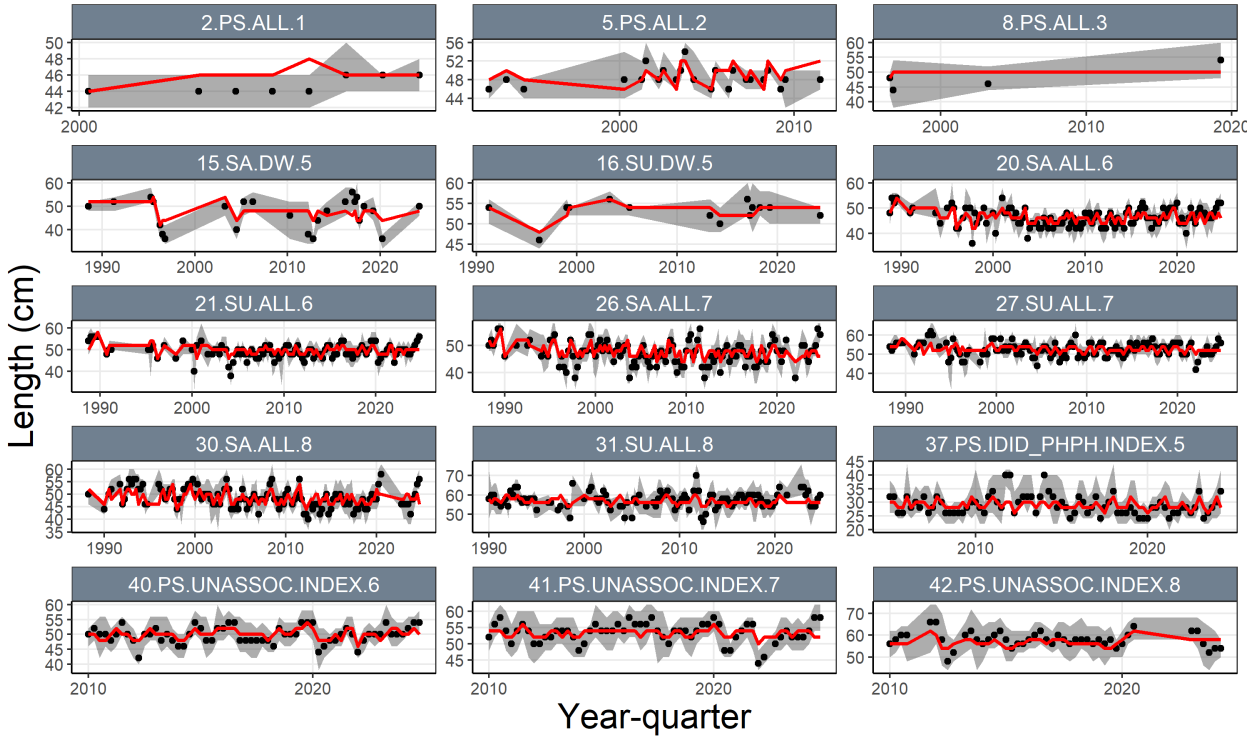

Figure 53: A comparison of the observed (black points) and predicted (red line) median fish length (FL, cm) for the purse seine extraction and CPUE indices for the diagnostic model. The uncertainty intervals (gray shading) represent the values encompassed by the 25% and 75% quantiles.

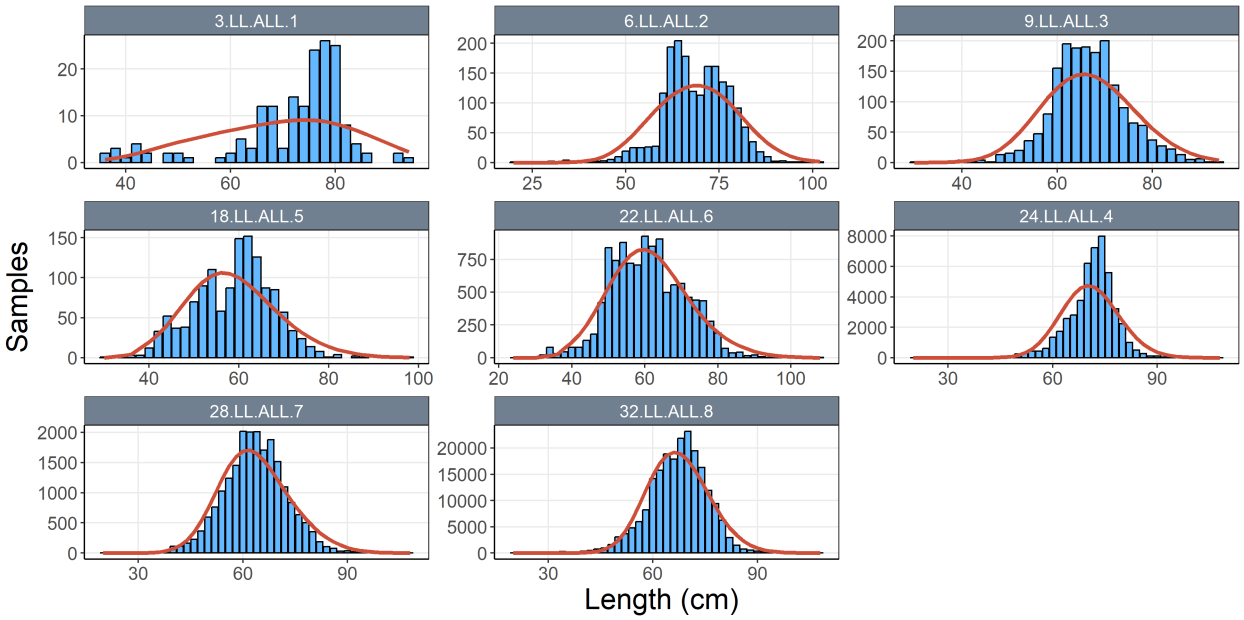

Figure 54: Composite (all time periods combined) observed (blue histograms) and predicted (red line) catch-at-length for the longline extraction fisheries in regions 1–8 for the diagnostic model.

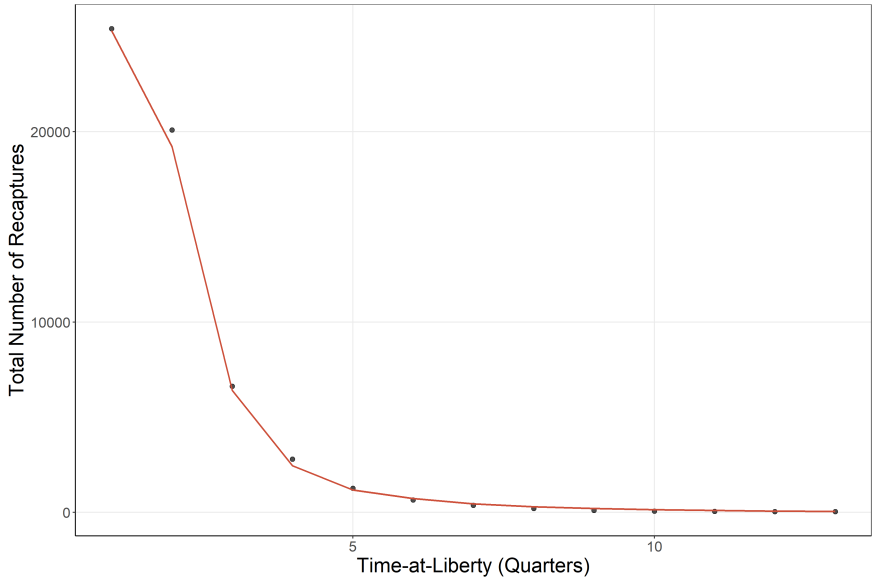

Figure 55: Observed (points) and model-predicted (red line) tag attrition across all tag release events for the diagnostic model.

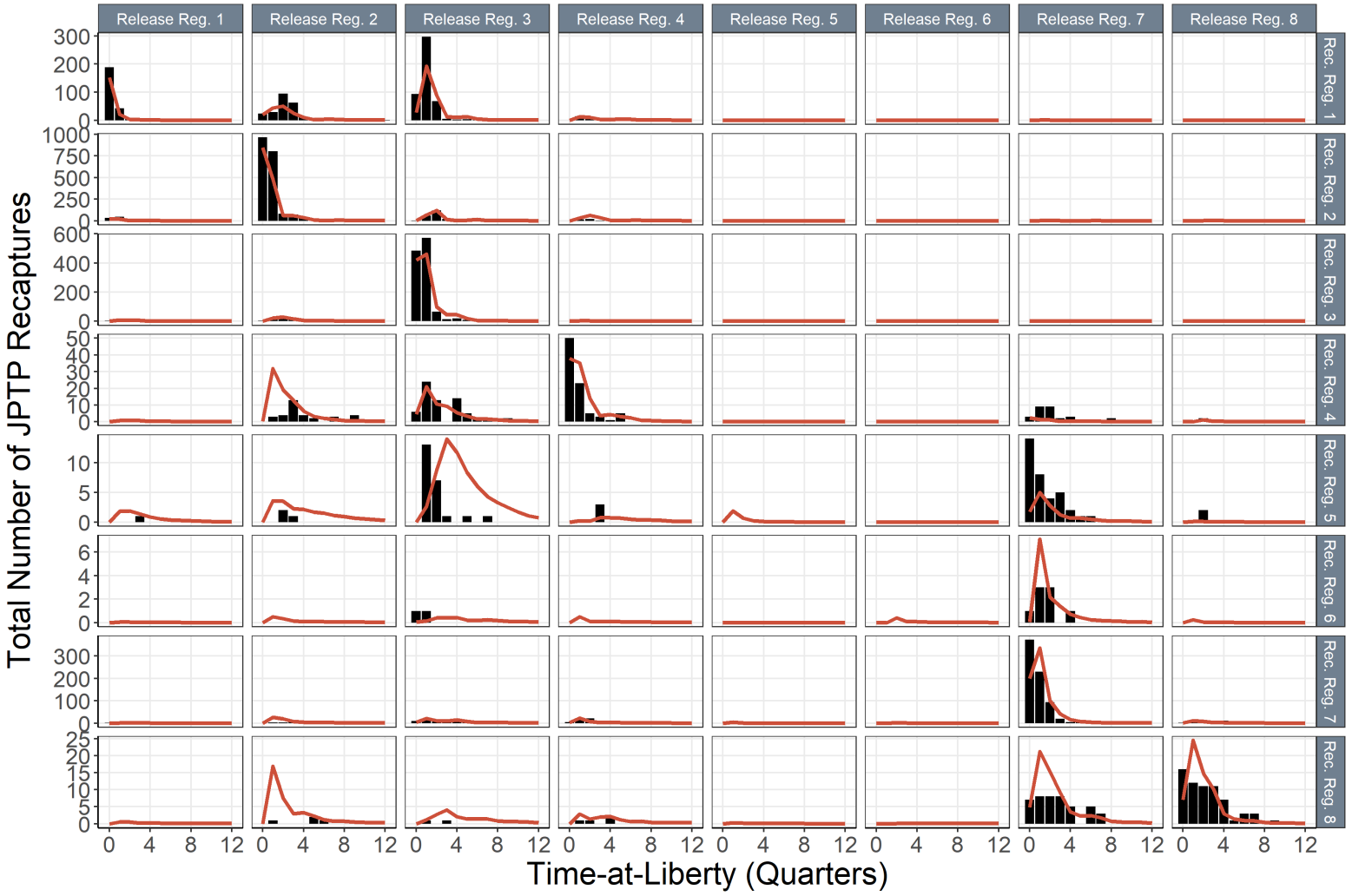

Figure 56: Observed (columns in black) and model-predicted (red line) tag attrition for all Japanese Tagging Program tag release events by release region (across) and recapture region (down) for the diagnostic model.

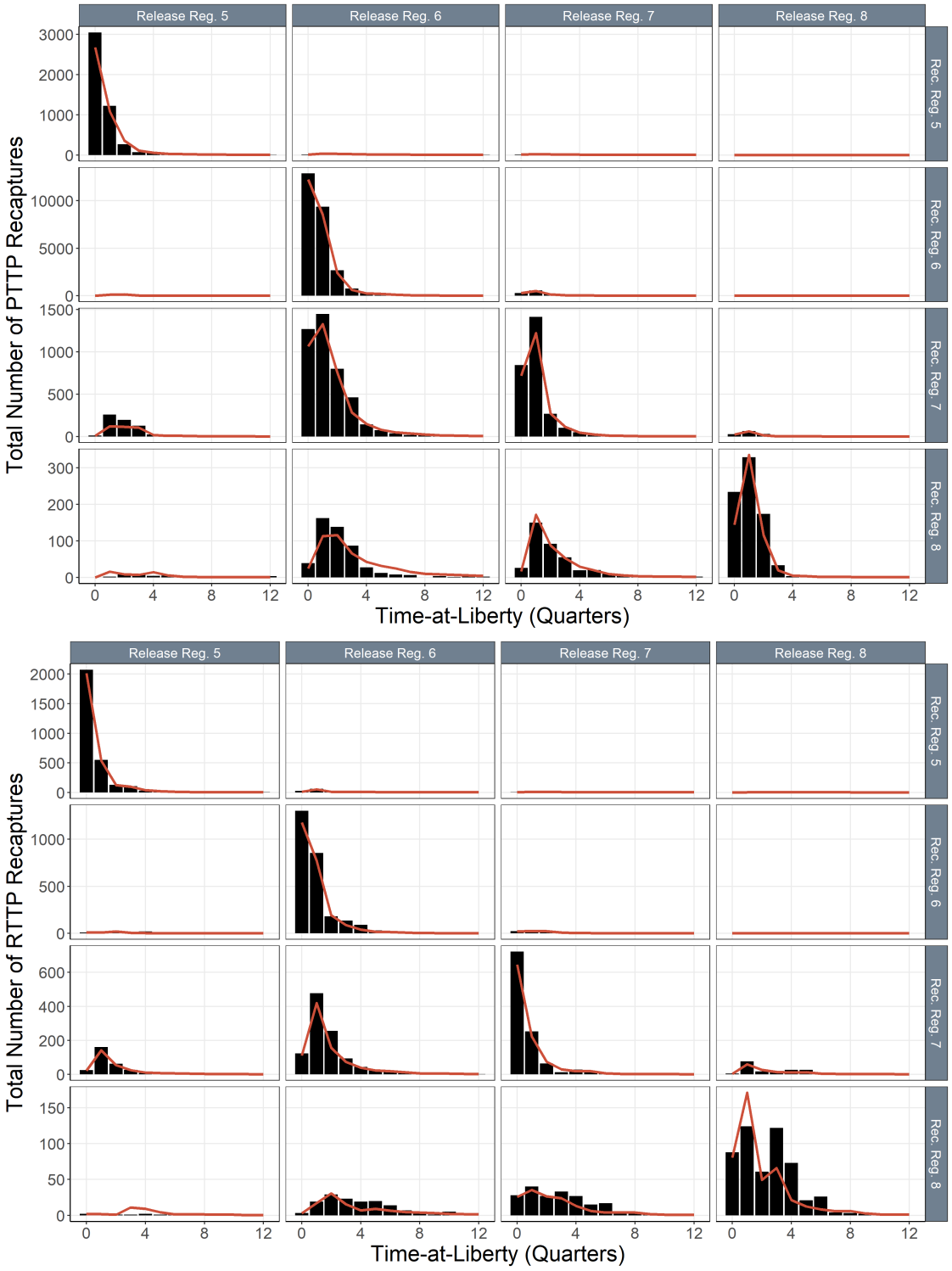

Figure 57: Observed (columns in black) and model-predicted (red line) tag attrition for all Pacific Tuna Tagging Program (PTTP) and Regional Tuna Tagging Program (RTTP) release events by release region (across) and recapture region (down) for the diagnostic model.

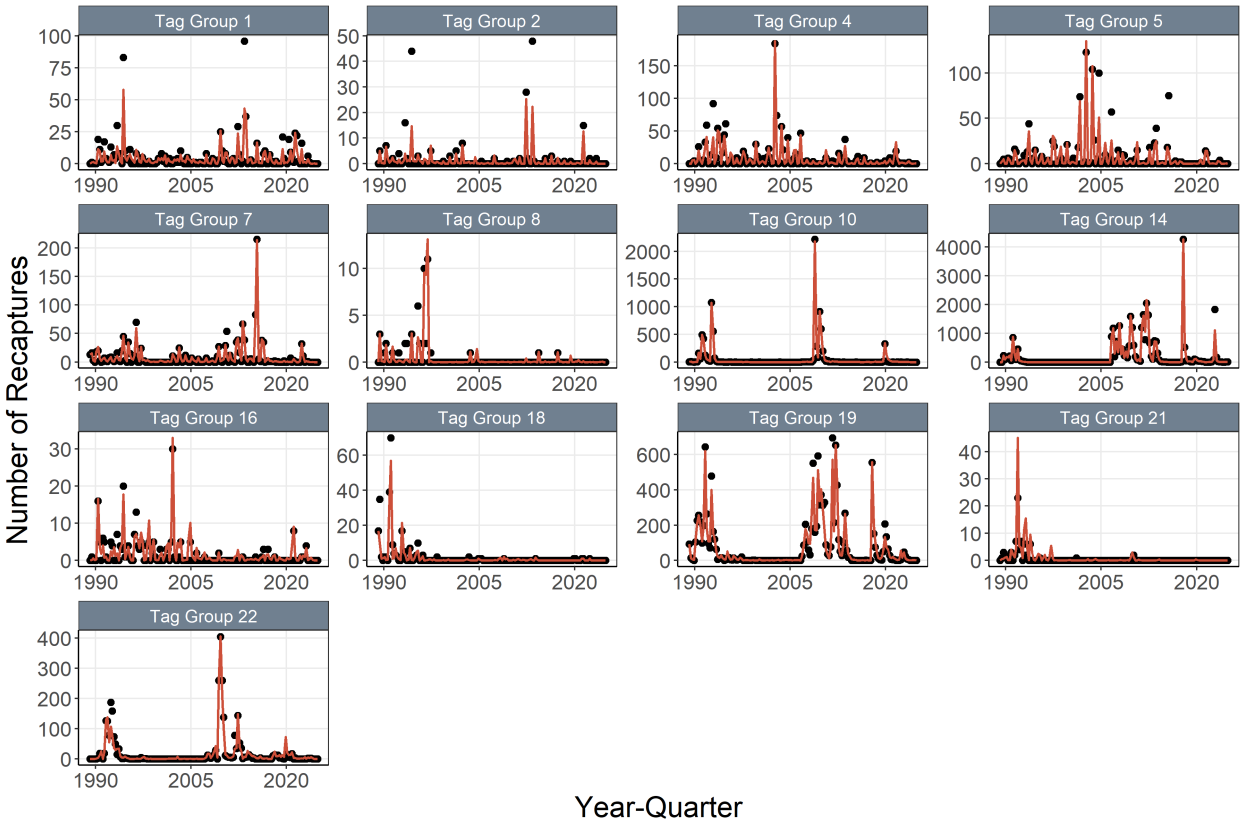

Figure 58: Observed (points) and model-predicted (red line) tag returns over time for the diagnostic model across all tag recapture groups (see Table 2 for group definitions by fishery).

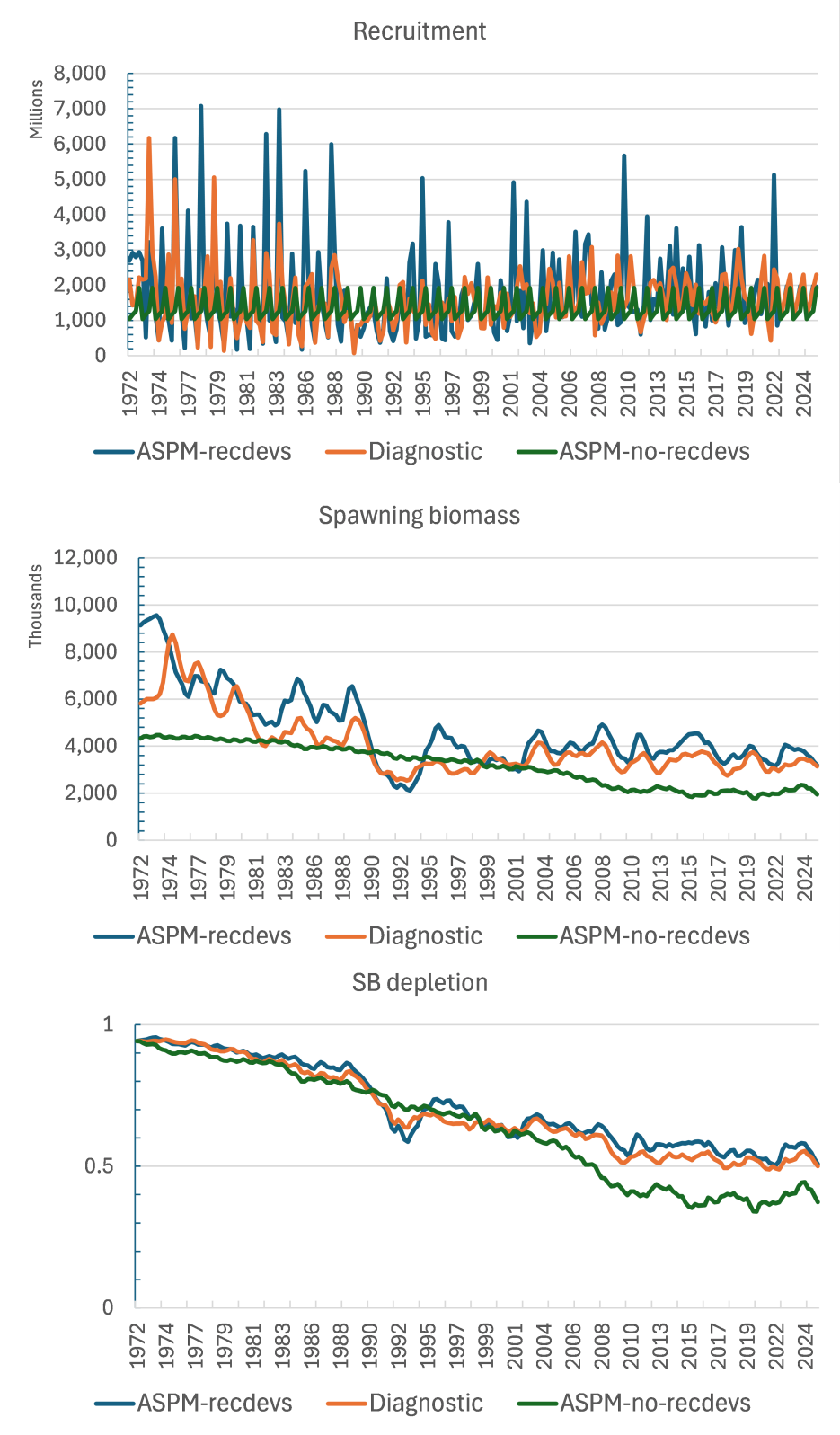

Figure 59: Recruitment, spawning potential (SB) and $SB/SB_{F=0}$ (SB depletion) estimates for the diagnostic case and for ASPMs that included (ASPM-recdevs) and excluded (ASPM-no-rec-devs) recruitment variability.

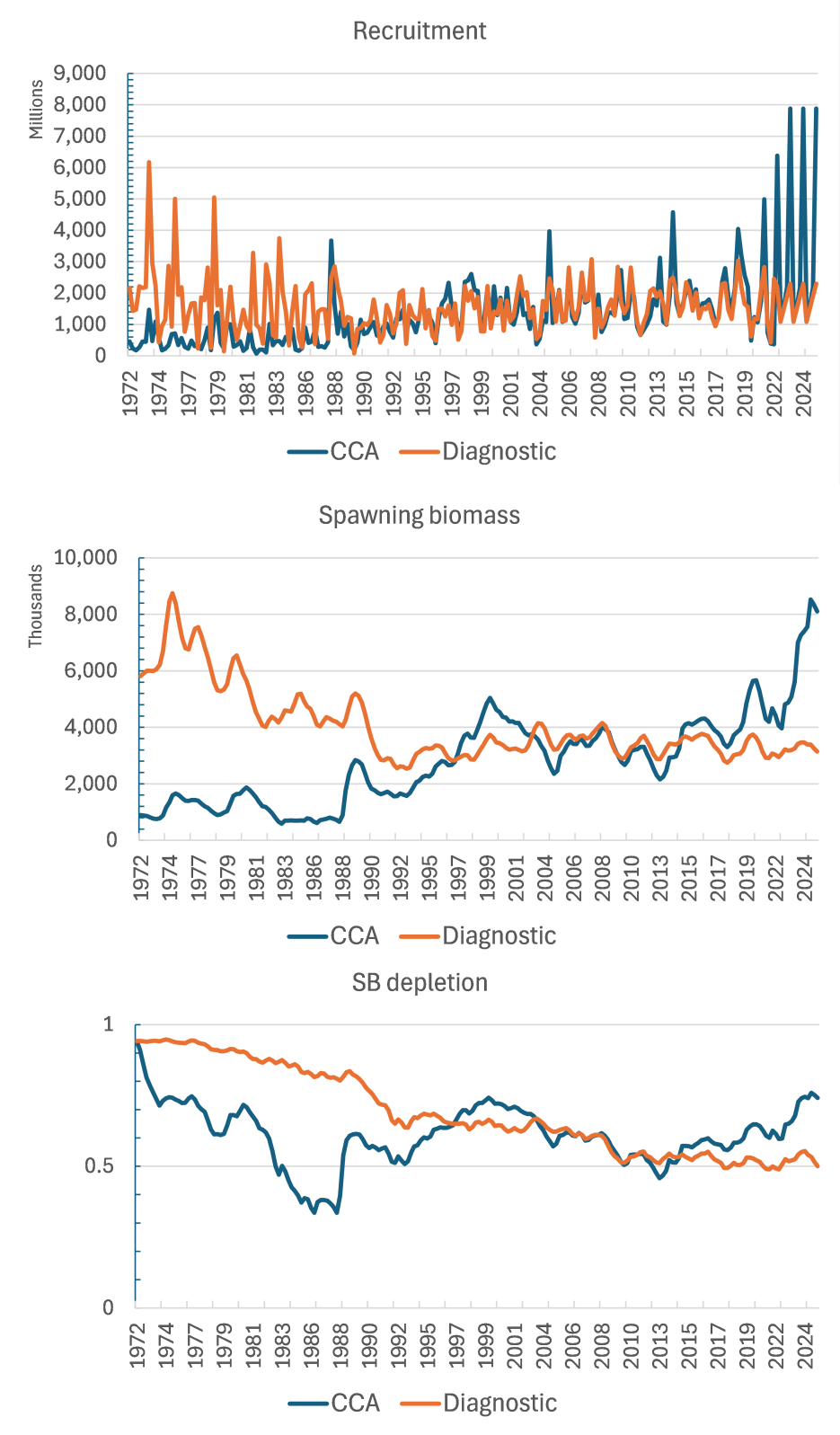

Figure 60: Recruitment, spawning potential (SB) and $SB/SB_{F=0}$ (SB depletion) estimates for the diagnostic case and for a catch curve analysis (CCA).

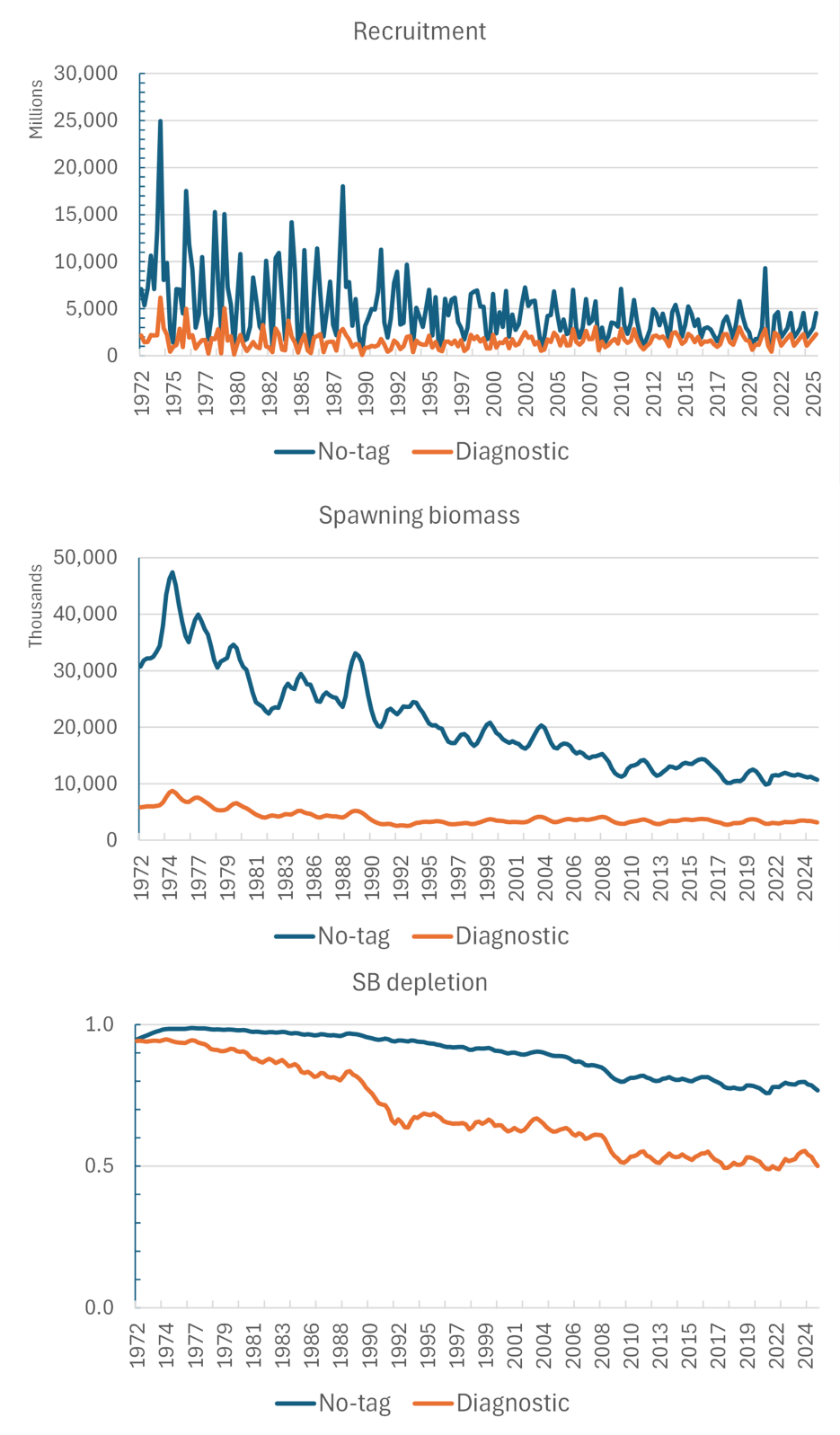

Figure 61: Recruitment, spawning potential (SB) and $SB/SB_{F=0}$ (SB depletion) estimates for the diagnostic case and for a model that excludes the tagging data (No-tag).

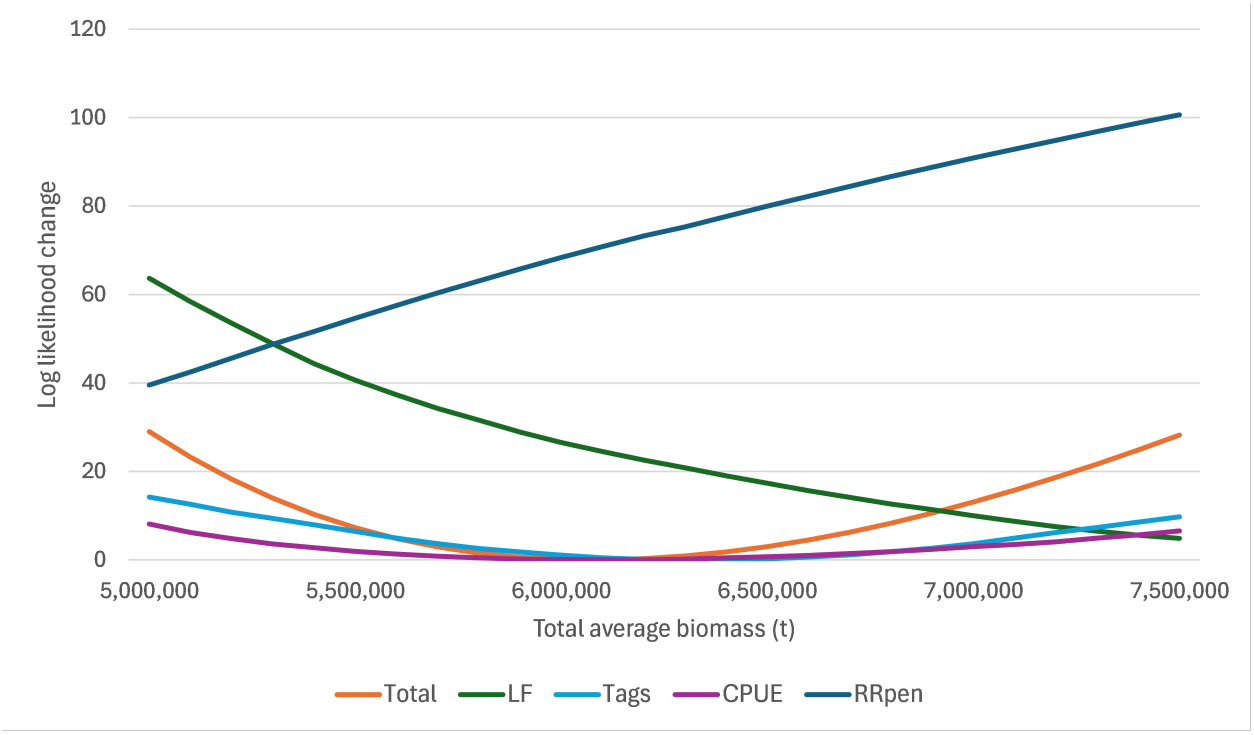

Figure 62: Likelihood profiles for data components (LF data, tagging data, CPUE indices) and the penalty resulting from reporting rate priors (RRpen).

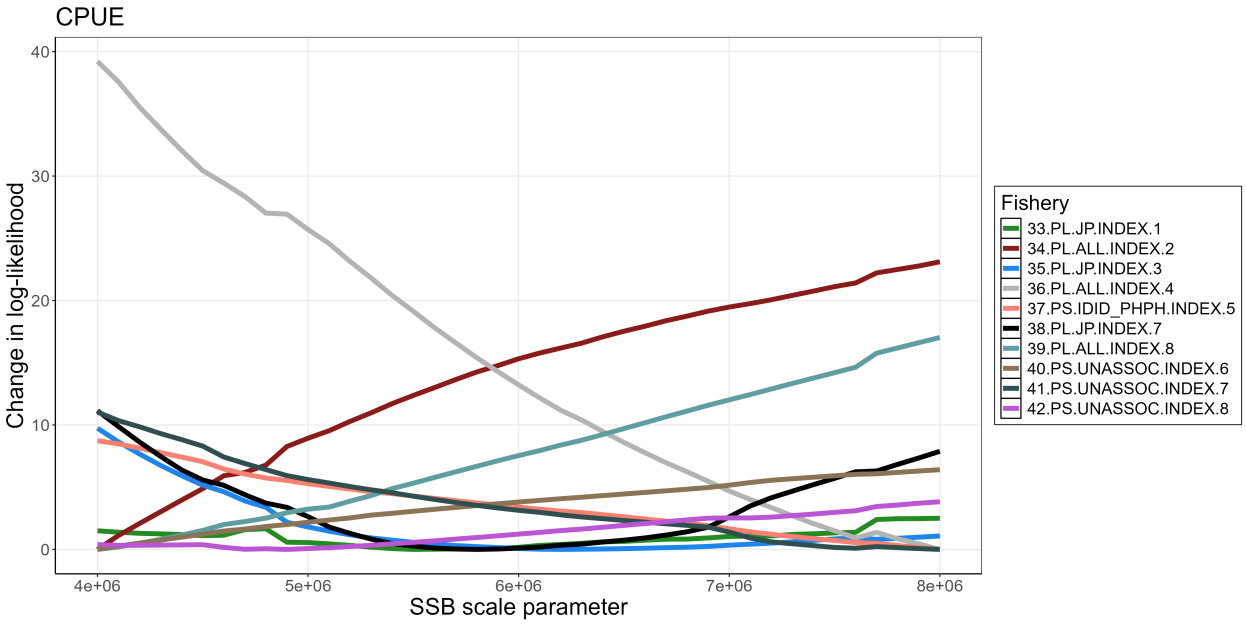

Figure 63: Likelihood profiles by fishery for CPUE indices.

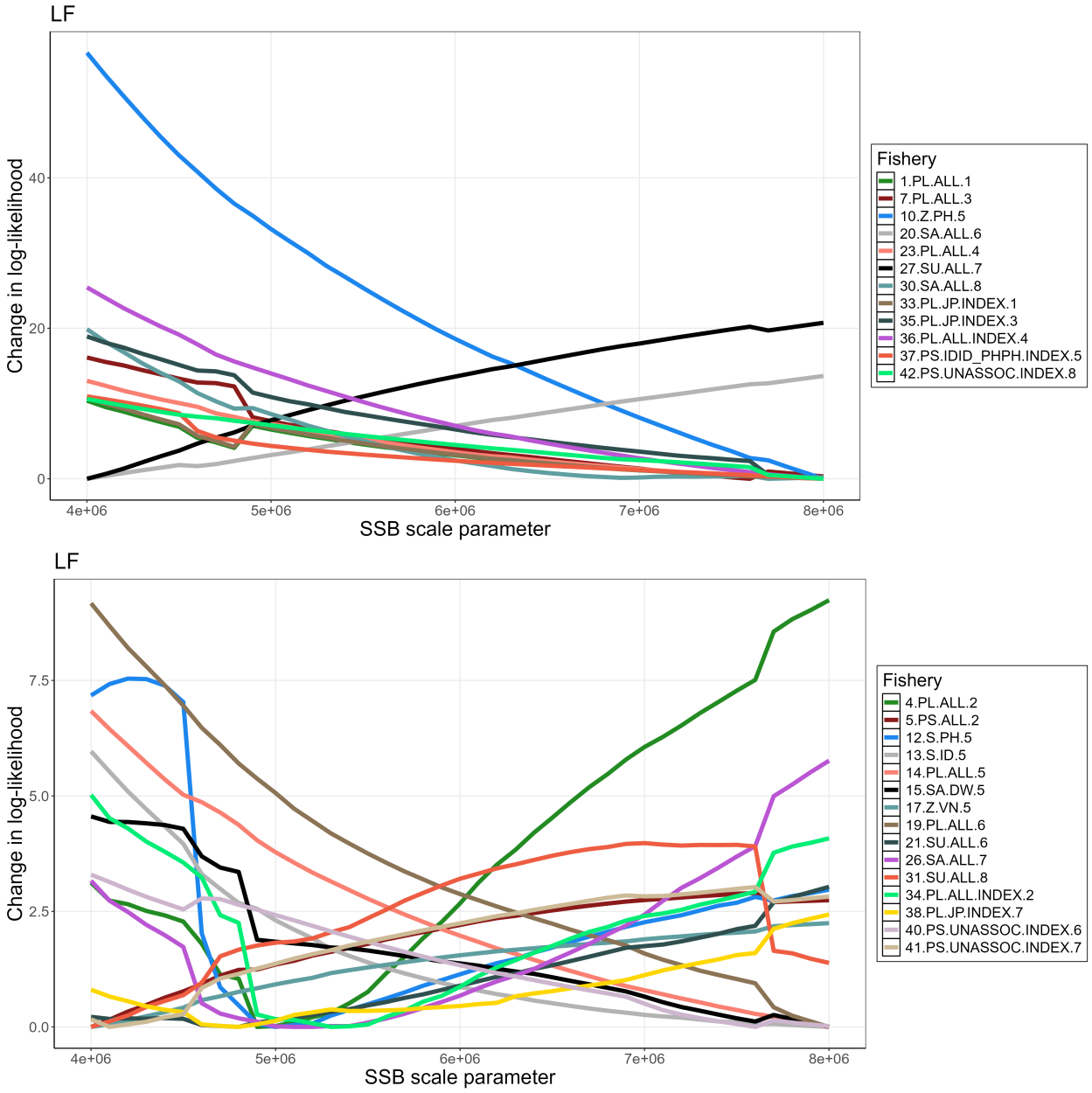

Figure 64: Likelihood profiles by fishery for LF with Δ likelihood > 10 (top) and LF with Δ likelihood ≤ 10 and > 1.96 (bottom).

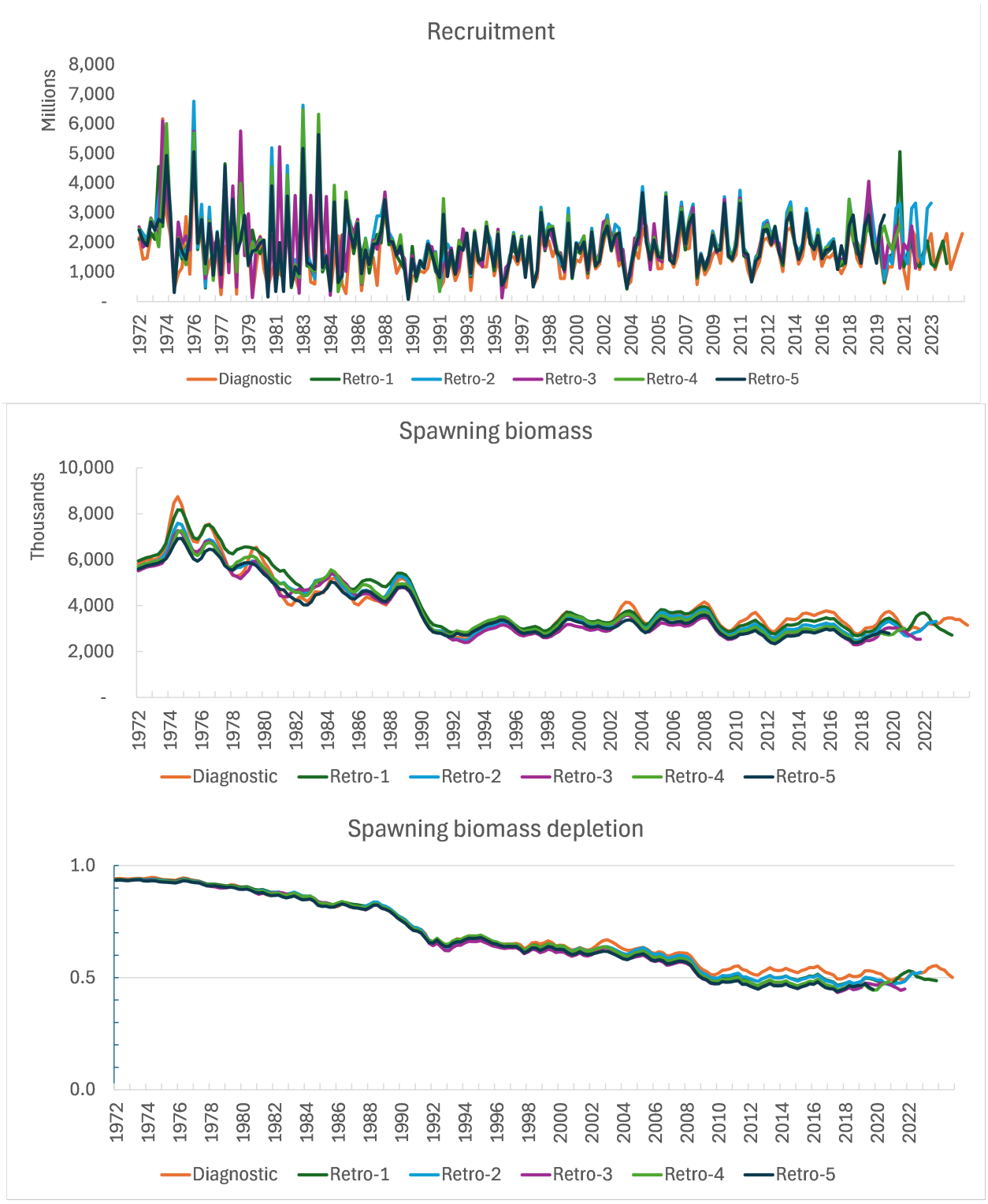

Figure 65: Retrospective analysis for recruitment, spawning potential (SB) and $SB/SB_{F=0}$ (SB depletion).

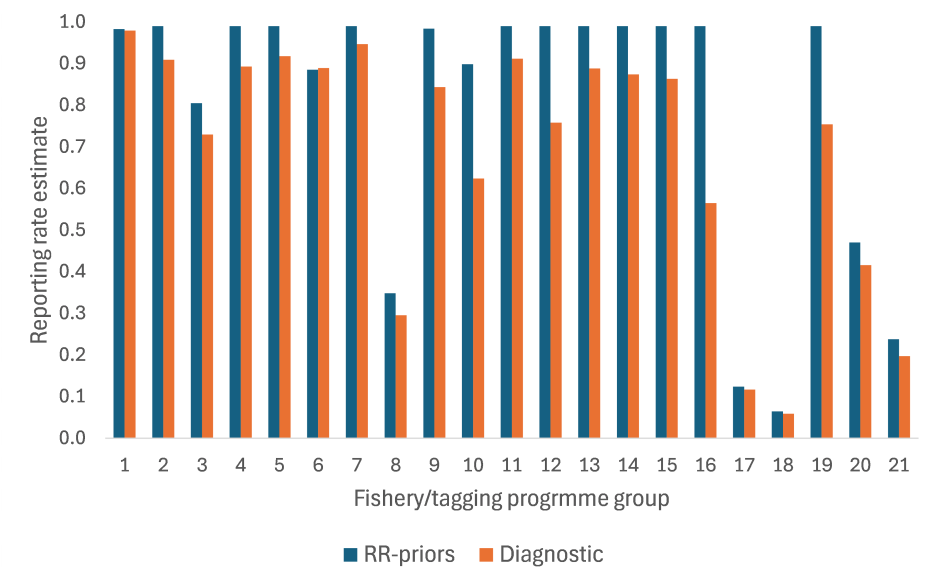

Figure 66: Estimates of reporting rates for fishery/tagging programme groups for the diagnostic model and for a model in which the priors for the reporting rates had been made to be uninformative (RR-priors).

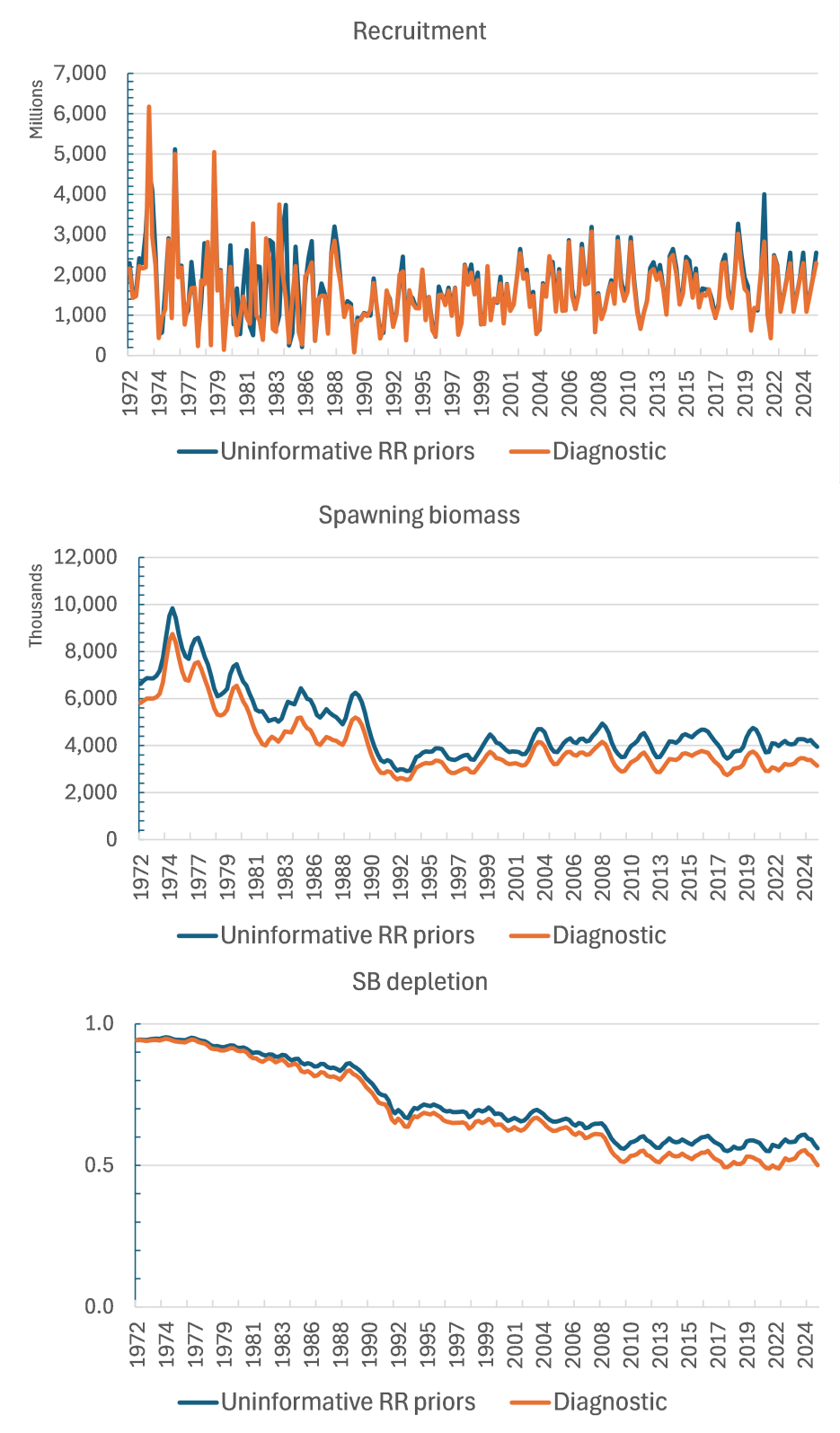

Figure 67: Estimates of recruitment, spawning potential (SB) and $SB/SB_{F=0}$ (SB depletion) for the diagnostic model and for a model with uninformative reporting rate priors.

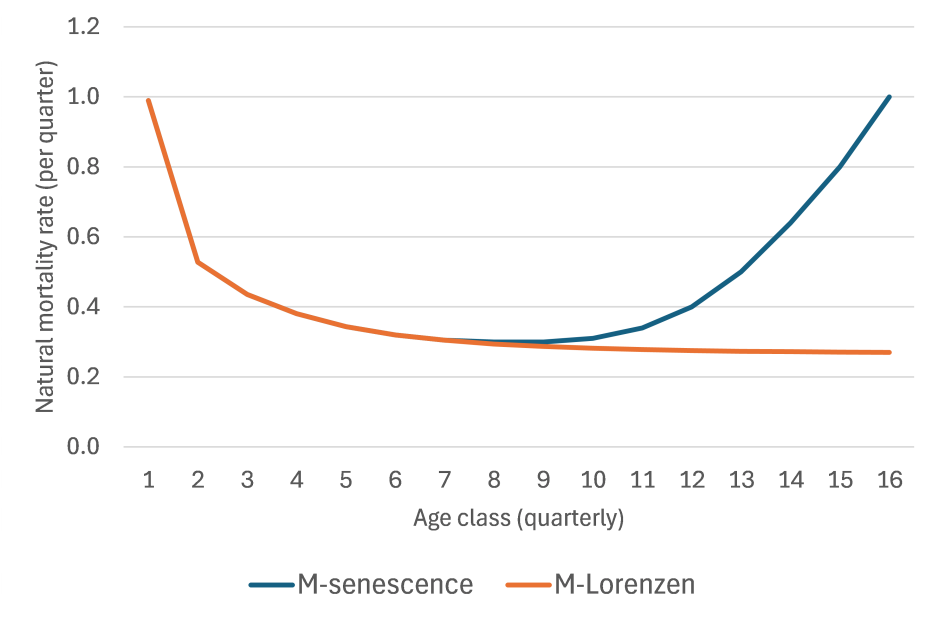

Figure 68: Estimates of natural mortality (M) by quarterly age class for the diagnostic case (M-Lorenzen) compared to a model constructed to recognise senescent mortality (M-senescence).

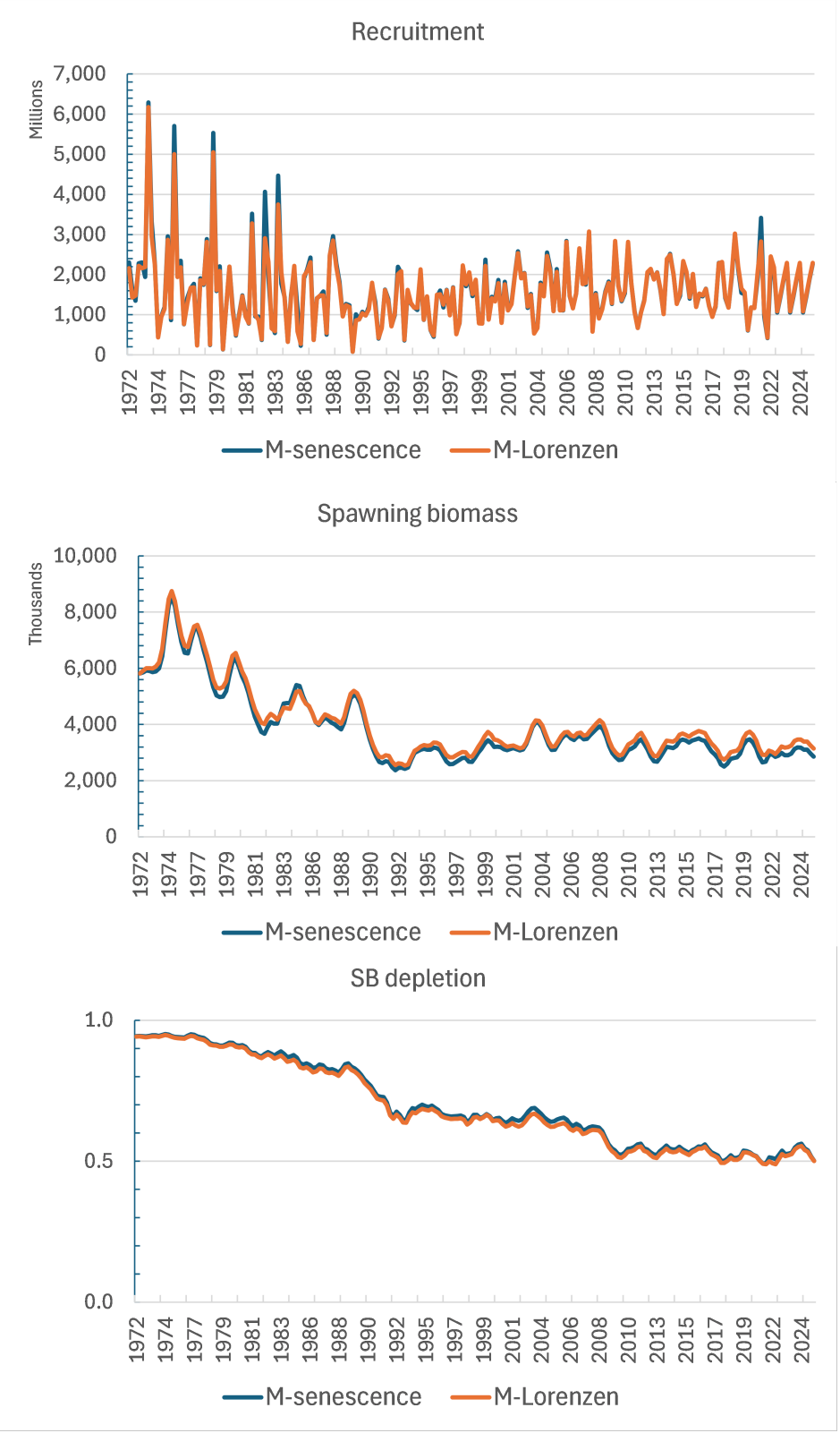

Figure 69: Estimates of recruitment, spawning potential (SB) and $SB/SB_{F=0}$ (SB depletion) for the diagnostic model (M-Lorenzen) and for a model with senescent natural mortality (M-senescence).

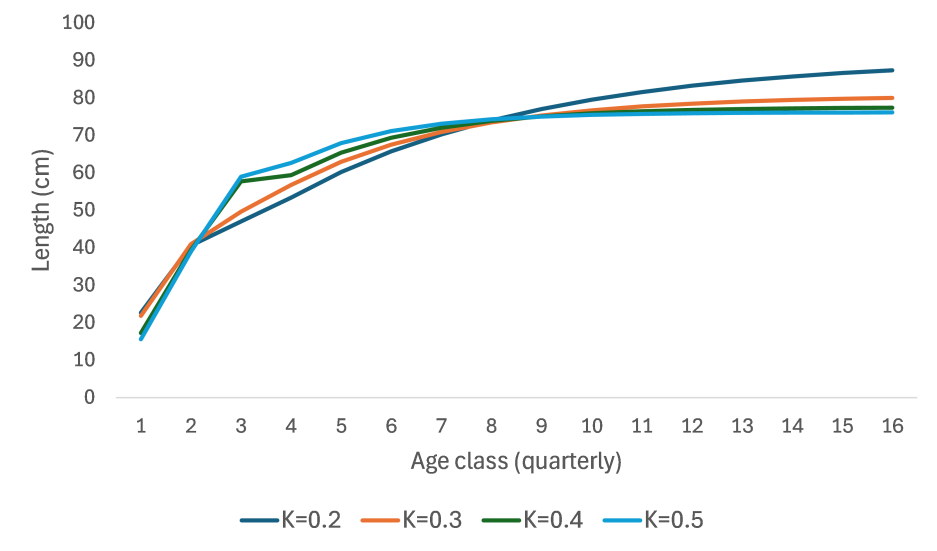

Figure 70: Alternative internally estimated growth curves for skipjack estimated for von Bertalanffy models with fixed growth coefficient k, and estimating $L1$, $L16$ and growth offsets for age classes 2 and 3.

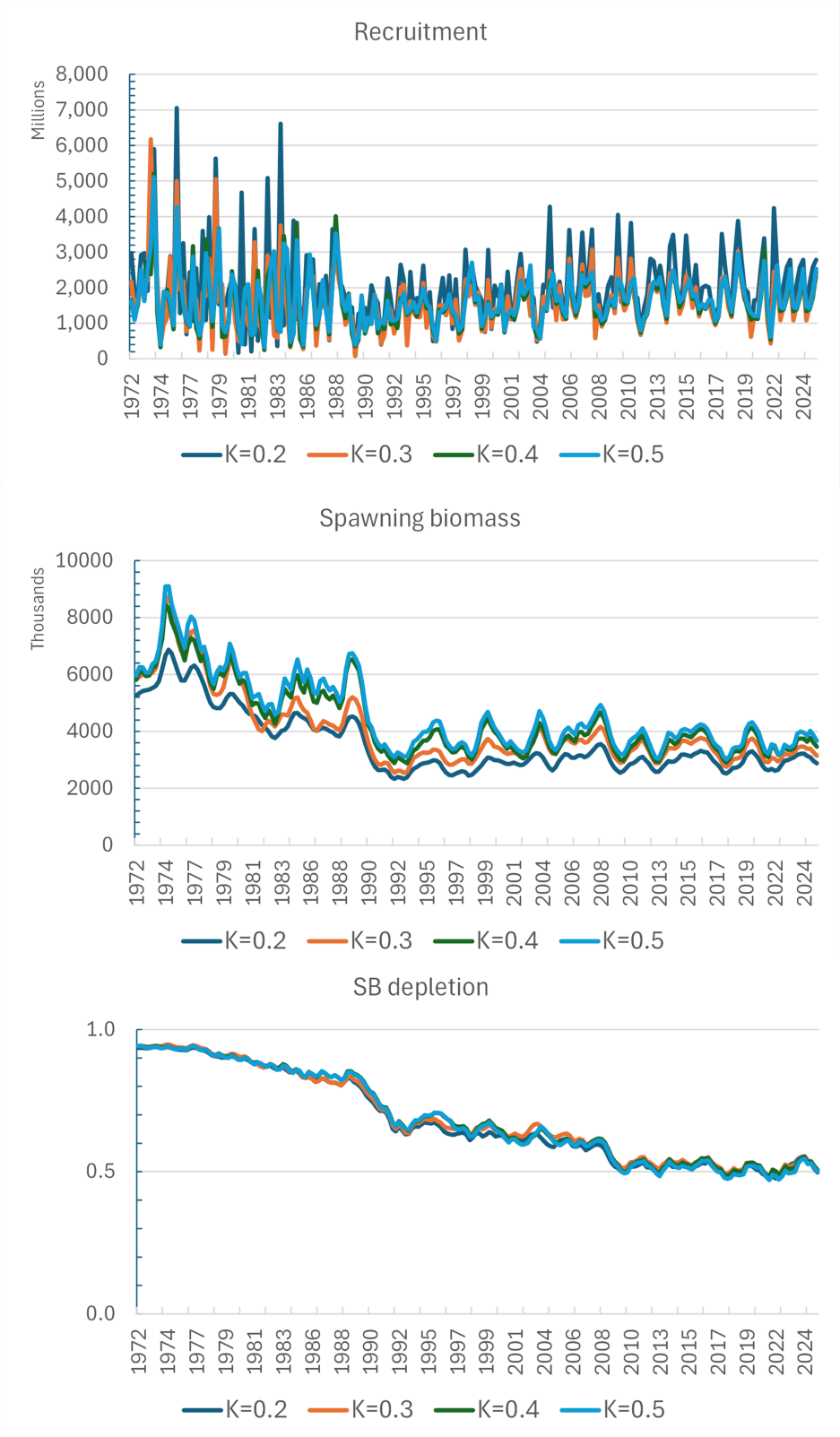

Figure 71: Estimates of recruitment, spawning potential (SB) and $SB/SB_{F=0}$ (SB depletion) for the diagnostic model (K=0.3) and for models with alternative fixed values of k.

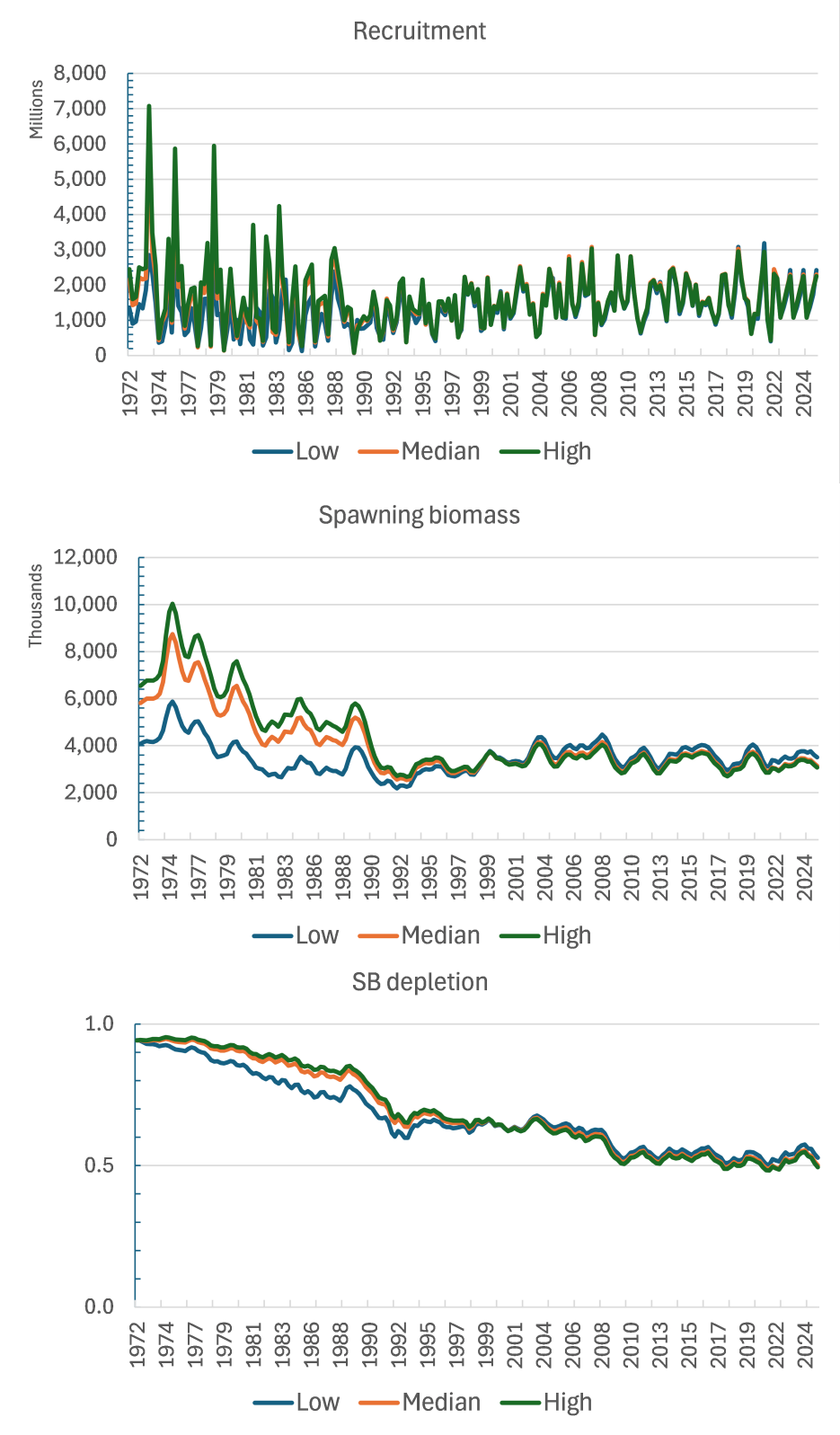

Figure 72: Estimates of recruitment, spawning potential (SB) and $SB/SB_{F=0}$ (SB depletion) for the diagnostic model (median effort creep of 4x terminal effective effort) and for models with low (2x terminal effective effort) and high (5x effective effort) levels of effort creep in the pole-and-line index fisheries.

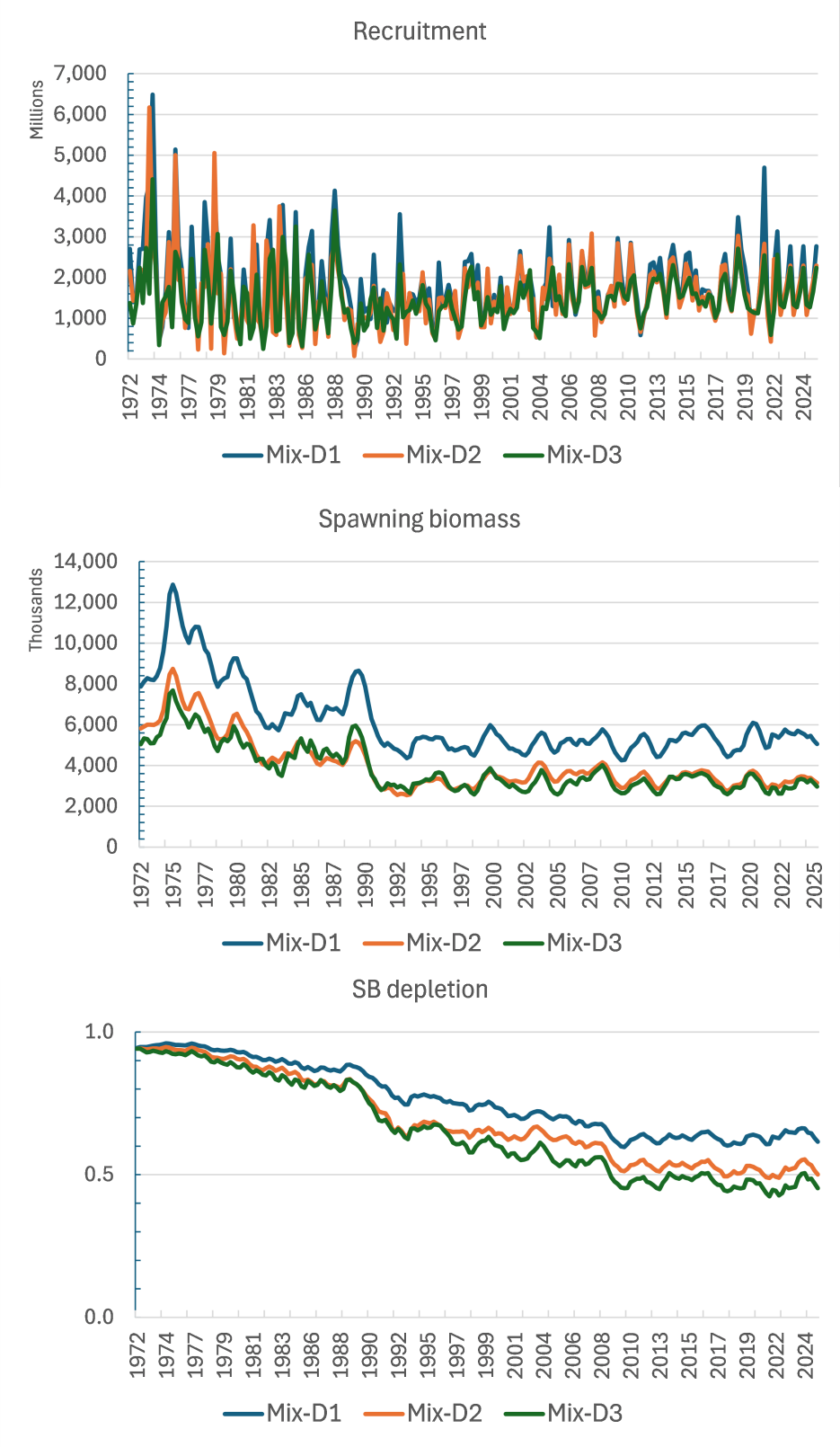

Figure 73: Estimates of recruitment, spawning potential (SB) and $SB/SB_{F=0}$ (SB depletion) from models with different tag mixing scenarios. Mix-$K1$ applies the strictest criterion (K <0.1) and results in longer mixing period, whereas Mix-$K3$ applies the most lenient criterion (K <0.3) and results in shorter mixing periods. The diagnostic case model (Mix-$K2$) applied an intermediate criterion (K <0.2).

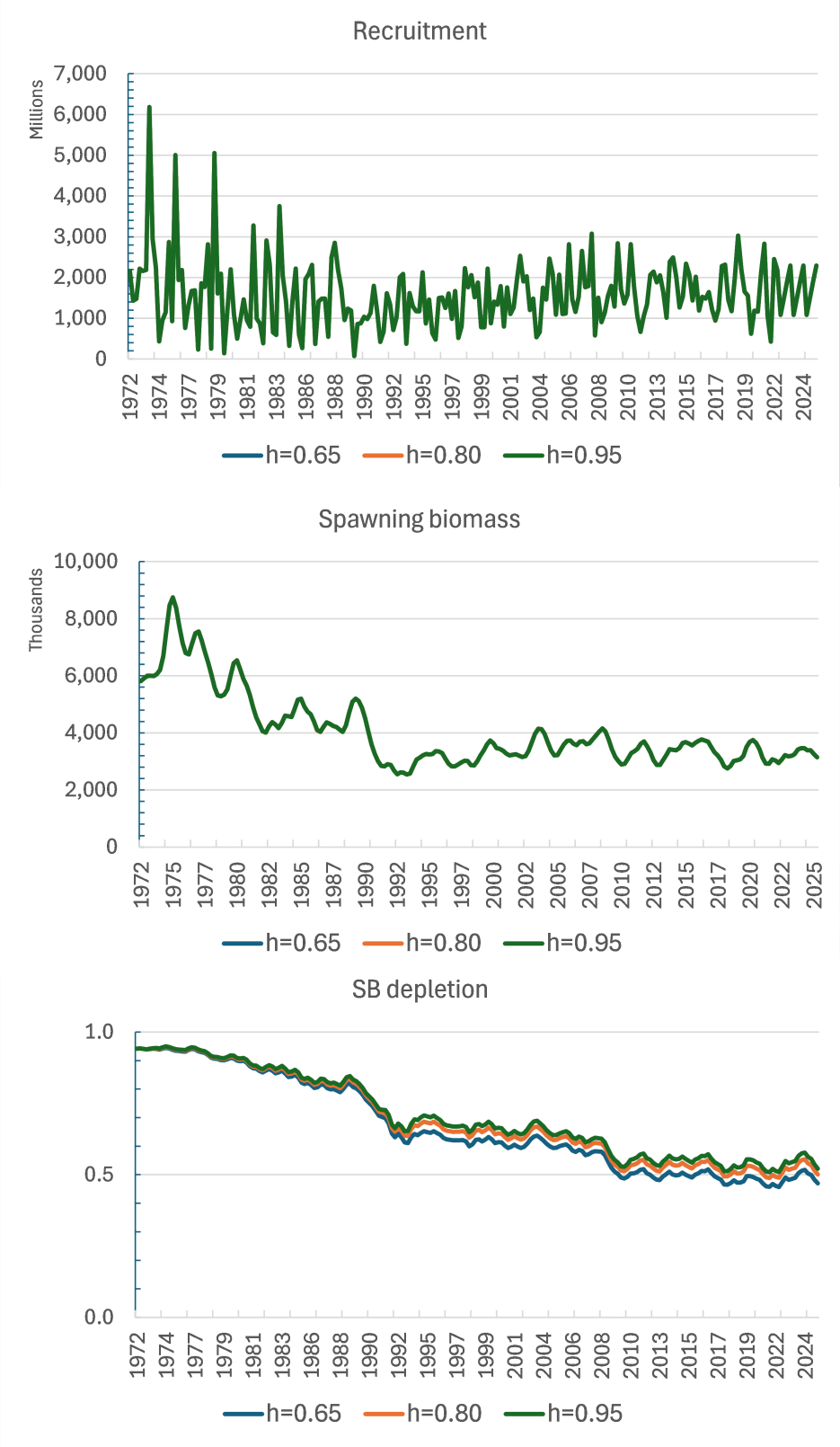

Figure 74: Estimates of recruitment, spawning potential (SB) and $SB/SB_{F=0}$ (SB depletion) for three levels of steepness.

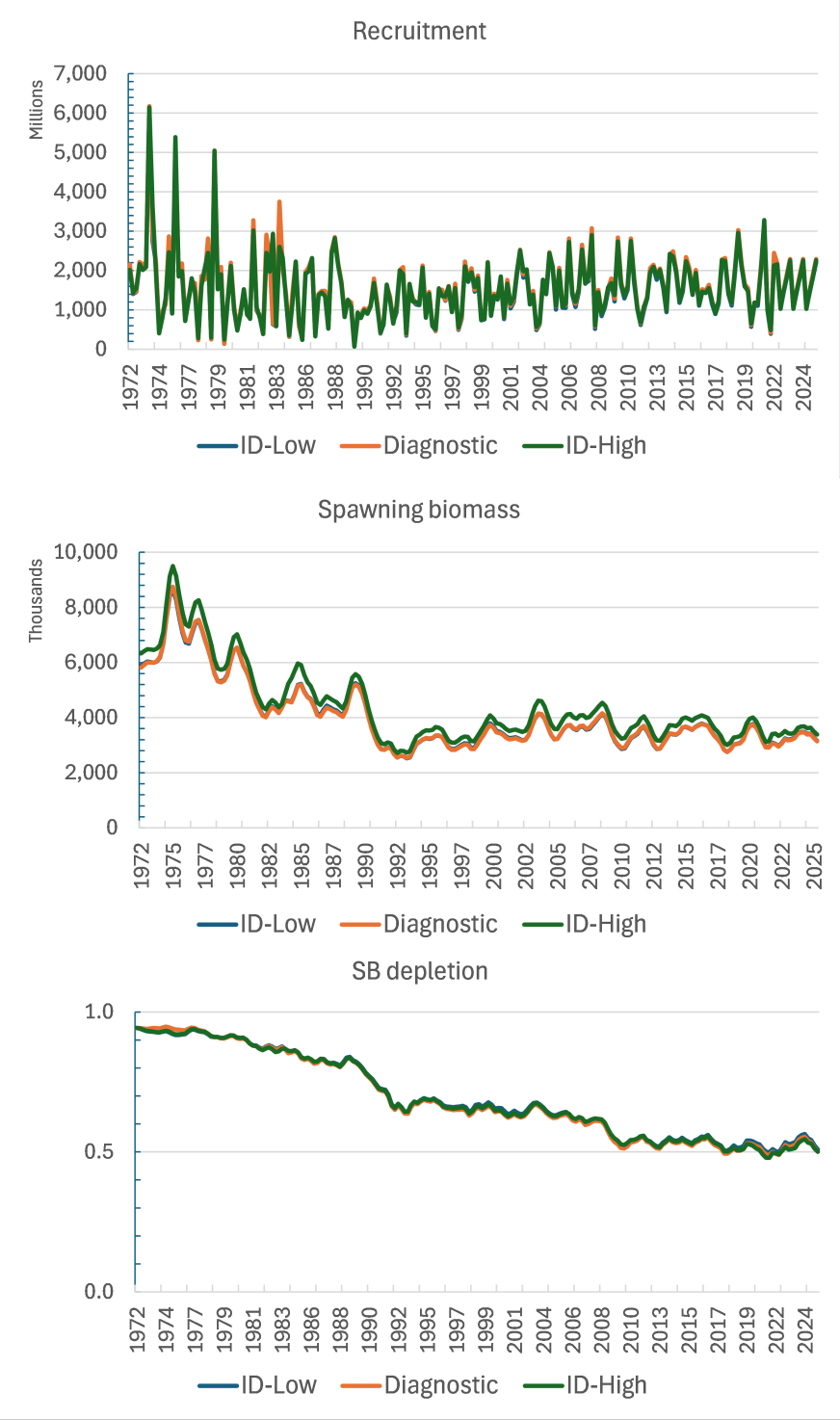

Figure 75: Estimates of recruitment, spawning potential (SB) and $SB/SB_{F=0}$ (SB depletion) for models that varied the catch of the Indonesian domestic fisheries by + (ID-High) and – (ID-Low) 20% from the diagnostic model.

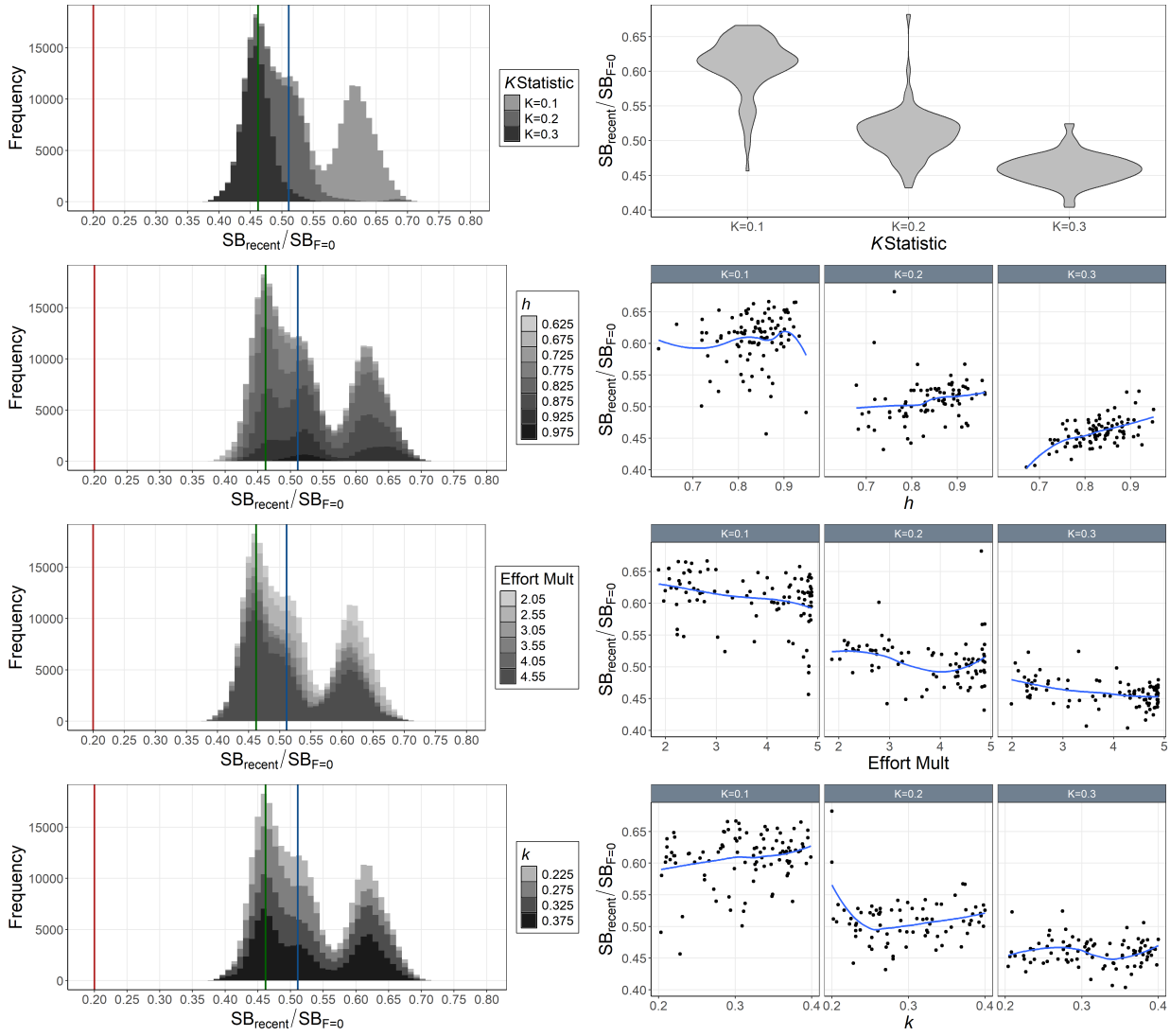

Figure 76: Histograms of Monte-Carlo estimated model uncertainty for $SB_{recent}/SB_{F=0}$ by mixing period (K statistic, top-left), h ($2^n d$-left), effort multiplier (Effort Mult; $3^r d$-left), and k (bottom-left) with mode (green line), median (blue line), and $SB_{recent}/SB_{F=0} = 0.2$ (red line). Also includes estimated $SB_{recent}/SB_{F=0}$ by mixing period (K statistic; top-right), h (2^{nd}-right), effort multiplier (Effort Mult; 3^{rd}-right), and k (bottom-right) for each model in the ensemble with loess smoother.

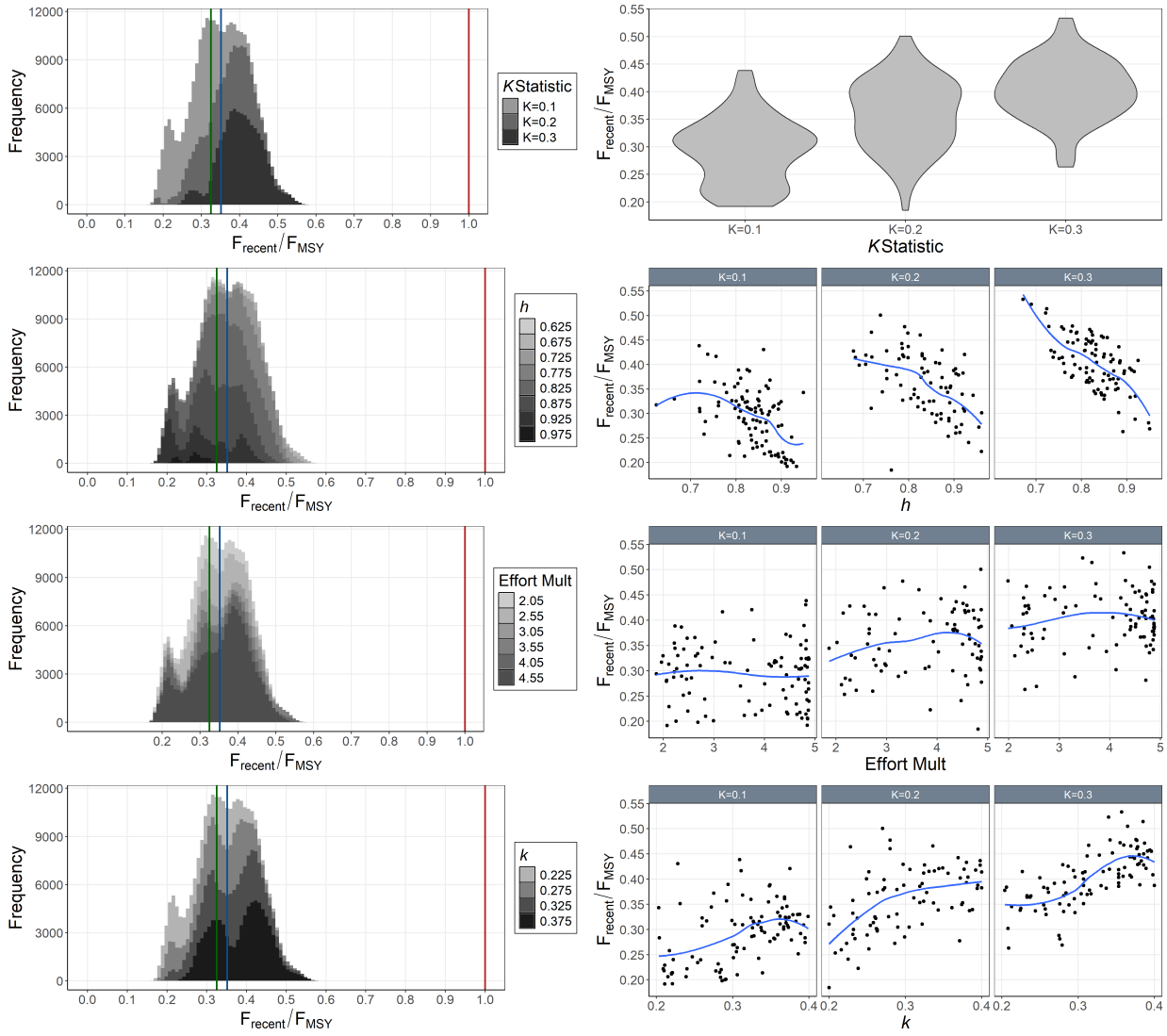

Figure 77: Histograms of Monte-Carlo estimated model uncertainty for F_{recent}/F_{MSY} by mixing period (K statistic, top-left), h ($2^n d$-left), effort multiplier (Effort Mult; $3^r d$-left), and k (bottom-left) with mode (green line), median (blue line), and $F_{recent}/F_{MSY} = 1.0$ (red line). Also includes estimated F_{recent}/F_{MSY} by mixing period (K statistic; top-right), h (2^{nd}-right), effort multiplier (Effort Mult; 3^{rd}-right), and k (bottom-right) for each model in the ensemble with loess smoother.

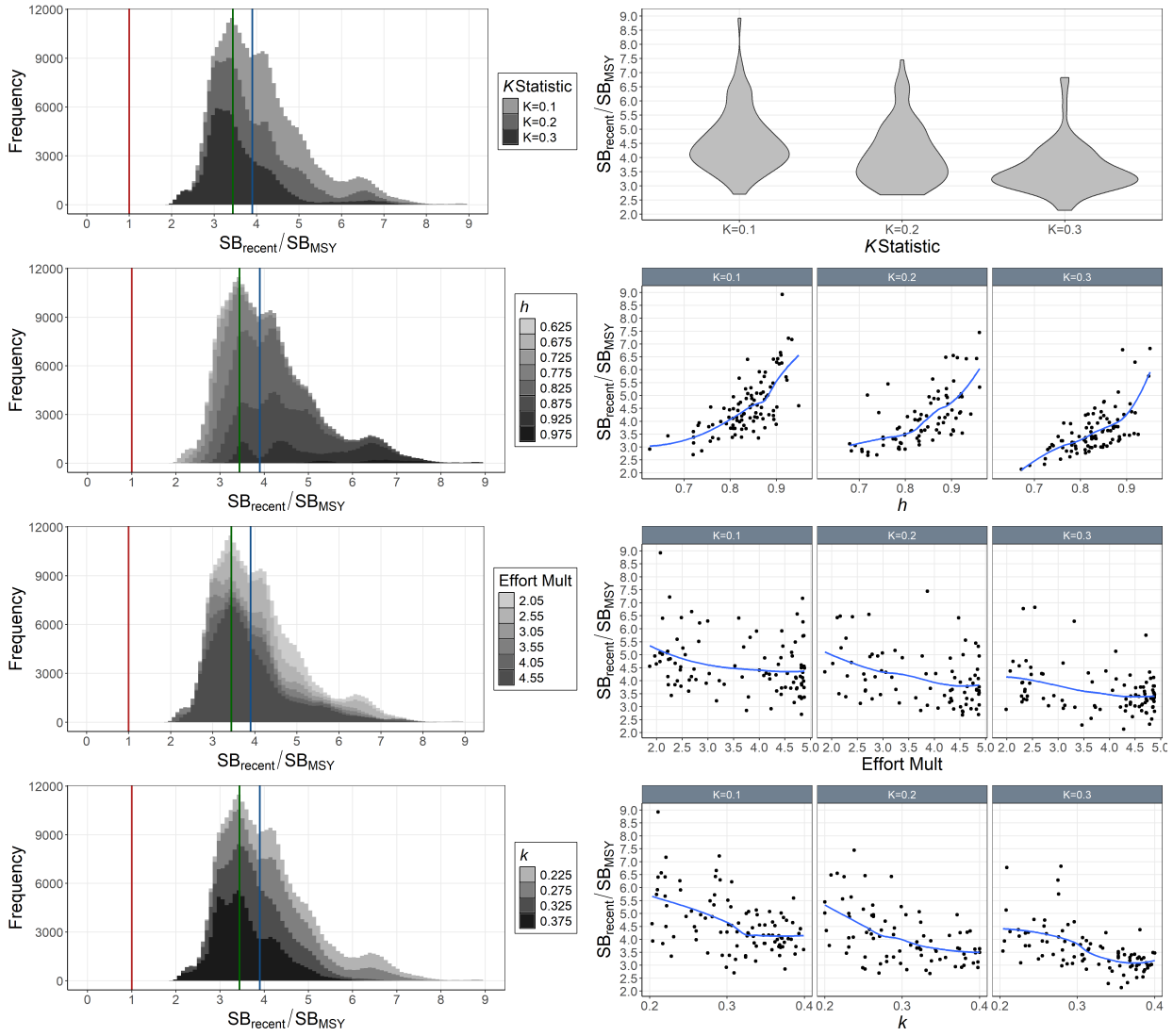

Figure 78: Histograms of Monte-Carlo estimated model uncertainty for SB_{recent}/SB_{MSY} by mixing period (K statistic, top-left), h (2^{nd}-left), effort multiplier (Effort Mult; 3^{rd}-left), and k (bottom-left) with mode (green line), median (blue line), and $SB_{recent}/SB_{MSY} = 1.0$ (red line). Also includes estimated SB_{recent}/SB_{MSY} by mixing period (K statistic; top-right), h ($2^{n}d$-right), effort multiplier (Effort Mult; $3^{r}d$-right), and k (bottom-right) for each model in the ensemble with loess smoother.

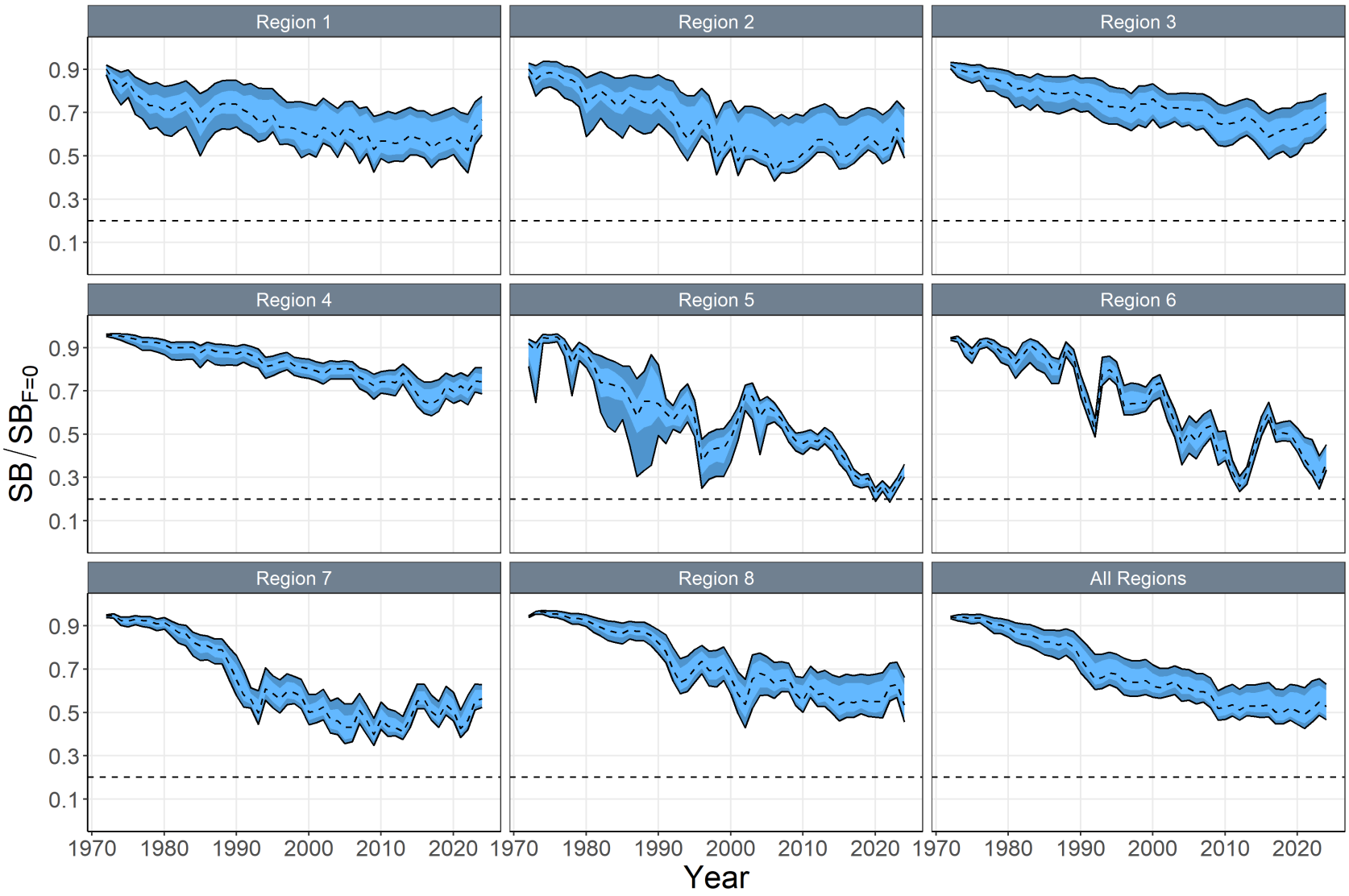

Figure 79: Annual estimated 90% (dark blue) and 75% (light blue) quantiles of $SB_t/SB_{F=0(t)}$ by region from the model ensemble. The dashed line within the interval indicates the median.

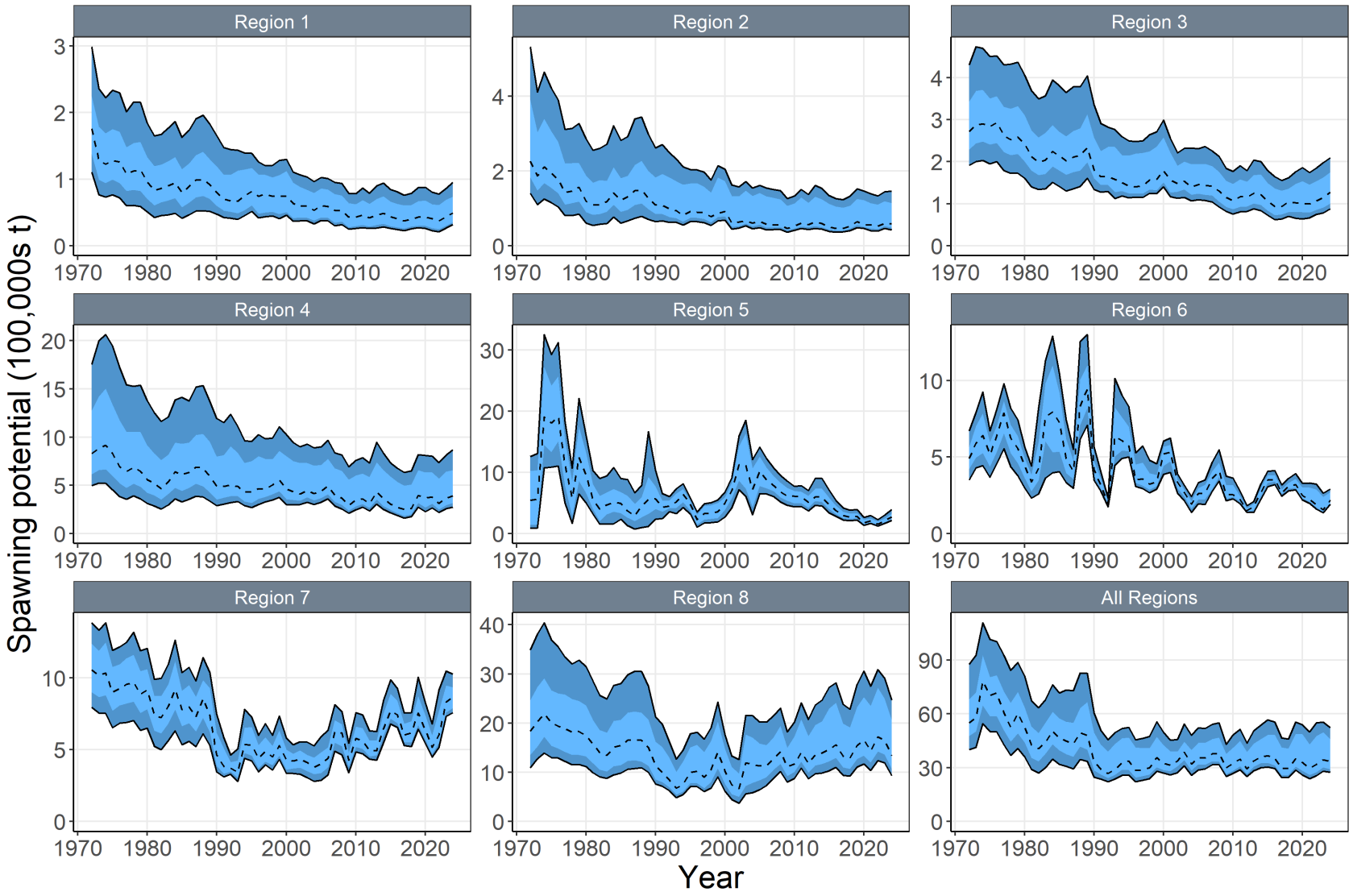

Figure 80: Annual estimated 90% (dark blue) and 75% (light blue) quantiles of SB by region from the model ensemble. The dashed line indicates the median.

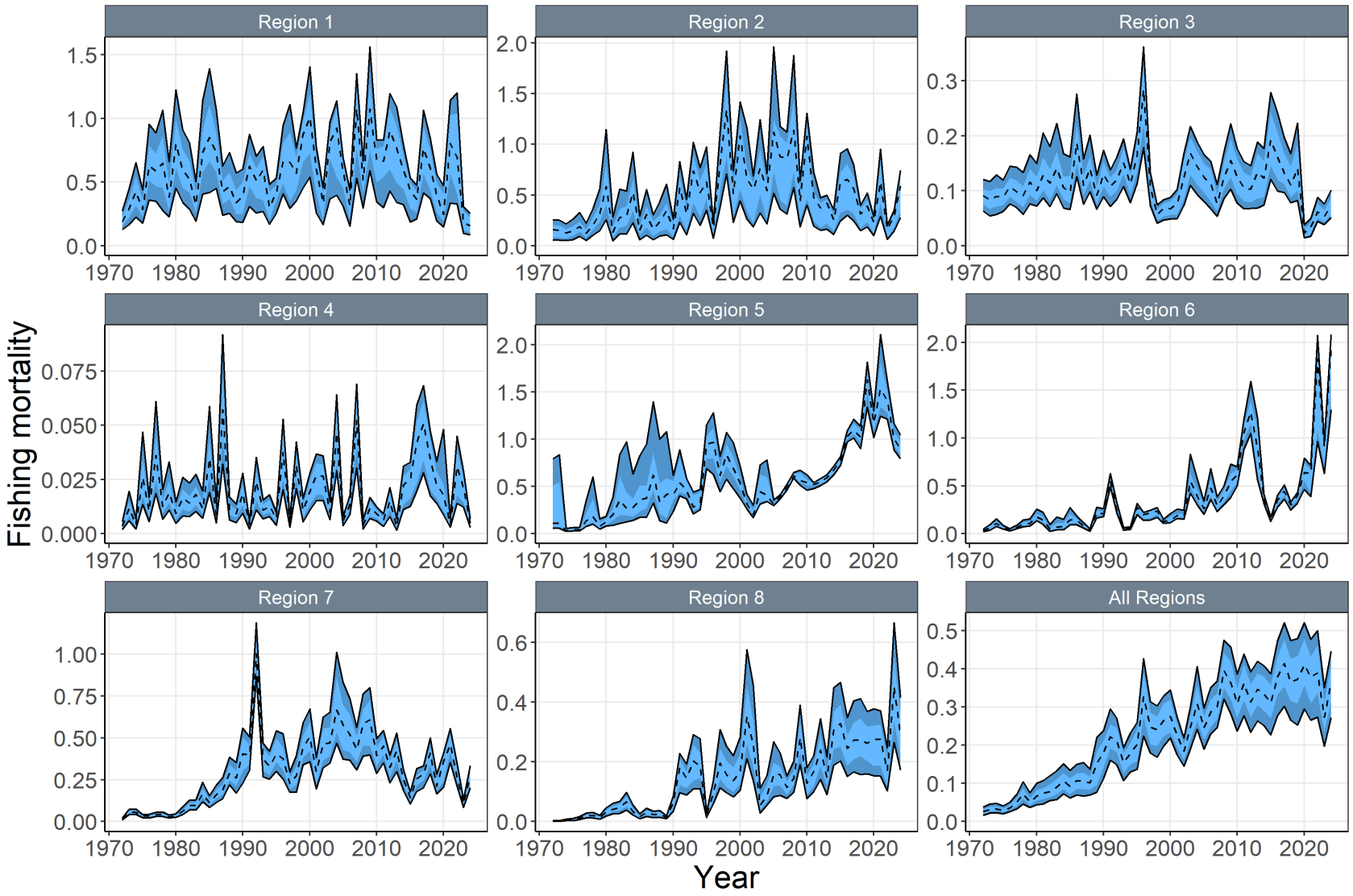

Figure 81: Estimated 90% (dark blue) and 75% (light blue) quantiles of annualised age aggregated fishing mortality (weighted by numbers-at-age) by region from the model ensemble. The dashed line indicates the median. Note the difference in scale among regions.

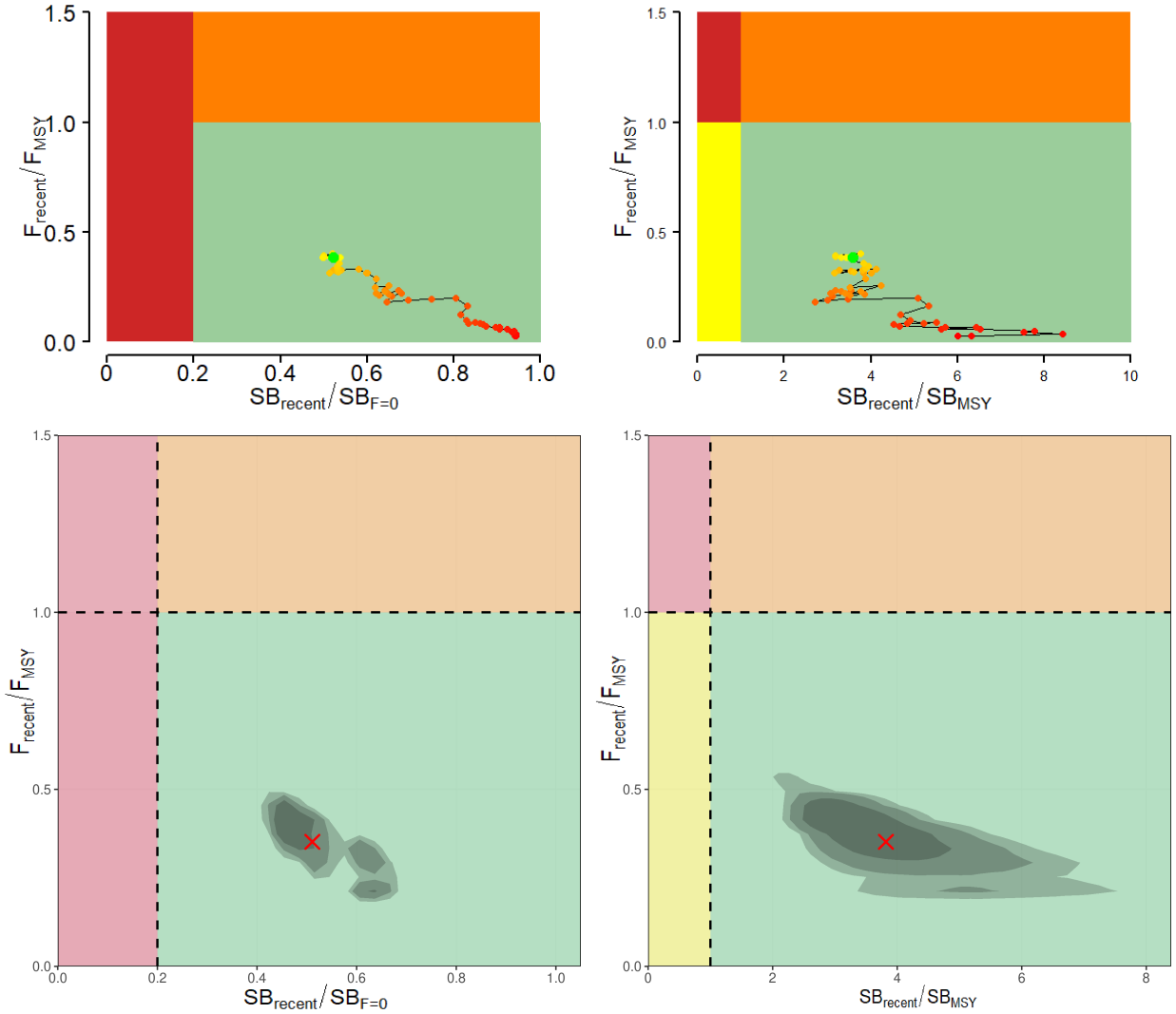

Figure 82: Majuro plots (left) and Kobe plots (right) summarising the results for the dynamic MSY analysis (top) and the Monte-Carlo random draws from the model ensemble (i.e., including estimation uncertainty) for the recent period (2021–2024; right). Colors for dynamic MSY go from red to green over time. Shading of model ensemble results indicate 50^{th}, 80^{th}, and 90^{th} highest density regions. The red X in model ensemble represents the median.

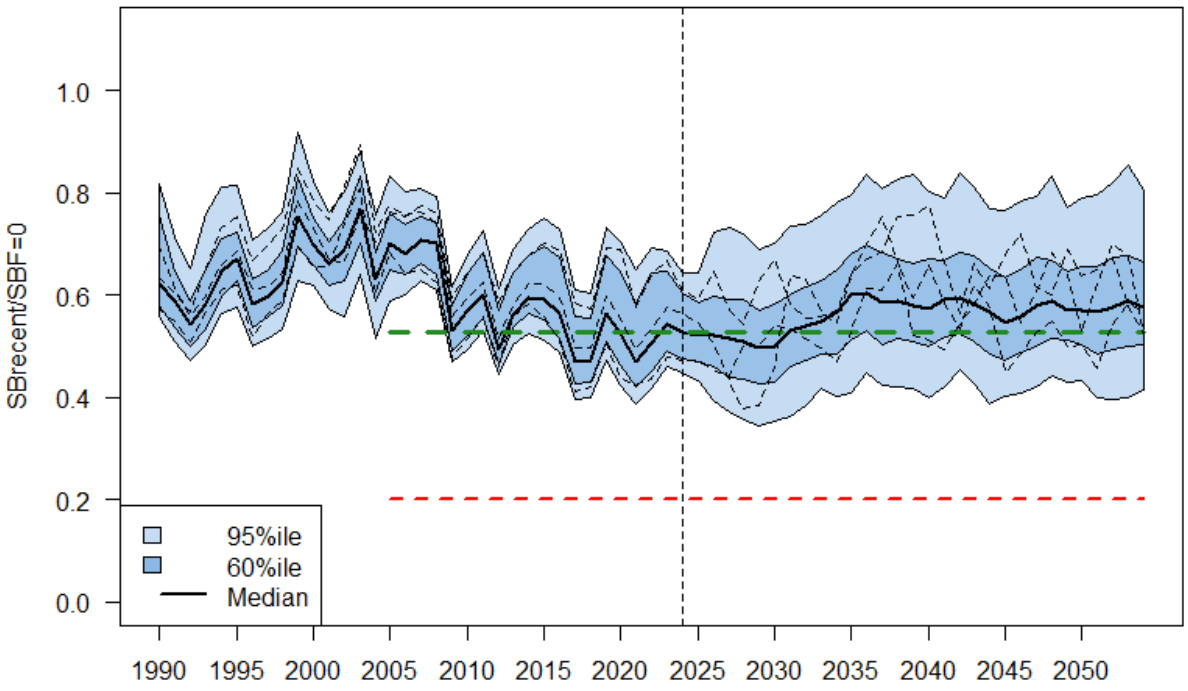

Figure 83: WCPO skipjack tuna SB depletion from the uncertainty grid of assessment model runs for the period 1990 to 2024 (the vertical line at 2024 represents the last year of the assessment), and stochastic projection results for the period 2025 to 2054 assuming catch and effort levels in 2024 continued. Prior to 2025 the data represent the 60^{th} and 95^{th} percentiles of the uncertainty grid from the assessment models and the median. During the projection period (2025-2054), levels of recruitment variability estimated over the period used to estimate the stock-recruitment relationship (1984-2020) are assumed to continue in the future. The dashed lines indicate three example trajectories (chosen randomly out of 8,100) from the model grid. The red dashed line represents the WCPFC agreed limit reference point (0.20). The green dashed line represents the re-calibrated skipjack TRP level.

17 Appendix 1: Doitall file

The text below (known as the "doitall" file) provides the flag settings and phase operations for running the diagnostic case model within a bash shell.

```
# ——————————
# Create initial 00.par file
# ——————————
# mfclo64 skj.frq skj.ini 00.par -makepar # does not work within a script
# ——————————
#
# ——————————
# PHASE 1 - initial fit with control phases
# ——————————
#
mfclo64 skj.frq 00.par 01.par -file - PHASE1
#
#————————————————————————————————————————————-
# Initial Phase Control option
1 32 7 # control phase - keep growth parameters fixed
1 387 0 # optimised scaling
#————————————————————————————————————————————-
# Catch conditioned flags
# general activation
1 373 1 # activated CC with Baranov equation
1 393 0 # activate estimation of: kludged equilib coffs, and implicit fm level regression pars
2 92 2 # specifies the catch-conditioned option with Baranov equation
# - catch equation bounds
2 116 80 # value for Zmax fish in the catch equations
2 189 80 # the fraction of Zmax fish above which the penalty is calculated
1 382 300 # weight for Zmax fish penalty - set to 300 to avoid triggering Zmax flag=1. Found by T&E
# De-activate any catch errors flags
-999 1 0
-999 4 0
-999 10 0
-999 15 0
-999 13 0
# – survey fisheries defined
# Index wt Time varying CV
```

-33 92 27 -33 94 1 -33 66 1 # PL JP 1
-34 92 28 -34 94 1 -34 66 1 # PL JP 2
-35 92 18 -35 94 1 -35 66 1 # PL JP 3
-36 92 19 -36 94 1 -36 66 1 # PL JP 4
-37 92 19 -37 94 1 -37 66 1 # PS PH 5 (appended based on Thom's review of CPUE analysis
-38 92 22 -38 94 1 -38 66 1 # PL JP 7
-39 92 24 -39 94 1 -39 66 1 # PL JP 8
-40 92 27 -40 94 1 -40 66 1 # PS UNA 6
-41 92 15 -41 94 1 -41 66 1 # PS UNA 7
-42 92 23 -42 94 1 -42 66 1 # PS UNA 8
– Grouping flags for survey CPUE
-1 99 1
-2 99 2
-3 99 3
-4 99 4
-5 99 5
-6 99 6
-7 99 7
-8 99 8
-9 99 9
-10 99 10
-11 99 11
-12 99 12
-13 99 13
-14 99 14
-15 99 15
-16 99 16
-17 99 17
-18 99 18
-19 99 19
-20 99 20
-21 99 21
-22 99 22
-23 99 23
-24 99 24
-25 99 25
-26 99 26
-27 99 27
-28 99 28

-29 99 29
-30 99 30
-31 99 31
-32 99 32
-33 99 33 # PL index fisheries grouped initially
-34 99 33 #
-35 99 33 #
-36 99 33 #
-37 99 34
-38 99 33 #
-39 99 33 #
-40 99 35 # PS index fisheries grouped initially
-41 99 35 #
-42 99 35 #
Recruitment and Initial Population Settings
1 149 100 # penalty on recruitment devs n/10 so for 100 = 1/sqrt(2*100/10) - CV 0.22
1 400 4 # set the last 2 recruitment deviates to 0
1 398 0 # Sets terminal recruitments at geometric mean
2 113 0 # estimate initpop/totpop scaling parameter
2 177 1 # use old totpop scaling method
2 32 1 # totpop estimated from this phase
2 57 4 # 4 recruitments per year
2 93 4 # 4 recruitments per year
2 94 1 # Use equilibium initial population
2 128 102 # Initial Z is M*1.02
2 95 0 # Use average Z for first 20 periods for equil. init. pop.
– kludged initial survival relationship
1 374 0 # Spline degree for initial survival
1 375 0 # penalty weight on initial survival
1 379 0 # penalty wt on high (4) spline degrees for kludged equilib coeffs
#————————————————————————————————————-
Likelihood Component
1 141 3 # Robust normal likelihood function for LF data
1 111 4 # Negative binomial likelihood function for tags
-999 49 100 # Divisor for LF sample sizes effective sample size

#————————————————————————————————————-
Tagging Related Flags
#

1 33 99 # Maximum tag reporting rate for all fisheries is 0.99
2 198 1 # Turn on release group reporting rates which are specified in the .ini
1 305 1 " " # Estimate the variance parameter of the negative binomial
-999 43 1 # Var parameter estimated for all fisheries
-999 44 1 # All fisheries grouped for estimating tag neg bin var parameter
2 96 12 # Tags are pooled across release groups after 12 periods CHECK THIS - LOWER AND WOULD SPEED UP

——————————————————————————————————————
Selectivity grouping and form 1=logistic 2=doublenormal 3=cubic spine or length specific
-N 24 X is the selectivity grouping
-N 57 3 is cubic spline selectivity
-N 61 X establishes that there are X nodes in the spline
-999 26 3 # Use length-based selec
-999 3 16
1 359 1000 # penalty to keep sel coeffs away from lower bound
Grping Form (spline) No. nodes Asymp zero sel age classes
-1 24 1 -1 57 3 -1 61 4
-2 24 2 -2 57 3 -2 61 4
-3 24 3 -3 57 3 -3 61 3 -3 16 1 -3 75 3
-4 24 4 -4 57 3 -4 61 4
-5 24 5 -5 57 3 -5 61 4
-6 24 6 -6 57 3 -6 61 3 -6 16 1 -6 75 3
-7 24 7 -7 57 3 -7 61 4
-8 24 8 -8 57 3 -8 61 4
-9 24 9 -9 57 3 -9 61 3 -9 16 1 -9 75 3
-10 24 10 -10 57 3 -10 61 6
-11 24 11 -11 57 3 -11 61 5
-12 24 12 -12 57 3 -12 61 5
-13 24 13 -13 57 3 -13 61 5
-14 24 14 -14 57 3 -14 61 6
-15 24 15 -15 57 3 -15 61 4
-16 24 16 -16 57 3 -16 61 4
-17 24 17 -17 57 3 -17 61 5
-18 24 18 -18 57 3 -18 61 3 -18 16 1 -18 75 3
-19 24 19 -19 57 3 -19 61 4
-20 24 20 -20 57 3 -20 61 4
-21 24 21 -21 57 3 -21 61 4
-22 24 22 -22 57 3 -22 61 3 -22 16 1 -22 75 3

-23 24 23 -23 57 3 -23 61 4
-24 24 24 -24 57 3 -24 61 3 -24 16 1 -24 75 3
-25 24 25 -25 57 3 -25 61 4
-26 24 26 -26 57 3 -26 61 4
-27 24 27 -27 57 3 -27 61 4
-28 24 28 -28 57 3 -28 61 3 -28 16 1 -28 75 3
-29 24 29 -29 57 3 -29 61 4
-30 24 30 -30 57 3 -30 61 4
-31 24 31 -31 57 3 -31 61 4
-32 24 32 -32 57 3 -32 61 3 -32 16 1 -32 75 3
-33 24 33 -33 57 3 -33 61 4
-34 24 33 -34 57 3 -34 61 4
-35 24 33 -35 57 3 -35 61 4
-36 24 33 -36 57 3 -36 61 4
-37 24 34 -37 57 3 -37 61 5
-38 24 33 -38 57 3 -38 61 4
-39 24 33 -39 57 3 -39 61 4
-40 24 35 -40 57 3 -40 61 4
-41 24 35 -41 57 3 -41 61 4
-42 24 35 -42 57 3 -42 61 4
#——-
Fishery groupings for tag return data
-1 32 1
-2 32 2
-3 32 3
-4 32 4
-5 32 5
-6 32 6
-7 32 7
-8 32 8
-9 32 9
-10 32 10 # PH DOM
-11 32 10 # ID DOM
-12 32 10 # PH small PS
-13 32 10 # ID small PS
-14 32 10 # ID PL
-15 32 10 # PS ASS R5
-16 32 10 # PS UNA R5
-17 32 11

-18 32 12
-19 32 13
-20 32 14 # PS ASS R6
-21 32 14 # PS UNA R6
-22 32 15
-23 32 16
-24 32 17
-25 32 18
-26 32 19 # PS ASS R7
-27 32 19 # PS UNA R7
-28 32 20
-29 32 21
-30 32 22 # PS ASS R8
-31 32 22 # PS UNA R8
-32 32 23
-33 32 24
-34 32 25
-35 32 26
-36 32 27
-37 32 28
-38 32 29
-39 32 30
-40 32 31
-41 32 32
-42 32 33
Turn on weighted spline for calculating maturity at age from length observations
2 188 2 " "
Start with Lorenzen M-at-age
#
2 109 3 # M-at-age from ini file, age pars(2)
#
#
PHASE1
#
———
PHASE 2
———
mfclo64 skj.frq 01.par 02.par -file - PHASE2
#

```
2 113 0 # Turns of rec init diff estimation
1 1 500 # Sets no. of function evaluations for this phase
1 50 -2 # convergence criterion is 1.00E+01
# Estimate movement coefficients
2 68 1 # Estimate movement parameters
2 69 1 # Use movement parameters
2 27 -1 " " # Set penalty for movement coefficient to 0.1
#
PHASE2
#
# ———
# PHASE 3
# ———
mfclo64 skj.frq 02.par 03.par -file - PHASE3
#
2 70 1 # Estimate time-series changes in recruitment distribution
2 71 1 # est. time series of reg recruitment
2 178 1 # constraint on regional recruitments
#
PHASE3
# ———
# PHASE 4
# ———
mfclo64 skj.frq 03.par 04.par -file - PHASE4
# Estimate regional distribution of recruitment
-100000 1 1
-100000 2 1
-100000 3 1
-100000 4 1
-100000 5 1
-100000 6 1
-100000 7 1
-100000 8 1
#
#
PHASE4
# ———
# PHASE 5
# ———
```

```
mfclo64 skj.frq 04.par 05.par -file - PHASE5
#
# Dirichlet Multinomial (no random effects) settings
1 141 11 # selects DM-noRE likelihood
1 320 5 # implements tail compression
1 342 5000 # maximum ESS
-999 89 1 # Estimate relative sample size covariate
-999 69 1 # Estimate exponent of sacalar of LF sample size multiplier
-999 49 0 # Turn off RN sample size multiplier setting
# – grouping flags for DM parameters (by gear type - PL/PS, ID/PH/VN, LL)
-1 68 1
-2 68 1
-3 68 2
-4 68 1
-5 68 1
-6 68 2
-7 68 1
-8 68 1
-9 68 2
-10 68 3
-11 68 3
-12 68 3
-13 68 3
-14 68 1
-15 68 4
-16 68 4
-17 68 3
-18 68 2
-19 68 1
-20 68 4
-21 68 4
-22 68 2
-23 68 1
-24 68 2
-25 68 1
-26 68 4
-27 68 4
-28 68 2
-29 68 1
```

-30 68 4
-31 68 4
-32 68 2
-33 68 1
-34 68 1
-35 68 1
-36 68 1
-37 68 3
-38 68 1
-39 68 1
-40 68 4
-41 68 4
-42 68 4
#
PHASE5
———
PHASE 6
———
mfclo64 skj.frq 05.par 06.par -file - PHASE6
#
1 1 500 # How many function evaluations
2 145 1 # Penalty wt. for SRR CV=0.7
2 146 1 # Make SRR parameters active
2 147 1 # No. time periods for recruitment lag
2 182 1 ” ” ” #” Annualized recruitments and average biomass
2 148 20 # Years (year quarters) from last year for avg. F
2 155 4 # But not including last 4
1 149 0 # Turn off recruitment penalties against mean - frees up recruitment - should improve fit to compositions
2 162 0 # Estimate steepness 0 IS THE DEFAULT meaning not estimated
2 163 0 # BH-SRR is parameterised using steepness. Value of 0 IS THE DEFAULT meaning it is parameterized with steepness
2 199 0 # start time period for yield calculation [4.5.11], made consistent with 2014 assessment - starts in 1982
2 200 4 # end time period for yield calculation [4.5.11]
-999 55 1 # Turn off fisheries for impact analysis [4.5.14]
2 193 1 # Turn on fisheries impact analyses
2 171 1 # Unfished calculations by estimated SRR
2 161 1 # Turn on the bias correction for the Beverton-Holt

2 116 200 # Increase Z bound for NR computations to 2
1 190 1 # Write plot.rep
1 187 1 # Write temporary tag report
1 188 1 # Write ests.rep
1 189 1 # Write .fit files
1 246 1 # Write independent variables report
#
PHASE6
———
PHASE 7
———
mfclo64 skj.frq 06.par 07.par -file - PHASE7
#
1 13 1 # Estimate L2
1 14 0 # k not estimated
#
PHASE7
———
PHASE 8
———
mfclo64 skj.frq 07.par 08.par -file - PHASE8
#
1 12 1 # Estimate L1
1 173 3 # Number of offsets estimated - 3 == age classes 2 and 3
1 184 1 # Estimate offsets
#
PHASE8
———
PHASE 9
———
mfclo64 skj.frq 08.par 09.par -file - PHASE9
#
1 15 1 # Estimate generic SD
1 16 1 # Estimate length-dependent SD
”# ”
PHASE9
———-
PHASE 10 - Estimate M scaling
———-

```
mfclo64 skj.frq 09.par 10.par -file - PHASE10
#
1 121 1 # Estimate M scaling
2 116 300 # Further relax the bound on Z
1 50 -4 # Convergence criteria - if achieved phase will terminate before full no. evaluations made
1 1 1000 # How many function evaluations
#
PHASE10
# ———-
# PHASE 11 - OPR (Orthogonal Polynomial Recruitment)
# ———-
mfclo64 skj.frq 10.par 11.par -file - PHASE11
# OPR settings
1 155 51 1 221 51 # Sets degree for year effect
1 217 1 # Sets degree for season effect
1 216 10 # Sets degree for region effect
1 218 51 # Sets degree for region-season interaction effect
1 202 3 # Common year effect for last 3 years
1 210 3 # Likewise region effect
1 212 3 # Likewise season effect
1 214 3 # Likewise region-season interaction effect
1 183 0 # Common year effect for initial x years
1 204 0 # Common region effect for initial x years
1 206 0 # Common season effect for initial x years
1 208 0 # Common region-season interaction for initial x years
PHASE11
# ———-
# PHASE 12 - ungroup indices and their selectivity
# ———-
mfclo64 skj.frq 11.par 12.par -file - PHASE12
# ungrp CPUE ungrp selectivity
-33 99 33 -33 24 33
-34 99 34 -34 24 34
-35 99 35 -35 24 35
-36 99 36 -36 24 36
-37 99 37 -37 24 37
-38 99 38 -38 24 38
-39 99 39 -39 24 39
-40 99 40 -40 24 40
```

```
-41 99 41 -41 24 41
-42 99 42 -42 24 42
#
PHASE12
# ———-
# PHASE 13 - allow LL fisheries to have decreasing selectivity
# ———-
mfclo64 skj.frq 12.par 13.par -file - PHASE13
-3 16 0
-6 16 0
-9 16 0
-18 16 0
-22 16 0
-24 16 0
-28 16 0
-32 16 0
#
PHASE13
# ———-
# Calculate Hessian & related diagnostics
# ———-
# Hessian
mfclo64 skj.frq 13.par hessian switch 1 1 145 1
# Compute eigenvalues
mfclo64 skj.frq 13.par hessian switch 1 1 145 5
# Compute dependent variables needed for reference points
mfclo64 skj.frq 13.par hessian switch 2 1 37 1 1 145 2
# Produce SD report
mfclo64 skj.frq 13.par hessian switch 1 1 145 4
#
```

18 Appendix 2: Parameter configuration

Table 6: Diagnostic model parameter (Param) configurations including region, fishery (or index), grouping, number of nodes in selectivity spline (Nodes), number of seasons (Seasons), number of parameters (No. params), whether the parameters are fixed or estimated (Fixed/Est), constraints, and comments.

Param	Region	Fishery	Group	Nodes	Seasons	No. params	Fixed/Est	Constraints	Comments
Selectivity	1	1	1	4	1	4	Est	Bounds penalties	
	1	2	2	4	1	4	Est	”	
	1	3	3	3	1	3	Est	”	
	2	4	4	4	1	4	Est	”	
	2	5	5	4	1	4	Est	”	
	2	6	6	3	1	3	Est	”	
	3	7	7	4	1	4	Est	”	
	3	8	8	4	1	4	Est	”	
	3	9	9	3	1	3	Est	”	
	5	10	10	6	1	6	Est	”	
	5	11	11	5	1	5	Est	”	
	5	12	12	5	1	5	Est	”	
	5	13	13	5	1	5	Est	”	
	5	14	14	6	1	6	Est	”	
	5	15	15	4	1	4	Est	”	
	5	16	16	4	1	4	Est	”	
	5	17	17	5	1	5	Est	”	
	5	18	18	3	1	3	Est	”	
	6	19	19	4	1	4	Est	”	
	6	20	20	4	1	4	Est	”	
	6	21	21	4	1	4	Est	”	
	6	22	22	3	1	3	Est	”	

Continued on next page

Table 6 – continued from previous page

Param	Region	Fishery	Group	Nodes	Seasons	No. params	Fixed/Est	Constraints	Comments
	4	23	23	4	1	4	Est	”	
	4	24	24	3	1	3	Est	”	
	7	25	25	4	1	4	Est	”	
	7	26	26	4	1	4	Est	”	
	7	27	27	4	1	4	Est	”	
	7	28	28	3	1	3	Est	”	
	8	29	29	4	1	4	Est	”	
	8	30	30	4	1	4	Est	”	
	8	31	31	4	1	4	Est	”	
	8	32	32	3	1	3	Est	”	
	1	33	33	4	1	4	Est	”	
	2	34	34	4	1	4	Est	”	
	3	35	35	4	1	4	Est	”	
	4	36	36	4	1	4	Est	”	
	5	37	37	5	1	5	Est	”	
	7	38	38	4	1	4	Est	”	
	8	39	39	4	1	4	Est	”	
	6	40	40	4	1	4	Est	”	
	7	41	41	4	1	4	Est	”	
	8	42	42	4	1	4	Est	”	
Sub-total						169			
Recruitment									
Year effects						51	Est		
Season effects						3	Est		
Region effects						70	Est		

Continued on next page

Table 6 – continued from previous page

Param	Region	Fishery	Group	Nodes	Seasons	No. params	Fixed/Est	Constraints	Comments
Region-season						1071	Est		
Sub-total						1195	Est		
Movement	1	2			4	8	Est	Bounds penalties	Weak prior on coefficients
	2	2			4	8	Est	”	
	3	4			4	16	Est	”	
	4	4			4	16	Est	”	
	5	3			4	12	Est	”	
	6	2			4	8	Est	”	
	7	5			4	20	Est	”	
	8	2			4	8	Est	”	
Sub-total						96			
Growth									
L1						1	Est	Bounds penalties	
L2						1	Est	”	
k						1	Fixed		
Offsets						2	Est	”	Weak prior of 0
V1						1	Est	”	
V2						1	Est	”	
Sub-total						6	Est		
						1	Fixed		
Natural mortality						1	Est		
Stock-recruitment									
Scale						1	Est		

Continued on next page

Table 6 – continued from previous page

Param	Region	Fishery	Group	Nodes	Seasons	No. params	Fixed/Est	Constraints	Comments
Steepness						1	Fixed		
Tag report rates									
RTTP	1	1	1			1	Fixed (0)	All have upper	
	1	2	1					bound of	
								0.99	
	1	3	1						
	2	4	1						
	2	5	1						
	2	6	1						
	3	7	1						
	3	8	1						
	3	9	1						
	5	10	2			1	Est		Weak prior
	5	11	2						
	5	12	2						
	5	13	2						
	5	14	2						
	5	15	2						
	5	16	2						
	5	17	1						
	5	18	1						
	6	19	1						
	6	20	3			1	Est		Informative prior
									(tag seeding)
	6	21	3						

Continued on next page

Table 6 – continued from previous page

Param	Region	Fishery	Group	Nodes	Seasons	No. params	Fixed/Est	Constraints	Comments
	6	22	1						
	4	23	1						
	4	24	1						
	7	25	4			1	Est		Uninformative prior
	7	26	5			1	Est		Informative prior (tag seeding)
	7	27	5						
	7	28	1						
	8	29	4						
	8	30	6			1	Est		Informative prior (tag seeding)
	8	31	6						
	8	32	1						
PTTP	1	1	1						
	1	2	1						
	1	3	1						
	2	4	1						
	2	5	1						
	2	6	1						
	3	7	1						
	3	8	1						
	3	9	1						
	5	10	7			1	Est		Uninformative prior
	5	11	7						
	5	12	7						

Continued on next page

Table 6 – continued from previous page

Param	Region	Fishery	Group	Nodes	Seasons	No. params	Fixed/Est	Constraints	Comments
	5	13	7						
	5	14	7						
	5	15	7						
	5	16	7						
	5	17	1						
	5	18	1						
	6	19	1						
	6	20	8			1	Est		Informative prior (tag seeding)
	6	21	8						
	6	22	1						
	4	23	1						
	4	24	1						
	7	25	9			1	Est		Uninformative prior
	7	26	10			1	Est		Informative prior (tag seeding)
	7	27	10						
	7	28	1						
	8	29	9						
	8	30	11			1	Est		Informative prior (tag seeding)
	8	31	11						
	8	32	1						
JPTP	1	1	12			1	Est		Informative prior (Japan)

Continued on next page

Table 6 – continued from previous page

Param	Region	Fishery	Group	Nodes	Seasons	No. params	Fixed/Est	Constraints	Comments
	1	2	13			1	Est		Informative prior (Japan)
	1	3	1						
	2	4	14			1	Est		Informative prior (Japan)
	2	5	15			1	Est		Informative prior (Japan)
	2	6	1						
	3	7	16			1	Est		Informative prior (Japan)
	3	8	17			1	Est		Informative prior (Japan)
	3	9	1						
	5	10	18			1	Est		Uninformative prior
	5	11	18						
	5	12	18						
	5	13	18						
	5	14	18						
	5	15	18						
	5	16	18						
	5	17	1						
	5	18	1						
	6	19	1						
	6	20	19			1	Est		Uninformative prior
	6	21	19						

Continued on next page

Table 6 – continued from previous page

Param	Region	Fishery	Group	Nodes	Seasons	No. params	Fixed/Est	Constraints	Comments
	6	22	1						
	4	23	20			1	Est		Informative prior (Japan)
	4	24	1						
	7	25	20						
	7	26	21			1	Est		Uninformative prior
	7	27	21						
	7	28	1						
	8	29	20						
	8	30	22			1	Est		Uninformative prior
	8	31	22						
	8	32	1						
Sub-total						21	Est		
						1	Fixed		
Length Data Dirichlet Multinomial									
	1	1	1			2	Est		
	1	2	1						
	1	3	2			2	Est		
	2	4	1						
	2	5	1						
	2	6	2						
	3	7	1						
	3	8	1						
	3	9	2						
	5	10	3			2	Est		

Continued on next page

Table 6 – continued from previous page

Param	Region	Fishery	Group	Nodes	Seasons	No. params	Fixed/Est	Constraints	Comments
	5	11	3						
	5	12	3						
	5	13	3						
	5	14	1						
	5	15	4			2	Est		
	5	16	4						
	5	17	3						
	5	18	2						
	6	19	1						
	6	20	4						
	6	21	4						
	6	22	2						
	4	23	1						
	4	24	2						
	7	25	1						
	7	26	4						
	7	27	4						
	7	28	2						
	8	29	1						
	8	30	4						
	8	31	4						
	8	32	2						
	1	33	1						
	2	34	1						
	3	35	1						

Continued on next page

Table 6 – continued from previous page

Param	Region	Fishery	Group	Nodes	Seasons	No. params	Fixed/Est	Constraints	Comments
	4	36	1						
	5	37	3						
	7	38	1						
	8	39	1						
	6	40	4						
	7	41	4						
	8	42	4						
Sub-total						8	Est		
Tagging Data Negative Binomial									
	1	1	1						
	1	2	1						
	1	3	1						
	2	4	1						
	2	5	1						
	2	6	1						
	3	7	1						
	3	8	1						
	3	9	1						
	5	10	1						
	5	11	1						
	5	12	1						
	5	13	1						
	5	14	1						
	5	15	1						
	5	16	1						

Continued on next page

Table 6 – continued from previous page

Param	Region	Fishery	Group	Nodes	Seasons	No. params	Fixed/Est	Constraints	Comments
	5	17	1						
	5	18	1						
	6	19	1						
	6	20	1						
	6	21	1						
	6	22	1						
	4	23	1						
	4	24	1						
	7	25	1						
	7	26	1						
	7	27	1						
	7	28	1						
	8	29	1						
	8	30	1						
	8	31	1						
Sub-total	8	32	1			1	Est		
TOTAL						1498	Est		
						3	Fixed		

19 Appendix 3: Table of model ensemble diagnostics

Table 7: Monte Carlo ensemble model iterations (Iter) with steepness (h), mixing period K statistic (Mixing), von Bertalanffy growth coefficient (k), effort multiplier (E-mult), total negative log-likelihood (Total), length-frequency negative log-likelihood (LF), CPUE negative log-likelihood (CPUE), Beverton-Holt negative log-likelihood (BH), tagging data negative log-likelihood (Tag), Japanese pole-and-line negative log-likelihood (JPPL), region 5 purse seine CPUE negative log-likelihood (PS-5), regions 6, 7, and 8 purse seine CPUE negative log-likelihood (PS-678), maximum gradient (Grad), and number of negative eigenvalues (Eigens).

Iter	h	Mixing	k	E-mult	Total	LF	CPUE	BH	Tag	JPPL	PS-5	PS-678	Grad	Eigens
1	0.90	2	0.32	4.35	321,261	299,873	-506	2.68	21,105	-563	41.8	14.3	7.48E-05	0
2	0.83	3	0.31	4.42	323,045	299,430	-502	3.24	23,401	-484	5.3	-23.7	8.50E-05	0
3	0.84	3	0.22	3.93	323,137	299,511	-481	2.88	23,411	-476	4.4	-9.4	6.98E-05	0
4	0.90	1	0.29	3.00	318,157	299,205	-720	2.82	18,782	-711	7.0	-16.3	9.82E-05	0
5	0.68	2	0.25	3.73	321,610	299,361	-415	2.87	21,867	-442	18.0	9.1	7.10E-05	0
6	0.87	2	0.32	4.75	321,403	299,380	-419	3.55	21,620	-454	24.4	10.7	9.49E-05	0
7	0.82	3	0.38	4.85	322,648	299,815	-540	2.82	22,640	-535	21.6	-26.2	6.86E-05	0
8	0.83	3	0.35	4.88	322,799	299,775	-504	2.96	22,801	-507	20.5	-17.5	6.77E-05	0
10	0.82	3	0.31	2.35	322,810	300,125	-664	3.83	22,632	-659	24.2	-28.8	6.92E-05	0
11	0.79	3	0.31	4.41	323,354	299,786	-507	3.28	23,360	-497	7.0	-16.6	7.94E-05	0
12	0.83	2	0.25	3.84	321,590	299,070	-458	3.30	22,178	-474	11.4	4.8	8.38E-05	0
14	0.88	1	0.33	4.20	317,579	299,477	-702	2.71	17,932	-763	46.8	13.8	8.69E-05	0
15	0.79	2	0.28	3.32	321,403	300,205	-569	2.63	20,985	-622	44.6	9.1	5.59E-05	0
16	0.89	2	0.32	2.02	320,860	299,388	-522	4.47	21,196	-586	29.7	34.3	9.29E-05	0
17	0.76	3	0.25	4.86	323,287	299,763	-551	2.83	23,375	-537	2.9	-17.8	8.85E-05	0
18	0.72	2	0.34	4.55	321,064	299,446	-425	3.15	21,235	-486	26.6	35.2	9.29E-05	0
19	0.83	2	0.28	3.64	321,446	299,261	-495	3.52	21,882	-508	15.1	-2.1	9.34E-05	0
21	0.91	1	0.21	2.08	318,360	299,041	-662	3.99	19,097	-699	14.8	21.7	8.89E-05	0
22	0.81	2	0.34	4.87	321,598	299,605	-499	3.78	21,681	-497	7.7	-9.5	9.61E-05	0
23	0.82	3	0.28	2.29	322,862	299,403	-613	4.02	23,377	-601	4.0	-16.1	9.81E-05	0

Continued on next page

Table 7 – continued from previous page

Iter	h	Mixing	k	E-mult	Total	LF	CPUE	BH	Tag	JPPL	PS-5	PS-678	Grad	Eigens
24	0.76	1	0.32	4.88	317,841	299,176	-688	3.42	18,464	-722	41.9	-6.9	3.74E-04	0
25	0.84	3	0.23	4.86	323,238	299,540	-446	2.95	23,445	-442	5.1	-9.2	7.47E-05	0
26	0.78	3	0.20	4.86	323,339	299,384	-413	2.81	23,670	-416	4.9	-1.9	9.15E-05	0
27	0.85	1	0.38	3.22	317,408	299,659	-751	2.75	17,615	-792	51.1	-10.2	9.50E-05	0
28	0.80	1	0.33	2.73	317,524	299,402	-734	3.51	17,975	-797	35.3	27.9	9.63E-05	0
29	0.89	2	0.30	2.18	321,291	299,380	-571	4.18	21,696	-587	11.8	3.9	9.77E-05	0
30	0.87	2	0.37	3.25	320,821	299,820	-543	2.70	20,742	-601	44.1	14.1	8.85E-05	0
31	0.90	2	0.22	4.61	321,642	299,298	-410	3.12	21,960	-446	19.5	16.8	8.06E-05	0
32	0.81	3	0.39	3.82	322,605	299,598	-498	3.07	22,776	-497	15.3	-16.7	9.15E-05	0
33	0.74	3	0.23	4.64	323,199	299,545	-457	2.91	23,413	-452	5.0	-10.2	9.85E-05	0
34	0.84	1	0.36	2.47	317,410	299,409	-763	3.08	17,876	-803	49.8	-9.3	8.54E-05	0
35	0.86	2	0.26	3.38	321,451	299,418	-517	2.64	21,762	-539	17.4	5.2	7.82E-05	0
37	0.89	3	0.40	4.88	322,992	299,923	-487	3.44	22,823	-485	15.1	-16.9	9.11E-05	0
39	0.85	1	0.40	4.34	317,407	299,750	-721	3.00	17,488	-761	48.3	-7.9	8.99E-05	0
40	0.87	1	0.31	4.87	317,956	299,117	-657	3.89	18,607	-687	28.6	0.5	7.58E-05	0
41	0.69	3	0.34	3.46	322,726	299,379	-491	3.33	23,110	-488	14.4	-17.8	7.20E-05	0
42	0.85	3	0.26	2.12	322,936	299,099	-566	4.16	23,699	-557	4.0	-13.3	9.50E-05	0
43	0.72	1	0.36	2.62	317,428	299,392	-744	3.02	17,891	-793	49.7	-0.1	9.99E-05	0
44	0.87	2	0.30	4.59	321,387	300,033	-491	2.50	21,049	-555	46.7	17.2	9.11E-05	0
45	0.87	1	0.29	3.03	317,822	299,758	-746	2.67	17,948	-800	48.6	5.4	5.16E-05	0
46	0.85	3	0.24	2.38	322,835	299,347	-561	3.65	23,354	-562	7.3	-6.1	9.14E-05	0
47	0.92	1	0.28	4.85	318,312	299,202	-622	3.51	18,843	-621	9.9	-11.2	9.56E-05	0
48	0.86	1	0.25	4.63	318,327	299,142	-595	3.13	18,896	-619	14.7	8.7	8.60E-05	0
49	0.80	2	0.23	2.95	321,573	300,205	-573	2.94	21,177	-635	51.1	11.2	9.44E-05	0
52	0.85	2	0.26	2.90	321,397	299,410	-535	2.74	21,737	-558	17.3	5.8	8.17E-05	0

Continued on next page

Table 7 – continued from previous page

Iter	h	Mixing	k	E-mult	Total	LF	CPUE	BH	Tag	JPPL	PS-5	PS-678	Grad	Eigens
53	0.89	1	0.40	4.00	317,274	299,280	-712	3.08	17,804	-752	33.5	5.6	9.84E-05	0
54	0.82	3	0.37	4.22	322,524	299,346	-530	3.45	22,958	-528	16.8	-18.9	9.16E-05	0
55	0.91	2	0.25	2.40	321,320	299,324	-534	3.50	21,749	-565	19.0	11.6	8.22E-05	0
56	0.82	1	0.29	4.78	317,913	299,765	-708	2.75	17,993	-761	45.1	7.2	8.44E-05	0
57	0.73	3	0.34	1.99	322,489	299,368	-603	4.87	23,009	-595	12.7	-20.5	9.93E-05	0
58	0.85	3	0.39	4.85	322,672	299,974	-553	2.80	22,525	-538	19.1	-34.5	6.96E-05	0
59	0.93	1	0.22	4.85	318,395	298,928	-582	3.23	19,167	-620	18.1	19.6	7.04E-05	0
60	0.87	1	0.21	4.87	318,470	298,924	-579	3.17	19,243	-616	17.7	19.4	9.20E-05	0
61	0.76	1	0.34	1.87	317,573	299,288	-731	4.53	18,121	-772	30.5	10.5	9.48E-05	0
62	0.80	1	0.35	2.22	317,434	299,579	-758	3.35	17,734	-809	50.8	0.3	8.93E-05	0
63	0.69	2	0.27	3.86	321,521	299,545	-513	2.52	21,699	-528	16.2	-1.4	9.02E-05	0
64	0.87	1	0.37	2.27	317,311	299,476	-766	3.26	17,714	-810	52.5	-8.7	8.24E-05	0
66	0.91	3	0.38	2.06	322,309	299,738	-639	4.14	22,485	-628	19.4	-30.9	6.21E-05	0
68	0.96	2	0.24	3.86	321,535	299,289	-503	2.75	21,961	-526	14.8	8.4	9.66E-05	0
69	0.79	2	0.38	4.71	321,043	299,497	-420	3.24	21,152	-471	22.9	28.0	6.78E-05	0
71	0.78	3	0.29	4.63	323,017	299,405	-520	3.26	23,420	-500	5.0	-24.6	9.75E-05	0
73	0.81	1	0.39	4.43	317,572	299,469	-713	3.26	17,927	-740	25.6	2.0	9.85E-05	0
74	0.83	1	0.35	2.36	317,464	300,084	-767	3.06	17,277	-819	50.5	1.9	6.94E-05	0
75	0.76	1	0.31	3.17	317,756	299,945	-753	2.65	17,699	-802	48.0	0.8	8.36E-05	0
76	0.93	2	0.23	4.47	321,719	299,496	-487	2.90	21,929	-514	14.8	12.1	8.35E-05	0
77	0.76	3	0.31	3.08	322,849	299,434	-574	3.51	23,283	-553	4.5	-25.4	9.58E-05	0
78	0.81	3	0.35	4.72	322,744	299,393	-489	3.43	23,111	-485	13.6	-18.2	9.35E-05	0
79	0.91	3	0.30	3.10	322,866	299,413	-579	3.40	23,330	-558	4.3	-25.5	9.94E-05	0
81	0.90	1	0.29	2.48	318,161	299,154	-724	3.73	18,845	-706	13.5	-32.0	8.24E-05	0
82	0.85	3	0.28	4.68	323,138	299,320	-496	3.24	23,602	-485	5.2	-15.8	9.25E-05	0

Continued on next page

Table 7 – continued from previous page

Iter	h	Mixing	k	E-mult	Total	LF	CPUE	BH	Tag	JPPL	PS-5	PS-678	Grad	Eigens
83	0.72	1	0.30	4.80	318,040	299,087	-666	3.60	18,729	-686	25.7	-6.0	9.73E-05	0
85	0.83	2	0.26	2.66	321,327	299,342	-536	3.23	21,725	-592	29.2	26.5	9.94E-05	0
86	0.91	1	0.31	2.84	318,092	299,291	-748	2.74	18,664	-726	8.8	-30.6	8.53E-05	0
87	0.87	2	0.25	3.23	321,445	299,358	-518	2.63	21,821	-543	17.7	8.1	9.31E-05	0
88	0.85	1	0.35	4.80	318,029	299,630	-638	3.54	18,142	-686	41.4	6.4	8.35E-05	0
89	0.91	1	0.29	2.69	318,155	299,175	-694	2.79	18,785	-688	7.0	-13.3	9.44E-05	0
90	0.74	2	0.27	4.86	321,487	300,055	-480	2.52	21,127	-551	51.0	19.1	5.12E-05	0
91	0.86	3	0.31	3.66	322,866	299,369	-550	3.60	23,328	-528	7.4	-29.2	9.99E-05	0
92	0.92	2	0.31	3.77	321,311	299,279	-489	3.40	21,713	-505	18.0	-2.1	9.28E-05	0
93	0.83	1	0.25	4.42	318,285	299,088	-607	2.94	18,921	-634	15.0	12.4	9.01E-05	0
94	0.77	3	0.31	4.63	323,134	299,988	-568	2.72	23,016	-552	3.8	-19.5	8.12E-05	0
95	0.87	1	0.36	2.07	317,615	299,271	-773	3.56	18,223	-802	43.6	-15.0	9.40E-05	0
96	0.89	1	0.28	4.46	318,292	299,184	-635	3.24	18,851	-634	8.9	-9.5	9.60E-05	0
97	0.90	2	0.29	4.84	321,867	299,597	-429	3.76	21,894	-447	15.9	2.3	9.30E-05	0
98	0.89	2	0.26	2.75	321,508	299,478	-590	4.05	21,833	-614	13.0	10.7	4.77E-05	0
99	0.73	1	0.22	4.83	318,556	298,622	-567	3.70	19,605	-572	7.1	-1.8	9.38E-05	0
100	0.62	1	0.30	4.23	318,566	299,537	-649	2.76	18,790	-641	10.7	-18.9	9.69E-05	0
102	0.75	3	0.31	2.29	322,765	299,366	-599	4.46	23,292	-577	4.6	-26.7	9.79E-05	0
103	0.79	2	0.21	4.87	321,821	298,690	-333	3.55	22,662	-356	8.1	14.9	9.58E-05	0
104	0.78	3	0.37	2.29	322,369	299,532	-605	4.33	22,731	-602	15.8	-18.7	4.41E-05	0
105	0.74	2	0.20	1.86	321,469	299,128	-524	4.22	22,085	-561	15.1	21.7	6.82E-05	0
106	0.83	3	0.26	2.47	322,971	299,308	-572	3.59	23,534	-558	2.8	-16.6	9.86E-05	0
107	0.82	2	0.26	2.97	321,478	299,077	-498	3.33	22,104	-515	11.5	6.1	5.94E-05	0
108	0.88	3	0.35	4.71	322,718	299,432	-507	3.54	23,066	-500	12.4	-20.0	9.82E-05	0
109	0.90	1	0.35	4.87	317,667	299,397	-673	3.43	18,053	-730	31.4	25.0	9.79E-05	0

Continued on next page

Table 7 – continued from previous page

Iter	h	Mixing	k	E-mult	Total	LF	CPUE	BH	Tag	JPPL	PS-5	PS-678	Grad	Eigens
110	0.85	2	0.26	4.80	321,667	299,594	-476	2.86	21,759	-504	17.4	11.0	8.05E-05	0
111	0.84	1	0.21	2.11	318,218	298,748	-652	3.67	19,241	-689	17.0	20.6	9.43E-05	0
112	0.85	1	0.28	4.10	318,263	299,180	-643	2.94	18,837	-644	9.1	-8.8	9.36E-05	0
113	0.81	3	0.39	2.33	322,279	299,355	-611	4.47	22,799	-606	16.0	-21.0	9.09E-05	0
114	0.81	1	0.33	4.84	318,559	299,752	-686	3.70	18,596	-662	5.6	-29.7	8.94E-05	0
115	0.86	1	0.21	4.44	318,555	299,166	-616	2.89	19,124	-646	16.1	14.4	9.79E-05	0
116	0.90	2	0.40	4.87	320,985	299,895	-475	2.90	20,758	-525	44.3	5.4	8.97E-05	0
117	0.96	2	0.26	4.86	321,599	299,399	-438	3.19	21,837	-497	34.9	23.4	4.79E-05	0
118	0.88	1	0.31	4.51	317,766	299,810	-710	2.66	17,799	-766	47.2	8.7	9.15E-05	0
119	0.75	2	0.25	4.63	321,576	299,361	-429	3.16	21,848	-456	17.6	9.3	5.74E-05	0
120	0.92	2	0.39	3.06	320,795	299,506	-508	3.37	20,989	-557	23.8	24.4	8.87E-05	0
121	0.81	3	0.26	4.87	323,212	299,308	-460	3.13	23,652	-458	7.8	-10.2	6.90E-05	0
122	0.78	2	0.36	2.79	320,841	299,367	-510	3.60	21,178	-559	27.7	22.0	9.90E-05	0
123	0.87	3	0.34	4.70	322,721	299,402	-500	3.46	23,093	-495	14.2	-18.4	8.92E-05	0
124	0.75	2	0.30	4.87	321,531	299,322	-441	3.76	21,846	-454	14.8	-2.5	8.64E-05	0
125	0.81	1	0.36	2.68	317,415	299,481	-758	2.92	17,808	-802	51.3	-7.8	9.58E-05	0
126	0.92	2	0.32	2.99	321,178	299,272	-511	3.64	21,602	-538	22.4	4.0	7.04E-05	0
127	0.81	1	0.35	2.23	317,394	299,920	-758	3.38	17,361	-819	53.7	6.8	9.39E-05	0
128	0.92	2	0.34	4.87	321,104	300,108	-470	2.53	20,668	-539	46.1	22.1	8.29E-05	0
129	0.85	3	0.26	4.40	323,264	300,122	-574	2.76	23,023	-570	16.0	-20.5	6.72E-05	0
130	0.88	3	0.21	4.12	323,234	299,382	-452	2.78	23,611	-453	4.2	-3.5	8.15E-05	0
131	0.88	1	0.24	3.95	318,261	299,023	-623	2.79	18,977	-655	16.0	15.8	5.87E-05	0
132	0.87	1	0.30	2.82	317,904	299,068	-728	3.59	18,676	-740	24.3	-12.6	7.17E-05	0
134	0.72	2	0.33	4.56	321,503	299,420	-463	3.13	21,744	-505	35.5	6.9	8.25E-05	0
135	0.83	1	0.37	4.62	317,370	299,211	-637	3.41	17,899	-692	48.9	6.0	8.35E-05	0

Continued on next page

Table 7 – continued from previous page

Iter	h	Mixing	k	E-mult	Total	LF	CPUE	BH	Tag	JPPL	PS-5	PS-678	Grad	Eigens
136	0.81	3	0.38	2.39	322,372	299,363	-604	4.01	22,880	-599	17.4	-22.5	7.34E-05	0
137	0.82	1	0.36	2.36	317,343	299,212	-739	3.81	17,972	-784	36.7	7.6	7.17E-05	0
138	0.71	2	0.31	4.55	321,390	299,237	-452	3.79	21,789	-468	17.6	-2.2	8.85E-05	0
139	0.84	1	0.33	4.71	317,682	299,342	-688	3.20	18,147	-745	34.1	23.5	8.55E-05	0
140	0.82	3	0.36	2.40	322,445	299,444	-596	4.22	22,878	-592	14.0	-18.8	9.85E-05	0
142	0.86	1	0.32	4.37	317,877	299,121	-673	3.58	18,537	-698	28.1	-3.2	8.73E-05	0
143	0.79	3	0.38	2.81	322,530	299,798	-576	3.94	22,595	-585	20.4	-11.2	8.20E-05	0
144	0.76	3	0.36	3.72	323,138	299,839	-549	2.91	23,102	-534	17.4	-32.0	7.20E-05	0
145	0.87	2	0.33	3.17	320,944	299,455	-478	3.20	21,165	-543	30.0	34.6	4.83E-05	0
146	0.95	3	0.28	2.55	322,928	299,655	-601	2.96	23,181	-584	2.6	-19.3	9.92E-05	0
147	0.86	3	0.28	4.80	323,160	299,669	-534	2.74	23,317	-519	2.5	-17.2	7.83E-05	0
148	0.84	1	0.30	3.53	318,025	299,117	-661	3.15	18,682	-683	26.9	-4.4	7.52E-05	0
149	0.81	3	0.28	4.87	323,130	299,382	-491	3.21	23,530	-483	5.7	-13.7	8.24E-05	0
150	0.85	1	0.39	1.99	317,224	299,577	-748	3.59	17,502	-805	53.7	3.8	8.91E-05	0
151	0.83	2	0.24	4.86	321,634	299,256	-404	3.25	21,984	-435	17.5	12.9	9.19E-05	0
152	0.82	3	0.33	3.71	322,658	299,438	-538	3.30	23,040	-536	15.8	-18.6	8.42E-05	0
153	0.83	3	0.38	4.33	322,607	299,557	-519	3.48	22,845	-519	16.0	-16.1	6.28E-05	0
154	0.80	1	0.34	4.87	317,633	299,453	-671	3.23	17,970	-739	35.5	32.5	6.79E-05	0
156	0.95	3	0.28	4.71	323,181	299,671	-526	2.73	23,328	-512	2.7	-16.9	8.95E-05	0
157	0.95	1	0.20	4.82	318,620	300,003	-720	2.90	18,481	-755	27.8	7.5	9.29E-05	0
158	0.77	1	0.32	4.82	317,628	299,336	-663	2.87	18,078	-730	49.9	17.3	9.34E-05	0
159	0.92	3	0.35	4.87	322,737	299,432	-500	3.59	23,076	-492	12.5	-19.8	4.29E-04	0
160	0.84	3	0.39	4.58	322,649	299,995	-566	2.73	22,493	-552	19.5	-33.8	8.53E-05	0
161	0.82	3	0.39	4.88	322,659	299,962	-551	2.80	22,521	-536	19.5	-33.9	6.96E-05	0
162	0.85	3	0.39	4.41	322,630	299,592	-499	3.40	22,806	-497	14.6	-16.5	5.90E-05	0

Continued on next page

Table 7 – continued from previous page

Iter	h	Mixing	k	E-mult	Total	LF	CPUE	BH	Tag	JPPL	PS-5	PS-678	Grad	Eigens
163	0.83	1	0.31	2.51	317,884	299,129	-733	3.87	18,599	-751	25.4	-8.0	9.76E-05	0
164	0.90	2	0.22	2.73	321,448	299,186	-492	3.18	21,973	-535	20.3	22.6	8.72E-05	0
165	0.83	1	0.31	4.14	317,703	299,338	-686	3.01	18,173	-753	36.4	29.7	7.76E-05	0
166	0.95	2	0.29	2.11	321,249	299,188	-544	4.22	21,806	-559	17.1	-2.5	9.32E-05	0
167	0.91	2	0.27	4.40	321,440	299,885	-448	2.37	21,225	-534	49.1	36.4	7.94E-05	0
168	0.72	3	0.39	3.64	322,539	299,945	-603	2.89	22,476	-586	18.3	-34.7	7.60E-05	0
169	0.88	2	0.34	4.50	321,184	299,377	-467	3.00	21,467	-523	41.6	14.3	5.56E-05	0
170	0.87	2	0.23	4.31	321,581	299,284	-421	3.09	21,923	-455	19.4	14.5	8.02E-05	0
171	0.88	1	0.34	4.64	318,596	299,817	-690	3.70	18,569	-664	3.7	-29.9	7.22E-05	0
172	0.72	3	0.37	4.78	322,626	299,427	-507	3.33	22,969	-506	16.5	-16.9	9.26E-05	0
173	0.84	3	0.26	4.72	323,238	299,343	-470	3.09	23,650	-458	4.9	-17.4	9.49E-05	0
175	0.74	3	0.29	3.13	322,918	299,393	-564	3.27	23,390	-555	5.6	-14.5	9.64E-05	0
176	0.87	3	0.32	4.29	322,912	299,417	-527	3.54	23,301	-507	8.3	-28.1	9.00E-05	0
177	0.82	1	0.26	4.86	318,175	299,283	-677	2.99	18,692	-730	42.6	9.8	5.75E-04	0
178	0.75	1	0.37	2.47	317,323	299,495	-745	3.08	17,684	-799	51.6	2.3	7.67E-05	0
179	0.89	2	0.21	2.17	321,701	299,093	-540	3.97	22,382	-555	9.2	5.9	5.71E-05	0
180	0.83	2	0.39	4.62	320,952	299,894	-499	2.81	20,752	-546	41.0	6.2	9.10E-05	0
181	0.72	1	0.31	4.82	317,958	299,094	-659	3.76	18,632	-683	27.2	-2.8	7.67E-05	0
183	0.87	3	0.35	4.33	322,660	299,428	-527	3.75	23,034	-518	12.3	-21.1	9.96E-05	0
184	0.88	3	0.31	4.13	322,954	299,423	-540	3.28	23,359	-519	3.8	-25.3	9.39E-05	0
185	0.80	2	0.40	2.14	320,677	299,919	-609	3.49	20,569	-656	41.3	5.9	8.84E-05	0
186	0.79	2	0.34	4.30	321,054	299,809	-498	2.63	20,961	-569	44.0	27.2	7.32E-05	0
187	0.78	3	0.38	4.31	322,598	299,793	-562	2.81	22,636	-556	20.9	-26.9	8.52E-05	0
188	0.91	3	0.35	4.51	322,731	299,429	-496	3.39	23,070	-489	12.5	-19.9	9.62E-05	0
189	0.92	2	0.27	4.35	321,427	300,010	-499	2.54	21,133	-569	52.5	17.8	6.99E-05	0

Continued on next page

Table 7 – continued from previous page

Iter	h	Mixing	k	E-mult	Total	LF	CPUE	BH	Tag	JPPL	PS-5	PS-678	Grad	Eigens
190	0.89	3	0.21	2.32	323,722	299,159	-499	3.54	24,352	-465	-10.5	-24.1	9.85E-05	0
191	0.79	3	0.39	4.72	322,613	299,552	-510	3.59	22,841	-508	14.7	-16.8	7.79E-05	0
192	0.88	3	0.30	4.87	323,005	299,328	-493	3.61	23,445	-475	8.9	-27.0	8.73E-05	0
193	0.76	1	0.34	3.32	317,631	299,298	-746	3.14	18,195	-792	29.9	16.0	9.74E-05	0
194	0.89	2	0.38	2.62	320,779	299,486	-524	3.60	21,013	-579	26.7	28.2	9.93E-05	0
195	0.71	2	0.25	4.82	321,615	299,350	-410	3.19	21,878	-439	17.9	10.8	6.27E-05	0
196	0.82	1	0.40	2.46	317,174	299,264	-749	3.67	17,759	-780	33.6	-2.8	7.70E-05	0
197	0.79	1	0.22	4.82	319,366	299,301	-655	3.99	19,834	-629	1.7	-28.3	4.58E-04	0
198	0.87	1	0.34	2.22	317,348	299,329	-746	3.47	17,886	-805	47.6	11.8	9.15E-05	0
199	0.67	3	0.36	4.28	322,736	299,514	-506	3.36	23,006	-502	13.7	-17.6	8.52E-05	0
200	0.83	2	0.40	2.66	320,607	299,352	-516	3.51	20,947	-566	30.0	19.8	6.88E-05	0
201	0.81	2	0.37	4.82	321,710	299,814	-399	3.54	21,471	-443	32.9	11.2	8.89E-05	0
202	0.91	1	0.22	4.74	318,410	298,939	-585	3.10	19,177	-624	18.5	20.2	9.62E-05	0
203	0.84	1	0.33	2.20	317,524	299,339	-749	4.17	18,055	-801	33.7	18.2	9.18E-05	0
204	0.74	1	0.38	3.75	317,451	299,875	-683	2.25	17,377	-747	48.8	15.4	7.54E-05	0
205	0.72	1	0.34	4.68	317,970	299,010	-698	3.90	18,751	-703	30.7	-26.2	9.63E-05	0
206	0.87	3	0.36	4.06	322,887	299,571	-563	2.97	23,140	-555	16.8	-25.4	6.59E-05	0
207	0.79	2	0.38	4.51	320,923	299,708	-480	2.77	20,884	-536	47.4	9.2	9.31E-05	0
208	0.83	3	0.37	2.92	322,460	299,774	-612	3.15	22,571	-601	20.1	-31.0	5.97E-05	0
209	0.75	2	0.33	2.27	320,861	299,399	-520	4.05	21,184	-584	29.9	34.5	6.81E-05	0
210	0.76	3	0.38	4.83	322,670	299,546	-497	3.54	22,893	-497	16.0	-15.8	9.02E-05	0
211	0.80	2	0.29	2.30	321,331	299,271	-562	4.03	21,833	-577	11.7	2.9	8.92E-05	0
212	0.93	3	0.40	4.69	322,734	300,084	-509	3.15	22,441	-521	21.1	-9.7	9.91E-05	0
213	0.82	3	0.38	2.71	322,456	299,918	-639	3.27	22,460	-623	18.3	-34.0	5.87E-05	0
214	0.82	3	0.24	4.61	323,106	299,361	-458	2.88	23,494	-463	9.3	-4.9	4.09E-05	0

Continued on next page

Table 7 – continued from previous page

Iter	h	Mixing	k	E-mult	Total	LF	CPUE	BH	Tag	JPPL	PS-5	PS-678	Grad	Eigens
215	0.89	1	0.39	4.33	317,271	299,513	-672	2.98	17,537	-740	39.8	28.5	9.04E-05	0
216	0.83	3	0.30	4.80	323,105	299,647	-506	3.08	23,256	-495	9.6	-19.7	7.93E-05	0
217	0.88	3	0.38	4.73	322,665	299,945	-560	2.78	22,555	-545	18.7	-34.1	4.79E-05	0
218	0.80	3	0.27	4.87	323,170	299,598	-527	2.74	23,390	-516	2.5	-14.2	8.31E-05	0
219	0.85	2	0.31	4.64	321,340	299,274	-436	3.49	21,684	-469	19.5	13.4	9.54E-05	0
220	0.81	3	0.23	4.66	323,278	299,670	-527	2.66	23,435	-519	4.7	-12.0	9.93E-05	0
221	0.88	1	0.37	2.11	317,297	299,500	-750	3.48	17,658	-804	52.3	2.1	9.20E-05	0
222	0.91	1	0.24	4.85	318,338	299,012	-589	3.31	19,033	-621	16.1	15.8	7.62E-05	0
223	0.89	1	0.37	4.21	317,488	299,501	-671	2.73	17,769	-729	48.5	8.9	9.56E-05	0
224	0.83	1	0.30	4.55	318,045	299,089	-663	3.80	18,730	-677	24.6	-10.3	7.87E-05	0
225	0.81	1	0.27	1.96	317,932	299,369	-751	4.27	18,446	-814	48.4	15.1	6.64E-05	0
226	0.90	1	0.37	4.83	317,461	299,638	-689	3.27	17,626	-745	48.5	7.0	8.80E-05	0
227	0.81	3	0.23	2.47	322,886	299,304	-541	3.57	23,423	-553	9.3	2.5	9.93E-05	0
228	0.87	3	0.33	4.51	323,039	300,100	-590	2.66	22,828	-563	3.1	-29.8	9.11E-05	0
229	0.84	1	0.22	3.70	318,394	298,926	-581	2.50	19,166	-619	18.0	20.1	9.66E-05	0
230	0.78	1	0.37	2.40	317,373	299,485	-763	3.15	17,766	-808	52.1	-7.3	9.38E-05	0
233	0.92	1	0.39	2.40	317,228	299,277	-734	3.69	17,783	-775	37.7	3.0	9.13E-05	0
234	0.83	2	0.38	4.20	320,944	299,608	-459	3.18	20,984	-511	24.8	27.1	8.90E-05	0
235	0.79	1	0.36	2.97	317,453	299,409	-745	2.78	17,900	-790	53.2	-8.5	8.95E-05	0
236	0.78	3	0.36	4.45	322,696	299,441	-488	3.33	23,009	-487	14.6	-15.4	7.69E-05	0
237	0.81	1	0.28	4.43	318,239	299,959	-715	2.66	18,135	-758	40.6	1.7	8.67E-05	0
238	0.86	1	0.26	4.85	318,171	299,282	-677	3.03	18,689	-730	42.9	10.2	5.58E-05	0
239	0.76	2	0.20	4.81	324,451	298,955	-108	4.45	24,769	-135	-6.5	34.1	9.94E-05	0
240	0.79	3	0.37	3.10	322,570	299,709	-559	3.48	22,704	-568	20.7	-12.5	8.27E-05	0
241	0.81	1	0.26	4.88	318,443	299,192	-635	3.72	18,993	-635	12.6	-12.4	6.77E-05	0

Continued on next page

Table 7 – continued from previous page

Iter	h	Mixing	k	E-mult	Total	LF	CPUE	BH	Tag	JPPL	PS-5	PS-678	Grad	Eigens
242	0.88	3	0.29	2.24	322,799	299,307	-599	4.50	23,388	-577	5.3	-27.1	8.78E-05	0
243	0.93	1	0.29	2.25	318,138	299,166	-740	3.92	18,822	-715	11.0	-35.3	6.48E-05	0
244	0.82	2	0.23	4.70	321,631	299,284	-402	3.17	21,952	-436	19.5	14.5	5.25E-05	0
245	0.78	2	0.23	3.92	321,661	299,284	-390	2.80	21,969	-424	19.8	14.5	6.86E-05	0
246	0.88	3	0.30	4.86	323,048	299,408	-501	3.34	23,429	-483	6.2	-24.1	9.94E-05	0
248	0.80	1	0.37	3.79	317,500	299,607	-686	2.49	17,695	-739	47.4	5.8	8.96E-05	0
249	0.86	2	0.23	2.28	321,471	299,511	-548	3.49	21,737	-575	16.9	10.2	9.79E-05	0
250	0.92	2	0.37	4.88	321,741	299,852	-499	3.53	21,575	-487	3.2	-14.4	5.26E-05	0
251	0.82	1	0.38	2.06	317,272	299,205	-746	4.15	17,911	-777	35.0	-4.7	7.81E-05	0
252	0.84	2	0.32	4.83	321,581	299,681	-488	3.06	21,577	-525	44.6	-8.1	7.67E-05	0
253	0.89	1	0.28	4.70	318,293	299,285	-622	3.28	18,741	-631	10.7	-1.3	7.88E-05	0
254	0.68	2	0.40	2.56	320,810	299,814	-521	3.98	20,717	-580	38.5	20.8	8.79E-05	0
255	0.66	1	0.39	2.29	317,219	299,213	-753	3.95	17,859	-780	31.7	-5.3	7.94E-05	0
257	0.73	1	0.20	4.67	318,502	298,926	-588	2.89	19,281	-625	16.9	20.0	9.94E-05	0
258	0.94	2	0.38	4.03	320,926	299,523	-464	3.20	21,058	-515	23.9	27.0	9.31E-05	0
259	0.76	3	0.21	2.31	322,993	299,246	-558	3.82	23,614	-563	6.3	-1.2	8.89E-05	0
260	0.83	2	0.32	2.66	321,056	299,851	-583	2.95	21,006	-638	41.7	13.4	7.63E-05	0
261	0.92	3	0.28	4.78	323,123	299,313	-489	3.45	23,582	-470	6.4	-25.4	9.99E-05	0
262	0.85	1	0.33	2.56	317,547	299,327	-748	3.72	18,089	-801	33.5	19.6	8.65E-05	0
263	0.85	3	0.33	2.36	322,548	299,435	-591	4.23	22,992	-587	15.1	-19.9	7.12E-05	0
265	0.83	1	0.37	4.73	317,586	299,586	-681	3.08	17,800	-743	33.2	29.0	4.19E-05	0
267	0.82	1	0.33	4.09	317,611	299,393	-694	2.95	18,033	-761	35.5	32.5	9.20E-05	0
268	0.78	3	0.26	2.45	322,950	299,338	-576	3.63	23,489	-562	2.9	-17.6	9.20E-05	0
269	0.81	1	0.38	2.64	317,380	299,634	-772	2.89	17,636	-810	51.1	-13.2	8.13E-05	0
270	0.86	3	0.40	4.50	322,668	300,015	-548	2.65	22,474	-534	20.4	-34.1	9.74E-05	0

Continued on next page

Table 7 – continued from previous page

Iter	h	Mixing	k	E-mult	Total	LF	CPUE	BH	Tag	JPPL	PS-5	PS-678	Grad	Eigens
271	0.85	1	0.27	2.23	317,822	299,618	-752	3.77	18,096	-823	53.8	17.3	7.29E-05	0
272	0.87	1	0.23	4.72	318,369	299,764	-713	2.57	18,468	-768	36.9	18.5	9.21E-05	0
274	0.83	3	0.21	3.59	323,158	299,421	-477	2.87	23,521	-476	4.2	-5.0	9.25E-05	0
275	0.90	2	0.39	4.32	320,945	299,901	-513	2.76	20,753	-560	40.8	6.0	9.63E-05	0
277	0.82	3	0.24	2.68	322,913	299,392	-591	3.35	23,418	-583	0.9	-8.6	6.97E-05	0
278	0.88	3	0.37	4.57	322,596	299,578	-511	3.35	22,806	-512	16.6	-15.2	9.40E-05	0
279	0.73	3	0.28	3.33	323,001	299,284	-545	3.36	23,557	-534	5.0	-16.7	9.91E-05	0
280	0.89	2	0.36	2.85	321,216	299,595	-568	3.17	21,384	-610	37.3	4.5	9.08E-05	0
281	0.86	1	0.37	3.67	317,440	299,269	-666	2.70	17,938	-716	36.5	13.9	5.65E-05	0
282	0.89	2	0.23	4.56	321,668	299,287	-388	3.10	21,970	-422	19.7	14.6	6.57E-05	0
283	0.77	2	0.29	4.33	321,463	299,302	-472	3.63	21,834	-484	15.4	-2.8	7.88E-05	0
284	0.86	3	0.32	4.84	322,985	299,399	-501	3.61	23,362	-481	8.1	-27.8	9.31E-05	0
285	0.89	3	0.34	2.71	322,628	299,703	-577	3.97	22,792	-581	19.6	-16.2	9.77E-05	0
286	0.86	2	0.38	4.73	321,026	299,833	-470	2.83	20,858	-520	44.2	6.0	9.22E-05	0
288	0.81	1	0.37	4.73	317,580	299,420	-677	3.40	17,947	-721	28.5	16.1	9.47E-05	0
290	0.89	3	0.37	4.84	322,620	299,547	-501	3.44	22,851	-503	16.3	-15.0	8.50E-05	0
291	0.83	2	0.35	4.34	321,006	299,722	-495	2.68	20,977	-553	44.1	14.4	8.91E-05	0
292	0.86	1	0.23	4.82	318,364	300,213	-731	2.39	18,026	-778	34.4	12.9	6.83E-05	0
293	0.89	1	0.22	3.60	318,415	298,936	-578	2.45	19,174	-617	15.4	23.2	7.79E-05	0
294	0.86	2	0.28	2.38	321,320	299,238	-547	3.80	21,838	-562	15.4	-0.9	9.22E-05	0
295	0.80	2	0.40	4.38	320,979	299,912	-470	2.65	20,729	-520	44.1	5.6	9.03E-05	0
296	0.78	2	0.37	4.07	321,080	299,654	-410	2.86	21,030	-478	27.2	40.9	9.98E-05	0
297	0.72	2	0.20	2.79	322,394	299,516	-313	3.67	22,395	-351	9.7	28.1	7.83E-05	0
298	0.82	1	0.37	2.77	317,335	299,621	-747	2.84	17,576	-799	52.0	-0.2	7.74E-05	0
300	0.82	1	0.22	3.82	319,075	299,845	-684	2.71	19,049	-684	20.1	-20.4	9.55E-05	0

20 Appendix 4: Additional model ensemble plots

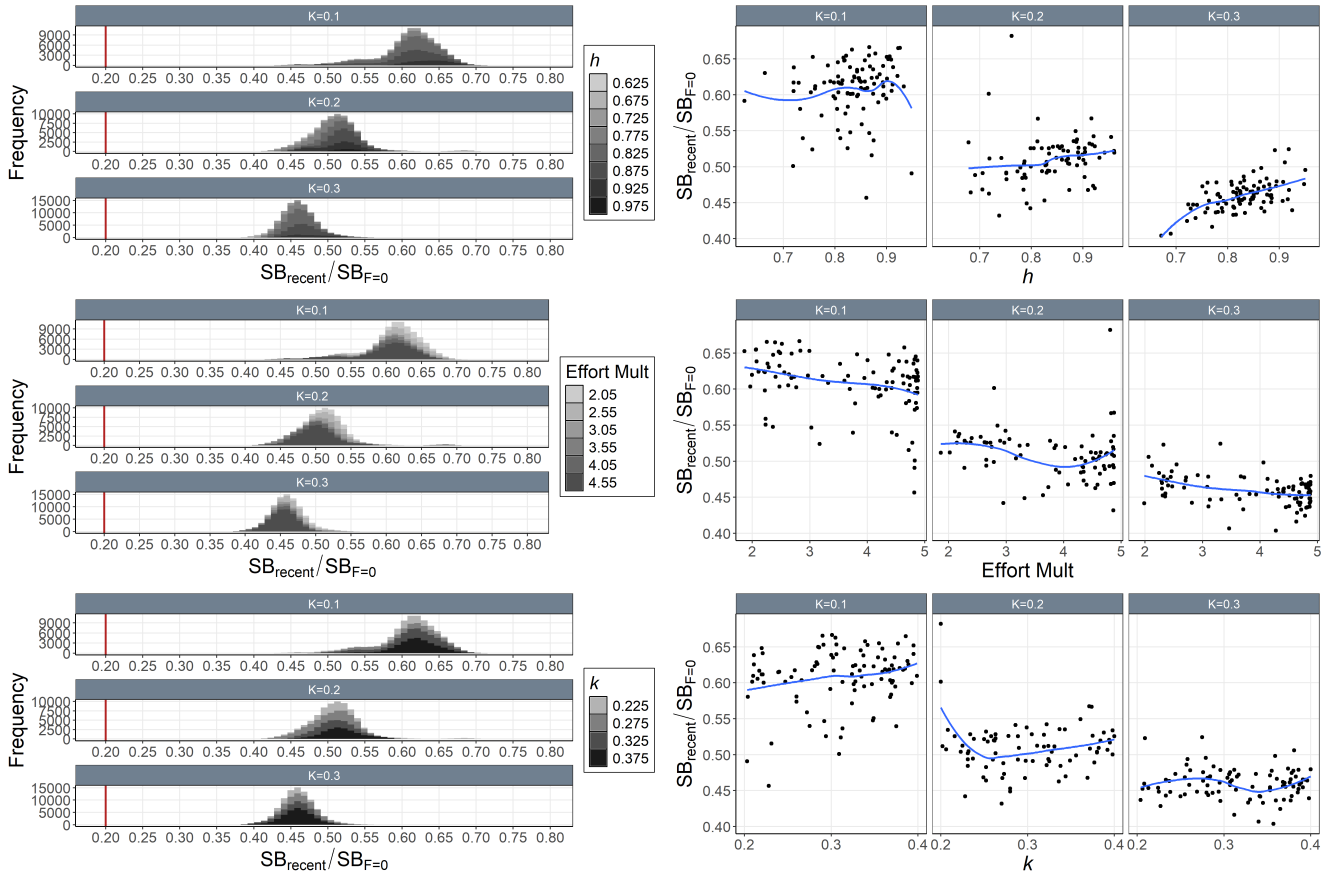

Figure 84: Histograms of Monte-Carlo estimated model uncertainty for $SB_{recent}/SB_{F=0}$ by mixing period (K statistic; grid facets), h (top-left), effort multiplier (Effort Mult; top-right), and k (middle-left) with median line (blue) and $SB_{recent}/SB_{F=0} = 0.2$ line (red). Also includes estimated $SB_{recent}/SB_{F=0}$ by mixing period (K statistic; grid facets), h (middle-right), effort multiplier (Effort Mult; bottom-left), and k (bottom-right) for each model in the ensemble with loess smoother.

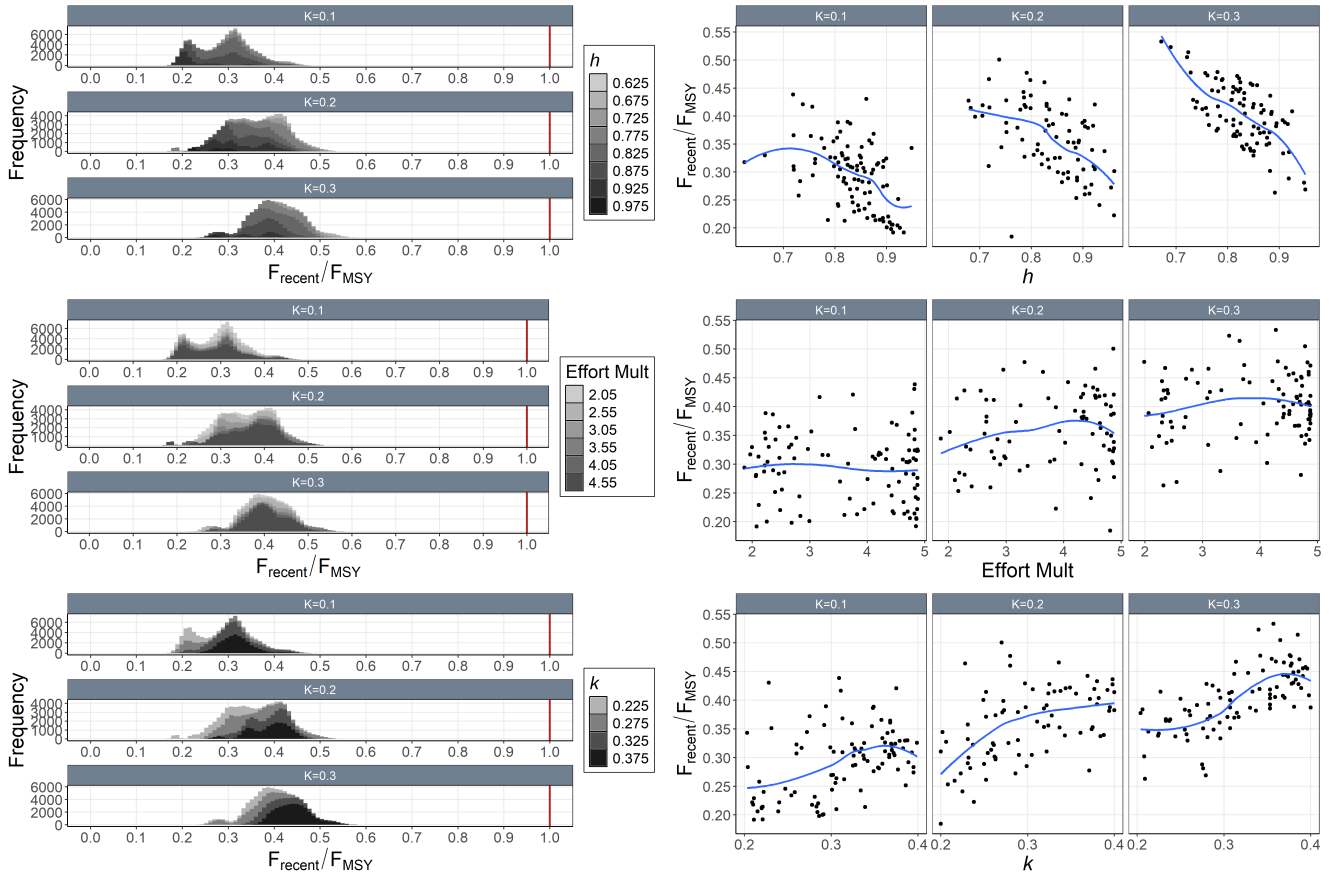

Figure 85: Histograms of Monte-Carlo estimated model uncertainty for F_{recent}/F_{MSY} by mixing period (K statistic; grid facets), h (top-left), effort multiplier (Effort Mult; top-right), and k (middle-left) with median line (blue) and $F_{recent}/F_{MSY} = 1.0$ line (red). Also includes estimated F_{recent}/F_{MSY} by mixing period (K statistic; grid facets), h (middle-right), effort multiplier (Effort Mult; bottom-left), and k (bottom-right) for each model in the ensemble with loess smoother.

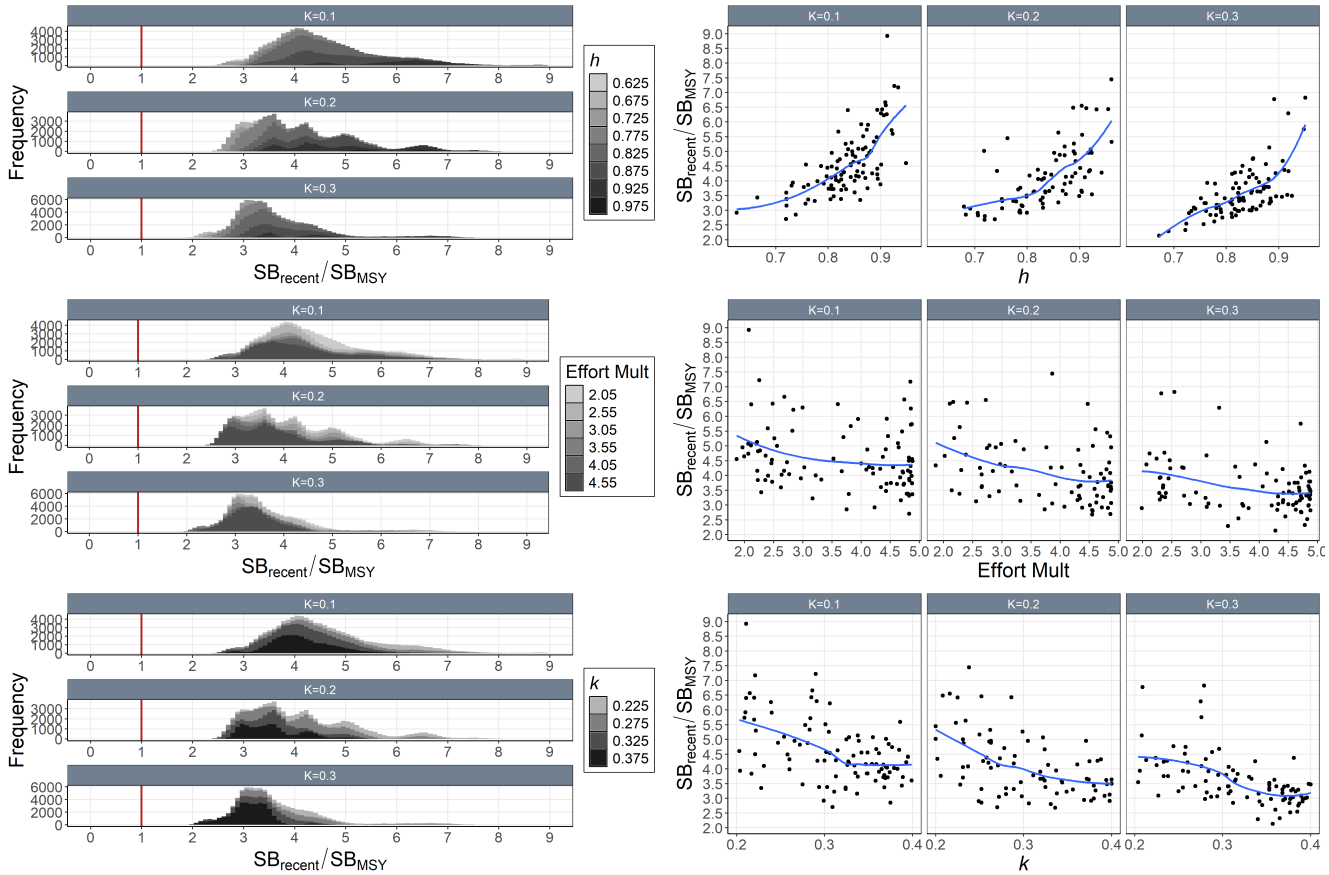

Figure 86: Histograms of Monte-Carlo estimated model uncertainty for SB_{recent}/SB_{MSY} by mixing period (K statistic; grid facets), h (top-left), effort multiplier (Effort Mult; top-right), and k (middle-left) with median line (blue) and $SB_{recent}/SB_{MSY} = 1.0$ line (red). Also includes estimated SB_{recent}/SB_{MSY} by mixing period (K statistic; grid facets), h (middle-right), effort multiplier (Effort Mult; bottom-left), and k (bottom-right) for each model in the ensemble with loess smoother.